PROGRESS REPORT ON
HIGH ALTITUDE PLASTIC BALLOONS
CONTRACT NONR-710 (01)
December 22, 1952 to December 3, 1953
VOLUME IX
CONFIDENTIAL INFORMATION

Copy No. 9

PROGRESS REPORT ON RESEARCH AND DEVELOPMENT IN THE FIELD OF HIGH ALTITUDE PLASTIC BALLOONS

CONDUCTED UNDER
CONTRACT NONR-710(01), NR 211 002
FOR PERIOD DECEMBER 22, 1952 to DECEMBER 3, 1953
WITH THE
OFFICE OF NAVAL RESEARCH

AND SPONSORED JOINTLY
BY THE ARMY, NAVY, AND AIR FORCE

PREPARED BY THE
DEPARTMENT OF PHYSICS
UNIVERSITY OF MINNESOTA
MINNEAPOLIS 14, MINNESOTA

PROGRESS REPORT ON CONTRACT 710(01)
From December 22, 1952, to December 3, 1953

VOLUME IX
Table of Contents

Section I. Organization . . . . . PP. I-1 to I-3

Section II. Balloon Design . . . . . PP. II-4 - II-72
A. Further Calculations of Balloon Shapes... II-4
P. Duct Appendix Size Calculations..... II-20
C. Flight Experiences with Cylinder Balloons II-49
D. Optimum Dimensions and Pressure of Cylinder Type Balloons..... II-58

Section III. Mylar Balloon Development Program. . . . . PP. III-73 - III-160
A. Initial Mylar Program..... III-73
B. Film Leakage Studies..... III-79
Appendix B-1: Kammermeyer Report #1..... III-82
Appendix B-2: Kammermeyer Report #2..... III-88
Appendix B-3: Kammermeyer Report #3..... III-98
Appendix B-4: Herb Shelly, Inc. Report... III-103
C. Superpressure Trajectory Balloons..... III-126
D. Glue Program..... III-128
Appendix D-1: Report on Sealing Methods for Mylar..... III-133
E. Photographs: Figures III-2 through III-37 III-136

Section IV. Radiation Heating of Balloons. . . . . PP. IV-161 - IV-209
A. Introduction and Statement of Problem.... IV-161
B. The Heat Balance Relation..... IV-162
C. Experimental Values for the Constants in the Heat Balance Relation..... IV-164
D. Examples of Heat Balance Calculations.... IV-196
E. Preliminary Infrared Flux Measurements... IV-200
F. Summary of Useful Information..... IV-207

Section V. Analysis of Balloon & Air Temperature Meas.. PP. V-210 - V-260
A. General Description..... V-210
B. Experimental Methods..... V-212
C. Properties of Thermistors..... V-217
D. Flight Summaries of the Temp. Flights.... V-221
E. Flight Summaries of Temperature-Instrumented Step Flights..... V-242
F. Description of Results from Other Temperature Measurements..... V-252
G. Analysis of Temperature Measurements..... V-253

Section VI. Vertical Flight. . . . . PP. VI-261 - VI-314
A. Step Flight Techniques..... VI-261
B. Analysis of Step Flights..... VI-282
C. Equations of Motion and Nomographs..... VI-299
D. Correlations with Other Flights..... VI-304
E. Fundamental Superpressure Calculations... VI-308

Section I

ORGANIZATION

Personnel, space and equipment for the Balloon Project remain essentially the same as reported in the second progress report. Dr. Charles Critchfield has resumed his professorial duties and his position as director of the project has been taken over by Dr. Edward P. Ney with Dr. John R. Winckler acting as alternate.

The current personnel fall into the following categories:

Experienced Research Men (Ph.D.)	6
Associate Scientists	2
Junior Scientists	3
Research Fellows	3
Electronics Mechanics	5
Engineering Assistants	7
Clerks	3
Sr. Lab Technicians	1
Non-scientific, miscellaneous, etc., equivalent	7
TOTAL	37

The names and experience of the senior men are:

Edward P. Ney, Associate Professor of Physics, Scientific Director of Project, Ph.D. 1947

John R. Winckler, Associate Professor of Physics, Alternate Scientific Director, Ph.D. 1946

Homer T. Mantis, Assistant Professor of Mechanical Engineering, Ph.D. (Meteorology) 1949

Ralph H. Upson, Professor of Aeronautical Engineering, Consultant during summer, M.E., A.E.

Raymond Maas, Research Associate, B.E.E. 1948

William F. Huch, Research Associate, B.S. (Aeronautical Engineering) 1942

A complete list of laboratory and office personnal, in addition to the six senior men listed above, is as follows:

Associate Scientists

Robert Howard
Logan Gilman

Junior Scientists

John Gergen
Donald Hinze
F. Willard Lewis

Research Fellows

Leland Bohl - ½ time
John Linsley - ½ time
Ferdinand Ohnsorg

Electronics Mechanics

Robert Anderson
Phillip Erickson
Donald Kruse
Joseph Merkl
James Stoddart

Engineering Assistants

Idar Anderson
Paul Chase
T. A. Erickson
Charles France
Joseph LeClair
Robert Mann
Bernard Welinski

Clerks

Antoinette Cheslik, Sr. Clerk
Robert Dahl - ½ time
Ethel Gold, Sr. Clerk

Sr. Lab Technicians

Rosalind Worthington

Non-scientific personnel

Berton Atkinson - Draftsman
Marlene Besaw - Secretary
Harold Carlson - Administrative Asst, part time
Charles Edwards - General Mechanic
Glen Erickson - Utility Man, ½ time
Donald Hanson - Sr. General Mechanic
Cecil Smith - General Mechanic

Winter operations are still made from Pierre, South Dakota, using a mobile communications unit. Prevailing westerlies prevent complete tracking of sustained flight when launched at Minnesota. "Step flights" have been made successfully during the summer at altitudes where the winds are 50 to 100 mile westerlies by launching from Minneapolis and recording at Minneapolis and at Green Bay, Wisconsin. The station used at Green Bay has been our portable "semi-" trailer station.

Very successful balloon flights were launched from Pyote, Texas, under a separate contract with ONR and are described more fully in Volume VIII.

In general, the project is receiving full cooperation from the University administration, representatives of ONR and CAA, the manufacturers of balloons and the hundreds of people who have helped in the recovery of gear and balloons.

Section II

BALLOON DESIGN

A. Further Calculations of Balloon Shapes

"NATURAL" BALLOON SHAPES WITH FABRIC WEIGHT

Introduction. A balloon tailored to an arbitrary shape (e.g., sphere-on-cone, etc.) will not necessarily assume that shape at ceiling altitude. There may be regions of excess fabric, resulting in the balloon not assuming its design volume. There may also be regions where the fabric is being stressed circumferentially (i.e., across the seams). The latter situation may be avoided by providing everywhere excess fabric, as is done in the case of a cylinder balloon. If the fabric weight of the cylinder balloon is negligible compared with the weight of the payload, the balloon will assume a so-called "natural shape". One may wish also to eliminate the excess fabric by tailoring the balloon exactly to this natural shape, thus keeping the circumferential stress just equal to zero.

If the fabric weight of the balloon is not negligible compared with the payload, then the cylinder balloon assumes a new, more oblate shape. In this case, the cylinder balloon shape is not the shape to which one would want to tailor a balloon of this fabric, since the excess fabric of the cylinder balloon now has weight which alters the shape. What has been calculated here is the "natural shape with fabric weight" and the results are applicable only to the design of tailored balloons. The results are applicable also only to balloons in which the bottom of the appendix is near the bottom apex of the balloon (i.e., neither super- nor sub-pressure balloons.)

The shapes given here are based on the solution of certain differential equations. Each shape is characterized by a value of the "balloon fabric parameter Σ", where Σ is a dimensionless parameter that enters the differential equations when the effect of finite fabric weight is taken into account. The method of obtaining the shapes from the differential equations was as follows:

Nine different values of Σ were chosen, and for each value the differential equations were solved using an electronic analogue computer, the shape coordinates being read off of dials on the computer. (The shape coordinates are given to four decimal places although, because of electronic limitations in the analogue computer, the results are probably accurate only to within 1%). These nine shapes were then normalized to give the shape coordinates r, z, s for balloons of unit gore length, where r and z give the profile of the balloon and s is the distance of a point on the profile from the bottom apex (measured up along the gore):

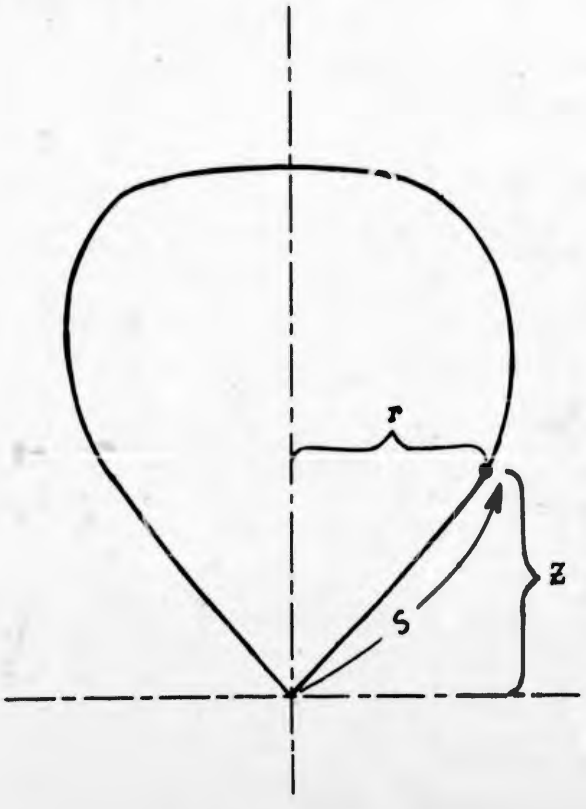

"NATURAL" BALLOON SHAPES
WITH FABRIC WEIGHT

NOMOGRAPH NO. 1

DETERMINATION OF BALLOON
FABRIC PARAMETER Σ

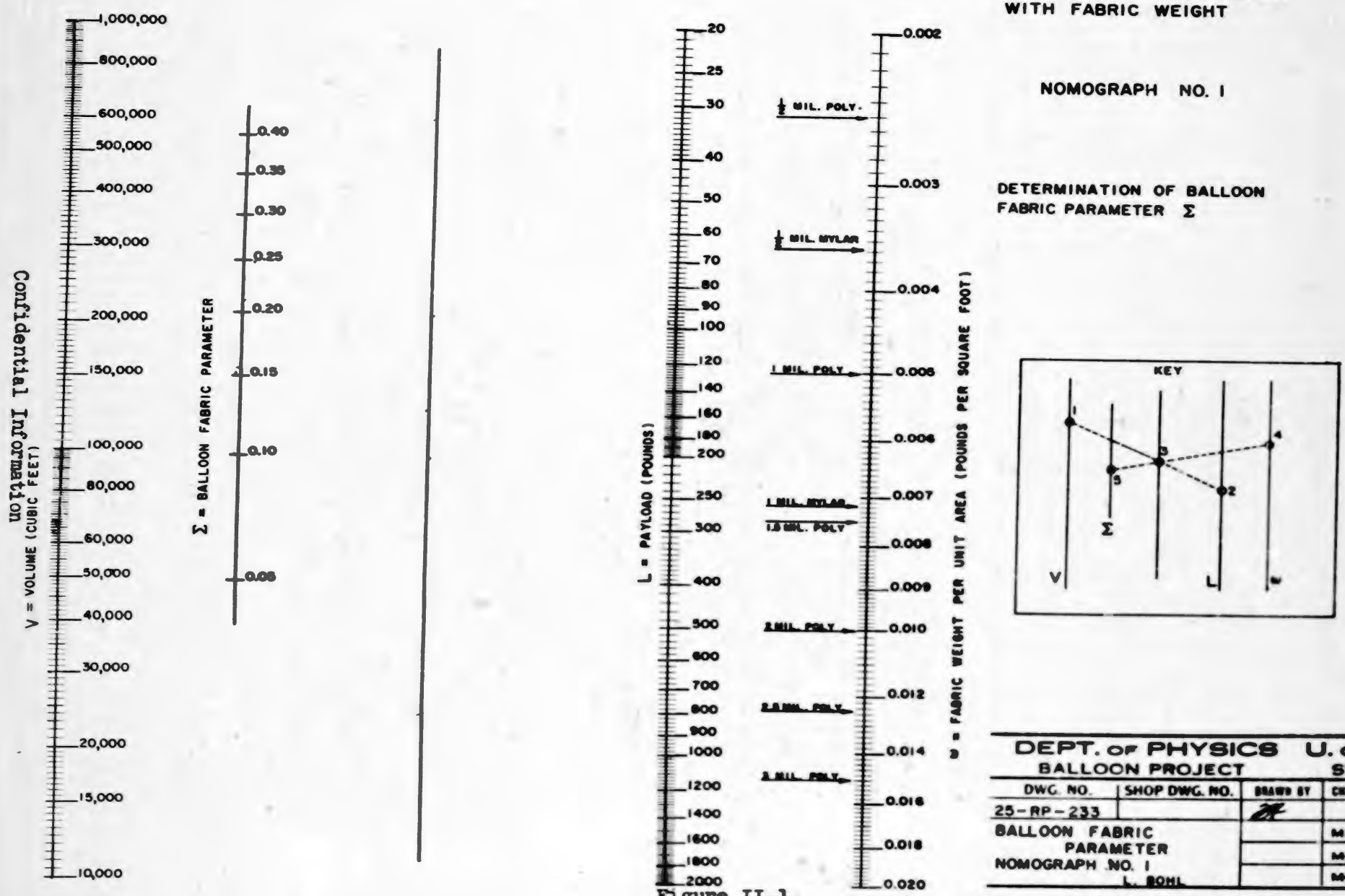

Figure II-1.

DEPT. OF PHYSICS U. OF MINN. BALLOON PROJECT			SECT. B B T	
DWG. NO.	SHOP DWG. NO.	DRAWN BY	CHECKED BY	DATE
25-RP-233				6-2-53
BALLOON FABRIC PARAMETER NOMOGRAPH NO. 1 L. BOHL			MOD. 1	
			MOD. 2	
			MOD. 3	

Each shape is characterized by a value of Σ, where $\Sigma = 0$ corresponds to the so-called "weightless natural shape", and larger Σ corresponds to the more oblate shape with heavier fabric weight. The proper value of Σ is uniquely determined by the following quantities:

(1) V = volume of fully inflated balloon (cubic feet),

(2) L = payload suspended from bottom apex (pounds),

(3) ω = weight of fabric material per unit area (pounds/square foot).

The value of Σ as a function of V, L, ω cannot be given in closed form, and so the relation is expressed in the form of a nomograph. Also given is a nomograph to determine the gore length S_λ as a function of V and Σ (this S_λ gives the factor by which to scale up the coordinates of the unit-gore-length balloon corresponding to Σ). A third nomograph is used to figure the gross load G, when L and Σ are known (this gives the total weight of the balloon fabric as G-L).

The use of the unit shapes and nomographs is discussed in the following.

Using Nomographs and Tabulated Values to Determine Shape Coordinates

One starts with the given conditions: volume (V cubic feet), payload (L pounds) and fabric material (ω pounds per square foot). In order to determine the shape coordinates it is necessary to determine two values:

(1) Σ = balloon fabric parameter

(2) S_λ = gore length.

The value of Σ selects the proper unit-gore-length balloon and S_λ gives the factor by which to scale up the coordinates of this unit balloon.

Σ is determined from Nomograph No. 1 (Figure II-1) by entering with V, L, ω, and reading off the value of Σ, as is shown in the key.

Using the volume V and the value of Σ just determined, the value of S_λ can be found from Nomograph No. 2. (Figure II-2.)

Thus, by picking the shape corresponding to Σ and scaling it up according to gore length S_λ, one has the desired coordinate data for the "natural shape with fabric weight" corresponding to the input conditions V, L, ω.

One can determine the gross load G (i.e., the payload weight plus fabric weight) by entering Nomograph No. 3 (Figure II-3) with L and Σ.

If the fabric weight ω is very small, one will get essentially $\Sigma = 0$, corresponding to the so-called "weightless natural shape" given in a previous report. The effect of non-negligible fabric weight ($\Sigma > 0$) is to make the natural shape more oblate.

In selecting the unit-gore-length shape, if the value of Σ obtained from the nomographs lies between any two of the nine values of Σ for which shapes are given, one can:

(1) Plot the two shapes given and interpolate between them.

(2) Choose the larger value of Σ (this will mean that the balloon will have volume V at ceiling but will have a slight excess of fabric).

(3) Choose the smaller value of Σ (this will mean that the balloon will be taut at ceiling with no excess fabric but with circumferential tension and with a volume slightly less than V).

The following examples illustrate the use of the nomographs and the tabulated data.

"NATURAL" BALLOON SHAPES
WITH FABRIC WEIGHT

NOMOGRAPH NO. II

DETERMINATION OF GORE LENGTH $S\lambda$

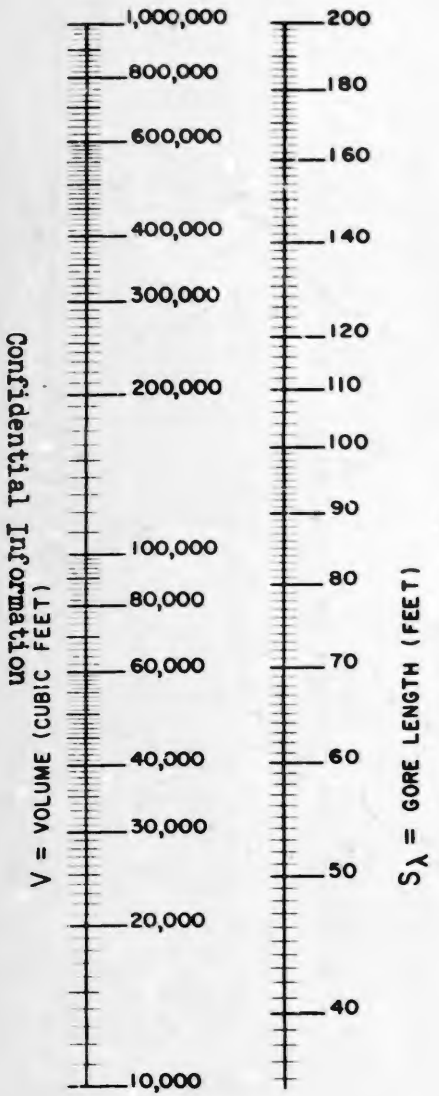

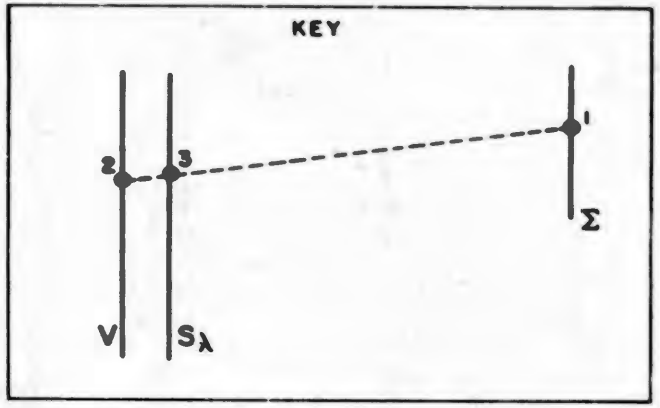

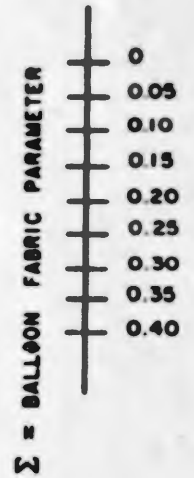

Figure II-2.

DEPT. OF PHYSICS U. OF MINN. BALLOON PROJECT SECT. B & T				
DWG. NO.	SHOP DWG. NO.	DRAWN BY	CHECKED BY	DATE
25-RP-234				6-2-53
GORE LENGTH NOMOGRAPH NO. 2			MOD. 1	
			MOD. 2	
L. BOHL			MOD. 3	

"NATURAL" BALLOON SHAPES
WITH FABRIC WEIGHT

NOMOGRAPH NO. III

DETERMINATION OF GROSS LIFT G

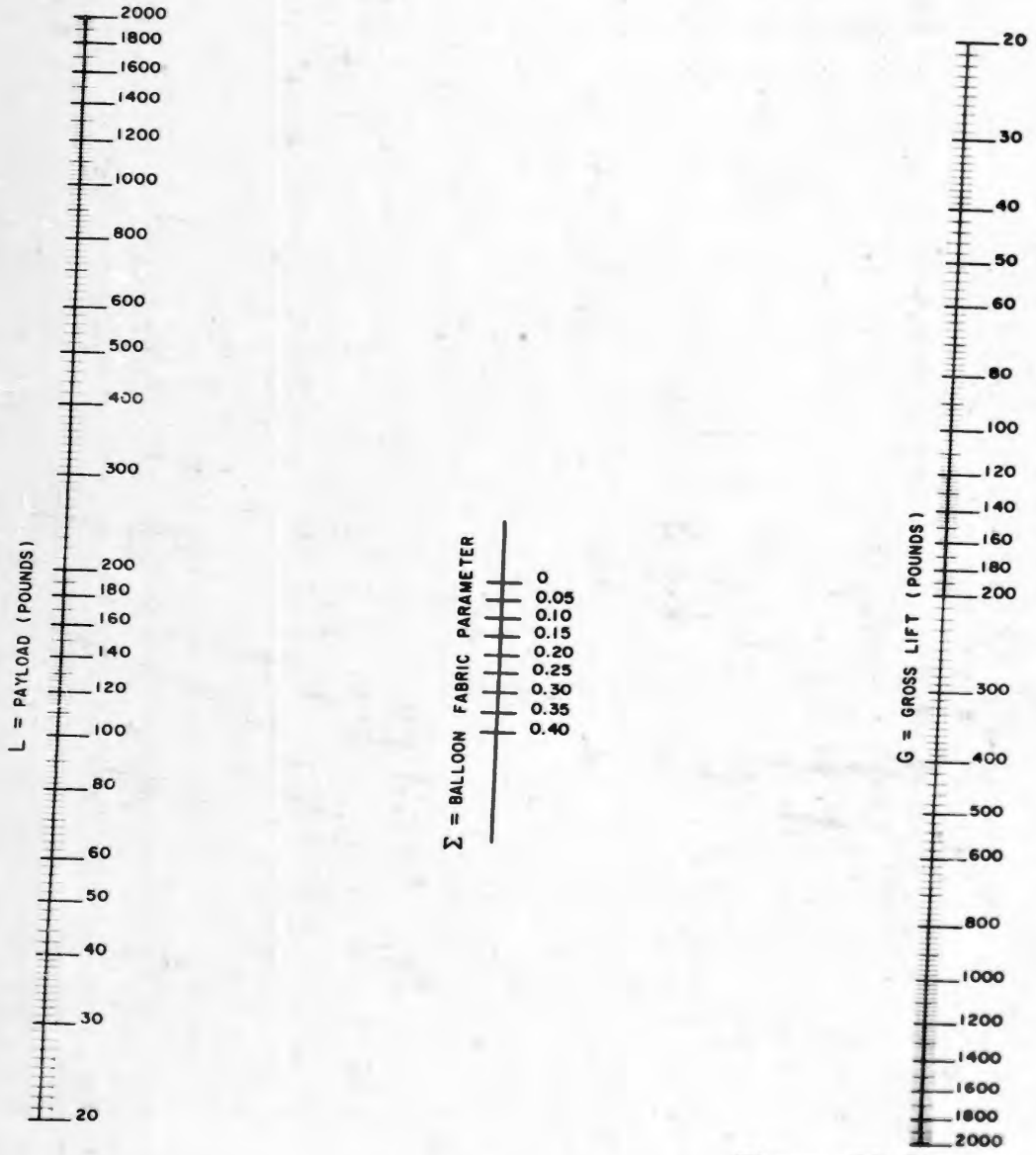

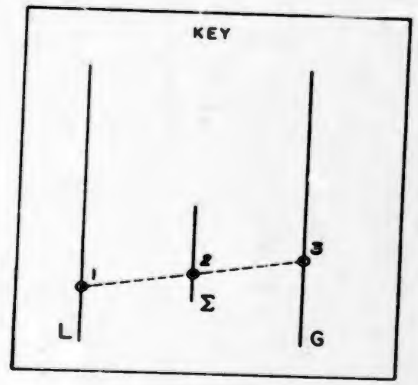

DEPT. OF PHYSICS U. OF MINN. BALLOON PROJECT SECT. 8 8 T				
DWG. NO.	SHOP DWG. NO.	DRAWN BY	CHECKED BY	DATE
25-RP-235		[illegible]		6-2-53
GROSS LIFT NOMOGRAPH NO. 3			MOD. 1	
			MOD. 2	
L. BOHL			MOD. 3	

Figure II-3.

Examples

(A) Suppose one wants a 100,000 cubic foot balloon of one-mil polyethylene to carry a payload of 100 pounds. From Nomograph No. 1, we find $\Sigma = 0.15$. From Nomograph No. 2, using $\Sigma = 0.15$ and V = 100,000 cubic feet, we find that the gore length should be $S_\lambda = 91.5$ feet. From Nomograph No. 3, using $\Sigma = 0.15$ and L = 100 pounds, the gross load of this balloon will be G = 156 pounds. Thus the fabric in this balloon will weigh 56 pounds. (The weight of the tapes, if any, is assumed to be included in L = 100 pounds.) Selecting the unit-gore-length balloon corresponding to $\Sigma = 0.15$, and using the scale factor $S_\lambda = 91.5$ feet, the coordinate data can be put into feet. Thus, for example, the height of the balloon will be 56.1 feet and the diameter of the balloon will be 63.9 feet.

(B) A half-million cubic foot balloon of two-mil polyethylene is to carry a load of 240 pounds. From Nomograph No. 1, $\Sigma = 0.275$. From Nomographs Nos. 2 and 3, using $\Sigma = 0.275$, we find $S_\lambda = 153$ feet and G = 560 pounds. Thus the balloon itself will weigh 320 pounds. For the shape of this balloon one will have to interpolate between the shapes corresponding respectively to $\Sigma = 0.25$ and $\Sigma = 0.30$. For example, the height of this balloon will be 89 feet and the diameter will be 110 feet.

$\Sigma = 0$ $S\lambda = 1.000$

S	R	Z
.0000	.0000	.0000
.0344	.0273	.0226
.0695	.0533	.0450
.1013	.0778	.0655
.1446	.1113	.0932
.1749	.1349	.1133
.2076	.1590	.1353
.2320	.1779	.1526
.2774	.2109	.1852
.3006	.2291	.2049
.3430	.2542	.2372
.3706	.2700	.2588
.4031	.2861	.2868
.4436	.3060	.3230
.4740	.3159	.3516
.5078	.3241	.3834
.5437	.3279	.4142
.5742	.3273	.4534
.6173	.3185	.4976
.6414	.3098	.5209
.6839	.2888	.5568
.7165	.2670	.5809
.7451	.2449	.5990
.7833	.2127	.6181
.8210	.1771	.6327
.8496	.1491	.6401
.8804	.1186	.6449
.9205	.0778	.6483
.9613	.0377	.6497
.9884	.0110	.6493
.9993	.0006	.6491
1.0000	.0000	.6491

$\Sigma = 0.05$ $S\lambda = 1.0000$

S	R	Z
.0000	.0000	.0000
.0373	.0299	.0228
.0616	.0491	.0377
.0930	.0739	.0572
.1283	.1031	.0790
.1622	.1304	.1003
.2002	.1601	.1250
.2274	.1807	.1427
.2571	.2043	.1636
.3003	.2347	.1960
.3290	.2538	.2179
.3575	.2720	.2402
.3869	.2888	.2653
.4295	.3095	.3027
.4568	.3199	.3275
.4951	.3325	.3647
.5218	.3359	.3921
.5560	.3375	.4290
.5904	.3333	.4650
.6169	.3175	.4917
.6499	.3111	.5226
.6839	.2933	.5503
.7202	.2691	.5762
.7516	.2437	.5956
.7908	.2081	.6138
.8146	.1865	.6226
.8529	.1473	.6313
.8837	.1160	.6362
.9165	.0820	.6379
.9458	.0538	.6388
.9810	.0211	.6381
1.0000	.0000	.6369

Σ = 0.10 $S\lambda$ = 1.0000

S	R	Z
.0000	.0000	.0000
.0356	.0295	.0205
.0656	.0536	.0379
.0899	.0738	.0515
.1305	.1079	.0755
.1505	.1246	.0871
.1908	.1573	.1117
.2240	.1840	.1329
.2448	.2009	.1466
.2808	.2294	.1728
.3144	.2514	.1975
.3444	.2704	.2199
.3735	.2883	.2442
.4100	.3080	.2749
.4365	.3197	.2986
.4702	.3322	.3297
.4938	.3384	.3538
.5292	.3433	.3900
.5567	.3411	.4199
.5872	.3381	.4519
.6249	.3271	.4890
.6541	.3122	.5136
.6908	.2904	.5428
.7177	.2714	.5612
.7471	.2486	.5798
.7739	.2246	.5928
.8132	.1878	.6064
.8369	.1643	.6125
.8782	.1220	.6188
.9075	.0943	.6214
.9413	.0586	.6214
.9685	.0320	.6209
.9997	.0002	.6184
1.0000	.0000	.6184

Σ = 0.15 $S\lambda$ = 1.0000

S	R	Z
.0000	.0000	.0000
.0326	.0283	.0180
.0563	.0471	.0306
.0902	.0762	.0494
.1230	.1046	.0680
.1554	.1326	.0862
.1755	.1488	.0976
.2089	.1758	.1176
.2400	.2014	.1374
.2759	.2289	.1622
.2949	.2432	.1758
.3331	.2686	.2043
.3595	.2829	.2218
.3896	.3037	.2503
.4196	.3186	.2757
.4523	.3325	.3059
.4791	.3412	.3325
.5105	.3478	.3651
.5348	.3491	.3906
.5758	.3457	.4346
.6039	.3382	.4610
.6285	.3290	.4852
.6641	.3102	.5162
.6889	.2943	.5348
.7240	.2674	.5600
.7535	.2443	.5762
.7814	.2188	.5883
.8123	.1900	.5997
.8454	.1560	.6075
.8656	.1374	.6111
.9013	.1004	.6137
.9314	.0696	.6150
.9614	.0395	.6143
.9854	.0152	.6137
.9990	.0009	.6126
1.0000	.0000	.6125

Σ= 0.20 $S\lambda$= 1.0000

S	R	Z
.0000	.0000	.0000
.0276	.0231	.0135
.0562	.0486	.0288
.0891	.0778	.0455
.1086	.0945	.0557
.1432	.1249	.0742
.1742	.1505	.0902
.1965	.1707	.1040
.2305	.1990	.1242
.2526	.2171	.1387
.2880	.2431	.1626
.3102	.2585	.1786
.3442	.2822	.2044
.3672	.2972	.2233
.4018	.3165	.2516
.4239	.3270	.2702
.4564	.3405	.3013
.4906	.3499	.3363
.5140	.3534	.3602
.5382	.3537	.3875
.5772	.3487	.4274
.6059	.3400	.4551
.6318	.3289	.4779
.6633	.3105	.5052
.6868	.2950	.5234
.7200	.2699	.5455
.7465	.2485	.5600
.7672	.2313	.5699
.7987	.2012	.5822
.8347	.1668	.5921
.8554	.1462	.5955
.8830	.1184	.5995
.9166	.0826	.6013
.9411	.0576	.6013
.9703	.0288	.6004
1.0000	.0000	.5996

Σ = 0.25 $S\lambda$ = 1.0000

S	R	Z
.0000	.0000	.0000
.0277	.0251	.0135
.0576	.0506	.0276
.0795	.0709	.0383
.1111	.0992	.0539
.1349	.1202	.0657
.1619	.1441	.0793
.1930	.1712	.0960
.2186	.1907	.1095
.2503	.2191	.1306
.2778	.2397	.1478
.3069	.2606	.1689
.3278	.2767	.1849
.3544	.2944	.2054
.3770	.3080	.2232
.4080	.3251	.2481
.4349	.3376	.2735
.4677	.3495	.3065
.4993	.3562	.3382
.5159	.3575	.3558
.5462	.3563	.3905
.5733	.3524	.4161
.6108	.3407	.4508
.6224	.3357	.4618
.6575	.3157	.4929
.6956	.2903	.5211
.7077	.2806	.5293
.7406	.2532	.5489
.7681	.2298	.5623
.8006	.2003	.5749
.8185	.1838	.5804
.8495	.1528	.5874
.8816	.1202	.5910
.9069	.0938	.5930
.9375	.0616	.5936
.9689	.0304	.5931
.9997	.0002	.5921
1.0000	.0000	.5921

$\Sigma = 0.30$ $s\lambda = 1.0000$

S	R	Z
.0000	.0000	.0000
.0261	.0241	.0119
.0486	.0440	.0213
.0763	.0695	.0333
.1022	.0931	.0453
.1261	.1148	.0562
.1582	.1436	.0713
.1845	.1664	.0837
.2069	.1870	.0965
.2336	.2095	.1114
.2566	.2279	1251
.2860	.2501	.1440
.3083	.2679	.1603
.3367	.2884	.1810
.3654	.3072	.2025
.3923	.3281	.2244
.4168		.2464
.4433	.3477	.2717
.4648	.3548	.2930
.4906	.3602	.3194
.5179	.3628	.3483
.5412	.3621	.3724
.5679	.3578	.3990
.5933	.3506	.4231
.6191	.3386	.4474
.6467	.3243	.4710
.6708	.3091	.4911
.7021	.2847	.5127
.7261	.2650	.5267
.7539	.2421	.5412
.7729	.2253	.5498
.7983	.2019	.5587
.8246	.1761	.5660
.8515	.1493	.5713
.8813	.1187	.5749
.9016	.0979	.5760
.9308	.0674	.5763
.9532	.0454	.5762
.9843	.0155	.5748
1.0000	.0000	.5740

$\Sigma = 0.35$ $s\lambda = 1.0000$

S	R	Z
.0000	.0000	.0000
.0222	.0203	.0090
.0518	.0476	.0213
.0714	.0661	.0288
.0964	.0896	.0395
.1261	.1173	.0525
.1474	.1362	.0615
.1728	.1594	.0730
.1960	.1804	.0851
.2166	.1987	.0961
.2452	.2212	.1110
.2743	.2453	.1287
.3035	.2690	.1496
.3262	.2856	.1656
.3390	.2949	.1749
.3565	.3065	.1879
.3686	.3136	.1977
.3871	.3254	.2128
.4221	.3440	.2451
.4464	.3536	.2678
.4662	.3600	.2879
.4884	.3644	.3099
.5190	.3667	.3426
.5391	.3658	.3634
.5539	.3636	.3784
.5940	.3522	.4174
.6157	.3432	.4371
.6447	.3274	.4619
.6615	.3164	.4757
.6897	.2963	.4965
.7186	.2736	.5148
.7391	.2563	.5264
.7692	.2286	.5410
.7821	.2169	.5459
.8171	.1837	.5565
.8448	.1566	.5626
.8668	.1332	.5657
.8935	.1066	.5680
.9166	.0833	.5687
.9364	.0642	.5692
.9722	.0284	.5685
1.0000	.0000	.5677

$\Sigma = 0.40$ $S\lambda = 1.0000$

S	R	Z
.0000	.0000	.0000
.0237	.0224	.0089
.0453	.0422	.0172
.0663	.0627	.0249
.0957	.0898	.0359
.1180	.1114	.0454
.1436	.1346	.0553
.1640	.1581	.0641
.1896	.1773	.0760
.2144	.1989	.0886
.2366	.2170	.1002
.2614	.2378	.1140
.2811	.2542	.1263
.3042	.2729	.1426
.3271	.2898	.1583
.3556	.3094	.1796
.3778	.3242	.1972
.4031	.3385	.2194
.4191	.3450	.2341
.4507	.3586	.2645
.4721	.3638	.2854
.4906	.3675	.3043
.5169	.3686	.3323
.5413	.3676	.3108
.5626	.3631	.3787
.5879	.3558	.4029
.6115	.3460	.4245
.6336	.3344	.4446
.6571	.3197	.4631
.6810	.3031	.4806
.7016	.2877	.4950
.7328	.2607	.5136
.7474	.2482	.5211
.7722	.2247	.5323
.7954	.2041	.5403
.8175	.1825	.5465
.8466	.1547	.5520
.8699	.1310	.5551
.8947	.1067	.5574
.9136	.0869	.5580
.9894	.0613	.5586
.9621	.0385	.5583
.9850	.0159	.5576
1.0000	.0000	.5572

SUPPLEMENTAL INFORMATION TO " NATURAL BALLOON SHAPES WITH FABRIC WEIGHT"

This supplement is intended as an aid in applying the REAC balloon shape calculations to the actual design of a balloon.

The unit balloon shape data given in tabular form should first be plotted to a suitable scale and a smooth curve drawn between the points. Though the points are given to four decimal places, the accuracy is only about 1% and hence some scatter is to be expected (each point represents a recomputation from the bottom apex up to the point). This procedure should also prove of value in interpolating between the various values of the parameter, $\sum$.

The calculations were made under the assumption that the tape weight is negligible. If there is appreciable tape weight, it will tend to be mostly at the apexes, and should thus be added to the payload in determining the proper shape.

The balloon should have a flat top if no concentrated loads are to be placed at the top apex. To within the expected accuracy, the unit shapes given are flat-topped.

As can be seen from the discussion of use of the nomographs, the input data are the volume, V, the fabric weight per unit area, ω, and the payload, L. Thus (for $\sum > 0$) the balloon shape obtained is appropriate to only one value of payload. If the balloon is flown with a lighter payload, then at ceiling the balloon will develop circumferential stress. On the other hand, if the balloon is flown with a payload heavier than the design load, then the balloon at ceiling will not fill out completely,

and there will be a volume defect. In general, if a certain amount of circumferential stress is not intolerable, then the value of L used in the design would be the maximum load to be used on the balloon.

When design curves are inferred from the results given in the report, the most accurate value of the volume of the balloon is best obtained by integration of the scaled-up design curves by some appropriate method.

The unit shape data is taken directly from the computer. The nomographs given in the report are merely for convenience in selecting which unit shape is applicable to the design conditions. In fact the nomographs were constructed entirely on the basis of the REAC results that are given in Table I, which follows. In cases where optimum precision is desired, or where the design values lie outside of the range encompassed by the nomographs, the table should be used.

In using the table, the input data are combined to form the dimensionless number $\frac{L}{\omega V^{2/3}}$. With this number, the value of Σ that corresponds identifies which unit shape is applicable to the design conditions. The value of the dimensionless number $V/S\lambda^3$, when taken with the design volume, gives the gore length of the scaled-up unit shape. The last column gives the ratio of gross weight to load weight and, in effect, determines what the total balloon weight will be according to the relation for the balloon weight W.

$$W = L\left(\frac{G}{L} - 1\right)$$

Thus the table can be used to give completely the design coordinates for a "natural shape" balloon. Again, the volume of the balloon should

TABLE I

$\frac{L}{\nabla^{2/3}}$	Σ	$V/S\lambda^3$	G/L
∞	0	.128	1.00
33.43	.05	.130	1.16
15.06	.10	.133	1.34
9.15	.15	.135	1.56
6.14	.20	.138	1.84
4.441	.25	.140	2.14
3.309	.30	.143	2.53
2.541	.35	.145	2.99
1.9935	.40	.148	3.52

probably be figured directly from the final design curves for the shape, rather than taken as the input design volume V.

B. Duct Appendix Size Calculations

A design problem of some consequence is the calculation of the size of appendix to be used under a given set of circumstances. The discussion of this problem will be separated into four parts:

i - Inertial overshoot of balloons on reaching ceiling altitude;

ii - Altitude at which valving occurs;

iii - Calculations for open appendices;

iv - Effect of skirts and ducts.

i. Inertial overshoot of balloons on reaching ceiling altitude.

It will be convenient to refer to Figure II-4 to describe the sequence of events as a balloon approaches its "floating altitude". At point (A) the balloon becomes taut, but because the balloon still has free lift, it continues to rise. From (A) to (B) the free lift is decreasing because the now-constant balloon volume displaces air which is becoming more rarified, an effect only slightly offset by the fact that a small weight of helium is escaping through the valve. If G is the weight of displaced air and M is the weight of helium in the balloon, then the rate of losing free lift, F, is

$$\frac{dF}{dt} = \frac{d}{dt}\left[G - (M + W)\right] = \frac{d}{dt}(G-M) = \left(1-\frac{1}{\sigma}\right)\frac{dG}{dt} \qquad (1)$$

since the gross weight W is constant, and the air is taken to be σ times as dense as the helium. If the balloon is rising at a rate v, then the

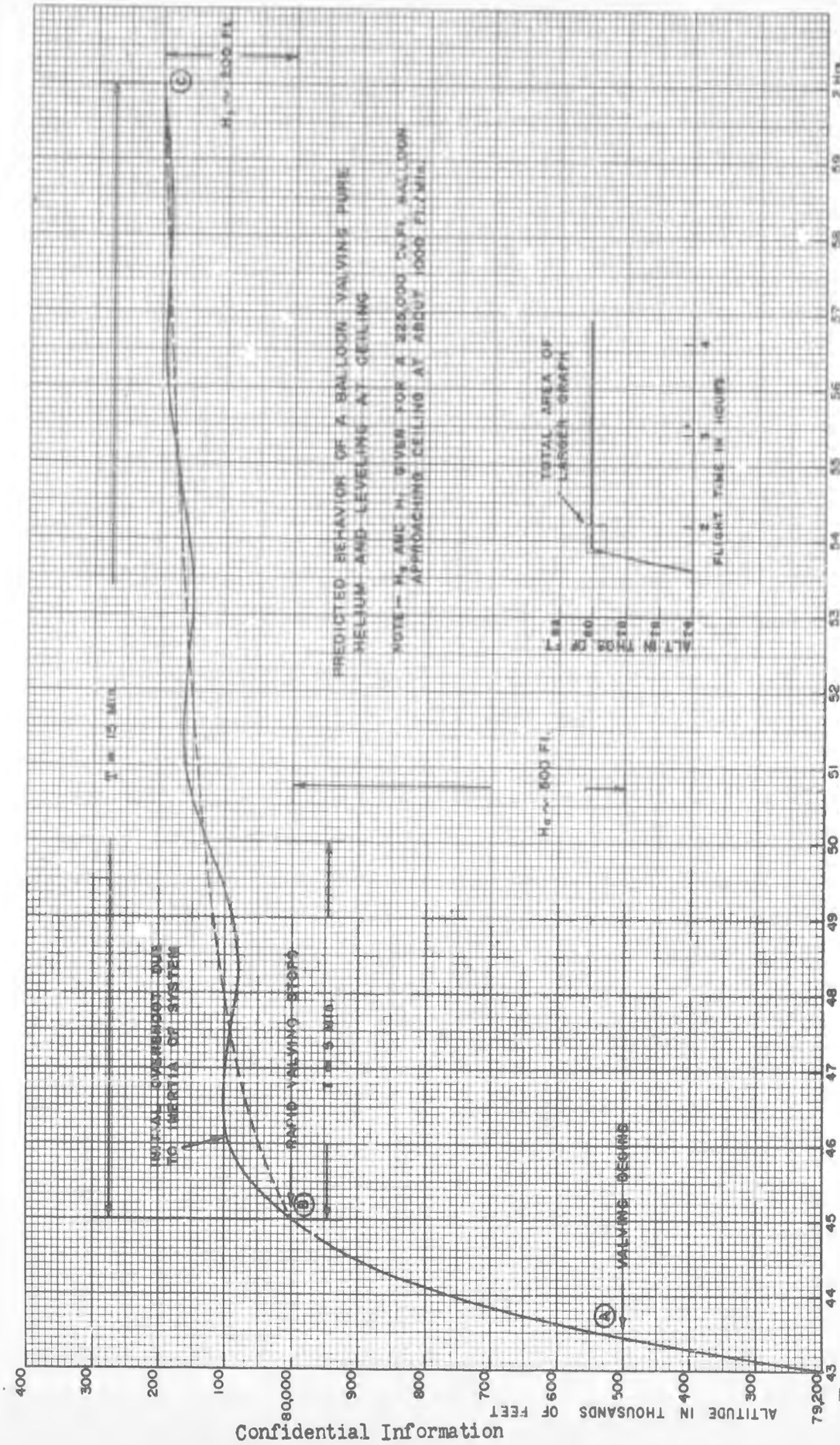

Figure II-4.

Confidential Information

fractional rate of change in the weight of displaced air is just

$$\frac{1}{G}\frac{dG}{dt} = -\frac{v}{Z_o} \qquad (2)$$

where Z_o is the atmospheric "e-folding distance" and is 20,000 feet in the stratosphere. Thus the free lift is being valved away at the rate (from (1) and (2)) of

$$\frac{dF}{dt} = -\left(1-\frac{1}{\rho}\right) G \frac{v}{Z_o} \qquad (3)$$

The gas in a balloon rising at a constant rate will, in general, be at a different temperature from that of the outside air due to the "thermal drag" effect. As the balloon slows its rate of rise, the gas will want to come to some new (and higher) steady-state temperature. But because the "relaxation time" of the gas (of order 15 minutes) is long as compared to the time interval in which overshoot occurs, it will be assumed in the following treatment that the temperature remains constant during the inertial effects. Thus when the free lift is small

$$\left(1-\frac{1}{\rho}\right) G \approx W = \text{constant},$$

and

$$\frac{dF}{dt} = -W\frac{v}{Z_o} \qquad (4)$$

The point (B) is the point at which all of the free lift has been valved away ($F = 0$, where F is understood to be the free lift not including the "thermal drag", that is, F is the net buoyancy of the balloon in the dynamic situation). In a sense, point (B) is the "ceiling" of the balloon, though the relatively slow warming of the gas will produce some free lift

and the balloon will finally rise to Ⓒ which is the floating altitude. This section, however, is concerned only with the height by which the balloon initially overshoots the point Ⓑ. The height above the point Ⓑ will be called h. Thus at Ⓑ (h = 0) there is no free lift (F = 0) but the inertia of the balloon carries the balloon on up a distance Δ h (the maximum overshoot) and the balloon at this point, having negative buoyancy, starts down. The subsequent behavior of the balloon is determined by the competition between the slow warming of the gas and the loss of lift by valving during overshoot.

The general expression for the amount of maximum overshoot is derived in Appendix I by solving the differential equation of motion for a valving balloon. There are two limiting cases, however, in which the maximum overshoot can be obtained more directly:

1) Assume that the rate of rise, v_o, is very small as the balloon starts to valve at Ⓐ. In this case, the effect of aerodynamic drag will be small, there will be only slight free lift, and valving will start very near the ceiling, Ⓑ. Thus one would expect the kinetic energy, $\frac{1}{2} W v_o^2$, would just be expended in doing work in going the distance of the maximum overshoot, Δh, against the force of negative buoyancy, $gG\frac{h}{Z_o}$, that is,

$$\frac{1}{2} W v_o^2 \int_0^{\Delta h} gG \frac{h}{Z_o} dh = \frac{1}{2} \frac{gG}{Z_o} (\Delta h)^2 \qquad (5)$$

so that the maximum overshoot would be

$$\Delta h = \left[\frac{WZ_o}{Gg}\right]^{\frac{1}{2}} v_o \qquad (6)$$

Since $\left[\frac{WZ_o}{Gg}\right]^{\frac{1}{2}} = 0.386$ minutes for a helium-filled balloon in the stratosphere and is independent of the size and loading of the balloon, it follows that the maximum overshoot is proportional to the rate of rise when that rate is sufficiently small.

2) When the rate of rise is very large, the situation is reversed, that is, the maximum overshoot is now independent of the rate of rise but is different for different size balloons. This can be seen from the following argument: Even though the balloon is valving lift, it has a kind of terminal (non-transient) velocity due to the aerodynamic drag force. Thus, not only is the free lift balanced by the aerodynamic drag

$$F = Kv^2 \tag{7}$$

where K is some constant, but since a quasi-equilibrium has been established, the rate of losing free lift must also be equal to the rate of losing aerodynamic drag:

$$\frac{dF}{dt} = \frac{d}{dt}(Kv^2) = 2Kv\frac{dv}{dt} \tag{8}$$

The rate of losing lift is proportional to the upwards velocity of the balloon (Equation (4)) so that

$$\frac{dF}{dt} = -W\frac{v}{Z_o} = 2Kv\frac{dv}{dt} \tag{9}$$

or

$$\frac{dv}{dt} = -\frac{W}{2KZ_o}$$

Equation (9) states that the balloon establishes a deceleration that is constant during valving and so the upward inertial force will have the constant value

$$W \cdot \frac{W}{2KZ_o} .$$

At the top of the overshoot, this force just balances the force of negative buoyancy,

$$g\,W\,\frac{\Delta h}{Z_o} = W \cdot \frac{W}{2KZ_o} \tag{10}$$

so that, for great rates of rise, the maximum overshoot is

$$\Delta h = \frac{W}{2Kg} \tag{11}$$

These results agree with the more general expression derived in Appendix I. The general expression is plotted graphically in Figure II-5.

It is the negative buoyancy developed as a result of this overshoot that drives the subsequent oscillations that sometimes occur as the balloon gas warms.

The expression for inertial overshoot has been derived under the assumption that the balloon is freely valving, that is, that no appreciable superpressure is built up in the balloon during the valving time. With the sizes of appendices commonly used, it turns out to be true that the valving superpressure is indeed inappreciable (c.f. Example 1 in Appendix II) in the case of a tailored balloon where the volume is constant. The volume of a cylinder balloon, however, is somewhat sensitive to superpressure as can be seen from the "volume defect" curve for cylinder balloons. It is conceivable that a restricted appendix opening in a cylinder balloon could result in super-pressuring to the extent of expanding the volume of the cylinder balloon so as to cause an overshoot of size comparable to the inertial overshoot effect. Such a case is calculated as Example 2 in Appendix II.

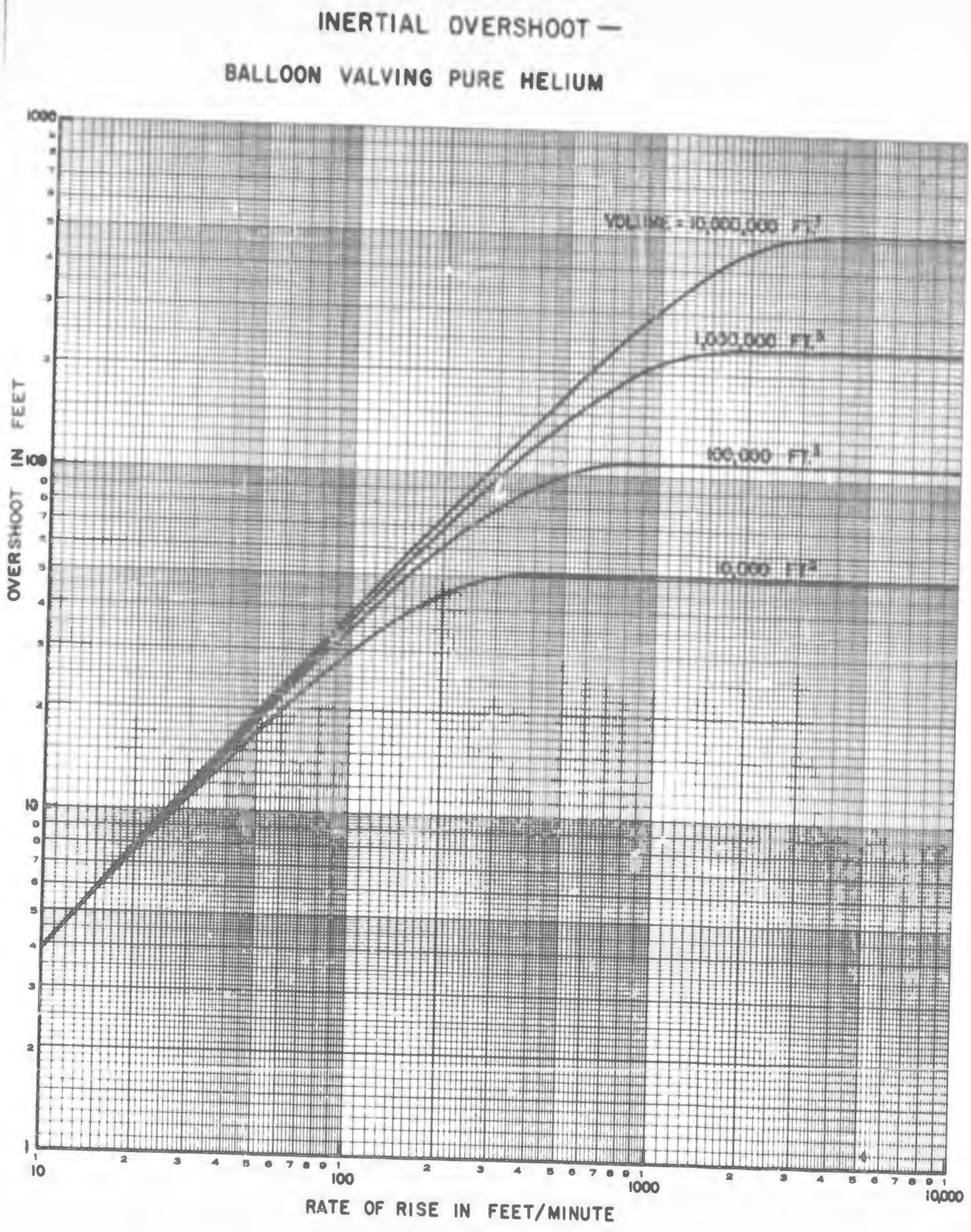
INERTIAL OVERSHOOT —
BALLOON VALVING PURE HELIUM
OVERSHOOT IN FEET
RATE OF RISE IN FEET/MINUTE
VOLUME = 10,000,000 FT.³
1,000,000 FT.³
100,000 FT.³
10,000 FT.³
1000
100
10
1
10
100
1000
10,000

Figure II-5.

Appendix I - General Expression for Inertial Overshoot

Consider a balloon rising and valving lift. There will be an upwards force on the balloon because of the free lift (net buoyancy) F, and a downward aerodynamic drag, Kv^2. In addition there will be an upward inertial force due to the deceleration of losing lift. These balance, giving

$$F = Kv^2 + \frac{G}{g}\frac{dv}{dt} \tag{12}$$

This can be made into a differential equation of motion by considering its time rate of change

$$\frac{dF}{dt} = 2K\frac{dv}{dt} + \frac{G}{g}\frac{d^2v}{dt^2} = -W\frac{v}{Z_o} \tag{13}$$

where equation (4) has been used to evaluate the rate of valving lift. If equation (13) is rearranged into the form

$$\frac{\frac{dv}{dt}\ \frac{d^2v}{dt^2}}{\frac{2Kg}{G}\frac{dv}{dt} + \frac{Wg}{GZ_o}} + v\frac{dv}{dt} = 0 \tag{14}$$

then an integration can be performed immediately, giving

$$\left[\frac{G}{2Kg}\right]^2\left[\frac{Wg}{GZ_o} + \frac{2Kg}{G}\cdot\frac{dv}{dt} - \frac{Wg}{GZ_o}\ln\left(\frac{Wg}{GZ_o} + \frac{2Kg}{G}\cdot\frac{dv}{dt}\right)\right] + \frac{v^2}{2} = \text{constant} \tag{15}$$

The constant of integration can be evaluated by noting that on reaching point (A) with velocity v_o the balloon had no deceleration ($dv/dt = 0$). This gives

$$\frac{2KZ_o}{W}\cdot\frac{dv}{dt} - \ln\left(1 + \frac{2KZ_o}{W}\cdot\frac{dv}{dt}\right) + \frac{2K^2gZ_o}{WG}\left(v^2 - v_o^2\right) = 0 \tag{16}$$

This integrated equation relates the deceleration of the balloon to the balloon's upward velocity. The maximum overshoot can now be evaluated by

noting that when the balloon is at the top of the overshoot ($v = 0$), the downward acceleration is due only to the negative buoyancy acquired by overshooting an amount Δh, that is,

$$\frac{dv}{dt} = -g\frac{\Delta h}{Z_o} \tag{17}$$

at the top of the trajectory. Evaluating equation (16) at the top of the trajectory, using (17), gives

$$\boxed{\frac{2Kg}{W}\Delta h + \ln\left(1-\frac{2Kg}{W}\Delta h\right) + \frac{2K^2gZ_o}{WG}v_o^2 = 0} \tag{18}$$

This transcendental equation relates the maximum overshoot Δh to the initial rate of rise v_o. The solution of this equation for a balloon valving pure helium in the stratosphere is given graphically in Figure II-5.

It is interesting to note that for very small values of v_o, equation (18) reduces to equation (6) given in the text, while for very large values of v_o, equation (18)reduces to equation (11), thus checking the result in the limiting cases.

Appendix II - Overshoot Due to Restricted Valving

By applying Bernoulli's principle to the valving of balloon gas, one can show that the volume rate of escape of gas is

$$\text{volume rate of escape} = A\left[\frac{2\Delta p}{\rho_{gas}}\right]^{\frac{1}{2}} \tag{19}$$

where A is the smallest cross-sectional area of the appendix, ρ_{gas} is the density of the balloon gas being valved, and Δp is the pressure difference across the appendix opening that is driving the valving.

If the balloon is rising with velocity v and valving, then the volume, V, is constant. Knowing the rate at which the atmospheric pressure, p, is decreasing, one can show that the build-up of valving pressure is given by the differential equation

$$\frac{d}{dt}\left(\frac{\Delta p}{p}\right) + \frac{A}{V}(2\sigma g Z_0)^{\frac{1}{2}}\left(\frac{\Delta p}{p}\right)^{\frac{1}{2}} = \frac{v}{Z_0} \qquad (20)$$

where Z_0 is again the 20,000-foot "e-folding" distance and σ is the ratio of air density to gas density. When the equilibrium valving pressure has been built up, the derivative term vanishes and

$$\frac{\Delta p}{p} = \left(\frac{vV}{Z_0 A}\right)^2 \frac{1}{2g\sigma Z_0} \qquad (21)$$

relating the fractional equilibrium valving pressure to the size and velocity of the balloon, and size of appendix opening.

Example 1. A skyhook flight used a tailored 3/4 million cubic foot balloon with an appendix 12 feet in diameter. At a rate of rise of 1000 feet/minute, according to equation (21), the balloon would build up a fractional valving pressure of only

$$\frac{\Delta p}{p} \approx 3 \times 10^{-6}$$

so that the balloon is really "freely valving".

Example 2. A 45-foot gore length cylinder balloon would have a volume (zero pressure) of about 8900 cubic feet. At a rate of rise of 850 ft/min, and with an appendix only one foot in diameter, one would expect a fractional superpressure of

$$\frac{\Delta p}{p} \approx 5 \times 10^{-5}$$

For a tailored balloon this valving pressure would have negligible effect on the overshoot, but this pressure (representing a pressure head of one foot) would be sufficient to cause a cylinder balloon to expand into a superpressure shape with a resulting increase in volume (in this case, $\Delta V/V \approx 1$ foot pressure head/45 foot gore length = 1/45) and the balloon would overshoot approximately

$$\frac{1}{45} \cdot 20{,}000 \approx 450 \text{ feet}$$

Roughly this behavior was observed with similar cylinder balloons on University of Minnesota Flights 60, 61, and 62. The inertial overshoot expected on these small balloons is given by Figure II-5 as 50 feet, so that for cylinder balloons the overshoot due to restricted valving can be important.

ii. Altitude at which valving occurs.

The altitude at which valving first occurs is determined by the rate of rise and by the ceiling altitude of the balloon. As the balloon approaches its ceiling altitude the gas within is cold due to the adiabatic expansion. It is convenient to consider the drag as composed of aerodynamic plus thermodynamic components. The thermodynamic drag represents the cooling of the gas due to its expansion. After the balloon has leveled at ceiling the gas will warm with a time constant of approximately fifteen minutes, thereby valving its "thermodynamic drag." Since the warming takes place slowly the orifice required for valving the thermodynamic drag could in principle be quite small.

In order that the balloon shall have a rate of rise at ceiling it must have a free lift equal to the sum of the aerodynamic and thermodynamic drags. As was pointed out, the thermodynamic part can be valved slowly. The part of the free lift which is equal to the aerodynamic drag must, however, be valved promptly. The ratio of the pressure at which valving starts to the ceiling pressure for the balloon will be equal to the ratio of the air displaced, including the aerodynamic drag, to the air displaced at ceiling. The aerodynamic drag nomograph in Section VI-C, Figure VI-7, allows estimation of the aerodynamic drag as a function of pressure, temperature, air displaced and velocity. For the purpose of calculating the valving altitude, we can approximate the equation for the aerodynamic drag by substituting the stratospheric temperature in the exact equation

$$P_A = 1.57 \times 10^{-3} \frac{p^{1/3} v^2}{T^{1/3} G^{1/3}} \qquad (1)$$

where P_A is the fraction that the aerodynamic drag is of the air displaced; p is the pressure in mb; v is the velocity in ft/sec; G is the air displaced in pounds and T is the stratosphere temperature.

One obtains

$$P_A = .268 \times 10^{-3} \frac{p^{1/3} v^2}{G^{1/3}} \qquad (2)$$

P_A also can be expressed as a function of the distance in feet below ceiling altitude at which distance valving begins

$$P_A = \frac{h}{2.1 \times 10^4} \qquad (3)$$

where h is the distance below ceiling in feet at which valving commences,

2.1×10^4 feet is the stratospheric scale height. Combining (2) and (3)

$$h = 5.62 \frac{p^{1/3} v^2}{G^{1/3}} \qquad (4)$$

Expressing v in ft/min gives

$$h = 1.56 \times 10^{-3} \frac{p^{1/3} v^2}{G^{1/3}} \qquad (4a)$$

with h in feet; p in millibars; G in pounds air displaced and v in ft/min.

The factor $\frac{G}{p}$ is proportional to the balloon volume and $\left(\frac{G}{p}\right)^{1/3}$ is proportional to the radius or diameter of the cell. For this reason equation (4a) can be rewritten, assuming a spherical shape

$$h = 3.55 \times 10^{-2} \frac{v^2}{V^{1/3}} \qquad (4b)$$

In equation (4b) v is in ft/min, V in cubic feet and h in feet.

For a 225,000-ft balloon approaching ceiling at 1000 ft/min, the above equation gives h = 580 ft. The fact that a balloon starts valving so close to its ceiling is responsible for the very sharp corner on time-altitude curves in which no air intake has occurred. The result of equation (4b) is shown in Figure II-6.

After the aerodynamic drag has been valved, the slow valving of the thermodynamic drag does not produce much change in altitude because the change in altitude only corresponds to the weight of helium which is valved. To take an example, suppose the gas warmed 15° on a flight displacing 500 pounds of air. The fractional change in pressure due to the valving of the gas as it warms would be $\frac{\Delta p}{p} = \frac{\Delta T}{T} \frac{1}{7.2}$

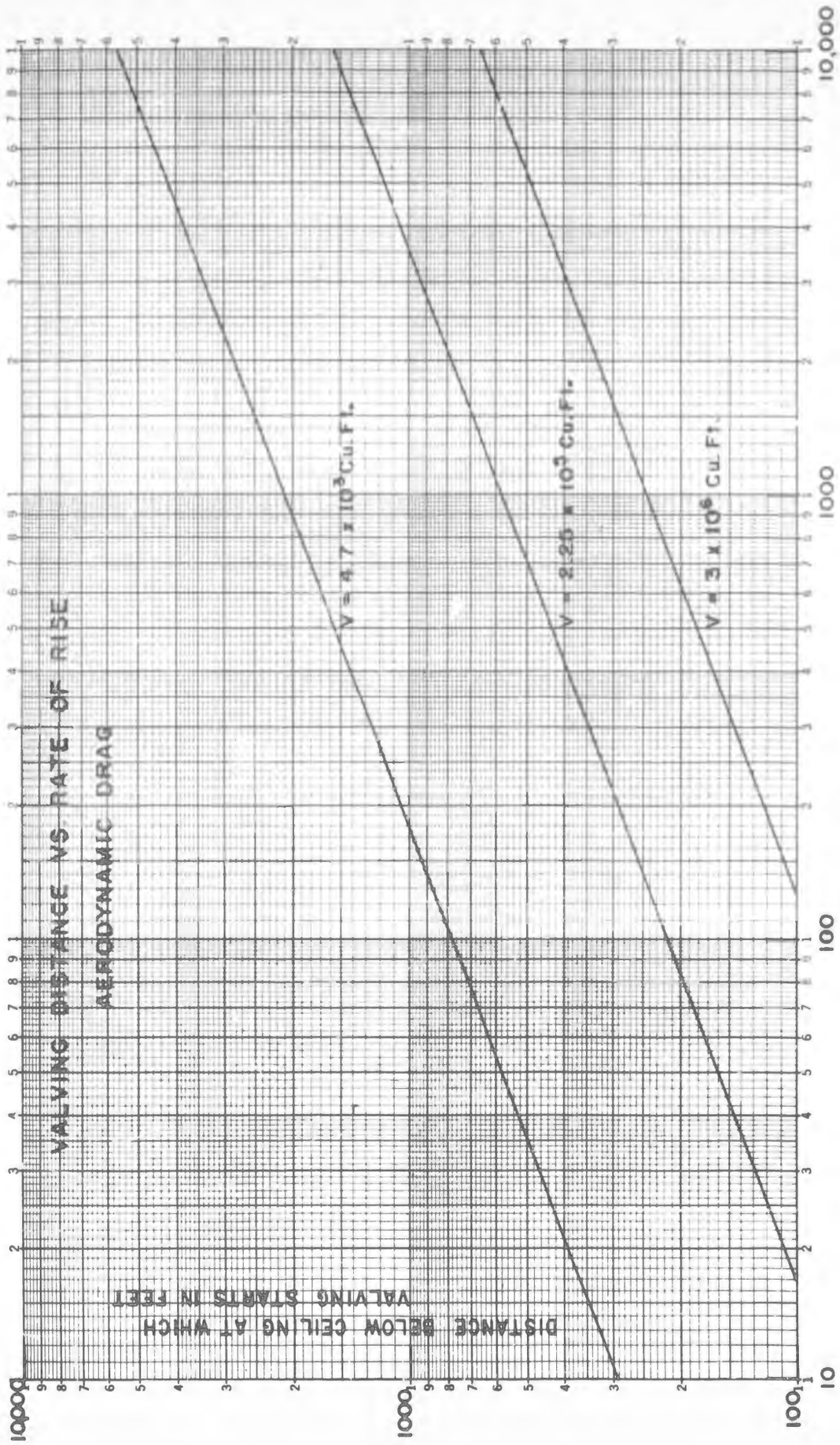
VALVING DISTANCE VS RATE OF RISE
AERODYNAMIC DRAG
V = 4.7 x 10³ Cu Ft.
V = 2.23 x 10⁴ Cu Ft.
V = 3 x 10⁶ Cu Ft.
DISTANCE BELOW CEILING AT WHICH VALVING STARTS IN FEET
RATE OF RISE Ft./Min.
10000
1000
100
10
1000
100
10,000

Figure II-6.

$$\frac{\Delta p}{p} = \frac{16}{200} \times \frac{4}{28.5} = .011 \text{ or } 1.1\%$$

The corresponding change in altitude would be .011 (2.1×10^4) = 230 ft.

If P_T is the <u>percent</u> thermodynamic drag on reaching ceiling, the change in altitude due to the warming will be

$$h = P_T \, 2.1 \times 10^2$$

iii. <u>Calculations for open appendices</u>

One can determine the valving superpressure at a given rate of rise by equating the volume flow of gas out of the appendix to the rate of change of volume of the gas in the rising balloon.

Equations (1), (2), and (3) relate the quantities determining the flow through the appendix.

$$\Delta p = \tfrac{1}{2} \rho_g \mu^2 \qquad (1)$$

$$\mu A = \frac{dV}{dt} \qquad (2)$$

$$\frac{dV}{dt} = \sqrt{\frac{2\Delta p}{\rho_g}} \; (A) \qquad (3)$$

where: Δp = valving superpressure (poundals/ft^2)

μ = flow velocity (ft/sec)

A = effective discharge average (ft^2)

V = gas volume (ft^3)

ρ_g = density of gas valved (#/ft^3)

The rate of change of volume from (3) can be compared with the rate of change of volume of a fixed quantity of gas moving up through the atmosphere.

$$\frac{dV}{dt} = \frac{V}{h_o} v \qquad (4)$$

where V = balloon volume (ft^3)

h_o = the atmospheric scale height in feet

v = the rate of rise in ft/second

Combining (3) and (4)

$$\frac{V}{h_o} v = \sqrt{\frac{2\Delta p}{\rho_g}} \; A$$

and

$$\Delta p = \frac{V^2 v^2 \rho_g}{2 h_o^2 A^2} \qquad (5)$$

Equation (5) can also be expressed in terms of air displaced. If one observes that

$$\rho_g = \frac{M}{28.5} \frac{G}{V} \qquad (6)$$

then (5) becomes

$$\Delta p = \frac{V v^2 M G}{2(28.8) h_o^2 A^2} \qquad (7)$$

with Δp in poundals/ft^2; V in ft^3; v in ft/sec; h_o in feet; A in ft^2; and G in pounds. Equation (7) can be rewritten

$$\Delta p = 3.78 \times 10^{-10} \frac{V v^2 M G}{A^2} \qquad (8)$$

where Δp is in pounds per square foot

V is in cubic feet

M is molecular weight of gas valved

G is air displaced in pounds

A is equivalent valving area in square feet

v is rate of rise in thousand feet per minute

h_o is assumed to be 20,000 feet.

In order to decide on the size hole needed for valving one may compare (8) with the structural equation

$$\Delta p_g = 24 \frac{T\,t}{D} = 24 \frac{w}{D} \tag{9}$$

where T is tensile strength in pounds/in^2,

t is the film thickness in inches ,

D is the balloon diameter in feet,

Δp_g is the bursting superpressure in pounds/ft^2.

If the balloon is to be safe, Δp must be some fraction F of the bursting pressure Δp_g, equation (9)

$$(3.78 \times 10^{-10}) \frac{V v^2 M G}{A^2} = F\,(24) \frac{T\,t}{D} \tag{10}$$

Since $V = \frac{4}{3} \pi R^3 = \frac{\pi}{6} D^3$ (11)

one can write $F = 1.34 \times 10^{-10} \frac{M G}{T t} v^2 \frac{D^4}{d^4}$ (12)

where F is the fraction that valving superpressure is of bursting superpressure,

M is molecular weight of valved gas,

G is air displaced in pounds,

T is tensile strength in pounds/in^2,

t is material thickness in inches,

v is rate of rise in thousand feet per minute,

D is balloon diameter in feet,

d is equivalent hole diameter in feet (usually assumed about .7 or actual dia.)

It should be noted that in (12) M is the molecular weight of the gas valved. If a balloon can valve air M must be taken as 28.8.

In most cases the initial valving condition may correspond to valving air. Therefore a useful solution to (12) will be with M = 28. To take a specific example, consider a Skyhook flight with M = 28.8; G = 300; T t = 1 (1-mil polyethylene); v = 700 ft/min. Solution of (12) gives $F = 5.67 \times 10^{-8} \frac{D^4}{d^4}$. The value 1 for F gives the minimum appendix size, $\frac{D}{d} = 64$. For a 73-ft diameter balloon this indicates that the appendix should have an effective diameter of at least 1.2 feet or an actual diameter of about 2.0 feet in order not to exceed the bursting superpressure.

Examination of (12) leads to several interesting conclusions. Balloons that intake a large amount of air will have a low rate of rise which tends to compensate for valving the heavy gas (i.e. v^2 decreases more than M increases). Balloons valving pure helium have high rates of rise but M is only 4. However, balloons that take in only a small amount of air have high v and high M and may burst.

Nomographs for the solution of equation (12) are included for M = 28.8 (valving air) and M = 4 (valving helium). They are Figures II-7 and II-8. The nomographs solve the equation for F = 1 and give <u>effective</u> appendix diameters. <u>In practice actual appendix diameters should be 1.5 to 2 times the values indicated</u>.

<u>Instructions for use of hole size nomographs</u>

These two nomographs give the ratio of the balloon diameter to the <u>effective</u> appendix diameter for the case of valving air and for valving helium. For open balloon bottoms, even with skirt appendices, it is known

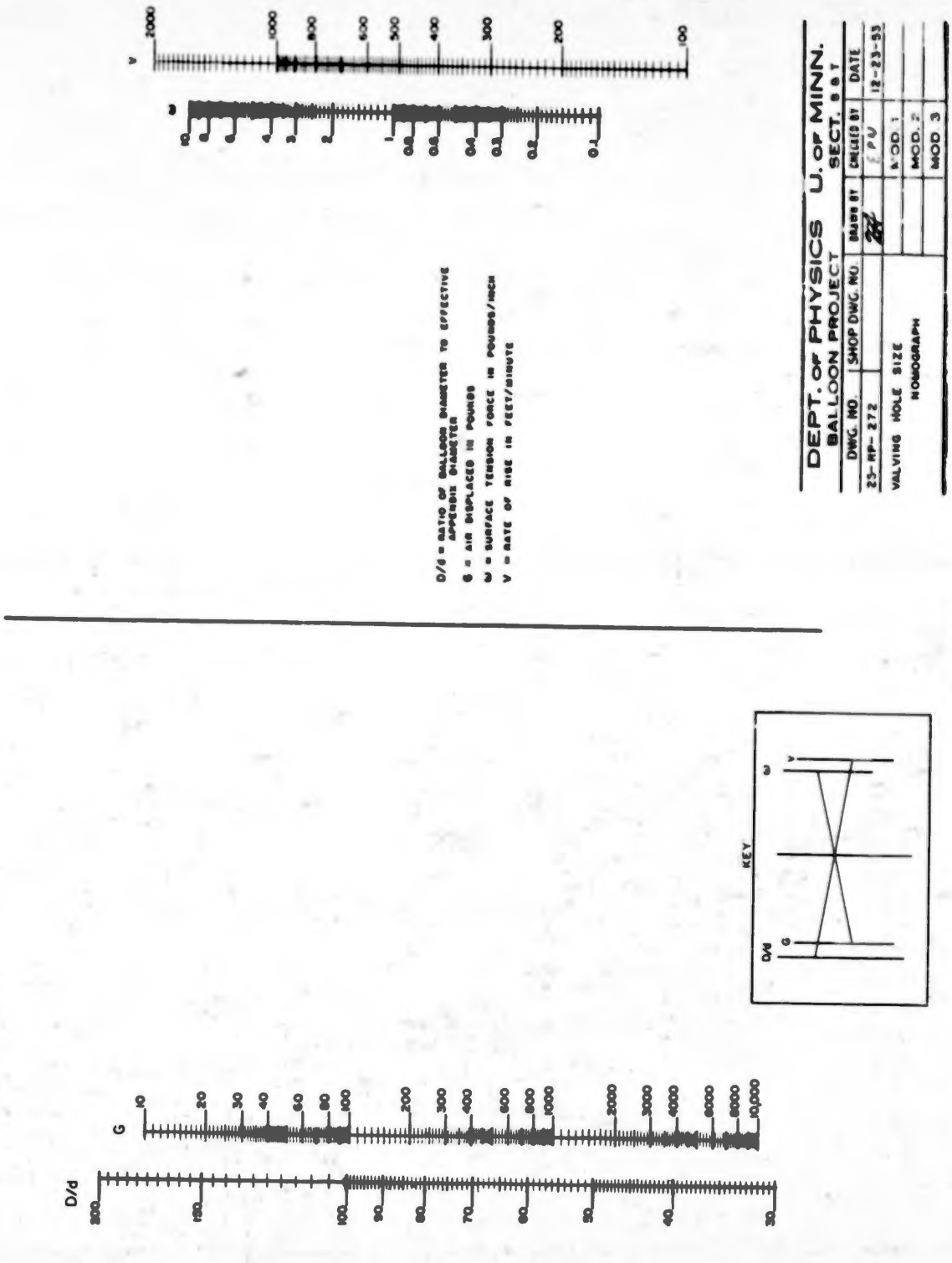
VALVING HOLE SIZE NOMOGRAPH
(FOR VALVING AIR)
V
ω
D/d = RATIO OF BALLOON DIAMETER TO EFFECTIVE APPENDIX DIAMETER
G = AIR DISPLACED IN POUNDS
ω = SURFACE TENSION FORCE IN POUNDS/INCH
V = RATE OF RISE IN FEET/MINUTE
DEPT. OF PHYSICS U. OF MINN.
BALLOON PROJECT
SECT. 861
DWG. NO. 23-MP-272
SHOP DWG. NO.
DRAWN BY
CHECKED BY EPV
DATE 12-23-53
VALVING HOLE SIZE NOMOGRAPH
MOD. 1
MOD. 2
MOD. 3
KEY
G
D/d

Figure II-7.

VALVING HOLE SIZE NOMOGRAPH
(FOR VALVING HELIUM)

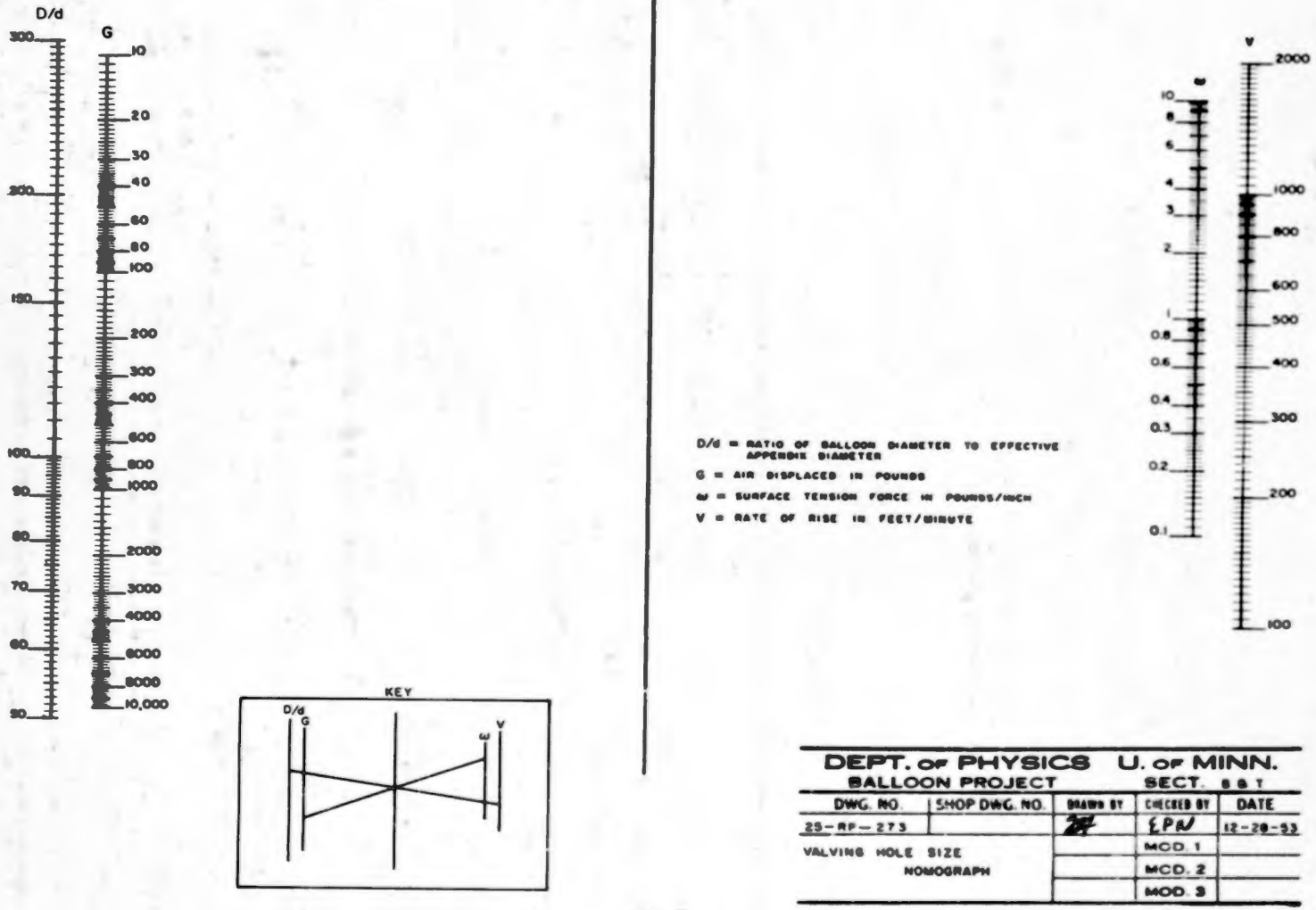

DEPT. of PHYSICS U. of MINN. BALLOON PROJECT			SECT. S & T	
DWG. NO.	SHOP DWG. NO.	DRAWN BY	CHECKED BY	DATE
25-RP-273		[illegible]	EPA	12-20-53
VALVING HOLE SIZE NOMOGRAPH			MOD. 1	
			MOD. 2	
			MOD. 3	

Figure II-8.

that air is taken in so it is believed that the air valving nomographs should be used to determine the effective hole diameter in these cases. In case of a duct appendix, since the gas is taken from the top of the balloon, one can safely use the nomograph for valving helium. In these nomographs the diameter given for the appendix is the effective diameter, which should be increased by at least 50% to obtain the actual appendix diameter. The rate of rise in a nomograph is given in feet/minute. The gross load is expressed in pounds. ω is the product of the required tensile strength of the material in pounds/in^2 by the thickness of the material expressed in inches. It therefore has the dimensions of pounds/in and is commonly referred to as the surface tension force. Typical values for the bursting surface tension force are 1 lb/in for 1-mil polyethylene which has a tensile strength of 1000 lbs/in^2 and a thickness of 1/1000 of an inch, up to a value of approximately 10 for 1-mil Mylar which has a tensile strength of 10,000 lbs/in^2. The nomographs give solutions for the ratio of balloon diameter to the effective diameter of the appendix.

C. Flight Experiences with Cylinder Balloons

The cylinder balloon was introduced at the time of the balloon meeting at the University of Minnesota held at the end of the first year of the high altitude balloon project. At the time of this balloon meeting a number of people attending were able to see some of the balloon shapes obtained by setting the zero pressure level with the duct at various positions in a balloon which was shaped like a cylinder and had its ends simply tied off. A number of causes motivated the introduction of the cylinder

balloon. It was believed and is probably true that the cost of production of the cylinder should be appreciably less than the cost of production of the shaped balloon. Since the heat seals are all straight seals, cylinder balloons can be made on a long table that does not have to have a curved design. However, the principal reason that we felt the cylinder balloon should be tried was that it allows one to dispense with the so-called "load-carrying" tapes currently present in most varieties of polyethylene balloons. The experience of the balloon project with these load-carrying tapes was that they often stuck on the balloon in places where they could later pull holes, opening the balloon up and causing a failure. This difficulty was largely circumvented on our project by flying a large number of double wall balloons, in which case the sticking tapes could only pull a hole in the outer layer of the balloon.

Still more recently, we attempted to weigh off on the ground for 24 hours a tethered balloon, and this experiment was performed at a time when the outside temperature was 25 degrees below zero. The inflation had hardly proceeded when it was observed that the polyethylene was beginning to come off the tape, and when the zero pressure had reached to about the middle section of the balloon all of the polyethylene pulled off of the tapes at the bottom of the balloon, rose to the zero pressure level, and opened holes creating a failure. This experience is undoubtedly related to the frequently observed experience that night-time balloon flights fail before reaching altitude. It is very likely that in the daytime the sun keeps the tapes warm and therefore sticky, whereas at night in the absence of solar radiation, the tapes can run essentially at the temperature of

the outside air instead of 30 or 40 degrees above it. Experiments are in progress to test this hypothesis.

The cylinder balloon of course is a natural shape balloon since it has adequate material at all points to disallow any circumferential stress. It has, in fact, enough material to make it the ultimate load-carrying balloon without circumferential stress, given a material with a definite ratio of tensile strength to density. Essentially, one can think of the balloon as a long rope of polyethylene which must support the load and, aside from the small geometric factor occasioned by the fact that the cone angle is not zero, this calculation allows one to determine the maximum load that a cylinder balloon may carry. The cylinder balloon has at all points the same meridional tension and takes on a flat topped appearance peculiar to natural shape balloons. Like all natural shape balloons with circumferential slack, it can change its volume quite appreciably on the application of a small amount of superpressure and although this fact was realized by the members of our project a certain amount of flight experience was necessary before we determined to what extent this slackness in the natural shape balloon could lead to problems. A large number of cylinder balloons have been flown for various purposes, some to study slack cylinder balloon behavior, some to study the properties of Mylar as a balloon material since Mylar could be sealed with straight seals in the cylinder balloons much more readily than in the shaped balloons, and some flights were made to attempt to utilize the high tensile strength and density ratio of Mylar in obtaining a superpressure balloon. The flights which used a cylinder balloon in some way are the following: 59, 60, 61, 62, 69, 70, 71, 72, 74, 75, 76, 77, 83, 84, 85, 88, 89, 93, 95, 96, 97, 98, 99, 100.

In discussing the results of these flights they are separated into several categories. The first of these is the behavior of slack Mylar cylinders, second the behavior of superpressure Mylar cylinders. We will discuss the slack Mylar cylinders first. Figure II-9, which contains a summary of a number of significant cylinder flights (Flights 60, 61, 62, 69 and 76), shows these flights on a contracted time and altitude scale. All of these balloons were 20-ft diameter Mylar cylinders with ducts one foot in diameter. The series of flights represented by the figure shows the development of the understanding of the flight characteristics of Mylar cylinders.

Flight 60 was the first cylinder balloon flown by our Project and was the first Mylar cylinder to be flown. It was manufactured by Herb-Shelly at Farmington, Minnesota. It shows a rather typical time-altitude curve. It was launched with a normal free lift that would have been used for our polyethylene shaped balloons of this size, and accelerated from 700 ft/min near the ground to approximately 1100 ft/min as it approached its ceiling. It was observed to turn around with some hesitation on the downward part of the time-altitude curve and establish a rate of 320 ft/min which it maintained to the ground. It was evident that the behavior of this cylinder was occasioned by the fact that the size of the duct dictated, in order to valve the free lift, a certain superpressure. This superpressure, in turn, was able to increase the size of the balloon because of the fact that the volume of the natural shape balloon changes very rapidly with superpressure in contrast to the behavior of a shaped balloon. It is obvious that at 1100 ft/min the superpressure required

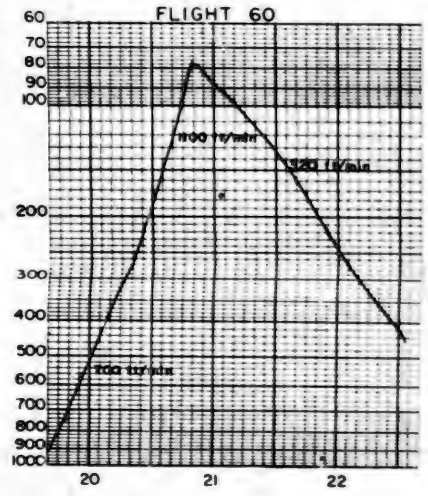

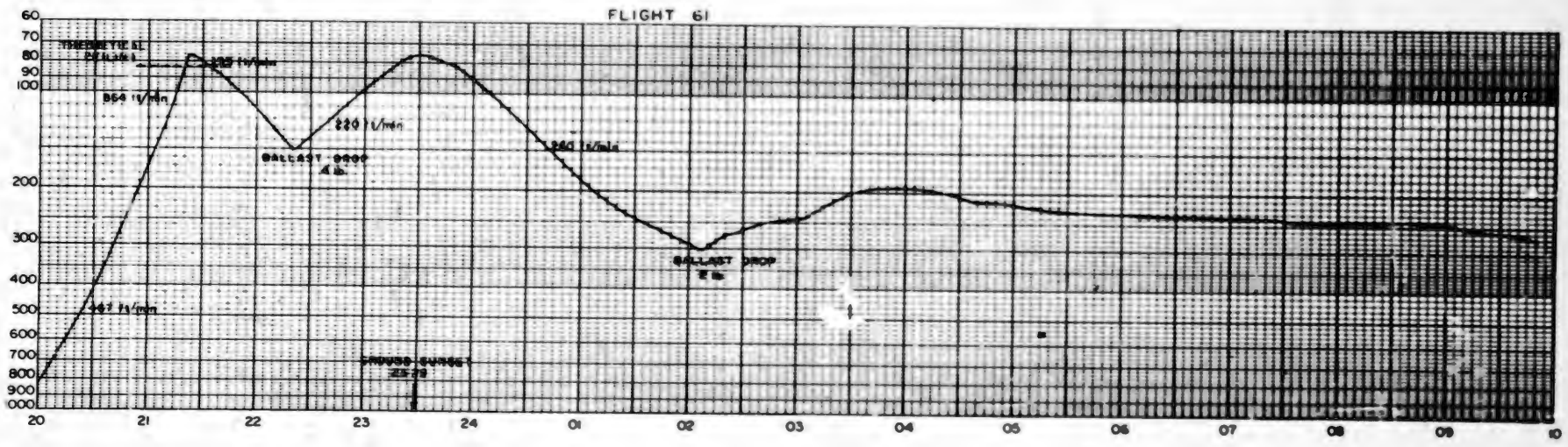

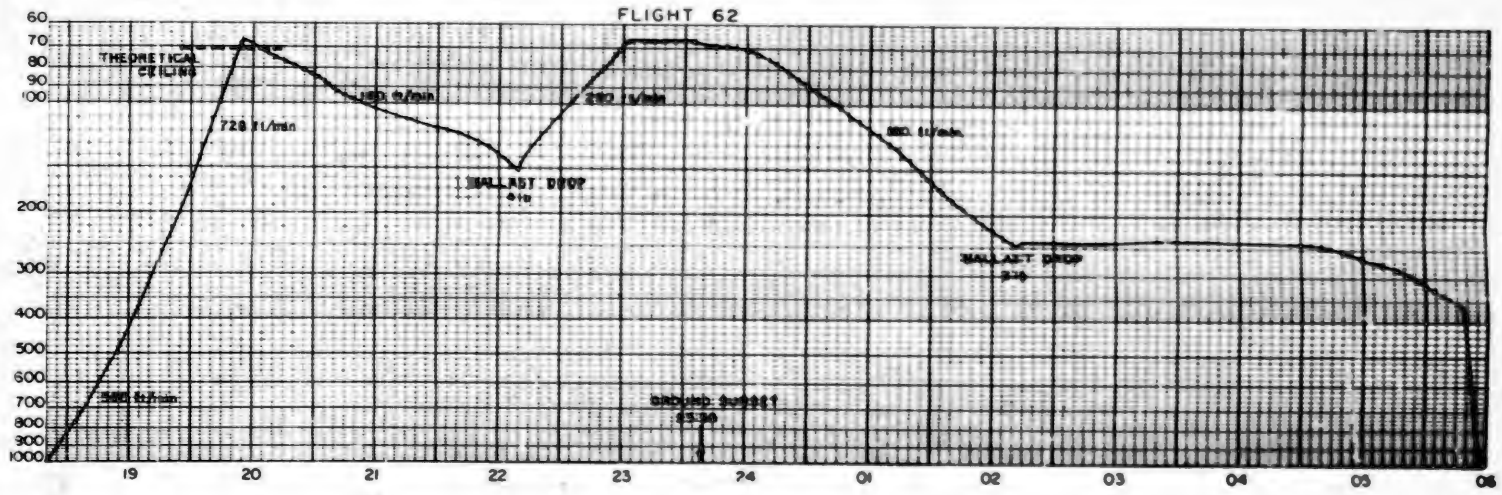

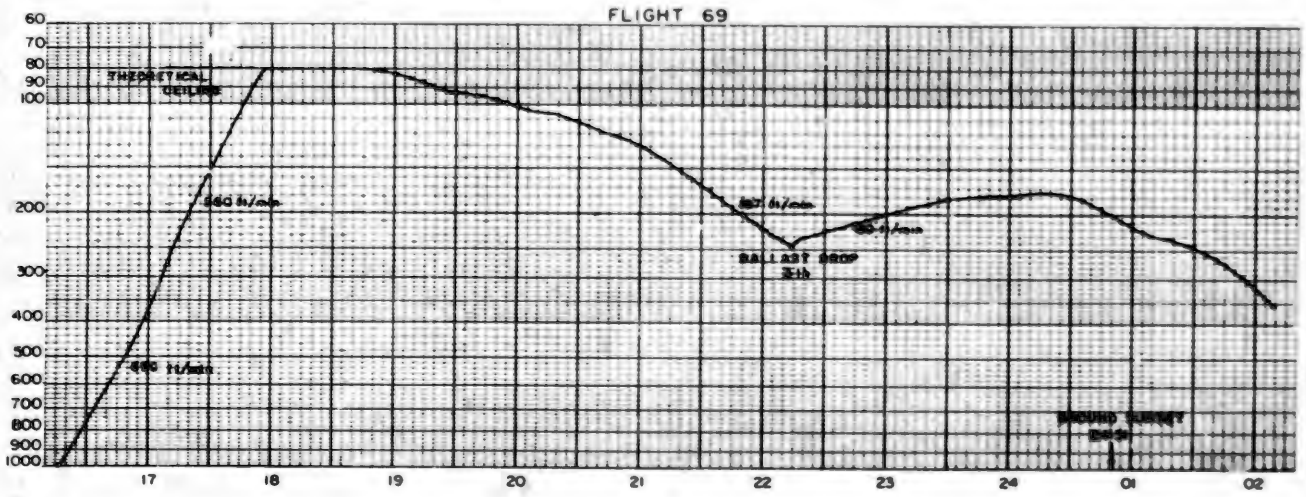

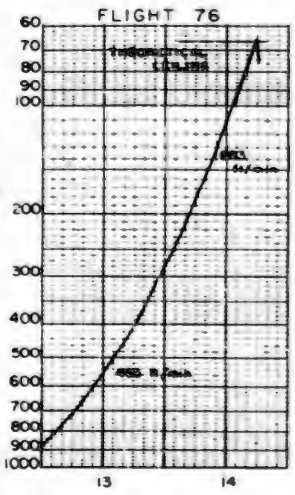

PRESSURE IN MILLIBARS

TIME IN HOURS (G M T)

Figure II-9.

to allow valving of the free lift gas was more than enough to greatly overshoot its ceiling due to the fact that its volume increased before the balloon became neutral. However, at this time the balloon begins to shrink because the superpressure disappears, and finds itself in an unstable situation from which it cannot recover unless the gas inside it can warm sufficiently to restore equilibrium. It is certainly true that there will be some rate of rise at which the overshoot occurring will be compensated for by the warming of the gas after the balloon overshoots. This warming can take place very rapidly because after the overshoot the balloon begins to descend, compress its gas, and thereby cause it to warm and become more buoyant. There is in Flight 60 some indication on the time-altitude curve of the slowing down of the downward descent rate occasioned by this warming of the inside gas. The phenomenon of overshooting, as was pointed out earlier in this report, is not limited to natural shape balloons but must occur in the case of all balloons. The fact that the balloons normally float level for approximately an hour at least after reaching ceiling is because of the warming of the gas, which can compensate for the overvalving of a balloon upon reaching ceiling.

In order to study this phenomenon in more detail, Flight 61 was prepared and it was decided we would drop the ballast to create a slower descent rate after the balloon had undergone some initial overshoot. We also carefully measured the gore length in order to determine the exact theoretical ceiling of the balloon, to be certain that the peculiar behavior was occasioned by overshooting of the original theoretical ceiling. Flight 61 did show that the balloon overshot the theoretical ceiling, in this case approaching ceiling at 864 ft/min. It descended at approximately

199 ft/min, somewhat less than Flight 60 because of the slower initial approach to ceiling. The ballast drop of 4 lbs produced a 220 ft/min rise rate. The balloon reached theoretical ceiling for the new gross load and leveled very briefly before sunset came upon it, producing a downward rate of 260 ft/min. The air displaced on Flight 61, as in all of the series of slack Mylar cylinders, was approximately 60 lbs. After descending to an altitude of 300 mb, the second ballast drop of 2 lbs more than compensated for the downward rate, and finally produced leveling of the balloon after three more hours. We felt that 2 lbs was probably a good estimate of the sunset ballast but it was not clear in this case since the sun set on the balloon just about at the time it reached ceiling. The timing was indeed somewhat unfortunate in this flight. One could not even be certain that the rate of 220 ft/min was low enough to keep the balloon from overshooting, since in principle one could argue that the sun had set on it just at the instant the balloon needed to valve and thereby leveled it without the need for overshooting.

It was therefore necessary to make another flight of the type of Flight 61 which is shown, on the same figure, as Flight 62. The initial approach to ceiling was in this case 720 ft/min, followed by 160 ft/min rate of descent, somewhat less than either 61 or 60 because of the smaller initial rate of approach to ceiling. The 4-lb ballast drop produced a rate of rise of 290 ft/min, after which the balloon leveled at theoretical ceiling, demonstrating that with this duct diameter-to-balloon diameter ratio a rate as high as 300 ft/min could be recovered from, whereas a rate as high as 728 ft/min occasioned overshooting of greater magnitude than could be compensated for by the warming of the gas. Sunset had occurred

on this flight after approximately 30 more minutes and the balloon descended at a rate of 180 ft/min. The ballast drop of 2 lbs or 3.3% exactly compensated for sunset and the balloon floated level for a period of two hours. After this time it found itself in the upper peninsula of Michigan passing between the two lakes, and at approximately 0430 it began descending at a slow rate and reached cutdown altitude at 0545. It is believed that this descent at the end of the flight was occasioned by the loss of infrared radiation as the balloon passed into the region which was more covered with water than land.

The fourth flight of this series was Flight 69 which was included here to show that a cylinder balloon can be launched and reach ceiling without overshooting. It is interesting to note that in all the previous flights, 60, 61 and 62, and in a subsequent flight, 76, the time-altitude curve showed the characteristic increase in rate of rise as the balloon rose to higher and higher altitudes. This was not true of Flight 69. The initial rate of rise in Flight 69 is higher than in 62 or 76. However, 69 shows a break at the tropopause and a decrease in rate in the stratosphere over the troposphere. Examination of the temperature soundings and weather situations for the days that these flights were made shows that the reason for a decrease in rate in Flight 69 was a decrease in infrared at high altitude caused by high cirrus clouds coupled with a stratosphere that was warmer than in the case of the other flights. Because of this, it was not possible for the balloon to warm continuously and thereby to show the acceleration. This is of course in line with the thinking about the rate of rise of a balloon being determined principally by the temperature field in which the balloon finds itself--that is, the free lift which

it has at rest at all altitudes in the atmosphere together with the combination of thermodynamic and aerodynamic drag which the balloon has in motion. Flight 69 is also interesting because of the fact that it shows a "Howell" effect, descending after approximately an hour of level flight. It now seems quite clear that the "Howell" effect, which was not understood for a long time, is undoubtedly occasioned by some change in the buoyancy of the balloon, sometimes produced by a change in infrared radiation. Updraft or downdraft at low altitudes will cause the balloon to descend and continue to descend after the period in which the balloon warms up to its final equilibrium temperature. The step flights have shown the fact that, in the daytime as the balloon descends to lower and lower altitudes, it finds itself heavier and heavier so that a balloon that begins to descend is in an unstable situation in the daytime. There appear to be certain portions of the atmosphere at night in which this is not true, and certain portions of the atmosphere show the opposite effect, namely that a balloon could descend gaining back free lift and reaching equilibrium because of the warming with altitude characteristic of that altitude and the particular time of day. In Flight 69 the three-pound ballast drop occurring at 250 mb was more than adequate to compensate for the loss of lift the balloon suffered after reaching ceiling. It rose at 80 ft/min until ground sunset produced a downward rate of approximately 187 ft/min, indicating here again that the sunset ballast demand was approximately 3 lbs. It should be pointed out that in Flight 62 the 2-lb ballast drop produced a thermodynamic bounce of the kind observed with large ducted balloons, only not as pronounced because of the fact that small balloons have a somewhat larger fraction of aerodynamic drag than do the large balloons.

It should be pointed out that cylinder balloons can be flown very successfully provided one realizes their limitations. In the series of flights described here, the ratio of balloon diameter to duct diameter was 20 to 1. With this balloon-to-duct diameter, the balloons overshot ceiling by more than they could recover due to warming at an upward rate of 800 ft/min. They could, however, approach ceiling at 400 ft/min and become stable. Since the valving superpressure goes as the fourth power of the ratio of balloon diameter to duct diameter, slightly increasing the size of the duct will have a pronounced effect on the rate at which a balloon can approach ceiling and become stable. We have learned that General Mills has flown a number of cylinder balloons with a diameter of 45 ft and a 2.85-ft diameter duct, giving it a balloon-to-duct diameter ratio of 16. With these balloons they have been able to approach ceiling at 800 ft/min and have the balloon become stable. This experience is definitely in line with the cylinder balloon behavior that was observed here and it should always be possible, by making the duct large enough, to have the balloon reach equilibrium stably at any rate of rise. When flying cylinder balloons with ballasting systems, one should be sure that the rates of rise are slow enough so that the balloon does not overshoot and does not overvalve. Cylinder balloons have also been flown successfully in other projects, principally by Howell of TUS and in some of the Air Force work.

Flight Experiences with Large Cylinder Balloons

A number of attempts were made to launch large cylinder balloons to study their behavior at ceiling as compared with the smaller Mylar

cylinders. These attempts brought out a shortcoming of the University launching method when applied to a cylinder balloon that arises because of the large amount of plastic present in this balloon. Figures II-10, II-11, and II-12 show various stages of the attempted launching of a cylinder balloon using the packed three-folding method. It can be quite clearly seen that because of the large amount of extra material on the cylinder this balloon becomes very cumbersome when three-folded. The extra material falls down to one side and when the balloon becomes airborne the gas transfer from the bottom level to the top may be impossible because of the great weight of plastic hanging down like a pigtail on one side. A modification of Winzen's method was also attempted on a cylinder balloon and this flight is shown on Figures II-13, II-14, and II-15. In this case our girdle was used as a means of attachment of a rope to the balloon, and was arranged to slide down later on in flight, as is the usual procedure. The balloon was not packed. To launch it one paid out line to cause the cylinder to become airborne downwind from the point at which the line pulley was secured. Examination of the pictures makes it clear how this method was carried out. Because of the single layer of polyethylene exposed to the wind, the upper bubble does get quite severely blown about, and Figure II-16 shows a failure at the top of the balloon which was created during this launching attempt. The balloon was repaired and launched, however, and rose to an altitude of 5,000 feet, floating there for several hours before descending. Although there may have been a small leak in the balloon, it is likely that this behavior was occasioned by too little free lift, probably produced because of the difficulty of weighing off in this system in the wind. Our experience

Figure II-10. Inflation of packed cylinder balloon in the horizontal position.

Figure II-11. The weight of the canopy shifting off center pulls the top of the bubble down.
Confidential Information

Figure II-12. The balloon is launched in this configuration. The canopy being heavier than the gondola lowered the top of the bubble so the gas did not transfer properly.

Confidential Information

Figure II-13. Letting the balloon up on the line.

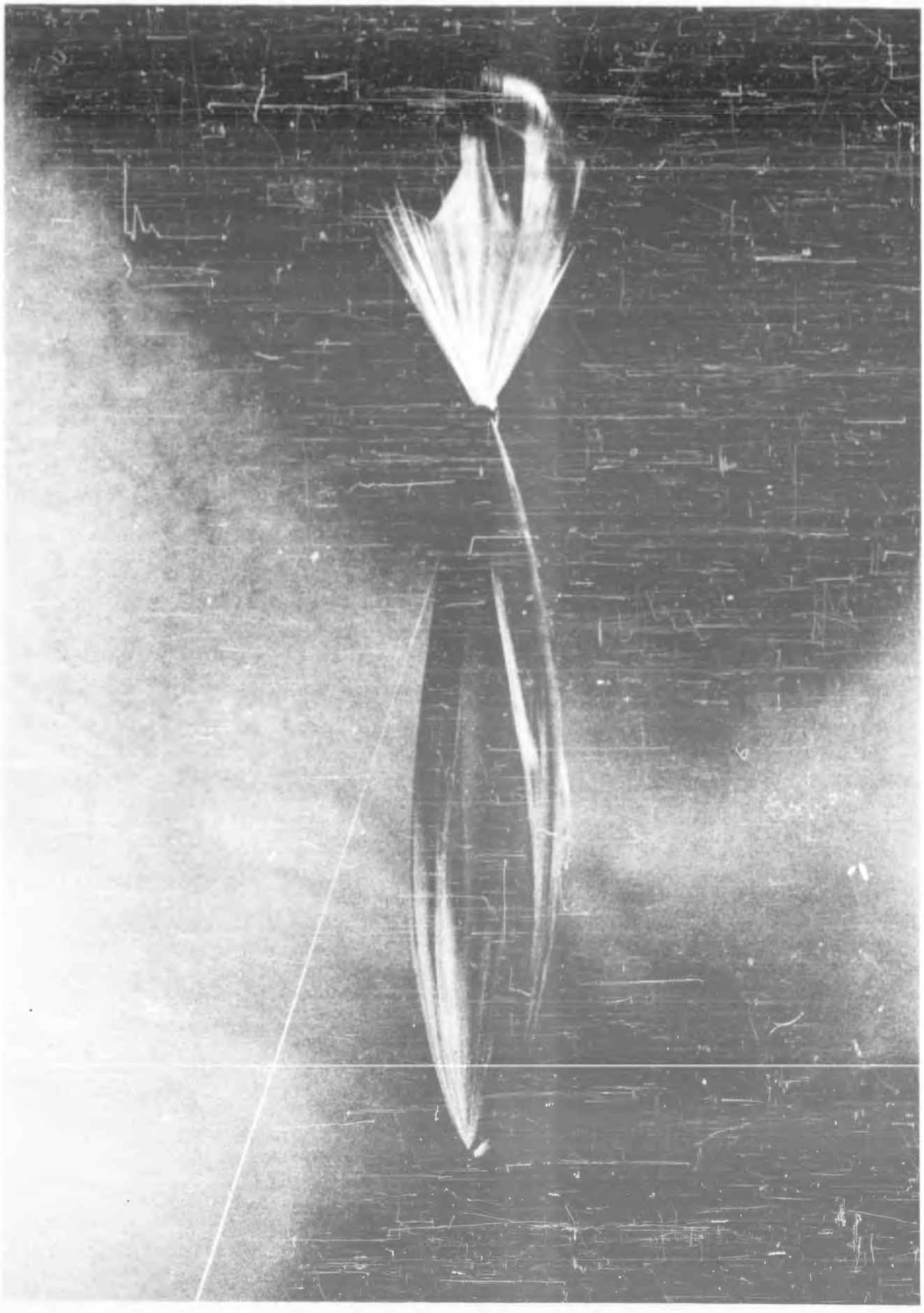

Figure II-14. Wind billowing the lower two-thirds of the balloon.

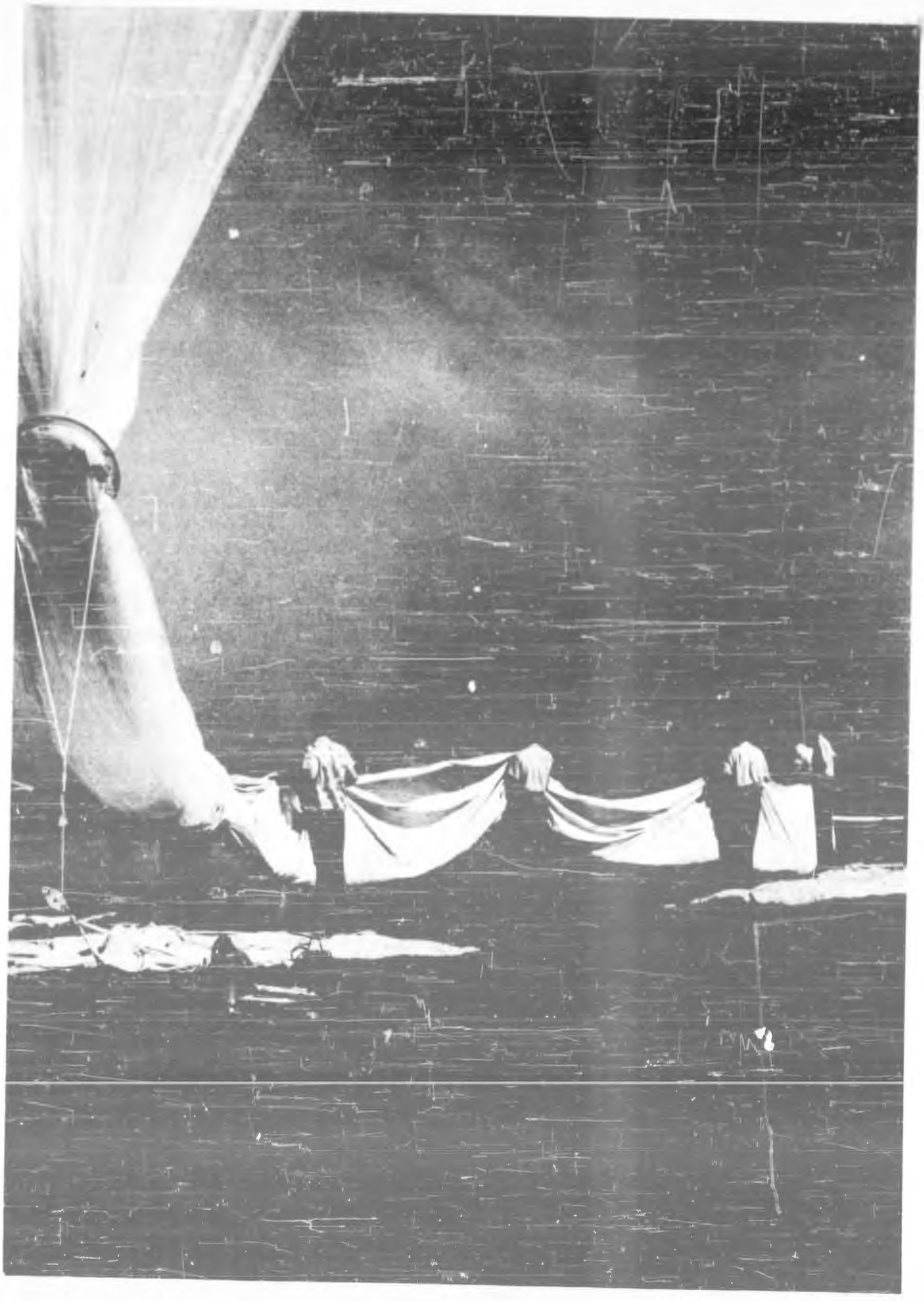

Figure II-15. Lowering the balloon after an observed loss of lift.

Confidential Information

Figure II-16. Balloon damage from wind buffetting.

with this method led us to believe that it was not an adequate solution to the launching problem for large cylinders and in fact indicated that it is not a very satisfactory launching system to pursue. There is actually no fundamental problem in launching the cylinder balloon from a platform and a number of cylinders have been launched from platforms by General Mills. Our attempts to launch these by the methods indicated here were occasioned because of our desire to be sure of the balloon's free lift. However, because of the difficulty of launching a cylinder balloon by any other method than the platform launch, it was decided to carry out these experiments in the future with the platform and to accept the uncertainty in the initial free lift.

D. Optimum Dimensions and Pressure of Cylinder-Type Balloons

Introduction

This study is concerned primarily with a balloon designed as a cylinder of uniform material around a vertical axis, the top and bottom edges being gathered into separate concentration points which will be termed the zenith and nadir, respectively. Further limitations will be assumptions that the circumferential stress is zero throughout and that the fabric weight is small enough to permit neglecting it in a first approximation of the meridian stress. The fabric is assumed perfectly flexible but substantially inextensible in all directions.

With these assumptions, it should be clear that the major results will be applicable far more broadly than to an actual cylinder balloon, since, within the limitations imposed, the only essential effect of the cylinder construction is to provide the same total section of material

around any circumference, cut normal to the surface. Due to the neglect of fabric weight, a further effect of this constant section is to make the meridian stress the same at all points. Thus the same general results, with secondary differences to be noted, can be had with: (1) a uniform cylinder with or without meridian tapes; (2) a multiplicity of meridian tapes inter-connected by a shaped gas holding film of negligible weight and stress compared to the tapes; and (3) a circumferentially uniform stress-carrying material whose thickness varies inversely as the radius of the designed shape.

Any of these types willautomatically produce a "natural" shape under the assumed flight conditions for which the design is set up. The actual balloon weight, however, may vary greatly depending on the pressure or gas head employed, on whether the envelope stress is a primary parameter or an incidental result,and on how the suspended load is carried (e.g. whether all at the bottom or part of it transmitted to the top). The primary purpose of this study is to determine the relative variation of balloon weight with gas head or pressure, while giving incidental attention to other effects.

Except as otherwise stated, the analysis will proceed on the assumption of an actual cylinder as designed,with dimensions and parameters pertaining thereto and with a required altitude and load to be carried. For the usual bottom suspension of the latter, a locally conical-bottom and flat-top natural shape is produced in flight.

Symbols (Figure II-17)

S - total length of cylinder, or meridian length of shaped balloon from nadir to zenith.

R - radius of cylinder, or maximum horizontal coordinate of shaped balloon.

A - axial length in flight, or straight-line distance from nadir to zenith.

θ - profile angle, referred to horizontal.

δ - unit lift of gas or gross lift/vol = $g(\rho_a - \rho_g)$.

w - unit weight of cylinder surface.

T - meridian tension per unit of cylinder circumference.

ℓ - T/w = critical length of material.

vol - enclosed volume, assumed all gas of uniform δ.

surf - surface area of cylinder (also of a sphere).

L - gross lift = δ vol.

W_b - total weight of envelope cylinder.

W_n - net suspended weight.

h - height of gas zero-pressure level below nadir.

Other subscripts: ℓ - lower (at nadir); u - upper (at zenith).

Optimum Dimensions and Basic Conditions

From reference 1① it will be apparent, for the weightless envelope and other assumptions, that: (a) The profile shape is fully determined by a given ratio of the gas head h to any other characteristic dimension such as the meridian or cylinder length S, and is independent of altitude,

① "Balloon Shape or Stress Analysis and Design of Thin, Axially Symmetric Fluid Containers", GeneralMills, Inc. Report, 30 September 1952.

unit lift, etc. (b) For any given value of h/S, the optimum dimensions of the cylinder are established by the ratio of R to S which makes R just equal to the equator coordinate X_e of the resulting natural shape. See second and third columns of Table II.

The optimum value of h/S will be here understood as that which involves minimum envelope weight for a given volume and lift, referred to two different major conditions:

I. A balloon employing a minimum or given unit weight of material, uniform for the assumed cylinder.

II. A balloon in which the envelope material is uniformly stressed to a maximum permissible value.

These conditions, each with optimum dimensions, will now be successively analyzed with the help of the results from the analog computer,② first for the condition $W_{nu} = 0$ and $\theta_u = 0$.

Case I: Given Material Weight

For any given unit lift, the gross lift will of course be determined by the volume; and for different values of h/S, a given volume will be enclosed by cylinders of varying dimensions of which the total surface will be $2\pi RS$. The relative envelope weight will therefore be given by the non-dimensional ratio:

$$\frac{(4\pi/3)^{2/3}\ \text{surf}}{4\pi\ \text{vol}^{2/3}} = \frac{(4\pi/3)^{2/3} RS}{2\ \text{vol}^{2/3}} = 1.30\ \frac{RS}{\text{vol}^{2/3}} \qquad (1)$$

adjusted to give unity for a shaped sphere.

---

② University of Minnesota High Altitude Balloon Project Report, Vol. V, pp. III-A-10 - III-C-40.

TABLE II

h	R/S	A/S	$Vol^{1/3}/S$	$Vol^{2/3}/S$	$1.3\frac{RS}{Vol^{2/3}}$	$S/Vol^{1/3}$	$\sin\theta_\ell$	$\frac{S/Vol^{1/3}}{\sin\theta_\ell}$	$\frac{Vol^{1/3}}{2\pi R \sin\theta_\ell}$
-0.3	.277	.748	.084	.192	1.88	2.28	.926	2.47	0.272
-.2	.300	.710	.103	.220	1.78	2.13	.833	2.56	.300
-.1	.317	.680	.116	.237	1.74	2.05	.725	2.83	.338
0	.328	.649	.125	.250	1.71	2.00	.637	3.14	.380
.2	.343	.608	.136	.265	1.69	1.95	.500	3.89	.475
.5	.358	.570	.145	.276	1.69	1.90	.365	5.22	.643
.7	.365	.550	.148	.280	1.70	1.89	.305	6.20	.757
1.0	.372	.535	.150	.282	1.72	1.88	.238	7.90	.955
∞	.383	.467	.152	.285	1.75	1.87	0	∞	∞

Data for zero and finite values of h/S are taken from Reference (2), with the zero value checked from Reference (1). The case of h/S = ∞ is from the mathematical theory of the elastica as brought out in Reference (1). Results for the bottom suspension are tabulated in Table II and plotted in Figure II-17. The relative meridian tension for this type is given by:

$$\frac{T}{\delta\, vol^{2/3}} = \frac{T}{L}\, vol^{1/3} = \frac{vol^{1/3}}{2\pi R \sin\theta_\ell} \qquad (2)$$

in the last column of Table II.

For given values of δ, w, and h/S, Case 1 will extend from a lower limit of size where $W_b = L$ to an upper limit where the allowable envelope stress is reached and where W_b/L is least. Within these limits the envelope weight varies as the two-thirds power of the volume.

Case II: Given Material Stress

For any given tension T per unit of circumference, the net load:

$$W_{n\ell} = 2\pi RT \sin\theta_\ell$$

and $$W_{nu} = 2\pi RT \sin\theta_u \qquad (3)$$

or for $\theta_u = 0$:

$$W_{n\ell} = W_n \approx L = \delta\, vol = 2\pi RT \sin\theta_\ell \qquad (4)$$

As $W_b = 2\pi w RS$, (5)

$$\frac{W_b}{L} = \frac{S}{\ell \sin\theta_\ell} \qquad (6)$$

Where $\ell = T/w$ = stress/density of the material.

As before, a non-dimensional criterion of envelope weight, good for any volume, lift, or material, can be expressed as:

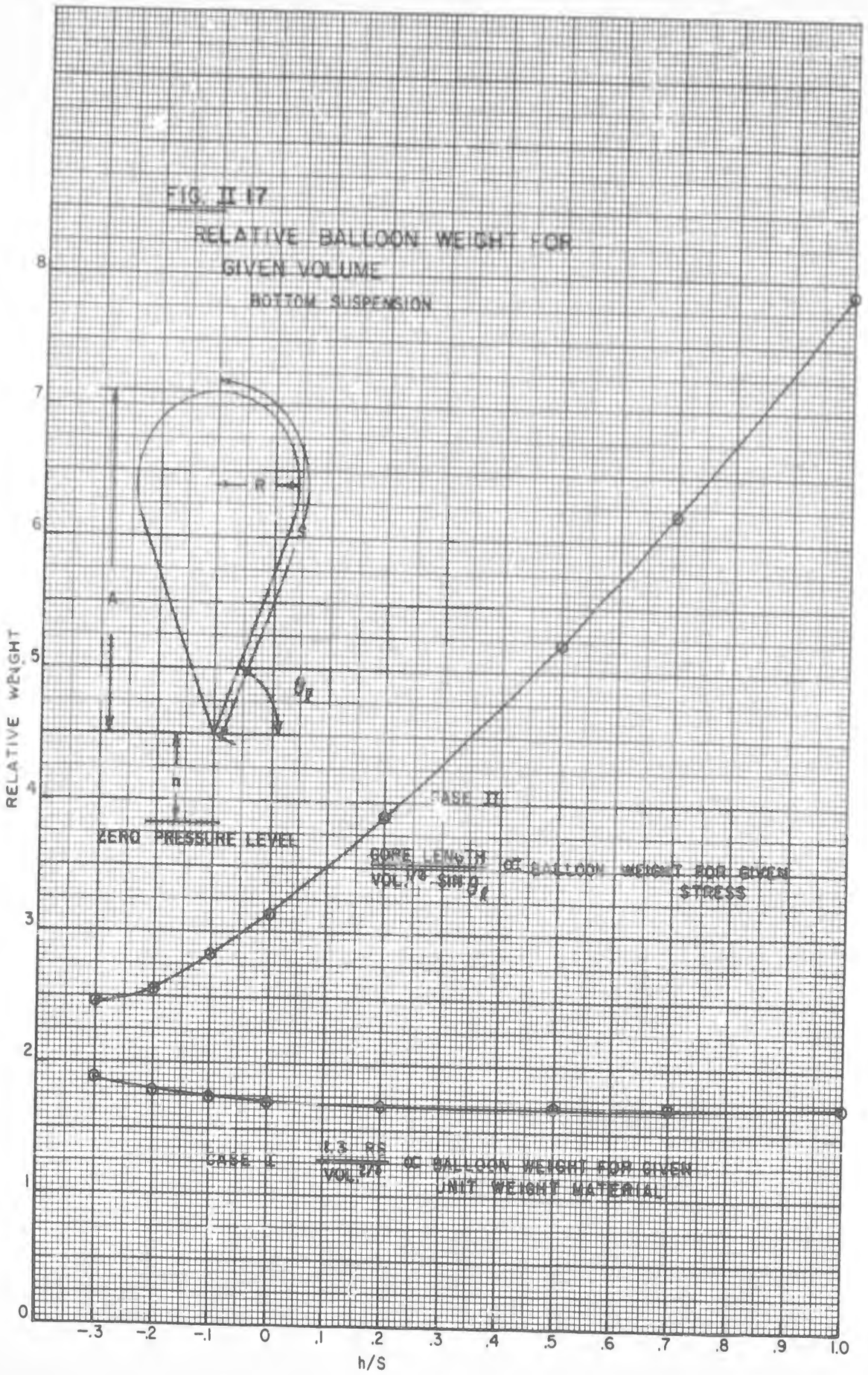

Confidential Information

$$\frac{\ell W_b}{vol^{1/3} L} = \frac{S}{vol^{1/3} \sin \theta_\ell} \qquad (7)$$

also tabulated in Table II and plotted in Figure II-17.

For given values of ℓ and h/S, Case II will extend from a lower limit of size, where the material thickness is a minimum and where W_b/L is least, to an upper limit where $W_b = L$. Within these limits the envelope weight varies as the four-thirds power of the volume.

Effect of Internal Suspension

The type of envelope here investigated is the heart-shape profile, Figure II-18, produced by carrying half of the net load through an axial tension member to the zenith; other assumptions the same as before. This type has hitherto been investigated on the analog computer in a preliminary way, not in the same series as the others, and at only one pressure: h = 0. Hence the results are only roughly comparative, being subject to check and to an extension to other pressures and perhaps to other divisions of load. The following dimensional characteristics are estimated from a shape in Reference 3③ which came close to meeting the above specifications.

$$\sin \theta_u = \sin \theta_\ell = 0.47$$

$$A/S = 0.45 \quad ; \quad R/S = 0.36$$

$$vol/S^3 = 0.133 \quad ; \quad S/vol^{1/3} = 1.96$$

For a given material, the index of balloon weight is then

$$\frac{1.30\ RS}{vol^{2/3}} = \frac{1.30 \times .36}{.260} = 1.80$$

Due to the equal division of load, the tension is half that given by equation (2) or:

---

③ Ibid, Vol. I & II, pp. 3-1 - 3-21.

INTERNAL SUSPENSION; EQUAL LOADS, TOP & BOTTOM

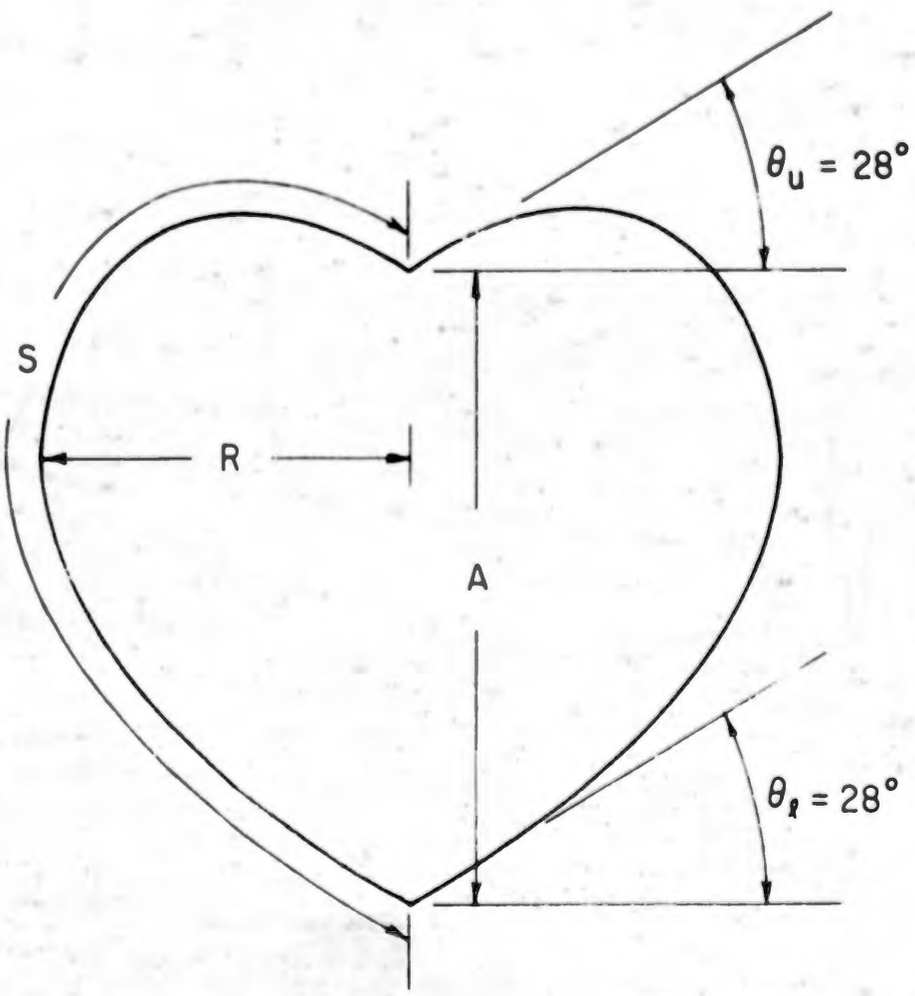

Figure II-18.

$$\frac{T}{L}\,vol^{1/3} = \frac{0.5}{2\pi \times .36 \times 1.96 \times .47} = 0.240$$

For a given stress, the relative envelope weight is again half that given by equation (7), or:

$$\frac{\ell W_b}{vol^{1/3}} = \frac{0.5 \times 1.96}{.47} = 2.08$$

The above figures neglect the weight of the axial member itself. If this member is the same material and carries the same stress as the envelope, the latter figure for a given stress must be corrected to a final index of structural weight:

2.08 (1 + .45 x .47) = 2.52 for the zero pressure condition

Comparison with the bottom-only suspension should be still more favorable at lower pressures.

Secondary Effects

With negligible envelope weight, the total net load $W_n = L$, as hitherto assumed; but finite envelope weight, of course, reduces this value by the increment W_b. The tension at any point y above the bottom is then:

$$T = \frac{W_b \ell}{4\pi R \sin\theta} + wy \qquad (8)$$

The tensile stress can be kept uniform if desired by varying either R or the thickness in proportion to T. The effect of including these factors in the computation of relative envelope weight, should usually be small. The optimum pressure in Case I will be slightly raised.

According to the elementary expression in Reference 4(4), the relative

(4) Ibid, Vol V, pp. VI-169 - 206.

temperature increment due to radiation should be proportional to the three-quarters power of the envelope-weight criteria as here presented. As this superheat equation makes no allowance for change of shape, however, its direct application in this case is invalid. A more realistic solution appears to be a variation in superheat simply in proportion to the 3/4 power of the envelope thickness for a given volume and altitude. This gives no variation in superheat for Case I, and a value proportional to T in Case II. The latter brings the pressure for minimum superheat slightly lower (more negative) than for minimum weight. For a given stress, the internal-suspension type will have definitely less superheat than any of the balloons in Table II; and, if designed for less pressure it will have still less.

With respect to leakage through holes, the only penalty of indefinitely reduced pressure is the increased surface for a given volume, and in Case II the decreased thickness. Evaluation of the latter effect must of course depend on tests of leakage vs thickness and stress of a given material, which are for the most part yet to be made.

A beneficial effect of high pressure is to stabilize the lift and altitude, particularly against loss of superheat. A pressure corresponding to h/S = 1.0 would take care of a temperature difference in the stratosphere on the order of $3^{o}F$. Thus to satisfy the full superheat condition, with materials at present in use, would require pressures outside the range of this investigation, especially considering the increased superheat due to the increased thickness in Case II. The leakage would then also be increased to probably prohibitive magnitude.

The aerodynamic drag will be somewhat increased by increased pressure

and by internal suspension. While this increase is usually favorable, it is probably of no importance in the stratosphere, but may be of appreciable help in damping movements in the troposphere.

Analysis has thus far been on the basis of a specific or design fullness. Unlike a shaped balloon with spherical top, which develops maximum stress at less than ceiling altitude, the natural shape always is most stressed at maximum fullness. The structural design must therefore be based on the maximum possible lift and pressure, but leakage and other characteristics can be based on expected or mean effective conditions. For a given lift, the stress at less than design altitude is reduced in proportion to $1/\sin\theta_l$, approaching a minimum as $\sin\theta_l$ approaches unity. For a small percentage fullness at low altitude, the example of the internal suspension type therefore carries less than half the full design stress, subject to special effects, not here considered, such as due to instability of the surplus fabric.

Concluding Discussion

Assuming the cylincer-type construction with all external load carried at the bottom and approximately equal to the gross lift, the first approximation of the actual envelope weight has been computed from the analog computer curves for two different cases: I. A given uniform thickness of envelope material; II. A given meridian stress with the balloon envelope adjusted to carry this stress. The diameter of the cylinder relative to its length is adjusted in each case to make the circumferential stress just zero with no slackmaterial at the equator. For Case I as shown in Figure II-17, the minimum envelope area and weight is attained with a

bottom gas head approximately 0.3 of the gore length, but the curve is very flat showing only about 4% increase in weight for a head of -0.15 of the gore length or for infinite pressure. It may be noted that this curve is plotted on a scale that makes the value unity for a perfect sphere with smooth surface and equal volume. Although the weight of the cylinder balloon is 69% more, this seeming advantage of the sphere is largely fictitious since, with a uniform surface, any concentrated load would cause infinite stress, and no spherical shape would be possible, short of infinite pressure. Case I implies that the envelope is understressed. A modification from the cylinder for Case I should preferably be sought by which the gores would be tailored to the natural shape above and below the equator as far as will keep the stress within the allowable limit. The cylinder shape can then be used for the remaining distance to the top and bottom on the principle of Case II.

When the envelope thickness is similarly kept uniform but adjusted to carry a given stress (Case II in Figure II-17), the weight variation with pressure head is much more marked. The minimum weight is now obtained with a gas head of -0.3 times the gore length. For zero head at the bottom, the weight is already up 28%; for a positive head of 0.3, it is 76% over the minimum; and for a head of 1.0, the weight is multiplied 3.2 times. An even lower pressure is recommended by the decreased leakage and superheat thus attainable, the only important exception being the possibility of a pressure-stabilized type.

For preliminary comparison, the relative envelope weight was computed for a heart-shaped profile carrying the total load equally divided between the top and bottom, again on the basis of analog computer results for

negligible envelope weight and with estimated volume coefficient. The results thus far are confined to the cylinder type or equivalent construction for the one case of zero bottom pressure. For a given envelope thickness, its surface and weight are about 5% more than for the flat-top or bottom-only suspension, but it carries 37% less stress for the full condition and about 50% less for a small initial-percentage fullness.

For equal stress in the full condition, the axial-suspension type has an envelope weight of 34% less than for the bottom-only suspension, but this saving is reduced to 20% if the weight of the axial member is included and computed for the same material as the envelope. Although these figures are on the basis of equal load division as above noted, the result is not thought to be so critically dependent on this equal division as to require a pulley type suspension. In fact, equal load division is not necessarily optimum, the true optimum being probably with slightly less than half the load on the top. The axial member will, of course, be eliminated if the top load can actually be placed on top, subject to a check of static stability.

The axial suspension or divided load will show still greater advantage at the lower pressures. If further work is done on this, it appears highly desirable on the basis of present evidence to carry further the analysis or development of this type at least to the extent of permitting optimum pressure to be estimated, and investigation of possible difficulties in actual construction and operation. Axial suspension becomes of decreasing advantage at the high pressures and would probably be of little or no value in a pressure-stabilized balloon.

The duct appendix is well suited for fixing the zero pressure level. It is thereby possible to achieve the condition in which the bottom of the balloon is under suction. This condition gave minimum envelope weight in Case II of Figure II-17.

A scientifically ideal construction for the major part of the gore length would be a material of varying thickness as noted in item (3) of the introduction, with further modification to allow for substantial fabric weight. Such variation can now be had in sheet metal, and there may be some technique to make it feasible in plastics. For example, a thickness variation in finite steps would be usable, in conjunction with appropriate tailoring of the gores, as already discussed in connection with Case I. The actual surface and leakage will then be minimized and difficulty with surplus fabric avoided. A closely equivalent construction could be had by means of tapes applied to a completely shaped envelope, provided the tapes and a suitable attaching cement without undue absorption of radiant heat can be developed.

Section III

MYLAR BALLOON DEVELOPMENT PROGRAM

A. Initial Mylar Program

The physical properties of Mylar film have made it an attractive candidate for balloon use since its introduction some three years ago. This highly transparent film could be extruded thinner than any other plastic film. In addition, it had high strength and good low temperature properties. It could be extruded with almost no leakage flaws and had very low gas permeability. The main obstacle to overcome was to find a means of fabricating a balloon of this material. If this could be done, it could be checked out on other qualities desirable in a finished balloon. The main questions remaining, which could be best answered with balloon experience, were the effects of its low tear resistance and its questioned susceptibility to ultra-violet and ozone in the atmosphere.

Previous attempts to heat seal Mylar had resulted in very weak, unreliable seams. Attempts to tape or glue the material were made, but the adhesives generally failed at stratosphere temperatures. In January 1953 the chance finding of a manufacturer who had successfully sealed samples of Mylar renewed interest in the material. By a carefully controlled process, Herb-Shelly, Inc. of Farmington, Minnesota, had obtained a reasonably strong bond with their heat sealing method.

This finding happened to follow immediately after the development of the cylinder balloon, described in the preceding report. In the cylinder design, balloon fabric is stressed primarily in the longitudinal direction. Since,the sealed panels can be placed with this orientation in a balloon,

the only stresses, being in line with the seals, need not involve the seals. In theory, no stress would occur across the seals. Actually, slight seal stresses do occur because of the irregularities of the folds under inflation and in ordinary handling of the fabric. The Mylar seal strength appeared adequate for this application, and efforts toward a Mylar cylinder balloon were begun immediately.

The first balloon manufactured was a subpressure shape corresponding to a shaped balloon with a 60° cone angle. It had a gore length of 40 ft which, in volume, corresponded to a cone-on-sphere balloon of approximately 20 or 25 ft in diameter. This balloon, which was of 1/4-mil material, was tested for its full ground inflation and successfully lifted over 500 lbs. A picture of this inflation, showing the cylinder balloon shape, was included in the last report.*

Subsequent to this test an attempt was made to fly this balloon with a gondola attached. It was launched from Pierre, South Dakota, in a 15 mph wind, and after rising about 100 ft it descended, whereupon the wind shredded some of the plastic. It was felt at the time that one factor which may have caused the descent was damage from the winds which buffeted it during launching.

This flight was followed by a series of four of the same type balloon, all of which were very successful. Not only did they prove Mylar to be an acceptable balloon material, but from these flights the first performance characteristics of the cylinder type balloon were also obtained. These results are discussed under the individual flight reports. It was determined

---

* Volume V, p. III-C-37.

from these flights that the sunset effect on the quarter-mil Mylar cylinder balloon was approximately two percent.

In general, the program planned consisted of subpressure, zero pressure level, and superpressure cylinders. One large Mylar balloon, Skyhook size, was also planned.

Next in order was the construction of a balloon of the same gore length with the zero pressure level at the base of the balloon. This additional pressure increased the volume from that of the subpressure balloon, and resulted in a fatter natural shape. More material was provided to accommodate the increase in circumference so that the stress in this direction would not be introduced. While the first of these was being inflated for a static test indoors, one of the seals gave way. Since the only stress across the seals is slight, due to asymmetrical filling, it appeared there must have been a local weak spot in a seal. Qualitative pull tests of seals in this balloon indicated that the strength of the seals was not too consistent. Some method of assuring that the seals were up to some minimum strength was needed.

The method devised to test each seal in the balloon during manufacture consisted of forming a test tube of the material on the backside of the seal in the balloon. This was done by running another seal three inches from the first. The long tube thus formed between the seals was held shut at one end. The other end was inflated with air. Internal pressure in the tube was measured and regulated to apply a predetermined stress across the seal. (See Figure III-1.) If the seal withstood the stress from this pressure it was left in the balloon. If it failed, another set of seals was made and tested. On the 1/4-mil balloons, the

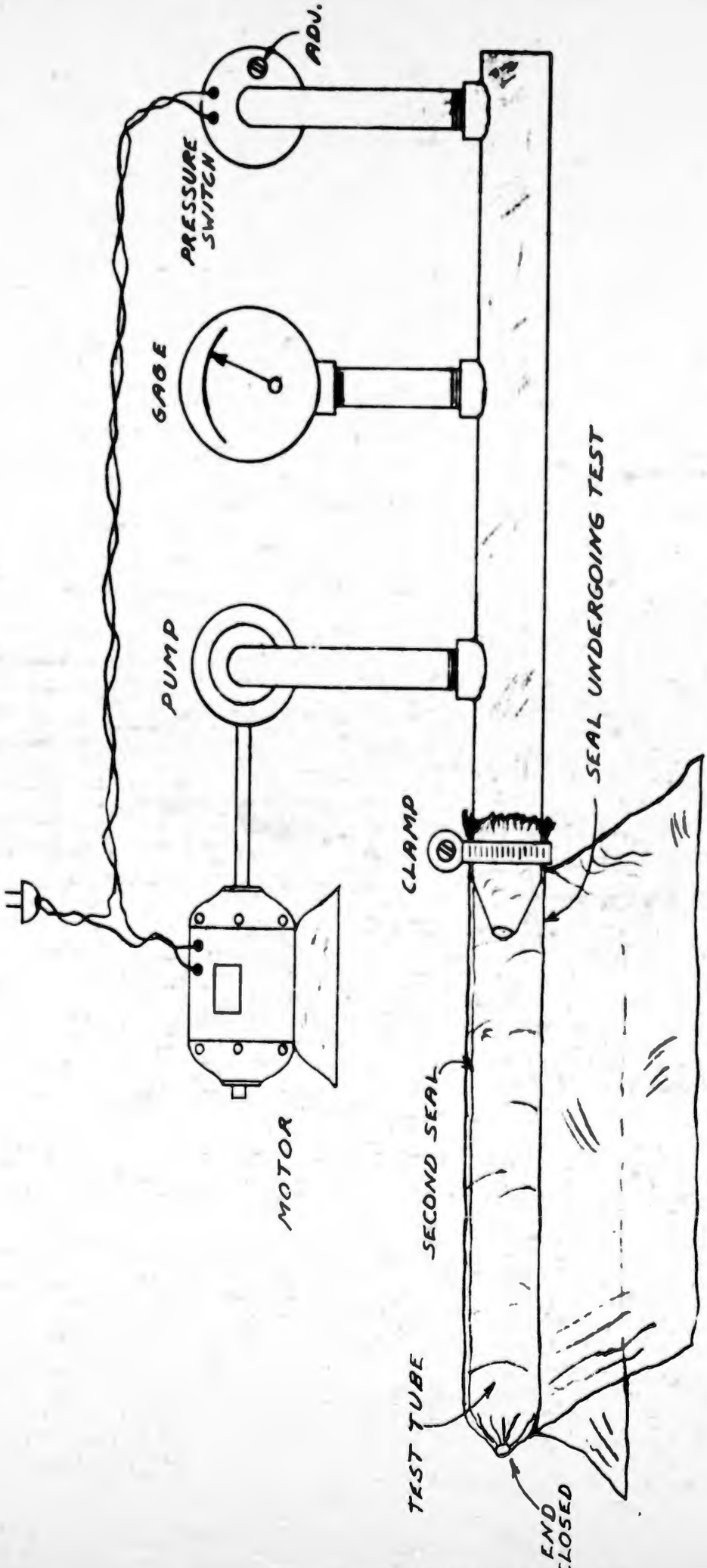
ADJ.
PRESSURE SWITCH
GAGE
PUMP
MOTOR
CLAMP
SEAL UNDERGOING TEST
SECOND SEAL
TEST TUBE
END CLOSED
PLASTIC FILM SEAL TESTER

Figure III-1.

tested seal strength was 0.9 lbs per linear inch, or 0.3 yield strength. By exercising great care in the sealing operation, failures could usually be held down to 5 or 10% of the total number of seals. There were times, however, when for no apparent reason a run of seals would not stand the test. In extreme cases progress was actually backwards in adding material to the balloon, as the test seals consumed more material than that being added by the good seals. The reason for such weak seals could not be traced to differences in material, temperature, humidity or other likely causes.

Following a series of flights of the zero pressure level balloons, some full superpressure balloons were manufactured. The first of these was test inflated with air, and superpressured to destruction. This effectively reproduces the forces in flight because the superpressure forces are extremely great compared to the forces from the lift of the gas and the load. This balloon failed at an average material stress of 7000 psi. (The yield point of Mylar is in the neighborhood of 12,000 psi.) The failure appeared to be in pure longitudinal tension, breaking across two gores and then down a seal. The torn edge across the gores had strained enough to show that it was at the yield point when it failed.

Because it is impossible to load all the material equally by having all gore lengths exactly equal, the shorter lengths reach the yield point first and fail before all the material is at the yield point. Consequently failure occurs at some point below the average yield stress for all the material. Similar tests on smaller sized balloons have resulted in average stresses of from 6,000 to 10,000 psi. On the basis of this, the design working stress in superpressure balloons was generally taken as 5000 psi.

In some 25 balloons made and tested to this working stress, none have failed.

The next series of the 40-ft cylinder flights was with a slightly superpressured balloon. The superpressure was to be achieved with a long duct which hung a half balloon height below the base of the balloon. All launchings of the balloons with long ducts involved difficulties of one sort or another. One balloon apparently was stopped in a temperature inversion, by moisture or by radiation cooling, and did not get to ceiling. On two others, the duct and gondola became twisted during launching and prevented the balloon from valving at ceiling. Another balloon was whipped by the wind during inflation and opened at a seal.

About this time in the program the 250,000 cubic foot cylinder of 1/4-mil Mylar was completed and ready for flight. This cylinder, 120 ft long and 80 ft diameter, was packed in the conventional manner for a University of Minnesota type launching. No trouble was had in handling the thin material during packing. However, during inflation of the balloon a basic weakness showed up. This came just after the balloon had enough gas to lift the top end of the packed balloon, and the top end was released so the balloon could stand erect, still folded in thirds, over the bottom tie-down. When this was done it was observed that helium was between the inner surface (the lower third) and the second surface (the center third). The inner third which should have been holding the gas evidently ripped from the slight action in tipping up from the horizontal position.

Since the balloon was damaged and the gas actually outside, it could not be flown. To allow the gas to escape, the corset was loosened at the bottom, allowing the canopy, which consisted of the upper two-thirds of

the balloon, to be lifted by the gas so it could dump. This action was very fast and practically disintegrated the balloon by shredding much plastic and seals. An on-the-spot inspection of a number of seals in this balloon showed that they were adequately strong in static tension, but failed readily under the sharp pull of shock loading. This weakness seemed to be a limiting factor in the use of this type seal on the larger balloons subject to shock loadings.

After the experience with this balloon it was clear that for large balloons a more suitable fabrication method, such as with glue or tape, would very likely be needed. Further efforts with this heat seal were, therefore, confined to the smaller balloons.

B. Film Leakage Studies

Assuming a uniform leak distribution in balloon fabric, the percentage leakage of an inflated balloon is a function of the area divided by the volume. The ratio of area to volume becomes increasingly great for the smaller balloons, varying according to the radius to the two-thirds power. Slight fabric leakage for these small balloons then becomes significant. This is especially true when the small balloon is superpressured, in which case the pressure forcing gas through the leaks is much greater than the static head pressure.

The first small balloons that were test inflated with helium under superpressure leaked excessively both in terms of the tested material diffusion and in terms of allowable leakage for a daytime duration superpressure flight. There was previous evidence of small leaks associated with the heat seals. This was observed when seal test tubes were inflated

under water. How to detect the location of these and other leaks in a finished balloon was not an easy matter. Attempts to find leaks and patch them did not noticeably improve balloons under test. Techniques tried were with a gas analyzer, and a sniffer probe, the use of ammonia with a chemical indicator and also by simply smelling for ammonia leaks. It quickly became obvious that the leaks, being small and well distributed, had to be eliminated from the start. This led to a joint effort on the part of Herb-Shelly, Inc., and Dr. Kammermeyer of Iowa University under subcontracts with the University of Minnesota.

The susceptibility to puncturing of the Mylar film by slightly rough surfaces or grit is brought out in their reports, which follow in this section. (See Appendices B-1, B-2, B-3, B-4.) With adequate precautions in the manufacture, including dust control, five test balloons were made which showed that leakage could be held down to a minimum which was actually less than material diffusion at higher pressure differences.

A meeting was held with representatives of the DuPont Corporation to show and discuss the results of these studies in the attempt to see what could be done about getting the best balloon material from DuPont. The representatives said they were aware of the puncturing type of film damage from hard surfaces and grit particles. They had been working toward fault-free material. Their production setup was such that a continuous check of the Mylar was not feasible at that time, but they did have a program of inspection and quality control in their plant. It was their opinion that the 1/4-mil material was so thin it might always be subject to some damage. The experience with 1/2-mil material indicated that this was thick enough so as not to be damaged by unavoidable minute impurities

or necessary handling. They stated that by exercising great care in the manufacturing and handling, 1/2-mil material could be produced practically fault free.

It appeared from this that a 1/2-mil material thickness, or possibly a light 1/2-mil (.356 to .4 mil) would be the thinnest material that could be used on the small superpressure balloons. The 1/4-mil could still be very useful in applications where minimum weight is of great importance and minute leakage is secondary, such as in the case of a balloon for an extremely high altitude.

APPENDIX B-1, Section III

Progress Report #1 for June and July 1953

to

Office of Naval Research

by

Karl Kammermeyer

Contract Nonr 875(00), Annex VII

1. Outline of Proposed Work and Methods

The primary purpose of the work under this contract is intended to be a study of the porosity of Mylar film. For film without mechanical flaws, that is, holes or tears, the meaning of porosity would become that of permeability to gas flow.

As originally planned, Mylar film samples were to be submitted by General Mills, Inc. or the University of Minnesota, so that permeability to helium gas could be studied at low temperatures, that is, about -78°C. This temperature was considered satisfactory, even though it is somewhat lower than actually needed. However, it is fairly easy to attain with solid CO_2 and therefore should simplify experimental work.

In order to ascertain that film samples were sound, it was decided to test sample sections at room temperature and compare the results with data which were obtained previously. This is obviously a necessary precaution. It also saves a great deal of time which would go to waste if

unsound films were tested in the low temperature apparatus. Low temperature tests are very time consuming.

Some of the test sections were to contain heat-seals, and porosity or permeability of such seals are naturally of great interest. Again, it is desirable to test first a plain section of such a sample to see if the film as such is sound before testing the seal itself. Then, a sample containing a seal should be tested at room temperature, and only if it shows a permeability value which is normal should the low temperature test be made.

2. Samples Received

The following shipments of samples were received.

Shipment #1: (Received 7/3/53) from Herb-Shelly, Inc. Farmington, Minn.

Description: Two panels of 0.25 mil. Mylar film sealed together by Herb-Shelly. Seal with pressure test tube. Seal tested to 0.9#/in. tensile.

Shipment #2: (Received 7/11/53) from Herb-Shelly, Inc.

Description: Part of one roll of 0.25 mil. Mylar film remaining from a roll which had been used to make a high altitude balloon.

Shipment #3: (Received 7/20/53) from Herb-Shelly, Inc.

Description: Six 0.25 mil. Mylar sample sheets from different rolls with identifying comments as follows:

A. April 320
CB 94075 #2683
25 "Mylar" A wt. 63.7
size 40
about 300 ft. had been taken from roll

B. Same shipment, different roll, re-rolled once.

C. Believe same shipment, different shine, harder to seal, apparently imperfections (lumps) noticed and taped. Rerolled once.

D. Older material rerolled once.

E. Material furnished by University of Minnesota, over two years old. Re-rolled on and off bent or broken core.

F. Believed same as E, but better re-rolling - core unbroken.

3. Testing and Results of Tests

Upon testing the first plain section (no seal) from the sample in the first shipment at room temperature, it became apparent that we were confronted by the problem of pin holes.

As a precautionary measure we retested a sound sample of our own Mylar film samples and found the Gas Permeability coefficient P was $.098 \times 10^{-9} \frac{(\text{std.cc})(\text{cm})}{(\text{sec})(\text{cm}^2)(\text{cm Hg}) \text{ press. drop}}$ at 27°C. This value compares favorably with our published data (see Appendix for copy of publication (Reference 1).*

When the various shipments of Mylar film were tested, a qualitative test method had to be used, as most film samples gave such high gas flow rates that the "rapid" permeability tests (Reference 2)* could not be used with a measuring capillary. For the purpose of the qualitative test

* The two publications referred to were not reproduced in this report, although they were incorporated into the original Kammermeyer report. They are: (Ref 1) Ind. and Eng. Chem. 45 p. 1148; and (Ref 2) Analytical Chem. 25, p. 424. (May 1953 and March 1953, respectively)

the capillary was disconnected from the tester and the vent valve on the downstream side was opened. The gas flow through the film was then observed at the vent valve (or at the capillary connection opening) by closing either one or the other, and watching the formation of soap bubbles from soap solution at the other low pressure side opening. In a very short time the operator was in a position to judge when a film was flowing much too fast. If there was the least indication that a film was tolerably slow, it was checked in the constant temperature bath apparatus using a capillary tube for volume rate of flow measurements.

While a person familiar with testing of films can readily recognize when the flow is greater than it should be, it is a good precaution to make a selenium sulfide print of the test specimen. Pinholes and imperfections become readily apparent on such prints. In order to eliminate the possibility of having mercury droplets getting under the film (thus giving a false indication) the film can be "printed" in several different relative positions.

[A selenium sulfide print made from a plain section (no seals) of the First Shipment sample is shown in the Appendix (Exhibit 1). The presence of numerous pinholes can readily be observed. The size of the dark dots indicates only relative size of holes, but not actual size, as the time of exposure determines how large the dots will grow.]* Several other film specimens were tested by selenium sulfide printing and in each case the presence of pinholes was definitely established.

---

* This print not reproduced, but see Plates 8-12 in Appendix B-4, this section, for typical examples of selenium sulfide prints.

The results of all tests which were actually carried out can be summarized as follows:

Of all specimens tested only one was found which was free of pinholes. The permeability values obtained are:

$P \times 10^9 = 0.12 \frac{(std.cc)(cm)}{(sec)(cm^2)(cm\ Hg)}$ at 50°C

$P \times 10^9 = 0.064$ " at 25°C

$P \times 10^9 = 0.030$ " at 0°C

This sample was obtained from Shipment #2. These values indicate that this film was somewhat slower than our previous samples, but for practical purposes the difference is not too significant.

Summary of all tests:

Sample	No.of samples (total tested)	Qualitative Test: Large Flow	Medium Flow	Slow Flow	Further test on slow flow
Ship.#1	15	6	4	5	All 5 too fast for tester. Rates 10 to 100 times of P.
Ship.#2	15	6	5	4	2 samples tested in tester. 1 sample about 30 times P. 1 sample satisfactory P.
Ship.#3					
A	4	1	-	3	Too fast for tester.
B	4	-	-	4	Too fast for tester. About 100 times P.
C	4	1	2	1	Too fast for tester.
D	4	1*	3	-	- - - - -
E	4	-	2	2	Too fast for tester.
F	5	4**	1	-	- - - - -

* very large hole
** one very large hole

Conclusions:

Straight Film Samples (No seals).

At the present time the whole problem is obviously one of obtaining films which have no pinholes,or at least very few and then only relatively small ones.

One wonders if the manufacture of a 0.25 mil. film will permit the production of flawless material.

While the disadvantage of using somewhat greater thickness is obvious, I believe consideration should be given to thicker films, perhaps 0.5 mil. Naturally, all efforts should first be made to locate a source of sound 0.25 mil. film. If this proves unsuccessful, the next step would be to check if 0.5 mil. film (perhaps 0.4 mil. might do) could be obtained without pinholes.

Low temperature testing has not as yet been carried out. It might be well to consider such a test,however, when more than one sound film sample has been found.

Testing of Seals

Although all but one film section gave unsatisfactory performance, a few test sections were prepared containing seals. Four samples from shipment #1 were tested as follows:

One sample: 2 seals in the same sheet (single film thickness)

One sample: 2 seals in the same sheet (double film thickness)

Two samples: 1 seal (single film thickness)

All qualitative tests showed very large to tremendously large flow rates. This would indicate that the seals were leaking as the rates were definitely greater than the one obtained on plain sections.

APPENDIX B-2, Section III

Progress Report #2 for August 1953

to

Office of Naval Research

by

Karl Kammermeyer

Contract Nonr 875(00), Annex VII

1. Film Testing for Porosity

A large number of production samples of 1/4 mil Mylar film, as well as some thicker films, were tested for presence of pinholes. The program was initiated by Mr. G. T. Schjeldahl of Herb-Shelly, Inc., who visited Iowa City on August 10, 1953. For the most part the testing work was carried out by Mr. E. N. Mitchell on August 10, 11 and 12, and by Mr. N. Horwitz on August 17 and 18. These men were assisted by Mr. Paul Nunn of our staff. The rapid permeability tester in our laboratory gave excellent performance and made it possible to test the many specimens in a reasonable time.

As it is expected that the details of the testing program will be reported by Messrs. Mitchell and Horwitz, it is not felt necessary to cover the results in this report. In a general way, the previously formed impression was substantiated, that is, it will be rather difficult to manufacture 1/4 mil Mylar film of a soundness to satisfy balloon service requirements. Therefore, an investigation of 1/2 mil film would probably be justified.

2. Low Temperature Testing of Mylar Film

As the comprehensive testing program for porosity did disclose that a number of sound sections were present, it was felt that a low temperature test with 1/4 mil film was worthwhile. Consequently, some 40 samples were screened on the permeability tester and one sound section was selected for the test.

The film tested with helium was Du Pont 1/4 mil Mylar A from bolt CB 2935-1364. The actual thickness was measured as 0.00030 in. using the Gardner Thickness Gage. (The sample was #41 of the group of films tested by Mr. Horwitz.) After bringing to equilibrium at about 50°C with a 50 psi pressure drop, the film was checked in the water bath apparatus at 27.8° and 48.7° C. The assembled flange with the film was then transferred to the low temperature testing equipment to avoid handling of the film itself.

The data which were obtained both at low temperatures and at the higher temperatures are summarized in Table I.

At first glance, there is quite a large spread of the values. Actually, the picture is not as bad as it looks. Due to the extremely small amount of gas which permeates, technique of operation becomes very important. The measurements are made with a traveling mercury plug in a capillary outside of the low temperature chamber. Some vibration is necessary to prevent sticking of the mercury plug, but too much vibration may result in impact movement of the plug as the pressure on both sides of the plug should remain essentially the same.

The values of readings 2, 3 and 4 appear to be closest to the true value and reading 5 is still a possibility. However, the other readings

TABLE I

Permeability Determinations on 0.0003 in. Mylar Film

Gas: Helium

Temp. °C.		Permeability Constant x 10^9 *	
48.7°		0.190	(7 determinations)
27.8°		0.808 **	(14 ")
-78.5° ***	1-	0.0000628	
	2-	0.000444	
	3-	0.000398	
	4-	0.000439	
	5-	0.000316	
	6-	0.000103	
	7 -	0.0000900	
	8-	0.000116	
	9-	0.000146	
	10-	0.000114	
	11-	0.0000999	
	12-	0.0000945	

* For definition of Permeability Constant refer to/Progress Report #1, Page 3. (Appendix B-1, Section III) (Page III-84.)
Kammermeyer

** This value compares with values of 0.098 (our own film at 27° C.) and 0.064 (Herb-Shelly film at 25° C.) reported previously on Pages 3 and 5 respectively of Progress Report #1. (Appendix B-1, Sec.III) (Pages III-84 & III-86.)

*** The equipment is set up with "dry ice" as cooling medium and the thermometer reading remains essentially constant.

in our opinion are definitely too low. Of course, our decision may seem somewhat arbitrary. However, a plot of the values on a 1/T versus log P graph shows that the expected extrapolation would give a reading of about 0.00044. We realize that this is somewhat of an indirect way to prove a point as there is no assurance that a straight line extrapolation will hold. However, from analogy with previous work on polyethylene films and helium, I believe the conclusion is reasonably well justified.

The graph is presented in Figure 1. It was originally laid out so that the temperature scale covered a distance of about 15 inches. This permitted the establishment of the slope of the line with considerable degree of accuracy.

Obviously, it would be well to make at least a few more low temperature determinations. This should preferably be done with 1/4 mil (nominally) film as difficulties in operation will increase materially when a thicker film is used. Nevertheless, if it is finally decided that 1/2 mil film were to be used it may be worthwhile to run a test with that thickness. It is my opinion that we will need only a very limited number of tests. In the first place, the permeability is so low that even a 100% variation, while objectionable, would not be too serious. Secondly, the tests are rather time consuming and the cost would not justify running a great many tests.

3. Selenium Sulfide Printing of Films

As the selenium sulfide printing method was again found to be a helpful tool, copies of the procedure are attached to this report for the sake of ready reference at a later date.

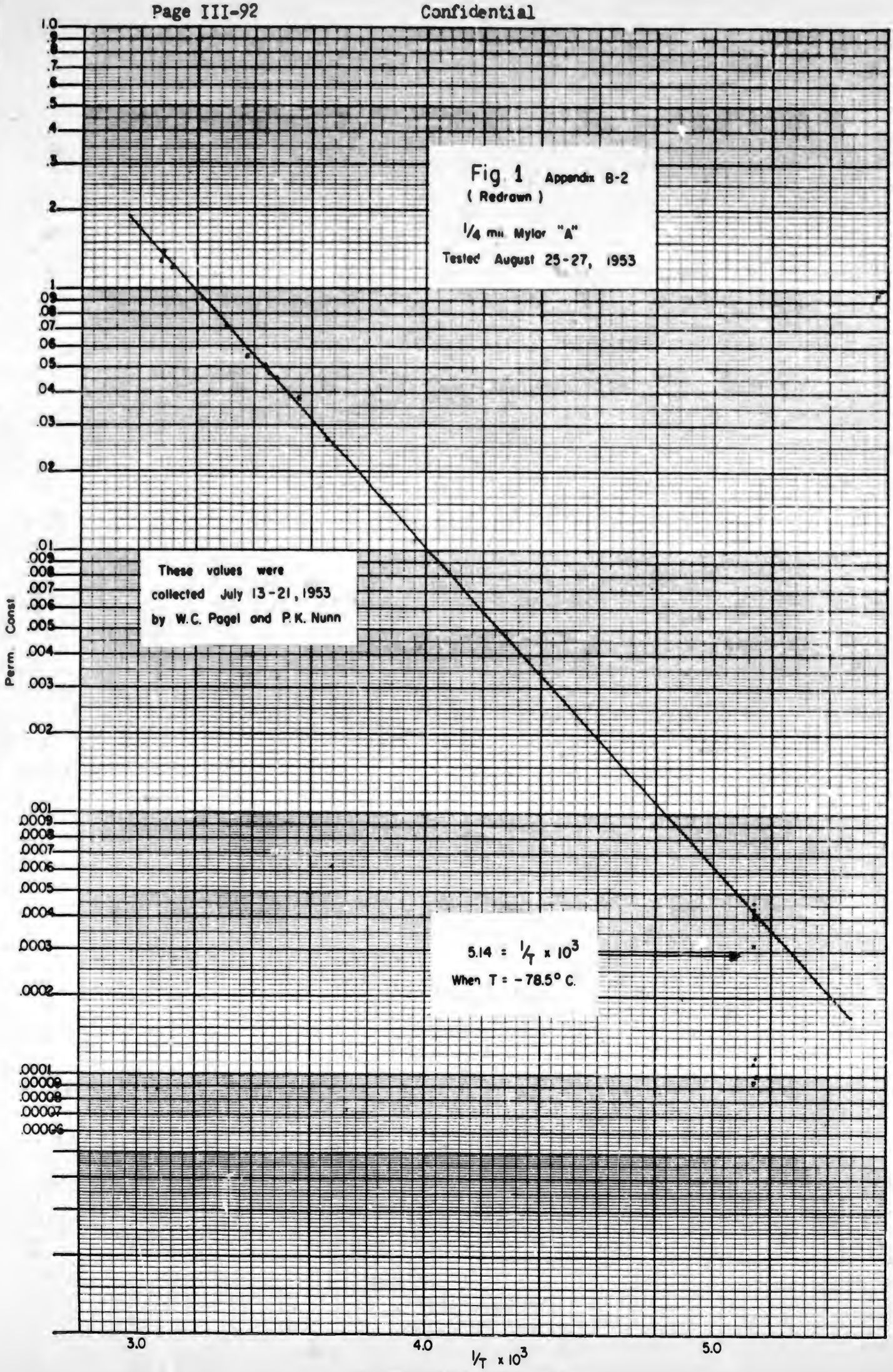
Fig 1 Appendix B-2
(Redrawn)
1/4 mil Mylar "A"
Tested August 25-27, 1953
These values were
collected July 13-21, 1953
by W.C. Pagel and P.K. Nunn
5.14 = 1/T x 10^3
When T = -78.5° C.
Perm. Const
1/T x 10^3
3.0
4.0
5.0

SELENIUM SULFIDE PRINTING

Porosity testing by means of gas permeation shows whether or not there are holes in a sample. If the exact location of the hole is desired, a selenium sulfide print must be used. The usefulness of this method seems to be limited to a search for the exact location of holes, since the long time necessary to make a print eliminates the method as a general test method for evaluating films. This report describes our experiences in using selenium sulfide prints to locate holes.

The general conditions for this test are as follows: a mercury vapor source above the film, and a treated selenium sulfide plate below. The mercury diffuses through the pinholes in the film and reacts with selenium sulfide to form a black product. From the position of black spots on the print, the position of the pinhole can be established.

As mentioned in previous reports, this process is patented by Dr. B. W. Nordlander, in U. S. Patent 2,310,111. If large-scale use of the method were made, some arrangement would be necessary with the owner of the patent.

PREPARATION OF TEST PAPER

Selenium Sulfide

The preparation of selenium sulfide was accomplished by following the directions from the literature. A flask was equipped with a gas-inlet, a liquid inlet, and a motor driven stirrer. In the flask a solution containing 100 mgs of $AlCl_3$ per liter was introduced. The solution then was saturated with H_2S gas, and a solution of 7.5% selenious acid was added very slowly. A sticky orange-yellow precipitate was formed. The precipitate was washed with water and air-dried at room temperature.

Selenium sulfide was also obtained from Dr. Nordlander, of the General Electric Company, who is the inventor of the selenium sulfide printing process. It was similar in appearance to that prepared in our laboratory.

Small particles of grit remaining on the paper tended to punch holes in the plastic film. Dr.Nordlander wrote that the method of preparation is very important in determining the suitability of selenium sulfide for making prints.

The paper used was master copy duplicator paper which is a glossy heavily calendered paper. A small amount of powdered selenium sulfide is rubbed lightly onto the paper with a wad of cotton. A static charge holds the powder on the paper. The more evenly the selenium sulfide is distributed on the paper, the better the print will be.

The amount of selenium sulfide required was not measured,but it is estimated to be in the neighborhood of 1 milligram per square foot of paper. Only a very light covering is necessary.

The sensitized paper should be stored in a place where it will not become exposed to mercury vapor.

The darkened areas on the print are caused by reaction of mercury vapor with the selenium sulfide. The most convenient source of mercury vapor is an amalgamated copper plate. Copper plates were ground smooth and amalgamated as follows: The plate was wet with a very dilute solution of nitric acid. The nitric acid acts as a flux, allowing the mercury to wet the surface. A few drops of mercury were then placed on the wet surface, and spread evenly with a clean cloth. The plate is then washed and dried, and excess mercury wiped off. This leaves a very smooth, bright surface.

Before a copper plate was obtained, an amalgamated plate was made by making an amalgam of mercury with copper powder. This amalgam was spread on a piece of cardboard which was covered with rubber cement. The amalgam hardened and served as a source of mercury vapor. The only disadvantage of this was that the amalgam contained hard rough particles which sometimes penetrated the film which was being tested.

The amalgamated plate was covered with filter paper for protection, since mercury vapor readily diffuses through filter paper. The amalgam gradually lost potency, and for best results the amalgam was renewed before each test.

TESTING

In the actual film testing there are several precautions which must be taken. When the film is placed on the treated selenium sulfide paper, it is held in place with drafting tape. The orientation markings on the film are continued on the plate so that when the film is removed, it may be replaced in the same position. The treated paper and the film are then placed on a thick sheet of plastic to prevent any diffusion of mercury from below. The amalgamated copper plate covered with filter paper is then placed on top of the film. On the treated paper the following information is recorded: film section number, location number, the time, and the date. A weight may be placed on top of the copper plate if convenient.

The whole assembly was placed in a covered box made of galvanized steel in order to keep the concentration of mercury vapor low in the air of the room. For the same reason, the plates should be stored in the box when not in use.

With a freshly amalgamated plate, larger holes will begin to appear as small black spots on the treated film after about four hours. If this film

is left for a longer length of time, the black spots will become blurred, making exact location of the pin holes more difficult. If the film contains very small holes, it may take up to 18 hours to get a print.

Dr. Nordlander mentions in his patent that the time required for a test may be considerably shortened by holding the temperature at 70°C. Above this temperature, a change takes place in the selenium sulfide which makes it useless for this purpose. We have not tried to make any prints at elevated temperatures; they were all made at room temperature.

Attempts to make a close correlation of print size for different times of exposure have not been successful, due to some extent to plugging of holes, as described later.

After about 18 hours, a curious pattern forms on the paper with some films. This pattern does not appear with films which have not been tested in the porosity tester. For those which have been tested, a definite pattern is obtained showing where the basket has compressed the film, and also other places where the film has been under stress. For this reason, the patterns are believed to be either strain patterns, caused by changes in the permeability of film when it is stressed, or due to differences in thickness due to plastic deformation. These patterns are easily distinguished from spots which indicate the presence of holes in the film.

After the film has been tested, a black deposit will appear on the film and may fill the pin holes. This deposit always appears on the side of the film next to the amalgamated plate, but it has never appeared on the filter paper between the plate and the film.

Small holes in the film also become filled with this deposit, and can be seen clearly. The exact nature of the deposit is not known. It may be possible that the selenium sulfide has enough vapor pressure, or

may decompose to give a vapor pressure of H_2S high enough to account for the deposit.

SOURCE OF ERROR

The most troublesome source of error so far encountered is that of small drops of mercury finding their way under the print paper or under the film in some way, causing a spot to appear where no hole exists. As a check, when a hole cannot be found by visual inspection, it is advisable to run a second print on a film. The probability of two false spots appearing at the same place is small, so that any area which shows a spot both times almost certainly contains a hole. One source of error in duplicate determinations may be that some of the very small pin holes could have been filled with the black deposit while making the first print and would not print in the second test.

APPENDIX B-3, Section III

FINAL REPORT

and

Progress Report #3 for September - December 1953

to

Office of Naval Research

by

Karl Kammermeyer

Contract Nonr 875(00), Annex VII

This report covers data obtained on 1/2 mil Mylar film and in addition presents a summary of previous work.

1. Low Temperature Testing of Mylar Film.

Previous work on 1/4 mil Mylar film indicated that such a thin film cannot readily be produced without having a certain number of small holes. This is a situation which one would expect. Therefore, the porosity of 1/4 mil Mylar film will in general be appreciable and thus nullify the film's normal excellent low gas permeation properties.

Consequently, it was considered worthwhile to make some helium permeation tests with the next higher thickness of film, that is, the nominal 1/2 mil film. A section of such film was received from Herb-Shelly, Inc., and the identifying label on the wrapper contained the following information:

DUPONT MYLAR
Polyester Film
Date: August 1478
Order: CB 3340
Kind: 50 "Mylar" A
Size: 40

The film actually measured 0.54 mils in thickness.

Two sections of "sound" film were selected by screening a number of pieces on the rapid permeability tester. Our expectations that the greater thickness would result in a lower incidence of imperfections, was borne out in the screening tests. Although we tested a fair number of sections we did not find any one sample which was unsatisfactory. The Mylar sheet showed a number of "line" surface impressions which could be guide or roll marks, or creases, and we wanted to be sure that there were no breaks in the film. Apparently, the markings did not have any deleterious effects.

As in previous cases, we found that it is rather difficult to get results with a completely satisfactory degree of reproducibility. We tested several samples in a qualitative manner, as we suspected that our method used to vibrate the glass capillary (Reference 2, Rept. #1) gave too great a spread in results. By using an improved "vibrator" we were able to get better agreement between check runs on the same film sample.

The final low temperature tests were made on two film samples. Helium permeabilities were obtained for both films at -78.5° C. (-109°F.) and at room temperature. The results are summarized in the following Table II.

TABLE II

Permeability Determination on 0.00054 in. Mylar Film
Gas: Helium

Film #1

°C.	1,000/T	P x 10^9 *
26.2	3.34	0.0151 (6 determinations)
-78.5	5.15	0.0000123
		0.0000147

Film #2

°C.	1,000/T	P x 10^9 *
31.2	3.285	0.0882 (7 determinations)
-78.5	5.15	0.000364
		0.000264
		0.000281
		0.000437

* For definition of P, see Progress Report #1, Page 3. (Page III-84.)

These data are both interesting and vexing. To be in proper perspective, they should be compared with data given in Table I of Progress Report #2 (Page 3), and also should be plotted on Figure 1 of Progress Report #2. (Pages III-90 and III-92, respectively.)

The practical interpretation of the findings on 1/2 mil film are:

(a) that the film thickness has no effect on the permeability constant (it affects the gas permeation directly, i.e., doubling the thickness gives one half the rate of flow), and

(b) the permeability constant curve presented in Figure 1 (Rept. #2) is satisfactory for use.

These conclusions seem to neglect the data obtained on Film #1. Actually, the procedure and the arrangement of equipment used to test Film #1 were such that there is some doubt in our mind regarding the validity of the data. Therefore, when we take into account all of the known factors and the over-all situation as it stands today, we feel that the above conclusions are justified.

It would be unwise, however, to simply want to ignore the unpleasant fact that we did again obtain some values for helium gas permeability constants which were appreciably lower than the values which we have come to consider as standards. We must, therefore, concede the possibility that the average value of 0.00044×10^{-9} for the helium permeability constant at $-78.5^{\circ}C$ is some 30 to 40 times as great as the "actual" permeability constant. This could mean that the "normal porosity" of Mylar film is such that the "permeability" value of 0.00044×10^{-9} can be expected from good quality film. Personally, I think this is the most significant conclusion.

At present, I do not feel that further permeability tests are necessary. Of course, on principle it would be well to look further into the discrepancies which we have encountered, and if it is considered desirable to do so, we would be interested in carrying out the necessary investigation.

2. Summary

The purpose of the work was an investigation of the helium permeability behaviour of Mylar film at low temperatures. For the sake of convenience, low temperature measurements were made at -78.5° C. which permitted the use of "dry ice" as control medium.

As in previous work with thin plastic films, the problem of "porosity", that is, the existence of small holes (mechanical defects) was encountered. This was the case, however, only for the 1/4 mil film. The 1/2 mil film appears to be essentially free of pin-holes. While we did not investigate a great many sections of 1/2 mil film, we still feel that we can make the above statement with a fair degree of confidence.

Helium permeability constants have been determined for both 1/4 mil and 1/2 mil film at room temperatures and at -78.5°C. Some discrepancies were encountered for different samples of the 1/2 mil film. It is quite possible that similar discrepancies might show up if testing of 1/4 mil film had been more extensive. In any case, however, it is felt that the temperature coefficient curve which has been presented for the helium permeability constant is adequate for present purposes.

The detailed findings and results have been reported in:

Progress Report #1 for June and July 1953,

Progress Report #2 for August 1953, and

Progress Report #3 for September to December 1953.

The latter report forms the first part of the present document.

We wish to express our appreciation of having had the opportunity to participate in this work.

Karl Kammermeyer

APPENDIX B-4, Section III

THE EVALUATION OF "MYLAR" WITH REGARD TO LEAKAGE PROPERTIES FOR USE IN BALLOON APPLICATIONS

Submitted by

HERB SHELLY, INC.

E. N. Mitchell, Consultant
Farmington, Minnesota.

TABLE OF CONTENTS

	Page
List of Plates	iii
Introduction	iv
Summary of First Tests by Herb-Shelly, Inc.	1
Summary of "Mylar" Conference with DuPont	2
Summary of Second Tests by Herb-Shelly, Inc.	3
First Tests by Herb-Shelly, Inc.	4
"Mylar" Conference with DuPont.	9
Second Tests by Herb-Shelly, Inc.	11
Appendix - Stenographic Report of "Mylar" Conference	

LIST OF PLATES

	Page
Plate 1 - Unopened roll of "Mylar"	12 (deleted)
Plate 2 - Unrolling process used for Mylar at Iowa	13 (deleted)
Plate 3 - Selenium Sulfide Print Maker	14
Plate 4 - General Mills Permeability Tester	15
Plate 5 - Abrasion of "Mylar" by crumpling	16 (deleted)
Plate 6 - Abrasion of film by rolling	17 (deleted)
Plate 7 - Abrasion of film by drawing over steel rod	18
Plate 8 - SeS print showing good film	19
Plate 9 - SeS print showing faulty film	20
Plate 10 - SeS print showing faulty film	21
Plate 11 - SeS print of film after abrasion by rolling	22
Plate 12 - SeS print of Herb-Shelly seal	23

INTRODUCTION:

The report contained herein describes work done by Herb-Shelly, Inc. for The University of Minnesota and the Office of Naval Research under University of Minnesota purchase order F-8762, Contract NONR-710(01) by E. N. Mitchell and N. Horwitz at the State University of Iowa and the University of Minnesota.

Herb-Shelly, Inc.

E. N. Mitchell, Consultant

First series of tests by Herb-Shelly, Inc. to determine leakage properties of "Mylar" film.

Purpose: We wished to determine whether new ¼ mil "Mylar" film had pin holes in it when it was received from Du Pont; the relative importance of leakage through pin holes as compared with leakage by diffusion, and whether pin holes were introduced into the film after we received it through handling.

Method: Samples of film were taken from three rolls of ¼ mil "Mylar" type A, and the amount of helium which passed through them when the film was subjected to a pressure difference was measured. The equipment used was built by General Mills, Inc. and located in the laboratory of Dr. K. Kammermeyer at the State University of Iowa.

Results: The samples taken from one roll indicated that there were no pin holes and that the gas passed through by means of diffusion only. About half the samples from the other two rolls did have pin holes, and the remaining half did not. We calculate that the rate of leakage of gas from a balloon under typical flight conditions is 40 to 250 times faster through the pin holes than via diffusion.

Conclusions:

(1) Extreme care in handling the film was exercised; therefore, we conclude that some of the new "Mylar" does have pin holes when it is received from Du Pont.

(2) The difference in the characteristics of the three rolls indicates that the film received from Du Pont does not have uniform properties with respect to leakage.

Conference with representatives of Du Pont regarding results of the first set of tests.

On August 17, 1953, a conference attended by the following people was held at the University of Minnesota.

Representing the balloon project at the University of Minnesota:

H. Kieth, Commander
J. Boarman
Dr. E. P. May,
Dr. J. R. Winckler
J. Fuch

Representing E I Dont DeNemours, Inc:

J. A. Ruby
R. L. Krueger
T. D. Secca

Representing Herb-Shelly, Inc.

P. Schjeldahl
R. J. Mitchell
I. Horwitz

Mr. R. J Mitchell described the results of the tests which indicated the existance of pin holes in the 2 mil "Mylar" film. The representatives from Du Pont stated that they could ship "Mylar" film which had passed more stringent tests and it was agreed that this should be done and upon receipt of the new "Mylar", Herb-Shelly, Inc., would repeat the series of tests previously described.

Conference with representatives of Du Pont regarding results of the first set of tests.

On August 17, 1953, a conference attended by the following people was held at the University of Minnesota.

Representing the balloon project at the University of Minnesota:

L. Kieth, Commander
J. Sparkman
Dr. E. P. Ney,
Dr. J. R. Winckler
W. Huch

Representing DuPont DeNemours, Inc:

J. A. Ruby
R. C. Krueger
T. D. Mecca

Representing Herb-Shelly, Inc.

G. Schjeldahl
E. N. Mitchell
N. Horwitz

Mr. E. N. Mitchell described the results of the tests which indicated the existence of pin holes in the $\frac{1}{4}$ mil "Mylar" film. The representatives from Du Pont stated that they could ship "Mylar" film which had passed more stringent tests and it was agreed that this should be done and upon receipt of the new "Mylar", Herb-Shelly, Inc., would repeat the series of tests previously described.

Tests made by Herb-Shelly, Inc., on second shipment of "Mylar"

Purpose: To see if the "Mylar" film which had passed the more stringent tests at Du Pont still contained pin holes.

Method: On August 21, 1953, Herb-Shelly, Inc., received from Du Pont 20 foot folls of $\frac{1}{2}$ and $\frac{1}{4}$ mil "Mylar" film which had passed more stringent tests at Du Pont. This film was taken to Dr. Kammermeyer's laboratory and tested as before, in the General Mills testing equipment.

Results: Samples from the first 3 feet of each roll contained a large number of pin holes. Samples from the rest of each roll were essentially free of pin holes and represented a substantial improvement over the films used in the first set of tests.

DETAILED REPORT ON THE FIRST SERIES OF TESTS BY HERB-SHELLY, INC., TO DETERMINE LEAKAGE PROPERTIES OF "MYLAR" FILM.

Objectives

We wished to determine the extent to which helium gas passes through "Mylar" film. In particular we were interested in the following questions.

a.) Does new "Mylar" film have holes in it when it is received from Du Pont?
b.) If the answer to a.) is yes, then how uniform are different samples of "Mylar" with respect to number and size of holes?
c.) If the answer to a.) is yes, then at what rate does helium gas pass through these holes? How large are the holes? How does the loss of helium through holes compare with the loss of helium through diffusion?
d.) At what rate does helium gas diffuse through "Mylar" film which has no holes?
e.) To what extent are holes introduced into the film through handling?
f.) What is the effect of diffusion on balloon performance? What is the effect of leakage through holes on balloon performance?

Method and Results.

Equipment to measure the rate at which helium passes through films has been built by General Mills, Inc., (See Plate 4) and used by Dr. K. Kammermeyer, at the State University of Iowa. This equipment, described in reference 1, essentially measures the time required for the helium, which passes through the film to be tested, to fill a capillary of known volume at known temperature and pressure.

A method of locating pin holes in films was developed by Dr. B. W. Nordlander. (See Plate 3)

Mercury vapor is allowed to pass through the holes and react with selenium sulfide placed under the film. The reaction discolors the selenium sulfide and this locates the pin hole. (See Plates 8-12)

To answer the questions posed in the previous section, tests were conducted at Dr. Kammermeyer's laboratory on $\frac{1}{4}$ and $\frac{1}{2}$ mil "Mylar" type A. Samples were taken from three rolls of "Mylar" which had never been removed from their original packing. (See Plate 1)* Extreme care was taken in the handling. For example, in unrolling the film the rolls were suspended in midair so that the film would not be subjected to the weight of the roll. (See Plate 2)* Pieces were cut from the roll while it was suspended. These pieces were then placed on clean cardboard, and circular samples 24cm in diameter were cut out and placed in the General Mills testing equip-

1. D. W. Brubaker and K. Kammermeyer Analytical Chemistry 25 424 March '53.

* Deleted.

ment. Samples were taken from the middle and both sides of the roll and from positions whose distance from the end of the roll varied in 5 foot intervals from 0 to 40 feet. (See fig. 1)

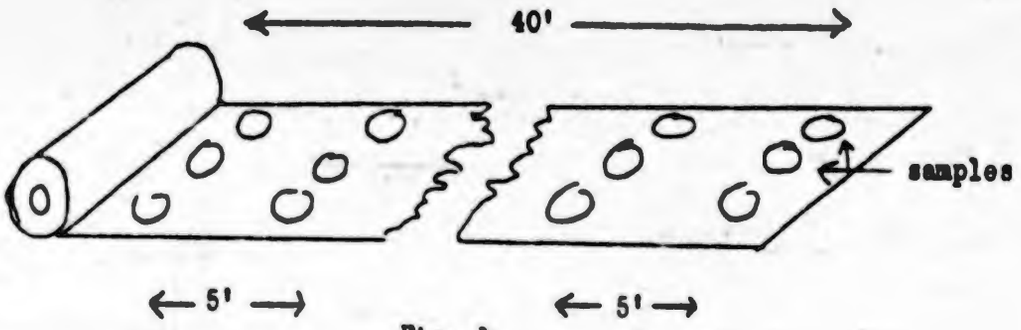

Fig. 1

In these tests helium was placed on one side of the film at a pressure of 64.7 pounds per square inch, the other side being at atmospheric pressure. The time required for helium to pass through the film and fill a $\frac{1}{2}$ cm^3 volume was measured. Fig. 2 shows the results of tests made on 48 samples.

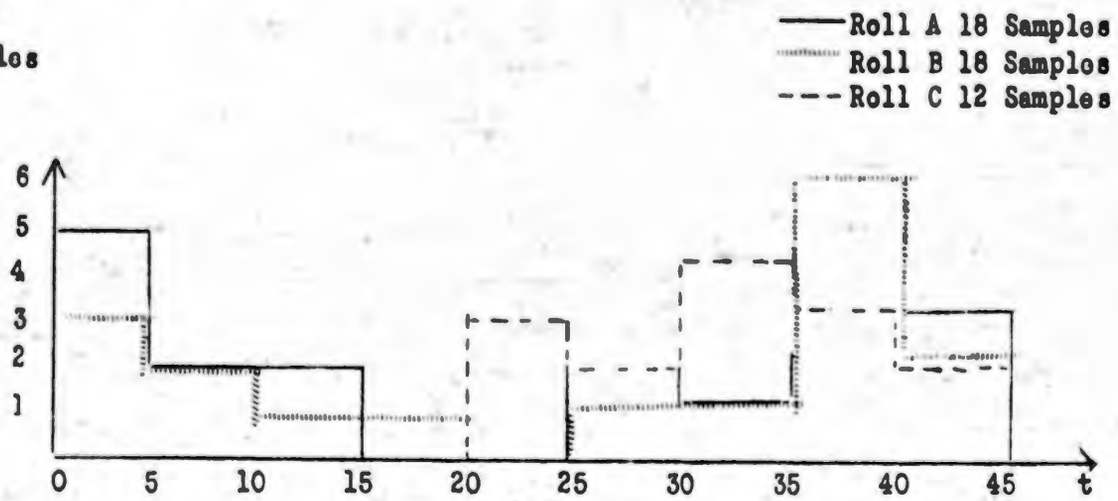

Fig. 2

The first thing to note is that there seems to be a natural subdivision at "t" approximately 20 seconds. We believe that samples for which "t" is greater than 20 seconds have negligible holes and the helium passes by means of diffusion only. Conversely, "t" less than 20 seconds indicates a sample with holes.

It should be pointed out that for samples with no holes, the time required will very until equilibrium inside the equipment is established. This takes about 20 minutes and in the above tests we did not feel it worthwhile to wait for this condition except in one or two cases. Therefore, although the data is spread from "t" equal 20 to "t" equal 45, we believe that had the time been taken in each case to establish equilibrium the results would have been more uniform. The effect of not waiting for equilibrium is to give times which are too short. In the few cases the gas was allowed to come to equilibrium the time crept up to a value of approximately 40 seconds and then remained constant. We have, therefore, taken the

value of 40 seconds to be the required time when the sample contains no holes and the gas passes through by means of diffusion only. For samples with holes equilibrium is reached in a matter of seconds, and, therefore, no correction is needed for the samples with "t" less than 20 seconds. Further evidence that the samples for which "t" equaled 40 seconds contain no holes is that the permeability coefficient calculated for these samples is .085 $x10^{-9}$ (std cc) cm/ cm^2 sec cm Hg pressure drop. This compared well with the value obtained previously by Dr. Kammermeyer[2] of .098 x 10^{-9}.

Discussion of Results (answers to the questions previously posed)

a.) EXISTENCE OF HOLES: Since extreme care was exercised in handling the film and since 33% of the samples of ¼ mil "Mylar" had "t" less than 20 seconds, we conclude that the new "Mylar" film does have holes in it when it is received from Du Pont.

b.) UNIFORMITY: The leakage time varies from less than 1 second to 45 seconds for samples from rolls A and B. The samples from roll C, however, have times which are all greater than 20 seconds. Thus, all the samples taken from roll C are essentially free from pin holes, but almost half of the samples from rolls A and B contain pin holes. We conclude that different rolls are not uniform in their leakage characteristics.

c. and d.) LEAK RATES AND DIFFUSION RATE: We have calculated the volume of gas at atmospheric pressure and 27° C which passed per second through one cm^2 of the film tested. The data was divided into the following groups and average values computed for each group:

Group 1 All 36 samples from rolls A and B
Group 2 All 16 samples from rolls A and B for which "t" was less than 20 seconds.
Group 3 All 36 samples from rolls A and B except one very bad sample for which "t" was much less than 1 second.
Group 4 All 16 samples for which "t" was less than 20 seconds except the one bad sample mentioned under group 3.

The reason for subdividing the data is that we would like to see how a balloon would behave if made of "average" film received from Du Pont and how it would behave if made entirely of film with holes. We assume that group 1 represent average film and group 2 represents film all of which has holes. There was one very bad sample for which "t" was approximately one tenth second. This high leak rate appreciably affects the average for the entire group and we felt it would be of interest to do the calculations including and excluding this one abnormal sample. Groups 3 and 4 are the same as groups 1 and 2 except that this bad sample is excluded.

2 K. Kammermeyer ONR Prog. Report #1 for June and July '53 Contract 875(00)

We define v_i to be the average volume of helium at 27° C and 745 mm Hg which passes per sec. per cm^2 through films in the i^{th} group, and v_D to be the volume under the same conditions which passes by diffusion only per second per cm^2 through a film with no holes. The results of the calculation are:

v_1	equals	74.3×10^{-5} cc/cm^2 sec
v_2	"	164.0×10^{-5}
v_3	"	27.2×10^{-5}
v_4	"	66.0×10^{-5}
v_D	"	3.8×10^{-5}

It should be pointed out that although the relative values are probably significant, the absolute values may be in error by a factor of 2 or 3.

In order to get a rough idea of the number of holes per cm^2 in the leaky samples and also to verify that samples with "t" less than 20 seconds did have holes a number of selenium sulfide prints are made. (See Plates 9 & 10) We found that there were approximately .05 holes per cm^2 and that an average hole diameter of one sixteenth mil would account for the observed leak rate.

e.) HANDLING: A sample of "Mylar" which did not leak was subjected to considerable crumpling, (See Plate 5) then retested. It was found that the sample still did not leak. On the other hand "Mylar" placed on a surface which was not extremely smooth and clean and then subjected to pressure was easily punctured. (See Plates 6 & 11)

f.) EFFECT ON BALLOON PERFORMANCE: We pose the following problem: If a balloon of volume V and area A flies at a height such that the pressure is p and is filled with helium to a superpressure Δp how long will it take to lose a fraction f of this superpressure if the balloon is made of "Mylar" typified by each of the above groups?

The calculation was made as follows: When a balloon has a superpressure of 1 millibar and flies at a height corresponding to 15 millibars, one can apply Bernoulli's equation for an incompressible fluid to the gas which escapes from the holes because practically no expansion takes place. One finds that

$$t_f = \frac{f V}{A g} \sqrt{\frac{M.W.}{2R T_B}} \quad \frac{\Delta p}{p}$$

where t_f is the time required for the balloon to lose a fraction f of its superpressure
M.W. is the molecular weight of the gas
g is the fractional area of the film which is holes
R is the universal gas constant
T_b is the temperature of the balloon

The problem then reduces to finding g from the data obtained from the General Mills equipment. We know the amount of gas which comes through the holes in a given time. Therefore, if we can find the velocity and density of the gas in the hole, we can calculate the size of the hole and thus get g. The density and velocity of the gas in the hole can be obtained by applying Bernoulli's equation to a compressible fluid undergoing adiabatic expansion. One finds that:

$$g = \frac{P_c V_c (M.W.)}{a_s R T_c \rho_h v_h t_c}$$

Where t_c is the time required to fill the capillary with helium
P_c is the pressure in the capillary
V_c is the volume of the capillary
T_c is the temperature in the capillary
a_s is the area of the sample
ρ_h is the density of gas in the hole
v_h is the velocity of the gas in the hole

The calculation was done for a balloon flying at 15 millibars, with one millibar superpressure. If t_i is the time required for the balloon to lose 10% of its superpressure when it is made of material from the i^{th} group then:

t_1 equals 1.36 hours
t_2 " .6 hours
t_3 " 4.25 hours
t_4 " 1.54 hours

To find the corresponding time for a balloon which lost gas via diffusion only we assumed that the amount of gas lost is directly proportional to the pressure difference across the film and extrapolated the results obtained with the General Mills tester (at Δp equal 50 lb/in^2) to balloon conditions (Δp equal 1 millibar), The result was:

t_D equals 163 hours.

g.) OTHER TESTS: A few samples of ½ mil "Mylar" were tested and all found free of holes. It was also found that these samples were closer to .6 or .7 mil than ½ mil.

A selenium sulfide print was made of one heat seal and a fairly large number of pin holes were found along the seal.(See Plate 12)

CONFERENCE WITH REPRESENTATIVES OF DU PONT REGARDING RESULTS OF THE TESTS DESCRIBED IN THE FOREGOING SECTION

On August 17, 1953, a conference attended by the following people was held at the University of Minnesota to discuss the problem of pin holes in "Mylar" film:

M. Kieth
Commander J. Sparkman
Dr. E. P. Ney
Dr. J. R. Winckler
W. Huch
R. C. Krueger
J. A. Ruby
T. D. Mecca
G. Schjeldahl
E. N. Mitchell
N. Horwitz

Mr. Mitchell reported on the tests described heretofore which indicated that new $\frac{1}{4}$ mil "Mylar" had pin holes. Mr. Krueger from Du Pont stated that Du Pont makes two types of $\frac{1}{4}$ mil "Mylar": type A and type C. Type C is subjected to a more selective quality control program. The material we had tested was of type A. Mr. Krueger suggested that he send us some type A "Mylar" which had been subjected to the same quality control standards as type C. It was agreed that this would be done and that upon receipt of the new "Mylar", Herb-Shelly, Inc. would conduct a series of tests identical to those performed before, and if this film proved satisfactory then Herb-Shelly, Inc., would proceed to use it in an attempt to make heat seals. Mr. Krueger estimated that through use of their more selective quality control program, they could ship "Mylar" which would leak at rates probably not to exceed 2 or 3 times the diffusion rate.

Mr. Krueger strongly urged that $\frac{1}{2}$ mil "Mylar" be considered and asked if there would be any interest in .33 mil "Mylar" should Du Pont decide to manufacture it. He felt there might be a critical thickness below which the probability of getting pin holes in the film rose rapidly. He suggested that $\frac{1}{2}$ mil or even .33 mill "Mylar" might prove to be appreciably better than $\frac{1}{4}$ mil in this respect. He stated that Du Pont had some $\frac{1}{2}$ mil "Mylar" which was actually closer to .4 mil and it was agreed that some of it would be sent to Herb-Shelly, Inc. to be tested along with the $\frac{1}{4}$ mil "Mylar".

There was some general discussion on the status of the "Mylar" program at Du Pont during which the following information was obtained:

Current Production

1.) Semi-works plant of about 50,000 square feet which includes both polymer and film equipment, located at Buffalo, N.Y.

2.) Production is very low - in the range of under 5000 pounds. They said that Herb-Shelly's stock of 400 pounds was more material than Du Pont had in inventory at the present time.

New Facilities

New plant being built at Circleville, Ohio, on a 600 acre plot. Will be in production late next year. Size of plant and production rates not mentioned.

Prices

On direct question by Mr. Schjeldahl, Mr. Krueger said the price of "Mylar" film would not go higher than it is at the present time. Mr. Krueger guessed that material price would eventually wind up 50% less than the current price. He did not, however, specifically mention gauge.

Method of Quality Control Used at Du Pont

Samples are taken at the beginning and end of each mill roll and the analysis is based on statistical methods.

TESTS MADE BY HERB-SHELLY, INC., ON SECOND SHIPMENT OF "MYLAR" FILM

Purpose

To see if the ¼ mil "Mylar" film which had been subjected to the more rigid quality control tests at Du Pont was appreciably better than the "Mylar" tested previously (part II of this report). Also to test some undersized ½ mil "Mylar".

Method and Results

The films were tested as before by using the General Mills testing equipment at Dr. Kammermeyer's laboratory at the State University of Iowa. The results are shown in fig. 4 and 5.

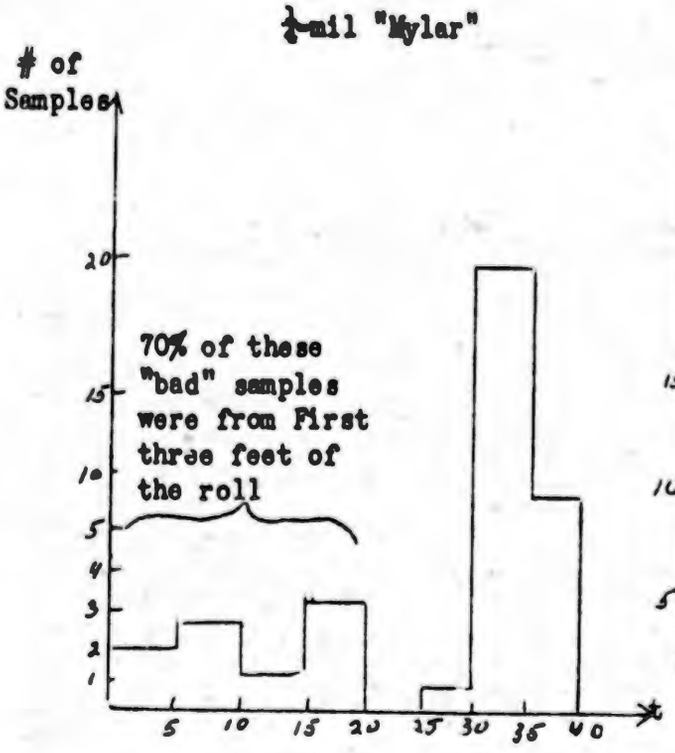

Fig. 3

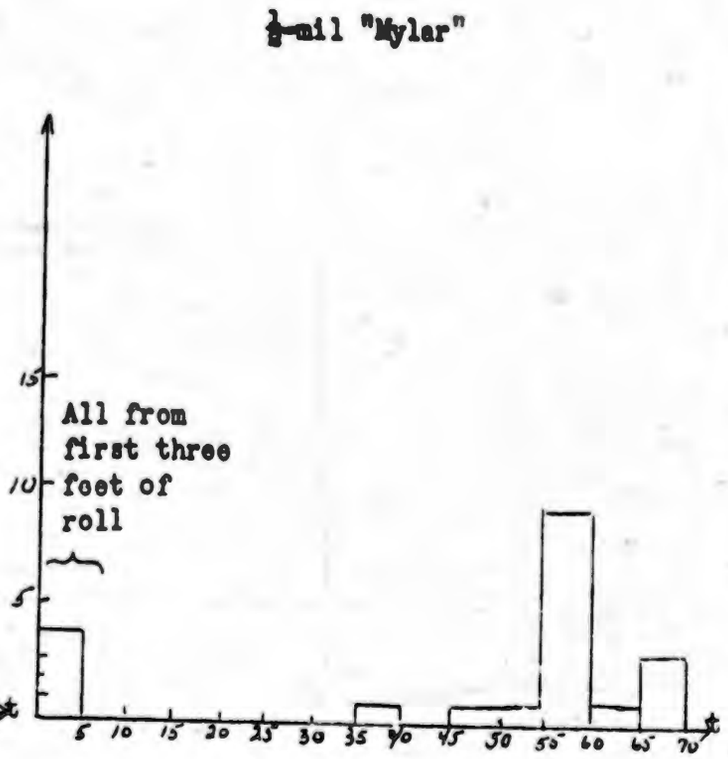

Fig. 4

Not counting the bad samples from the first three feet of the ¼ mil roll, the average time required for the helium to leak through is 33 seconds. Using this data to get an estimate of effect on balloon performance we calculate that a balloon made of this quality "Mylar" would lose 10% of its superpressure in about 100 hours. This is to be compared to 140 hours if the loss of helium were due to diffusion only, and ½ to 4 hours if the balloon were made of "Mylar" similar to the first samples tested (part II).

PLATE 3 --- Apparatus for making Selenium Sulfide prints

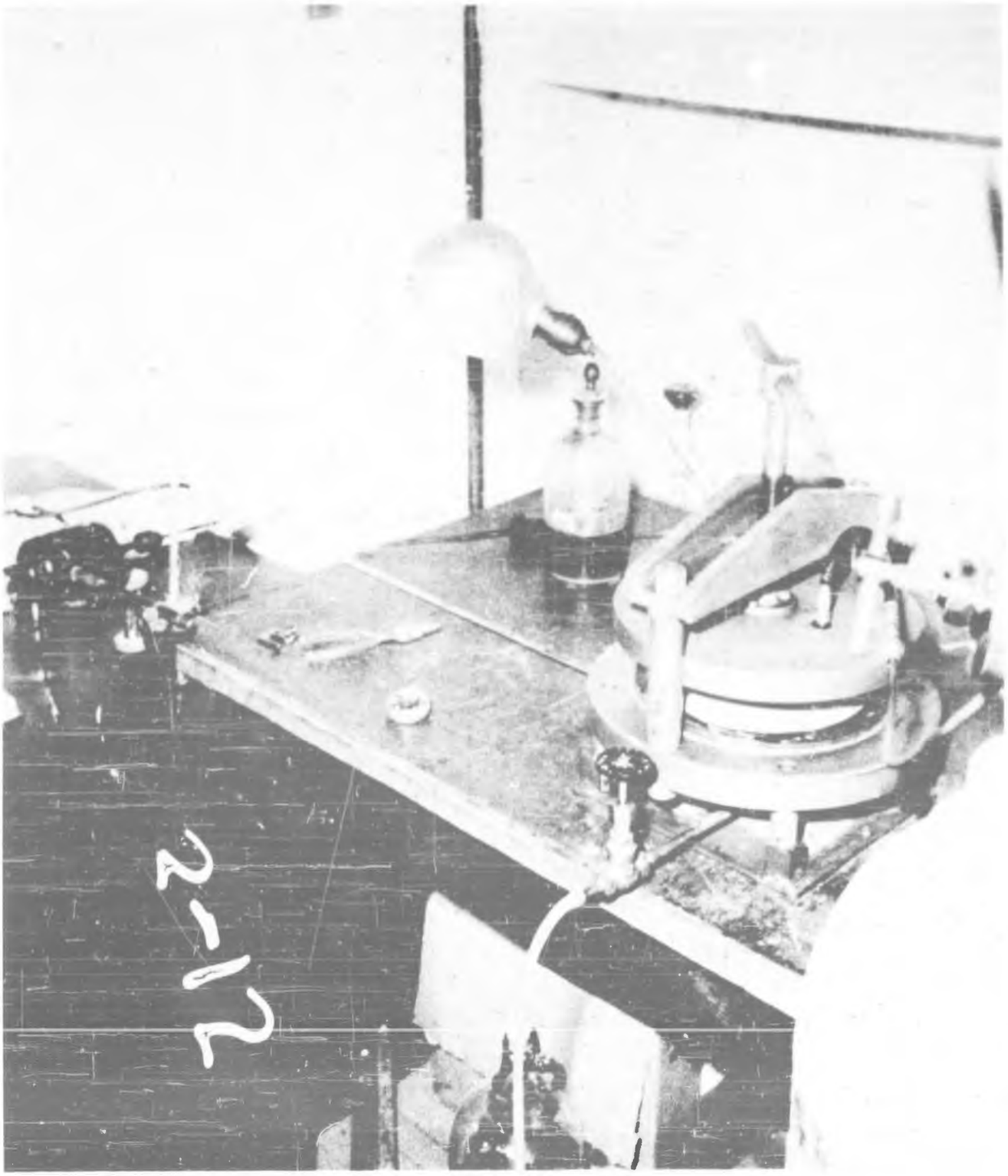

PLATE 4 --- Permeability Tester used for quantitative leakage tests.

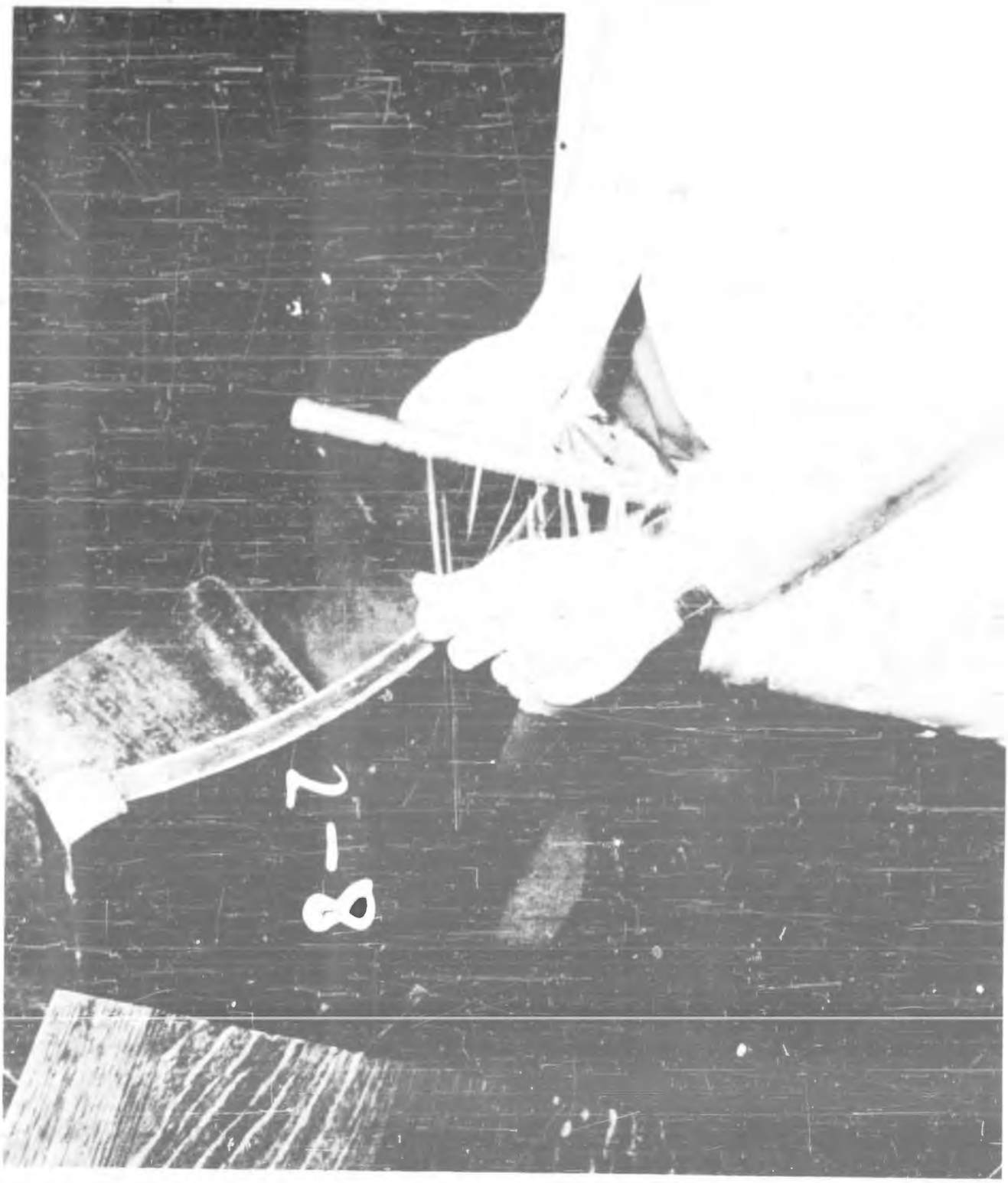

PLATE 7 -- Drawing of "Mylar" to measure resistance to abrasion.

PLATE 8 -- Selenium Sulfide print of good sample of "Mylar"

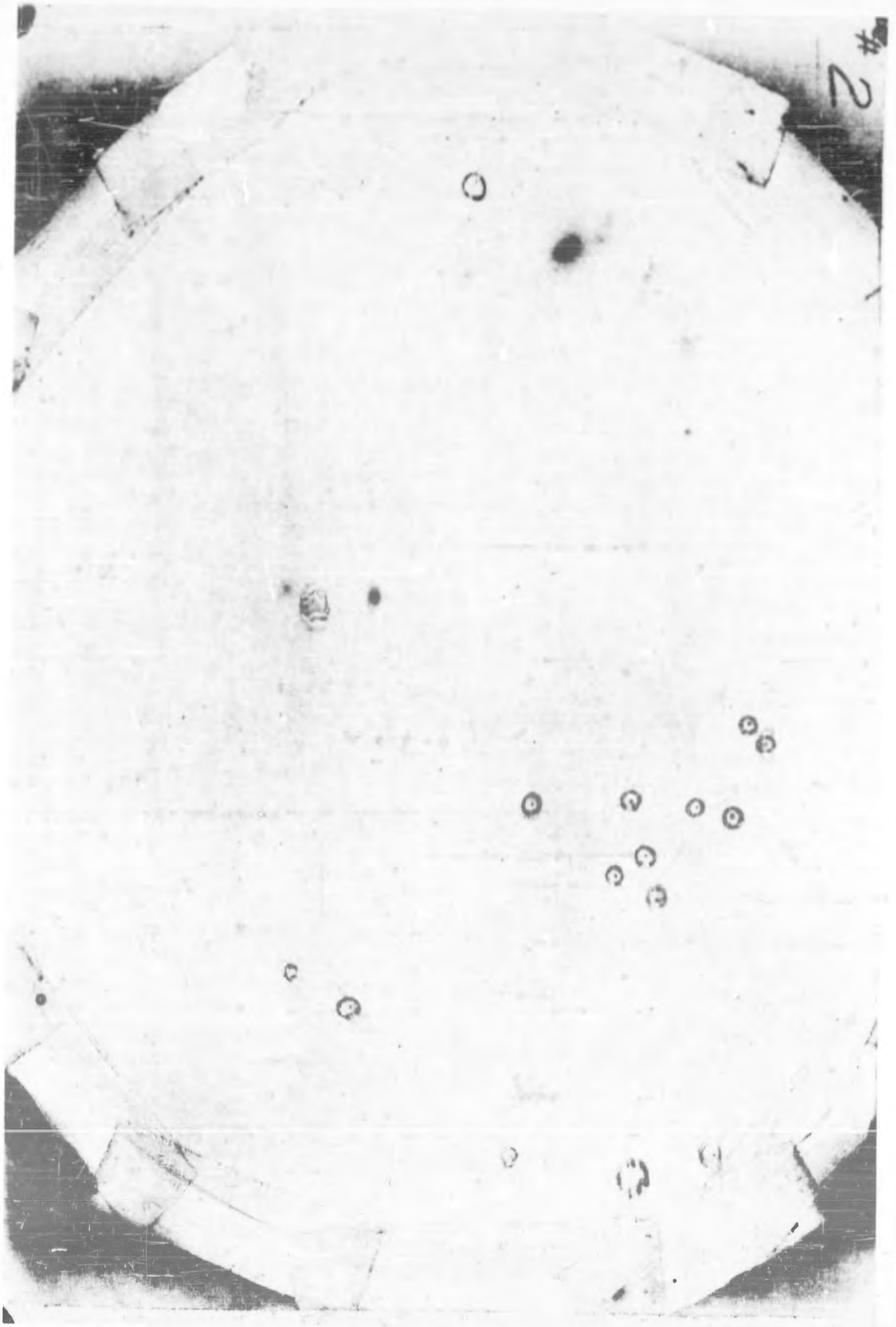

PLATE 9 -- Selenium Sulfide print of bad sample of "Mylar" showing pinholes (circled)

PLATE 10 -- Selenium Sulfide print of bad sample of "Mylar" showing pinholes (circled).

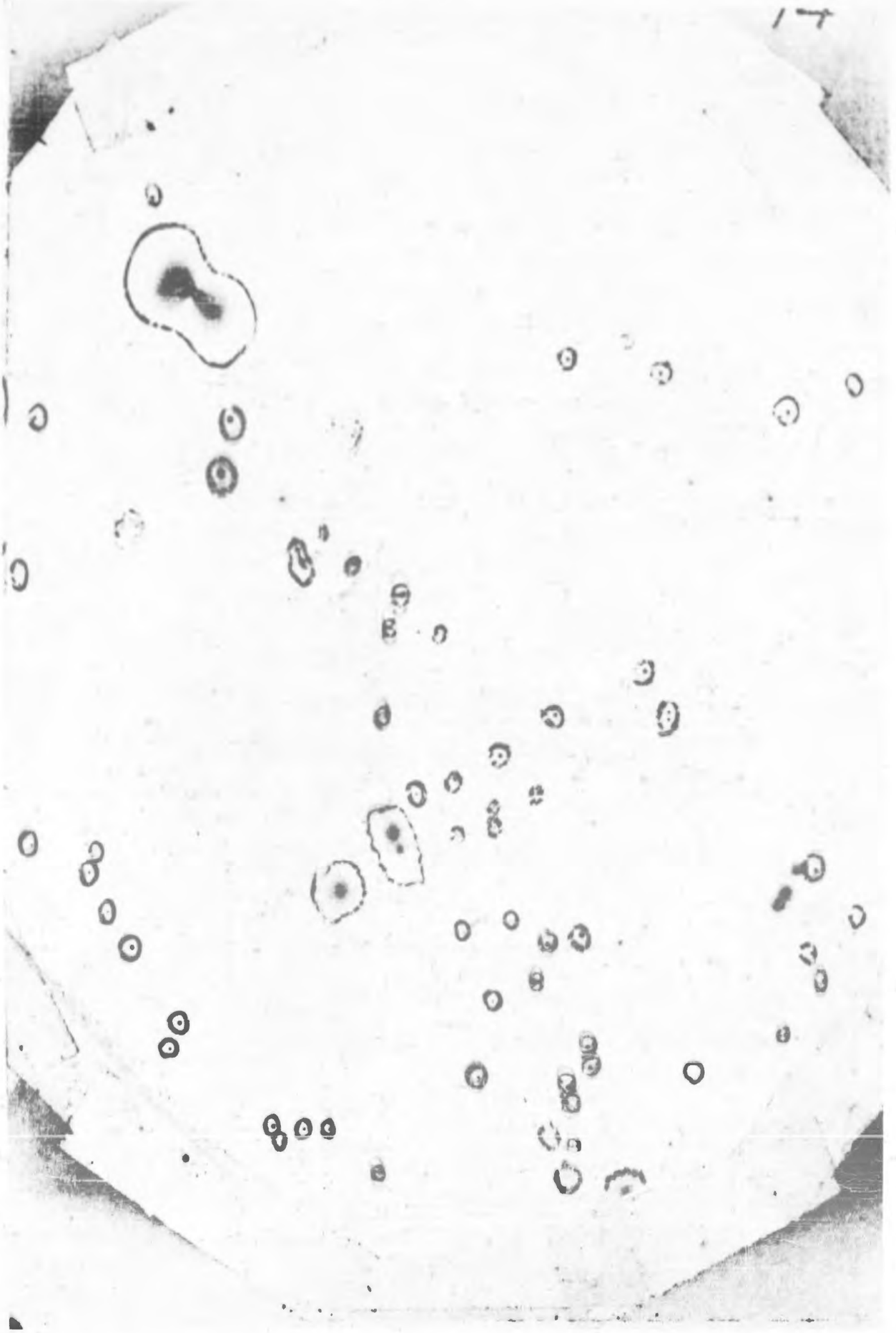

PLATE 11 -- Selenium Sulfide print of good sample of "Mylar" which had been treated by rolling and made to leak.

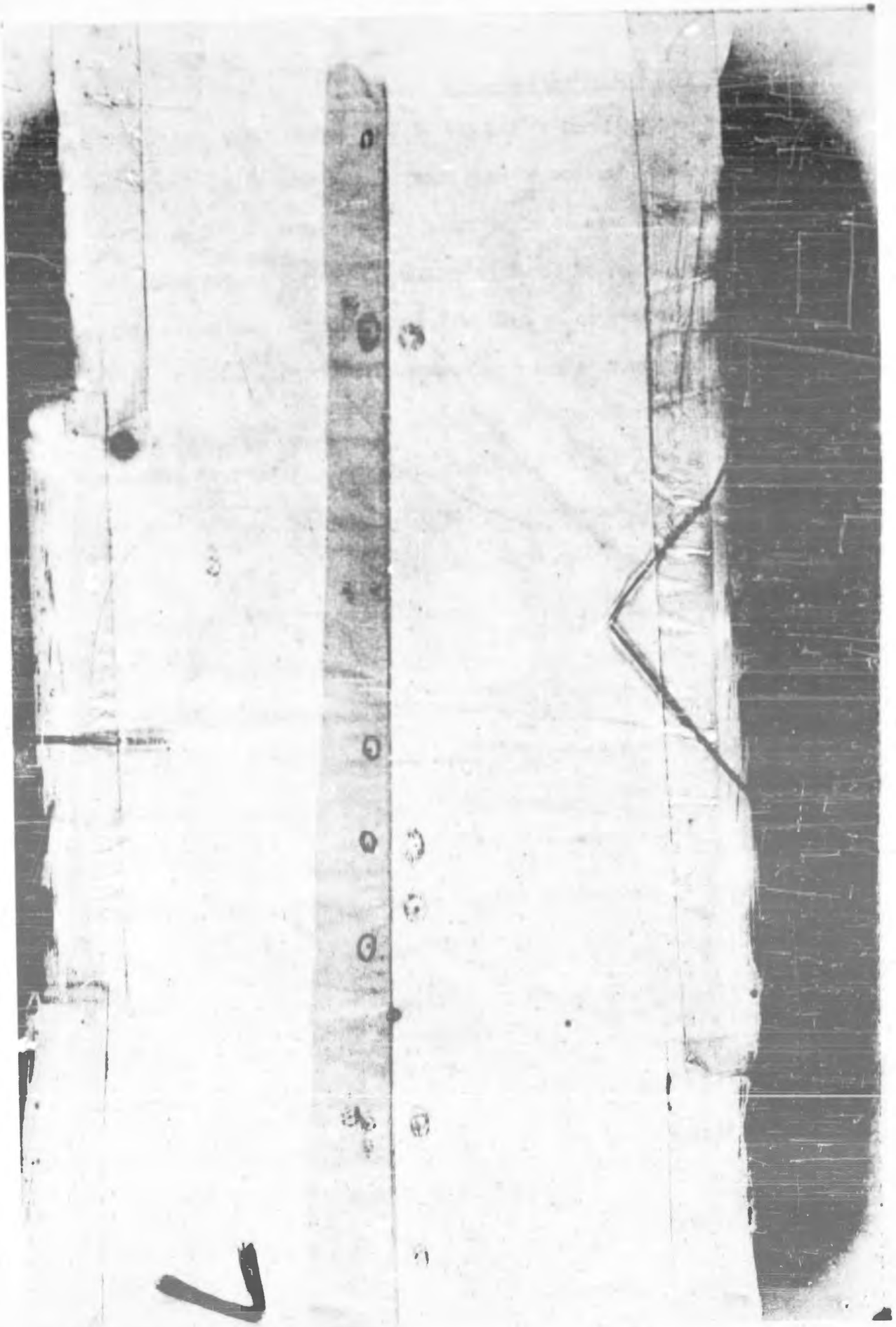

PLATE 12 -- Selenium Sulfide print of seal made by Herb-Shelly, Inc. (Pinholes are circled).

C. Superpressure Trajectory Balloons

The five test balloons at the end of the leakage study showed the small superpressure balloon to be a production possibility. Specifications for a balloon capable of carrying a down camera at 300 mb were made. These balloons, of about 360 cubic ft, closely approximated the test cells. They were to be made of 1/2-mil material and tested individually for leakage rate and superpressure strength.

These balloons were made to a nominal 14-ft gore length. At each end, the double ring end fittings were installed. Three-inch aluminum rings of 1/4-inch material were used for these. After the rings were installed, the measured gore length averaged about 13'2".

In the manufacture of this balloon a bubbler can is clamped in the fabric at its base with a hose clamp. The trimmed fabric edge beyond the clamp is sealed with Scotch Kote, a Minnesota Mining and Manufacturing sealing compound. In a similar manner, the top end of the fabric is clamped and sealed. The balloons, complete with harness and top line, weighed about 2 lbs 14 oz.

The bubbler can serves as a safety valve in flight. The center tube, clamped and sealed to the fabric, is immersed in a liquid contained by the outer can. Internal pressure in the balloon changes the levels of the liquid and at a maximum pressure the liquid levels will change enough to allow the gas to bubble through and escape. An inflation tube is also provided in this fitting to facilitate inflation of the balloon while there is liquid in the can. This tube is sealed with a cork after inflation.

Every balloon is pressure and leak-tested at the manufacturing plant before delivery. The maximum leak rate allowed is a superpressure drop

from 4 millibars to 1½ millibars in two hours. Of the first 25 balloons tested, all but one met this specification. After this test, the balloons are deflated and boxed for delivery.

By measuring the ambient pressure and temperature under test conditions, as well as the lift of the balloon, the volume can be quite accurately determined. This takes much of the guesswork out of calculating the floating altitude. A form has been devised to compute conveniently the weight to be added to bring the balloon and gondola down to the desired altitude. Because the balloons float according to density altitude, the pressure altitude will depend somewhat on atmospheric temperature. To date, the altitudes seem to come out quite close by assuming standard temperature. One peculiarity noted in some of the time-altitude curves is a slight drop in altitude after an hour or two of floating. Whether this is due to atmospheric conditions or balloon performance has not been determined.

For the flight, kerosene or Skelly "S" solvent is used in the bubbler can instead of the water used in testing. Care must be taken in order that the liquid does not spill in inflation or launching. Ten ounces of kerosene limits the maximum pressure to 4 millibars.

The balloon is inflated through the small tube in the bubbler can, and a vertical weigh-off made. A 1 3/4-lb free lift gives a rate of rise of approximately 500 ft/min. If it is necessary to inflate in limited vertical space in order to keep out of the wind, the top may be tied down temporarily to the base of the balloon with the top line. The balloon can be weighed off in this manner, and the top is released just before launching.

Of the 25 balloons tested and flown, two are known to have failed during the ascent. This is difficult to account for unless damage was made during deflation, packing, inflation or launching. With the exception of these two,the results have been very promising. One balloon which barely made minimum specifications floated at ceiling altitude for five hours, coming down in the latter part of the afternoon. Others have been observed to come down after sunset.

The initial superpressure of 4 millibars is normally sufficient to maintain good altitude control on these balloons during the daytime, but is not nearly enough to take care of sunset. To do this, something like 15 millibars superpressure would be necessary for this balloon system. This being greater than the material strength, changes in the direction of a larger balloon with thicker film, or a decrease in load, would have to be made.

D. Glue Program

Encouraging flight results from Mylar balloons, except for low shock resistance of the seals, provided the incentive to keep on the lookout for other means of fabricating Mylar. Glues tried previously had not held satisfactorily and the only solvent known for Mylar, carbolic acid, was too toxic to consider for this application. Pressure-sensitive tapes, which were heat-cured after application, showed promise until they were given a cold test. At low temperatures these parted from the plastic material quite readily.

It was not until August 1953, when a pouring resin (used in our shop for coating Olland Cycle drums) was tried as a glue, that it appeared

feasible to bond Mylar with an adhesive. Sample lap seals ½-inch wide had a seam strength stronger than the ½-mil parent material. They seemed very good in shock loadings and their strength was not affected by extremely low temperatures. The resin seal had two qualities that might be considered disadvantageous. The first was that the peel strength was quite low. Under a peel force, one or the other of the two Mylar sheets would separate easily. The other bad quality was that if there was a buildup of resin, as between wrinkles of material, the thick resin would be brittle after setting. When folded it would crack and very likely fracture the Mylar. Thick spots in the seal were consequently avoided in manufacture by using flat, stretched material.

Shortly after this adhesive was found, facilities were set up in the the Physics Building to glue together a 14-ft gore length superpressure cylinder balloon. Ten seals were made of this length in an average time of slightly less than 30 minutes for each. This time included the laying out of material, mixing of the resin, application of the resin, and forming the seal. The successive seals were stacked one on top of the other on the table, and were allowed to set for 24 hours. As the resin is very fluid before setting, it conforms to slight wrinkles in the material. An inspection after the seals were made disclosed several spots like this where the material was wavy. In some of these places there was insufficient resin to contact both surfaces and small channels or leaks resulted. These were plugged with additional resin. After these had set the ends were pleated and the end fittings installed. The top end was closed by sealing in a cup of resin. A bubbler can safety valve was installed at the lower end.

Under a superpressure inflation test, the pressure dropped from 4.1 millibars to 1.5 millibars in 2½ hours. In comparison with other tests this was good, with but slight leakage. This balloon was deflated after the test and flown on September 24. After climbing to altitude it leveled off and held a very constant altitude for two hours and 30 minutes. This balloon was subsequently recovered and diffusion-tested. Samples of a number of seals showed them to be excellent gas barriers after the flight.

Efforts were made in the direction of the possibility of super-pressuring out sunset by going to 1-mil material and a 22-ft gore length balloon. The process of assembling these balloons is illustrated and described in Figures III-14 to III-37. (See E, this section.) When the first 1-mil balloon, designated UM-2, was test-inflated, it was noticed that gas was being lost around the end fittings. Apparently the rough handling required to pleat the ends and squeeze them into the end fittings had separated some seals. It seemed that the loose flaps beyond the lap seal might provide a starting place for peeling.

On the next balloon, UM-3, the adhesive was applied wide enough to include both edges of material. This made a more trustworthy seal. In inflating this balloon, one of the aluminum end fittings failed in a poor weld at about 4 millibars superpressure.

The double ring end fittings, which we knew had adequate strength, were used on UM-4. The end seal in the resin cup was made at the extension of the material beyond the rings. The additional amount of plastic folding required for these was apparently too much for the glue seals on the heavy 1-mil material and leaks resulted between the rings and the end

fittings. In further efforts to prevent leakage in this region, that part of the seal which was woven through these rings was covered with tape to prevent separation of the glue seal. This was only partially successful.

To broaden experience in the development of glued Mylar balloons, the University informed the balloon manufacturers of this work and at the same time requested bids on the manufacture of two large 225,000 cu ft balloons of ¼-mil Mylar.* For light load high altitude work, a balloon of this size would compete favorably with the 3 million cu ft "Super Skyhook". Each could lift its own weight to approximately 125,000 ft.

The relatively long setting time and low viscosity of the resin has given some trouble in manufacturing. Any resin which runs onto the wrong fabric adheres well enough to cause a hole upon separation. Also if there is too thick a layer of resin it may crack upon folding and fracture the material with the sharp broken edges.

The use of additives to result in a more pliable resin is being investigated. Early tests show an increased setting time for these mixtures which is not the most desirable from the standpoint of manufacturing.

There is another area in which adhesives may be advantageous over heat sealing. So far heat seals have been successfully made only in straight lines. This has limited all balloons to the cylinder design Theoretically, a sphere can be superpressured twice as much as a cylinder. A possible way to obtain a spherical balloon of curved seams is with a glue adhesive. This would make possible a balloon with material stressed in two directions.

---

* See Appendix D-1, this section.

An order was placed with General Mills for the manufacture of two 10-ft spherical balloons of 10 gores each. The development of a spherical shape from flat sheets of non-extensible material will result in lap seams which will always have wrinkles; that is, the two sheets forming the lap will not lie flat with respect to each other. This, of course, added to the difficulties of glueing with the slow-setting low-viscosity adhesive. Two spheres were made, and although somewhat patchy in appearance gave evidence of what could be expected with the sphere balloon. Under pressure it became obvious that this sphere, developed from flat sheets, did not become stressed the way that a true sphere surface would. Transverse wrinkles across the seams appeared which indicated that the stress at this point was in only one direction. Actually then, the theoretical advantages of a sphere over the cylinder balloon could not be realized with flat Mylar film. A burst test of the first balloon occurred at a theoretical stress of 1,670 psi in the fabric, or 13% of the material yield strength. Failure occurred at the seams, so this does not represent the material stress limit. Judging on the manner of wrinkling, the upper strength limit with perfect seams would appear to be about 50% of the material strength. If this is true, there is no real advantage in going to a small spherical shaped balloon with a small number of gores, for the superpressure limit will be approximately that of an equivalent cylinder balloon.

APPENDIX D-1

October 20, 1953

To: General Mills, Inc.
Office of Naval Research
Herb Shelly, Inc.
Winzen Research, Inc.

From: Department of Physics, University of Minnesota

REPORT ON SEALING METHODS FOR MYLAR

The University of Minnesota in connection with their HAB research contract has investigated various means of sealing polyester film, "Mylar". Because of the high strength and the fact that Mylar can be extruded as thin as ¼ mil, it possesses very great advantages for some balloon applications. In addition to this it has been shown to have low temperature properties very much superior to polyethylene. In fact, the low temperature properties are so good that they are not a factor.

Three methods of manufacturing balloons from Mylar are being considered: the heat sealing method; taping with pressure sensitive tapes heat cured; and a glue seal utilizing polimerizing glue. The first method, heat sealing, is being studied under sub-contract by Herb Shelly, Inc., Farmington, and at the moment no final conclusions can be drawn on this subject. The method of sealing with pressure sensitive heat cured tapes produces a very adequate seal at room temperature but unfortunately this seal does not have the required low temperature properties for a balloon. The principal purpose of this note is to describe the third method of sealing, namely sealing with polimerizing glue. A number of seals have been made in our laboratory and one balloon constructed with these seals was satisfactorilyflown under superpressure. The seals have adequate

strength so that when test tube cylinders were made utilizing these seals, the failure under pressure occurred in the Mylar rather than the seal. The seal is extremely good at low temperature and can be immersed in liquid air without degradation. The only possible disadvantage of this seal is that when the glue does not completely come out to the edge of the Mylar it has a relatively low tear resistance. However, its shock resistance is high, its static strength is high and we believe that it is a completely adequate way to assemble Mylar into a balloon shape. A number of these glue seals have been tested for leakage. The one balloon which we constructed and flew was a ½ mil Mylar cylinder flown under super pressure corresponding to a tension in the material of 5000 pounds per square inch. The balloon floated stably at ceiling and was recovered and returned to us. Upon examination after return, the balloon having been bundled into a box, we found two tears in the balloon, presumably acquired when it landed. Neither of these tears was in the glue seals and, in fact, all nine of the glue seals on this balloon were intact after flight recovery and return to us. To make a quantitative test of the leakage, the center section of this balloon was cut out and 23 samples were tested for leakage. Thirteen of these samples had seals in them and 10 were samples from the material itself. Of these 23 samples, 20 showed leakage not exceeding diffusion leakage of the material. Of the three that leaked, two were material and the third was a sample which had a glue seal in it. Since the samples tested are about a foot in diameter, one would expect that if the material leaked, essentially as many leaky samples would be found with glue seals in them as without, so the indication we believe is that the leakage obtained on these samples is consistent with material leakage alone.

In our method of application of this glue seal to cylinder balloon construction, the glue is applied in a line along the material and the next sheet of material was flipped down over the glue seal. The surface tension of the glue causes it to pull the material down and create a very transparent and continuous seal. The adhesive that is used is a bakelite plastic no. BR 18774 with a bakelite hardener no. BRR 18812 which may be obtained from the Bakelite Company, Boundbrook, New Jersey. It is a polimerizing material and must be mixed in the following way: two and one-half parts of plastic by weight to one part of hardener by weight. The seal must cure for 24 hours before the full transverse strength is acquired.

Accompanying this note on seals is a request "For the construction of two 225,000 cubic foot $\frac{1}{4}$ mil Mylar balloons". This request for bid contains detailed specifications on this balloon.

E. Photographs

Figure Number	Title	Page
III-2 to III-10	Launching sequence of 45' Mylar Cylinder	III-137 - III-145
III-11	Four trajectory balloons readied for flight	III-146
III-12	14' gore length balloon airborne with its load.	III-147
III-13	Small glued Mylar sphere, 10-gore balloon.	III-148
III-14 to III-37	Fabrication sequence of Resin Adhesive construction	III-149 - III-160

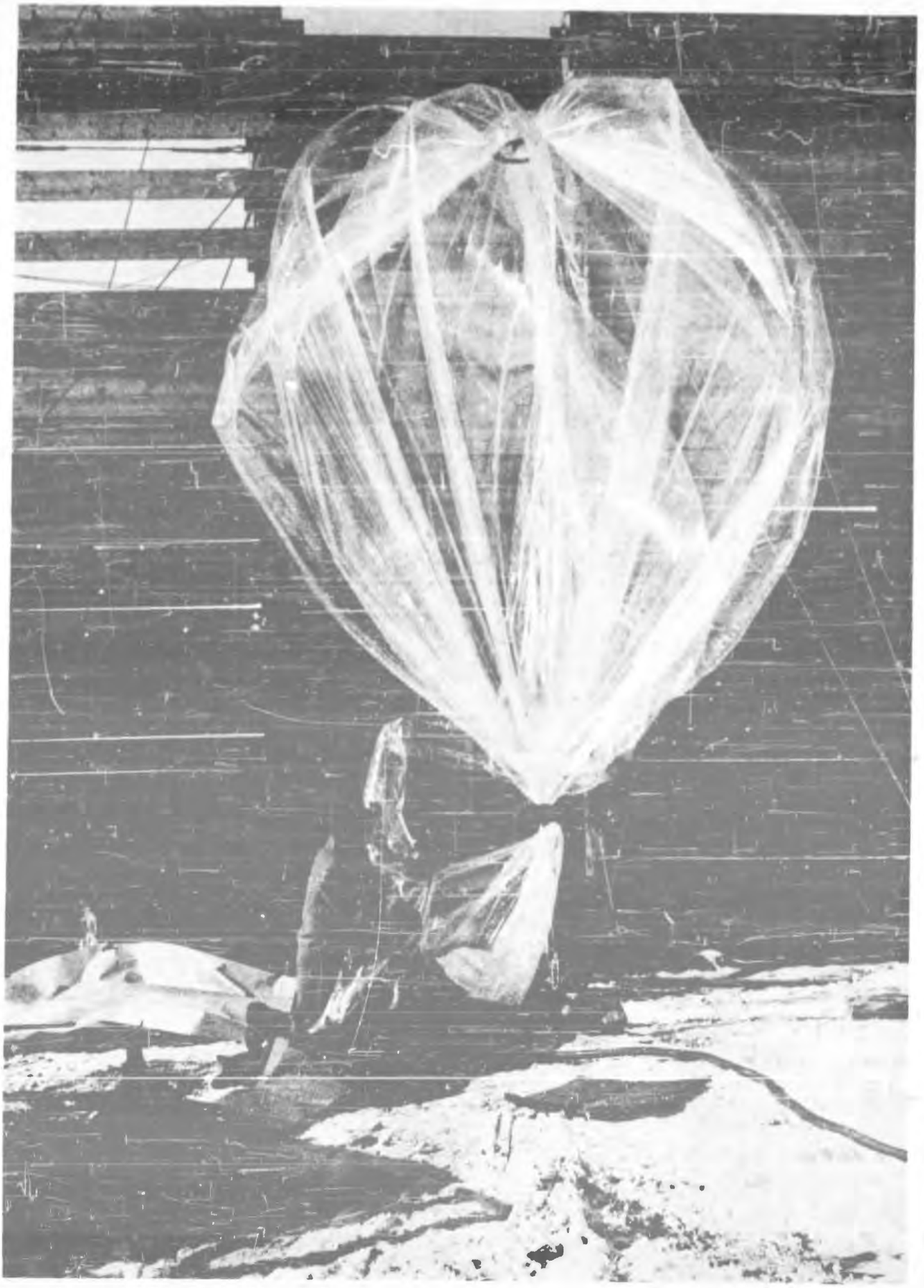

Figure III-2. Launching sequence of a 45' Mylar cylinder balloon. Top portion of balloon is inflated through duct. Material is held below bubble by a temporary tie to which weigh-off weight is attached.

Figure III-3. After the weigh-off the temporary tie is removed and the balloon is allowed to become vertical, controlled gently in a hand-over-hand manner.

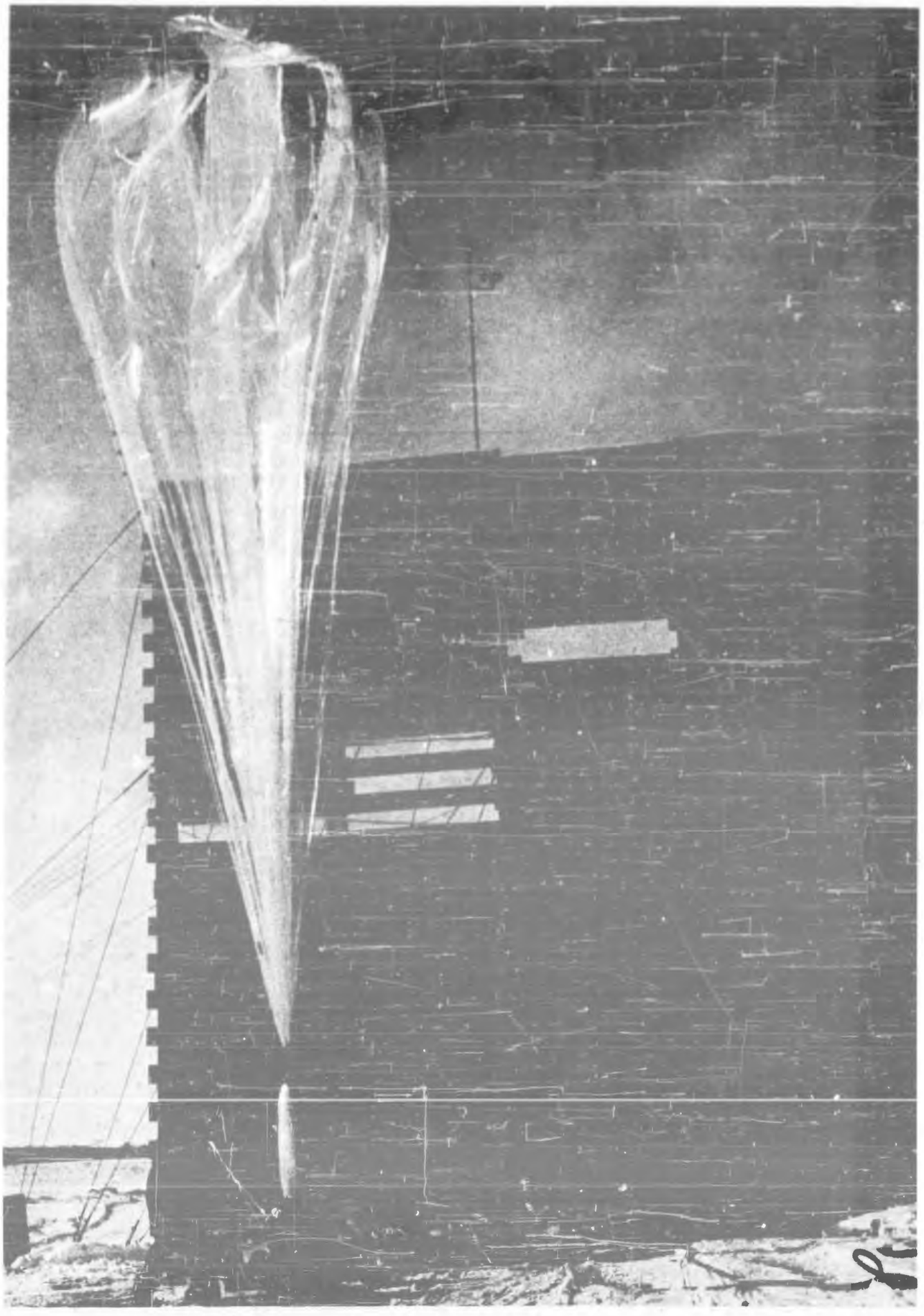

Figure III-4. The fully extended balloon is erected until it is over the gondola.

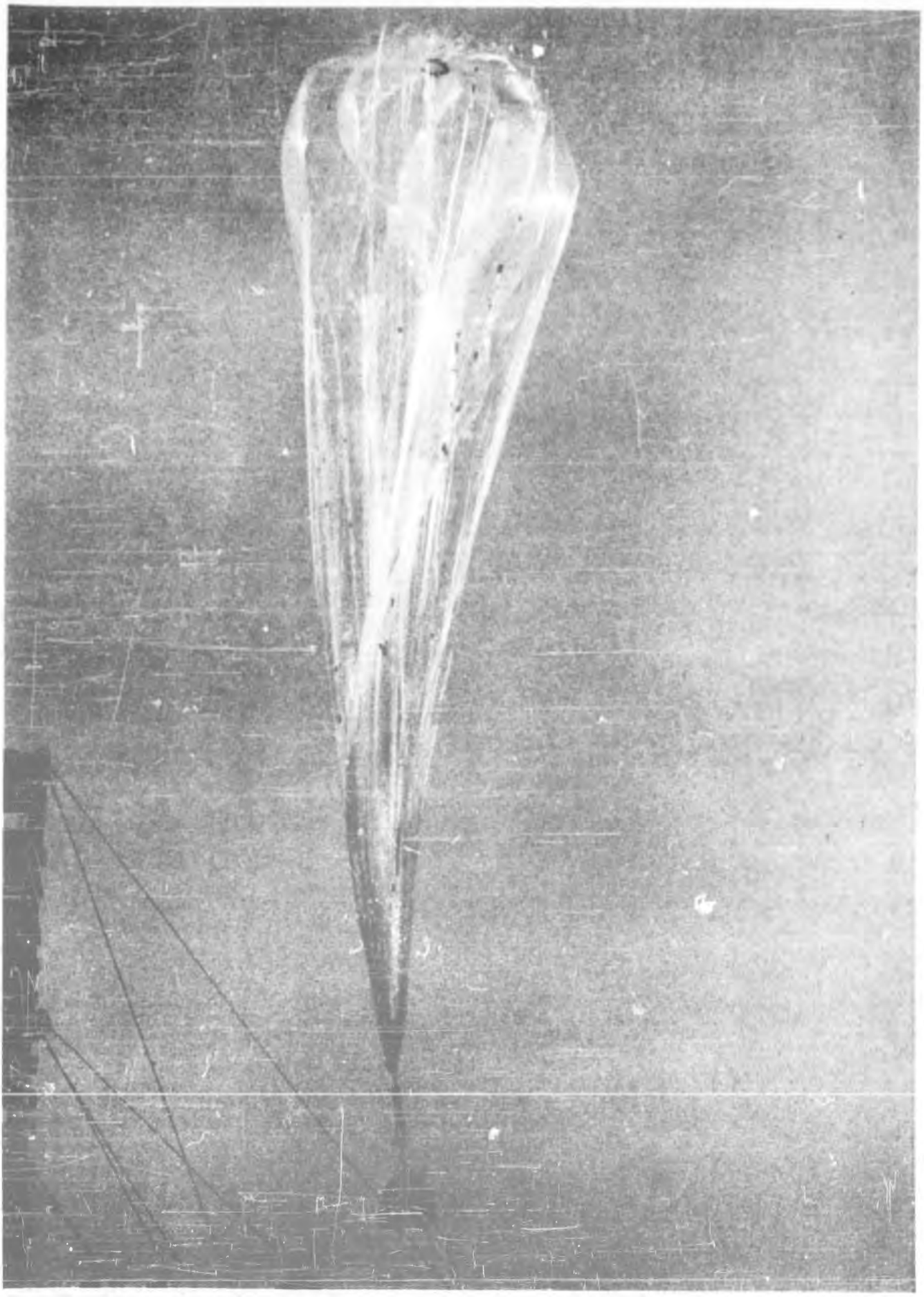

Figure III-5. The balloon and gondola are airborne.

Figure III-6. Superpressure test of (M-7) a 45' cylinder balloon. The seal orientation indicated by the presence of the seal test tubes is in line with the tension forces from the superpressure. An air inflation of 1.10 mb produced a total longitudinal force of 2200 lbs in the 1/4 mil fabric before failure. This effectively simulates flight stresses for the same superpressure.

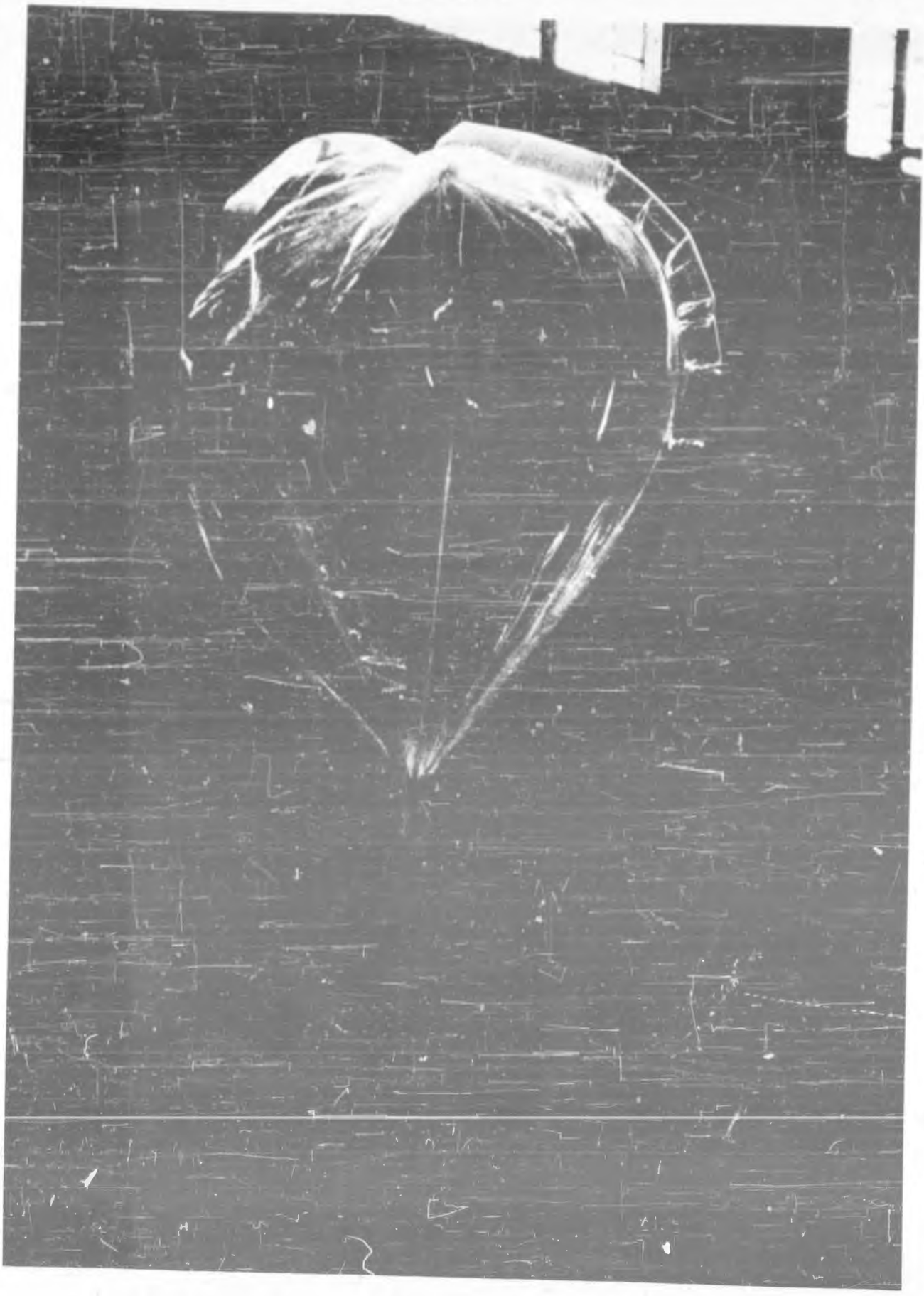

Figure III-7. The Mylar cylinder balloon of 14-ft gore length is shown inflated to a subpressure of .15 balloon height.

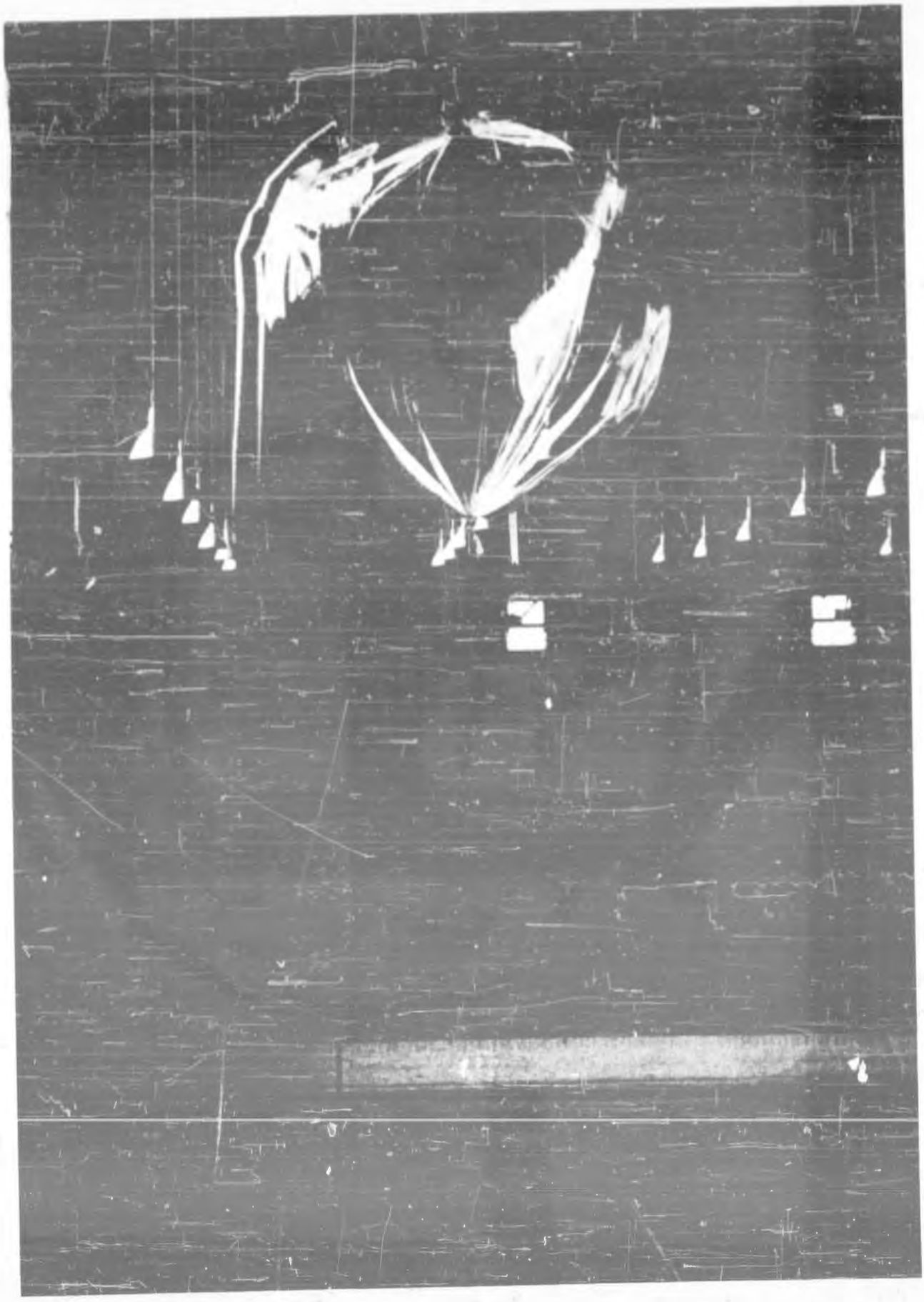

Figure III-8. With further inflation, the volume increases at .5 balloon height superpressure. The pressure level is evident by the inflation in the duct.

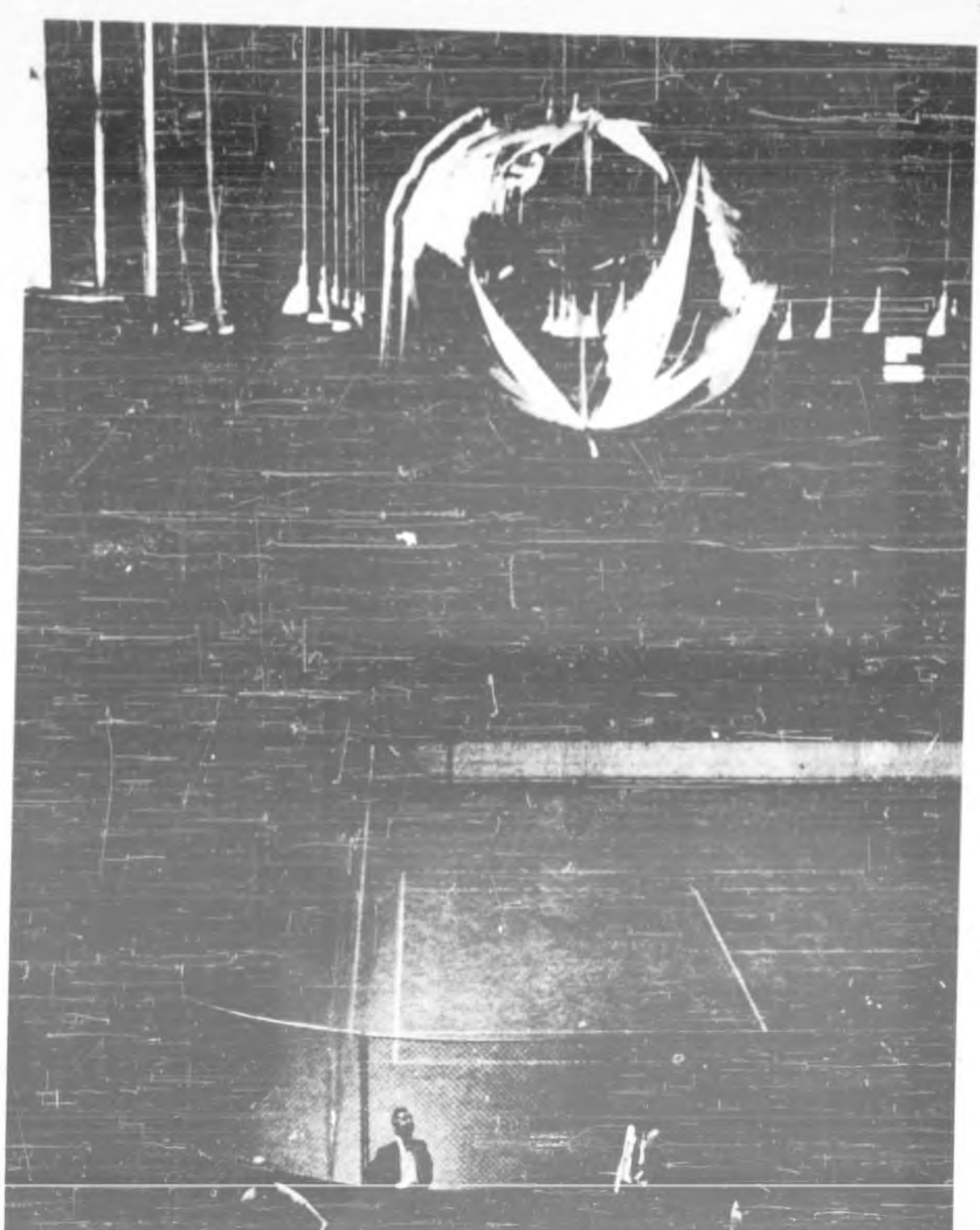

Figure III-9. As the pressure is increased to two balloon heights, the final shape and volume are very nearly approached.

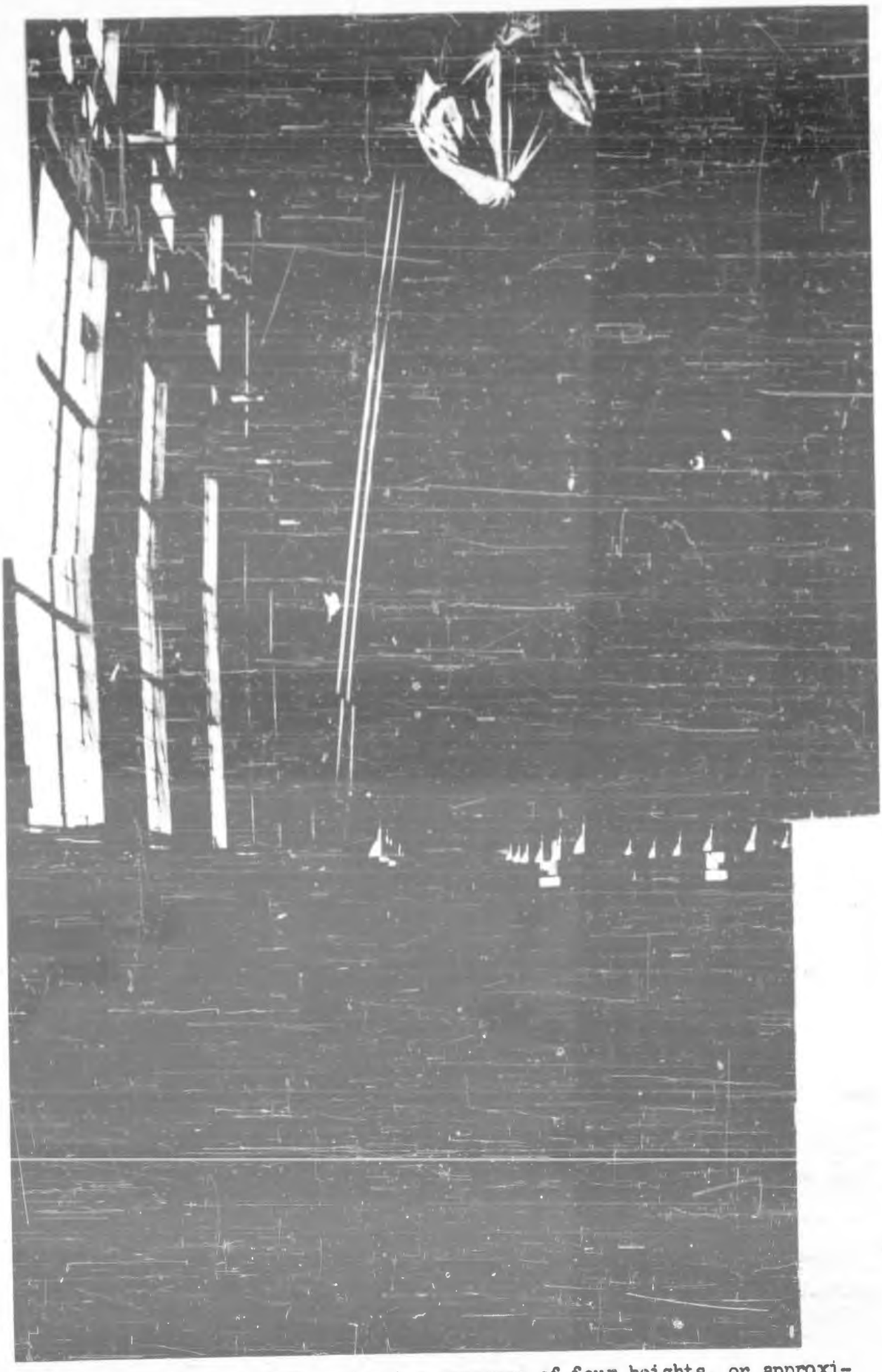

Figure III-10. The balloon is at a pressure of four heights, or approximately one millibar at the ground level. To produce 4 millibars superpressure at 300 millibars pressure, the duct length required is 300 ft.

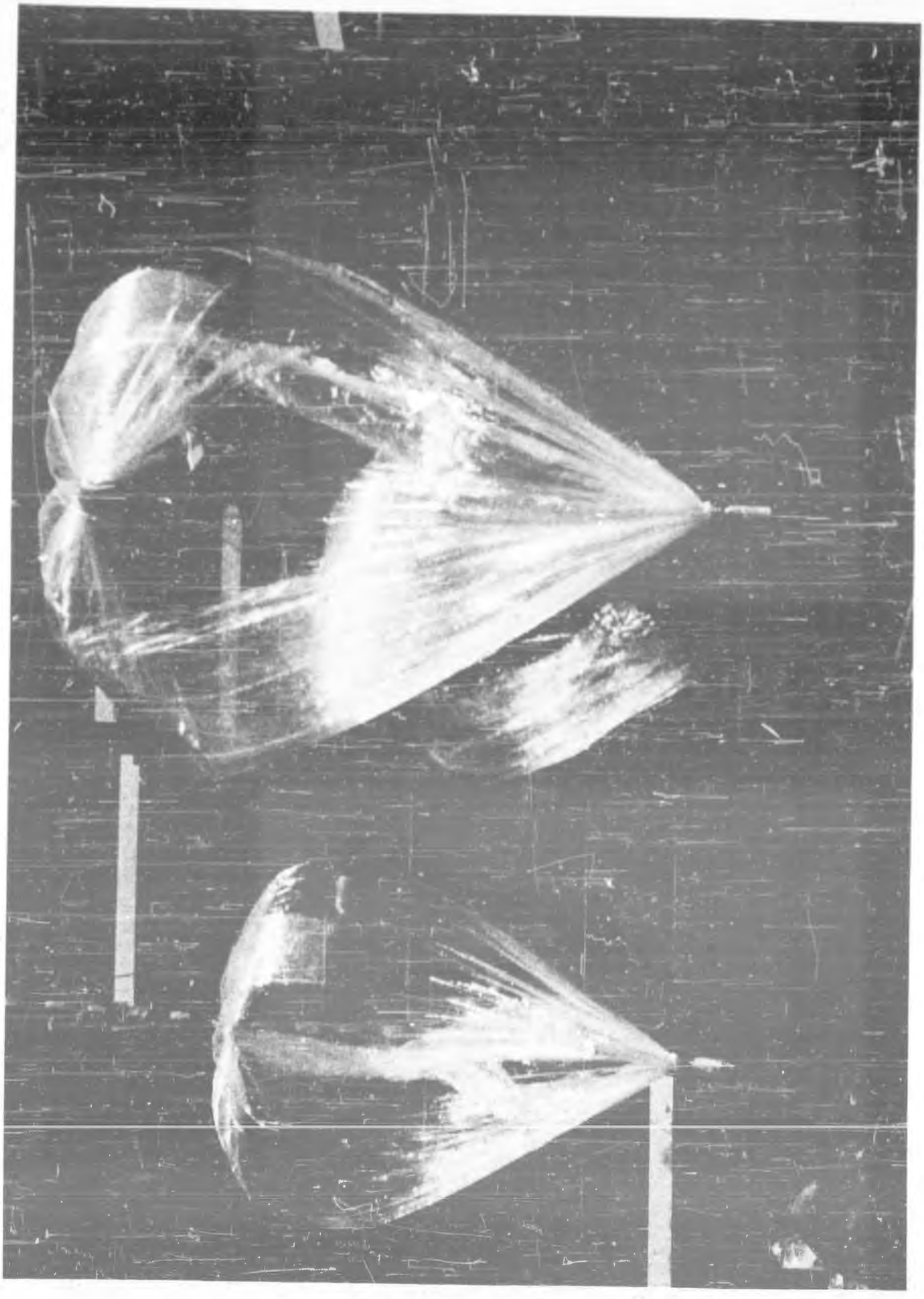

Figure III-11. Four trajectory balloons are readied for flight. Each is weighed down to float at a specific level.

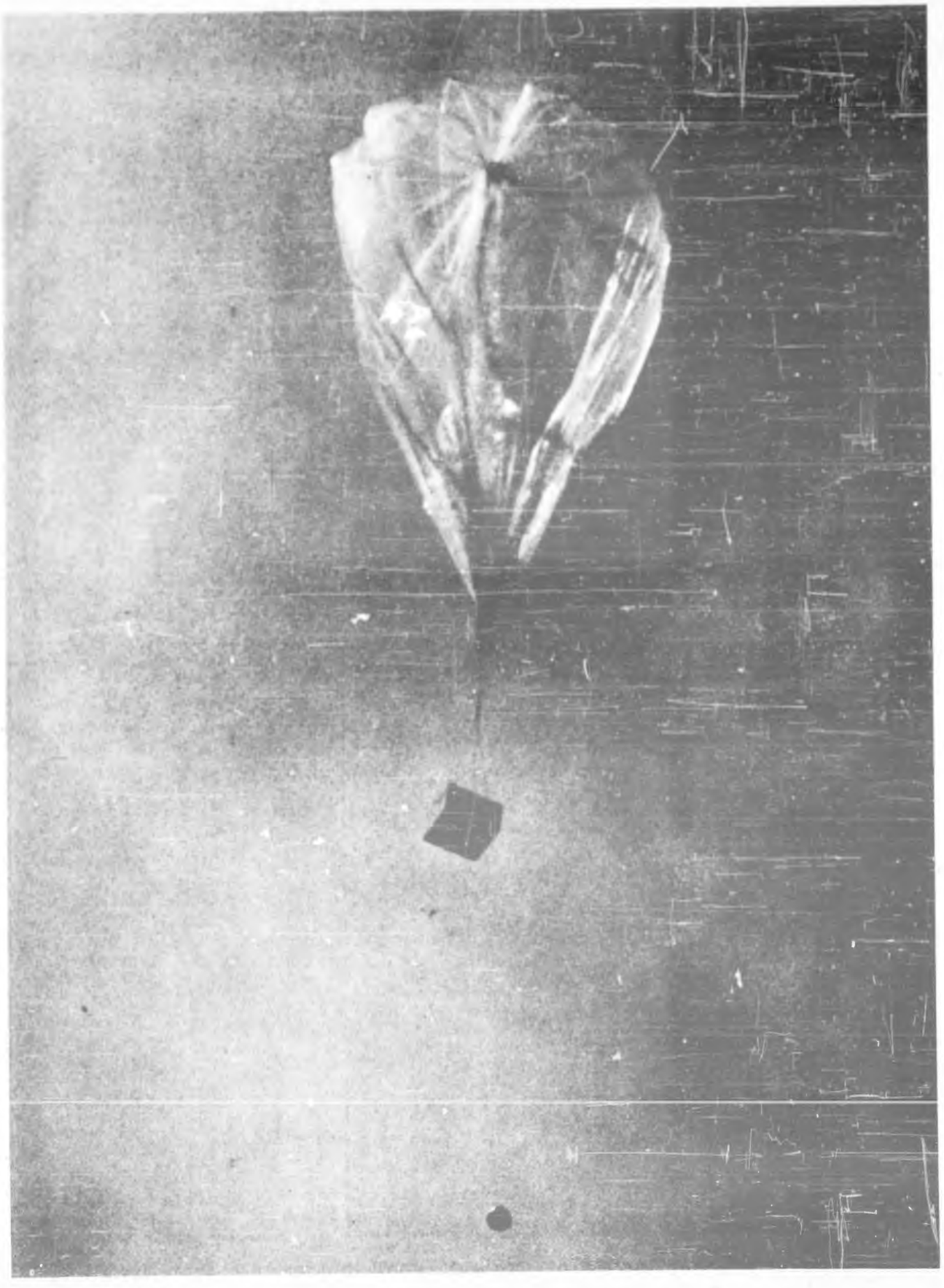

Figure III-12. The 14' gore length balloon airborne with its load. At 300 mb it will be fully inflated and held at 4 mb superpressure by the liquid levels in the bubbler can.

Figure III-13. The surface of the small glued Mylar sphere shows that in the 10-gore balloon the tensile stress does not occur in both directions all over the surface. Ripples down the seals indicate zero tension in this direction. Consequently, the full strength of the material cannot be used in this case, and the efficiency of the use of the fabric is no greater than in the cylinder balloon.

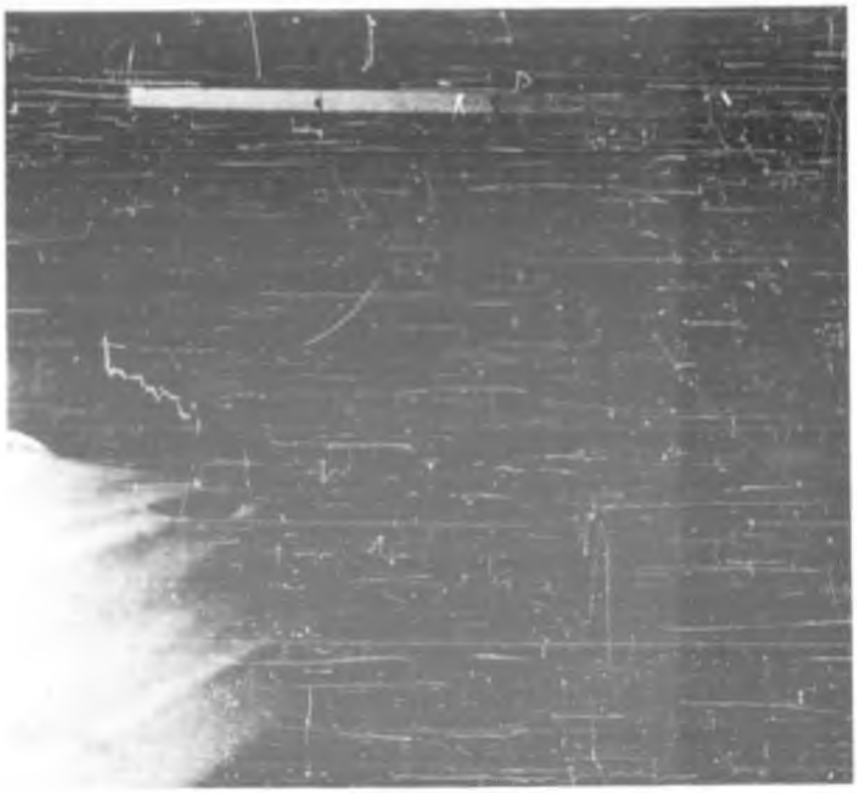

Figure III-14. The roll of material and a roll of wrapping paper are placed in position at one end of the balloon table. Two cutters are positioned to cut the paper into 8" strips. These strips are used as straight edges and separators for the Mylar seams.

Figure III-15. Near the free edge of Mylar from the previous gore, a paper strip is taped in place. The edge of the paper serves as a guide in folding the Mylar back for the next seal.

Figure III-16. The Mylar is folded over the paper and taped in position. Wrinkles are pulled out when both ends are taped simultaneously.

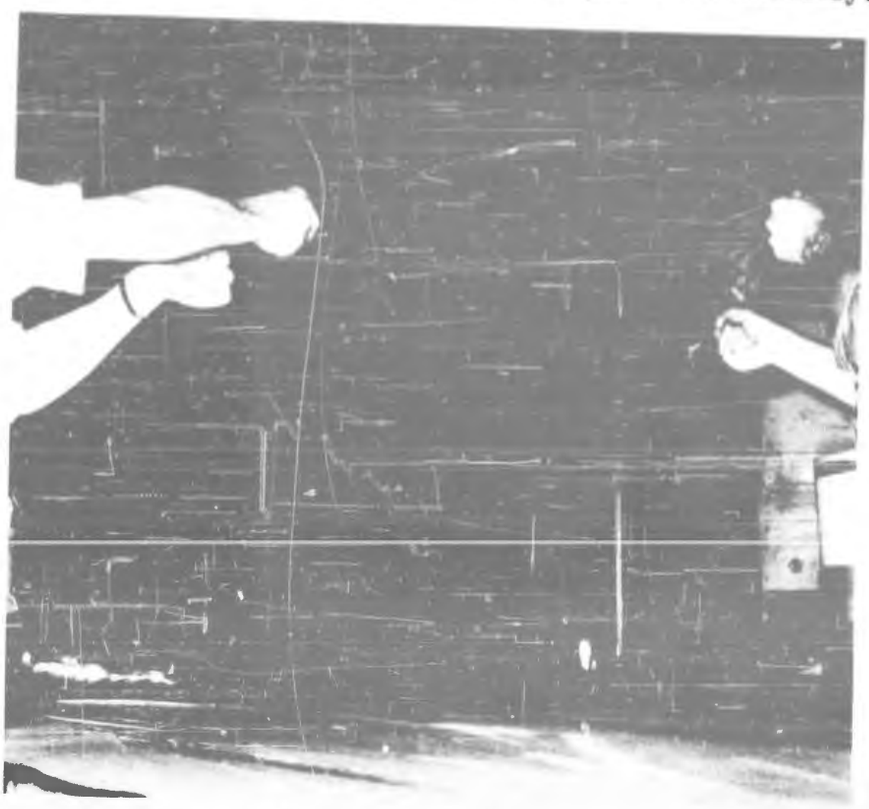

Figure III-17. Material for the next gore is unreeled from the roll, cut to length, and taped to the table so that it laps the previously folded edge by a seam width (about $\frac{1}{2}$ inch). This edge is then lifted up and folded back about two inches so the adhesive can be applied.

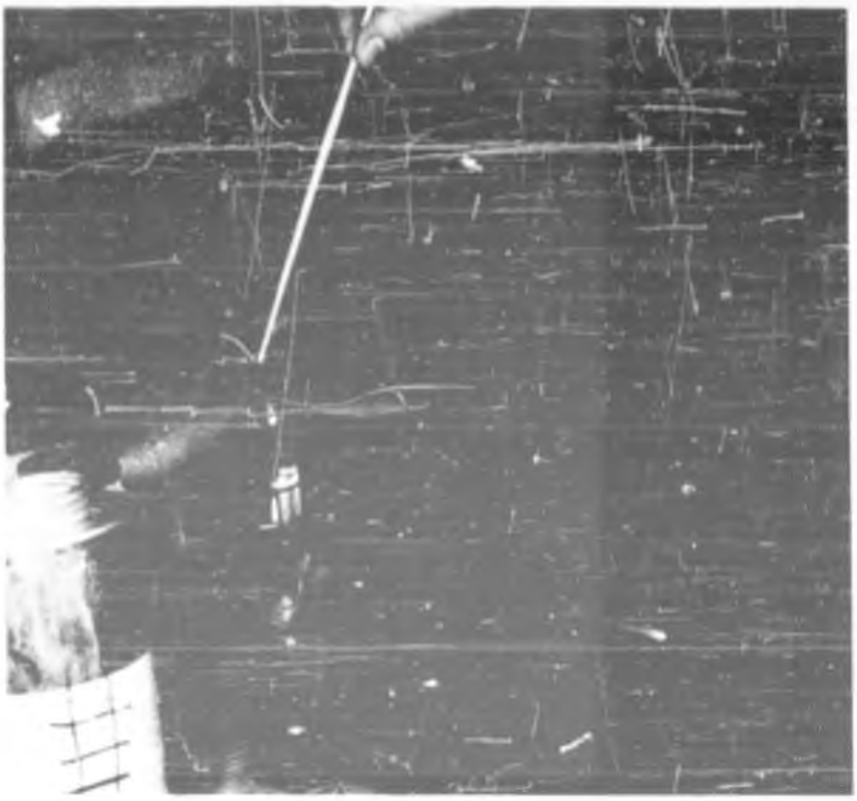

Figure III-18. The resin and hardener are mixed in the ratio of 2½ to 1. Small quantities are mixed at a time so the mixture can be applied before it sets. The quantity of resin shown is sufficient for three seals, which can be made within 1½ hours.

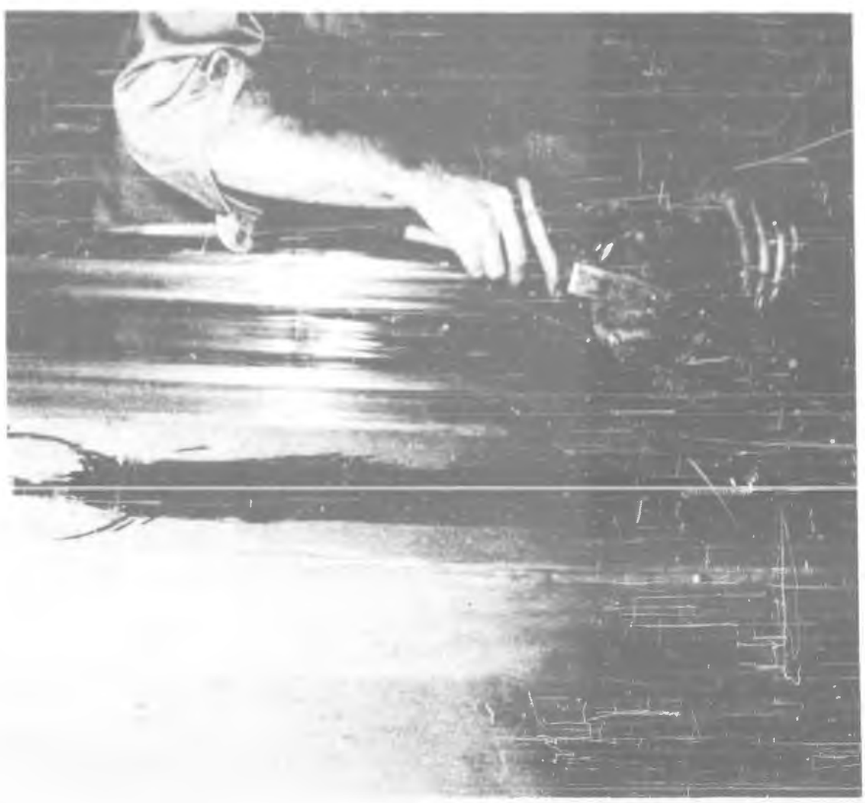

Figure III-19. A 3/8" wide rubber roller is first wetted with the resin, on a piece of paper (foreground), and then is rolled over the Mylar edge to be sealed.

Figure III-20. The edge is folded back and tipped up until it "flips" down in place on the adhesive. At this point the seal is carefully inspected for wrinkles which may form air channels through the seal. Large bubbles trapped by the seam are individually run to an edge by finger pressure.

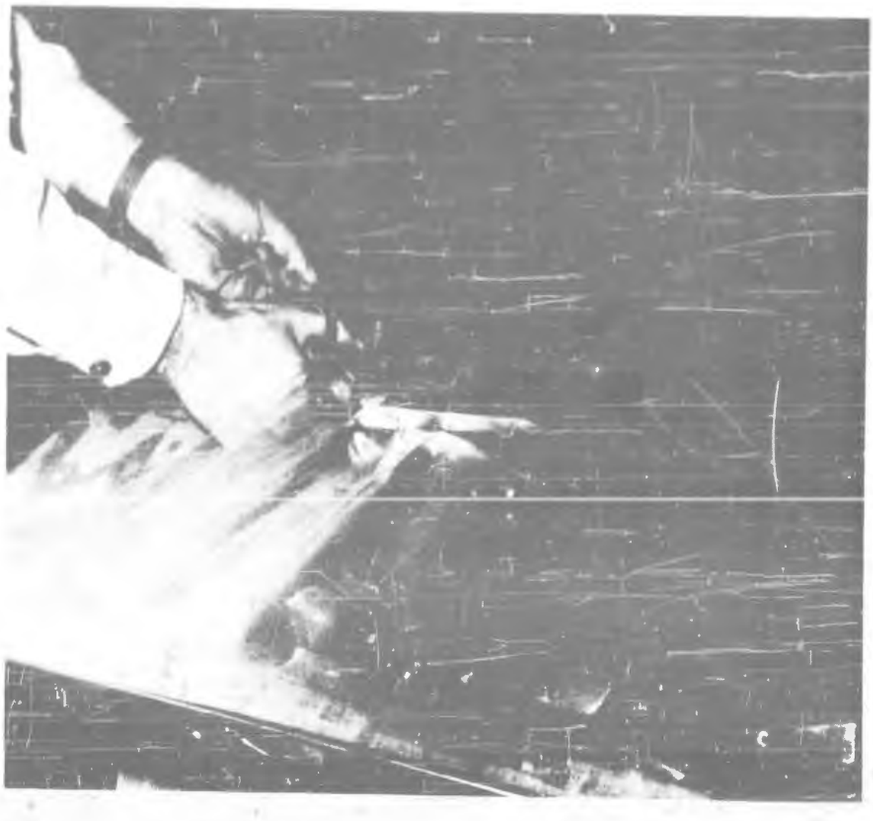

Figure III-21. The ends of each gore are marked with lines showing the correct length. After all the seals are made and have set, the tapes at the ends are removed and the excess material beyond the marks is cut away.

Figure III-22. One method employed to gather the ends of the cylinder was to punch holes in the edge and gather the edges on a wire. Here all the gores are punched at once. The paper slipsheet facilitates clean cutting with the punch.

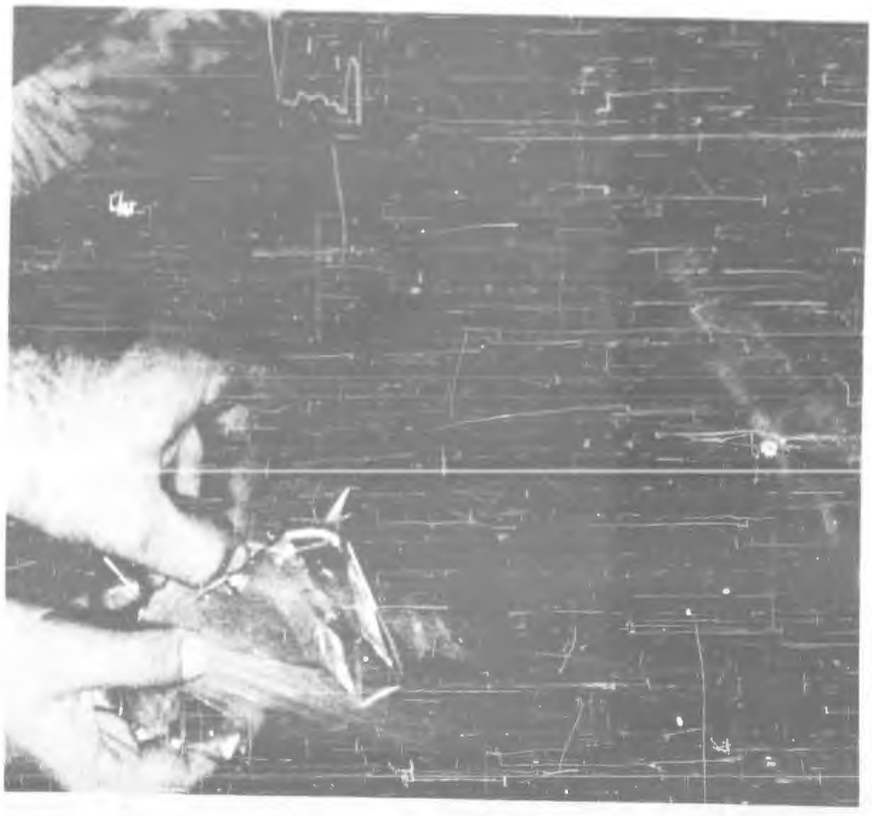

Figure III-23. To gather, the wire is woven in and out of the holes. One of the finished seams can be seen in the center of the picture.

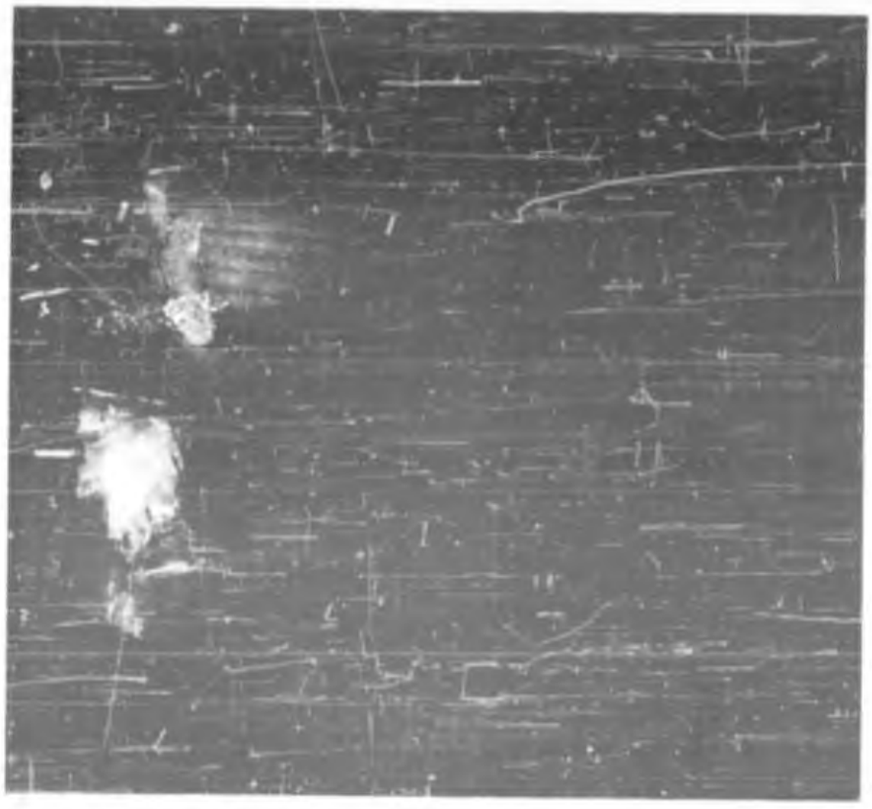

Figure III-24. The end of the balloon as it appears after it is gathered. It is important that the wrinkles be taken out in this region so that the same gore length will exist for each element of fabric. If they were of unequal length, loads would be taken up by the shorter ones first, greatly reducing the strength at failure.

Figure III-25. On balloon 2 and 3, the pleated ends were potted directly into the end fittings. The paper carton around the top fitting contains water to keep the temperature of the setting resin from becoming excessive.

Figure III-26. The material is potted around the val ing tube in the bottom fitting.

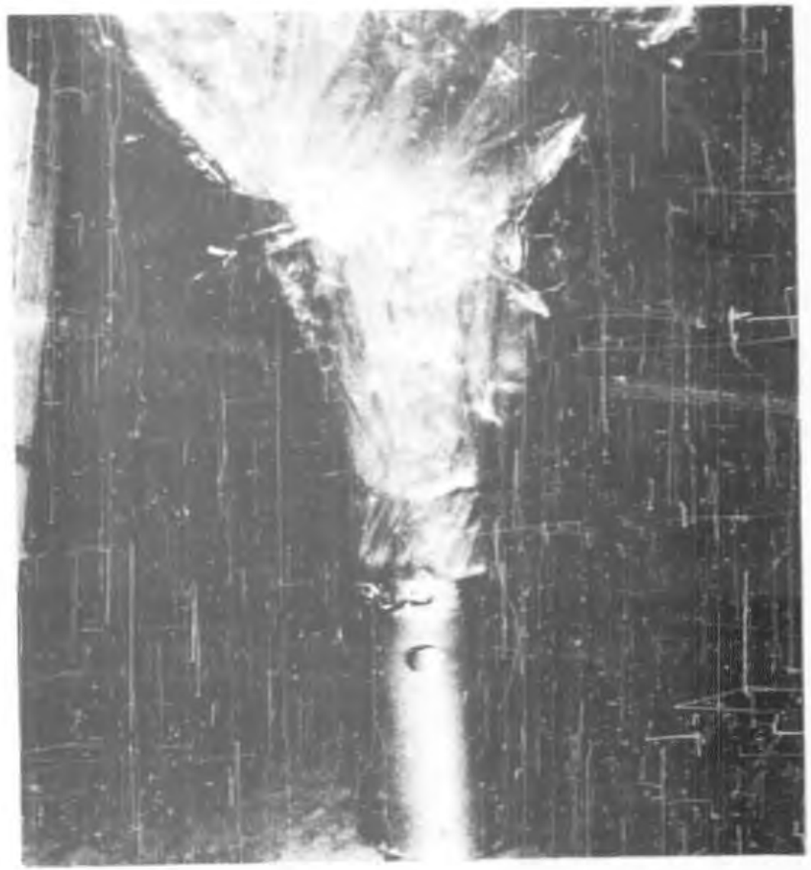

Figure III-27. The spiral formed by the pleats was found to be a point of weakness. Some of the fabric is potted shorter than the remaining, and this part tends to tear when a load is applied.

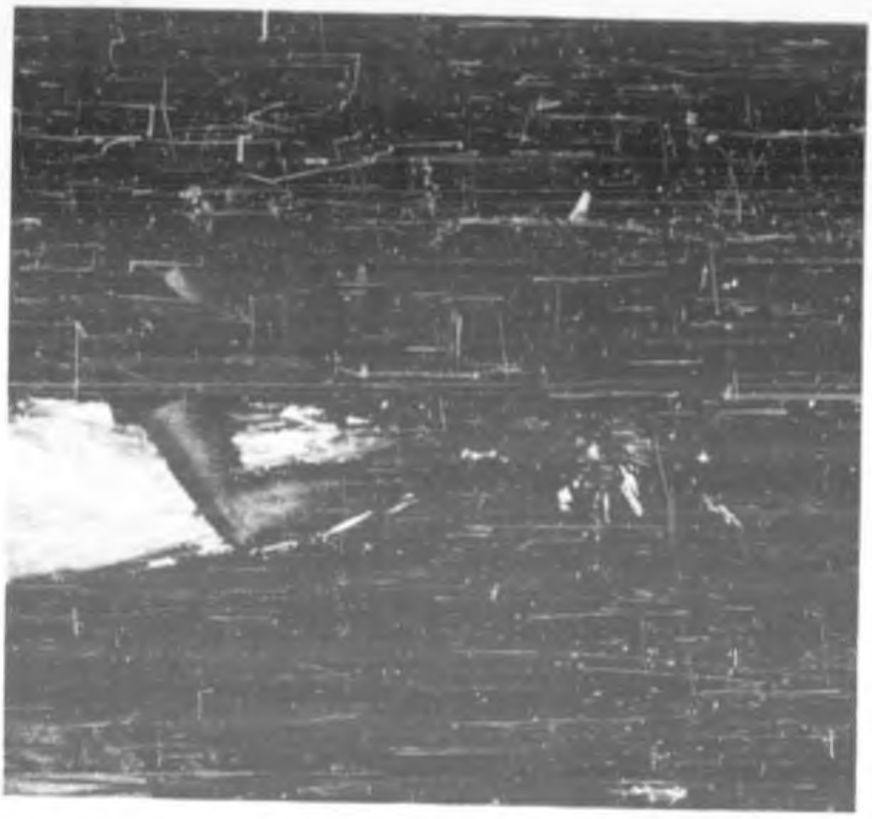

Figure III-28. Additional collars are placed above the potted fittings so that sharp points of the set resin do not cut material that is pulled over at 90°.

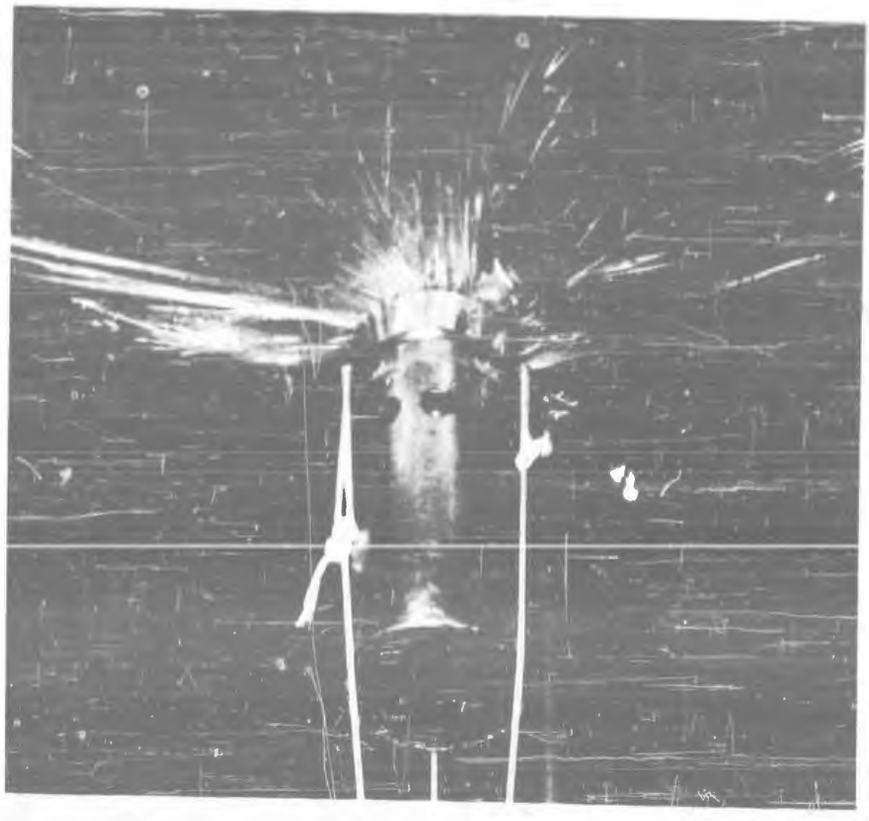

Figure III-29. The arrangement of the fabric under superpressure stress is shown. As the superpressure is increased from zero, individual folds straighten into alignment with very loud cracks and pops. The balloon lift at this time is about 80 lbs. The total fabric tension, however, is about 500 lbs per millibar of superpressure.

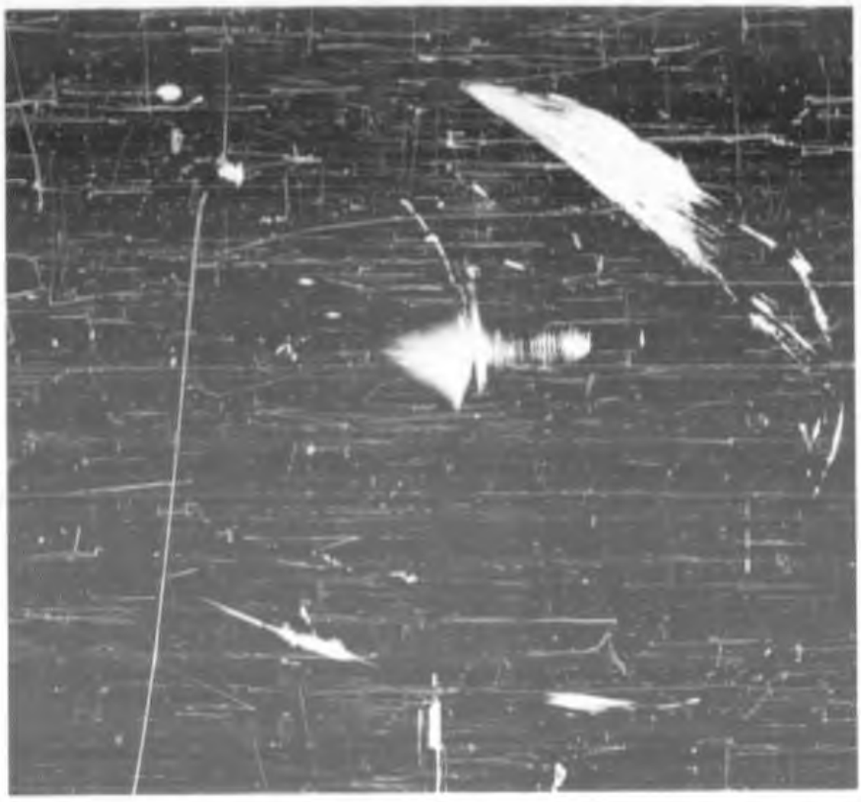

Figure III-30. The appearance of the balloon under superpressure. At about 4 mb superpressure the balloon burst the top collar fitting.

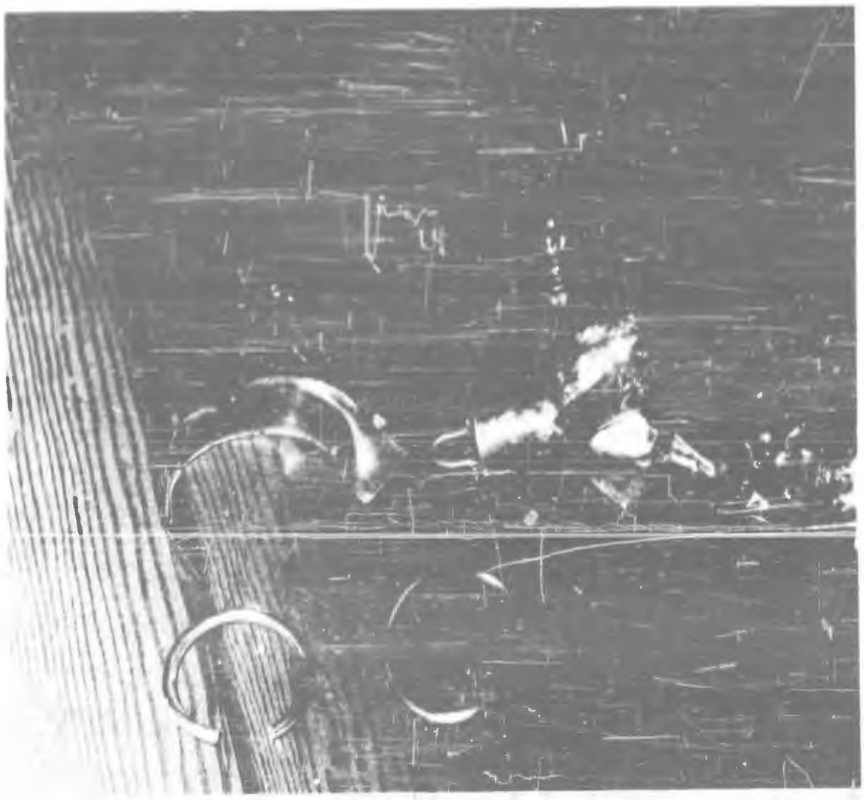

Figure III-31. The radial stress in the fabric is restrained by circumferential ring tension. The intensity of the forces is illustrated by the complete separation of welds in the top collar. In this fitting the weld was not nearly as strong as the rest of the ring.

Figure III-32. The double ring fitting installation is shown as it was made on balloon #4. The two rings take care of the fabric tension. A gas tight seal of the fabric has to be made in addition. After the balloon is pleated the rings are slipped over each end.

Figure III-33. Twelve inches of fabric are folded back over the first ring. An attempt is made to have the distribution of pleats at this fold as uniform as possible so that the loading on the pleats is more or less equal.

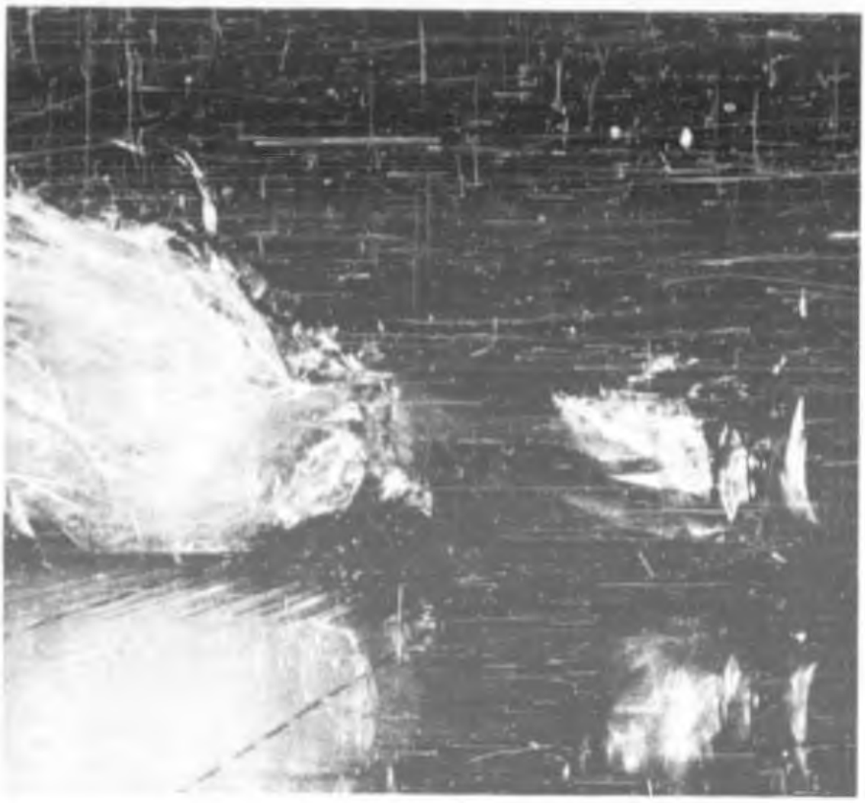

Figure III-34. The second ring is slipped over the folded fabric.

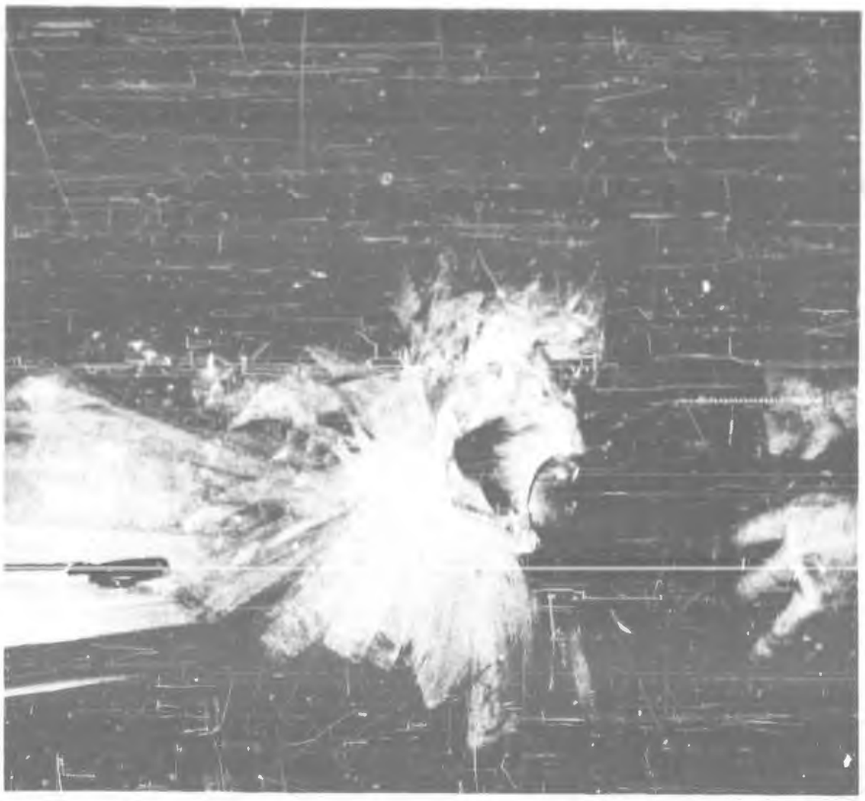

Figure III-35. The fabric is folded down once more and is then ready to be sealed to the bottom fitting. On this balloon the seal was made by potting the material in an annular cup. A hose clamp around the fabric has been used with more success on later balloons.

Figure III-37. The top seal is made by potting the material in an aluminum cup.

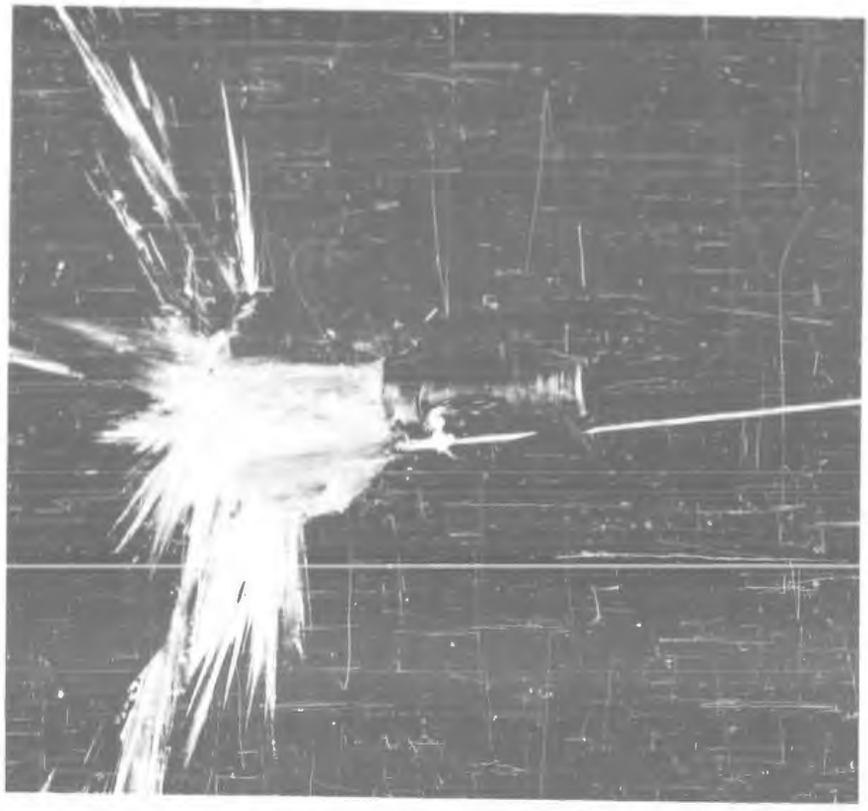

Figure III-36. The completed bottom bubbler fitting. The hose permits the internal pressure to be measured.

Section IV

RADIATION HEATING OF BALLOONS

A. Introduction and Statement of Problem

The effect of the radiation field in which a balloon finds itself is to establish the fabric temperature at some equilibrium value. If this temperature value differs from the ambient air temperature, convective flow to the air results and limits the temperature excursions resulting from the attempt to reach radiation equilibrium. Since the fabric temperature directly controls the buoyancy of the balloon, it is of the utmost importance to understand as completely as possible the details of the radiation processes, and also of the convection process. The radiation effects are so predominant as to profoundly affect most applications of balloons. Besides the familiar change of lift at sunrise and sunset, the work of the University of Minnesota project has demonstrated the "warming with altitude" effect. This term describes the changes of buoyancy with altitude due to the radiation field on the balloon. The effect depends on altitude, time of day, and also the season, and terrain details. In order to understand the mechanism by which stability (or instability) is produced in a balloon at various heights in the atmosphere, the experimental and theoretical details of the "warming with altitude" effect must be worked out.

Further observations that the drag force on a vertically moving balloon when it is set in motion is very different in the day than at night can be linked to the fabric temperature and its differences day and night. Also, several striking effects on Mylar balloons, where the

infrared radiation absorption is known to be large, have been observed during periods of flight when the balloon would fall or rise in response to changes of buoyancy.

It is also possible to introduce radiation-absorbing gasses into the balloon, such as ammonia. Ammonia-filled balloons have been flight-tested but the experimental and theoretical details of the radiation absorption process of ammonia and other infrared absorbing gasses in balloons have yet to be worked out.

In this section we shall summarize work on evaluation of the constants of materials and of the atmosphere which are necessary for a theoretical approach. The results of direct measurements from temperature and step flights are given in other sections of this report.

B. The Heat Balance Relation

The quantities which one needs to know to solve any given problem are contained in the heat balance equation for the balloon, as given in Volume I of this series, Page 4-14, and repeated here for convenience:

$$C_f \, m \frac{d}{dt} (T + \theta_1) = q_0 + q_1 + q_2 + q_3 - q_4 \qquad (1)$$

where

q_0 = heat convected per second from the gas to the fabric,

q_1 = power absorbed by the fabric from the solar radiation ($\lambda \approx 0.5\mu$),

q_2 = power radiated by the fabric because of its temperature ($\lambda \approx 10\mu$),

q_3 = power absorbed by the fabric from the terrestrial and atmospheric radiation ($\lambda \approx 10\mu$),

q_4 = heat convected per second from the fabric to the outside air.

C_f is the specific heat of the fabric of mass m, and at superheat θ_1, above the air temperature T.

If we consider the balloon fabric to be thin, so that the intensity of radiation is practically undiminished in passing through,* then we may write for the power absorbed from the sun

$$q_1 = E_s \cdot a_s \cdot m \qquad (2)$$

E_s is the visible flux (includes scattered light from earth and clouds), a_s the absorption coefficient of fabric for solar radiation per cm of thickness divided by the density of the fabric, and m the mass. Similarly, for the infrared radiation we write

$$q_2 = A_e \cdot b \cdot (T + \theta_1)^4 \cdot m \qquad (3)$$

where b is the radiation constant. A_e has the units of emissivity per cm of thickness divided by the density of the material in g/cm^3. Equation (3) may also be written

$$q_2 = K (T + \theta_1)^4 m \qquad (4)$$

where $K = A_e \cdot b$ = watts/g/(deg K)^4 for the material. There is also the relation

$$q_3 = E_e \cdot a_e \cdot m \qquad (5)$$

E_e is the flux of long-wave length radiation present at the balloon's location, and a_e the absorption per cm of the material divided by the density. Although balloon materials in general do not absorb selectively in the visible range, this is not true in the long wave infrared region near the maximum of intensity for earth radiation ($\lambda \approx 10\mu$). Therefore, in computing q_3 the spectral distribution of the atmospheric radiation in

---

* This is equivalent to assuming the differential absorption law $dI = -\lambda I dx$.

this region must be known, as well as the absorption spectrum of the balloon fabric. The spectral distribution of atmospheric radiation depends on the concentration of ozone, carbon dioxide and water vapor and can be evaluated as described in paragraph C-1. The relative spectral absorptivity of the fabric has been measured in the laboratory with infrared spectrometers. The average absolute absorptivity has been measured experimentally using black body methods.

The last term, q_4, limits the temperature excursions due to radiation, by convective heat exchange with the outside air, and may be expressed as

$$q_4 = H \theta_1^{4/3} \tag{6}$$

the exponent of θ_1 being that given by convection theory.* The constant H can be shown to be independent of altitude. It may be calculated theoretically but is best evaluated by experiments.

In the following pages the values of the constants in Equation (1) will be assembled insofar as they are known at this time, and some illustrative calculations carried out for special situations in balloon flight.

C. Experimental values for the constants in the heat balance relation.

1. The spectral absorption in the infrared region. This is shown in Figure IV-1** for polyethylene and Mylar films. Note that polyethylene has strong absorption bands at 3.5, 6.8, and 13.7 microns. These bands

---

* See Volume I, pp. 4-8 to 4-19, of this series of reports.

** Furnished by courtesy of Air Force Cambridge Research Center, from measurement by Baird Associates, Inc.

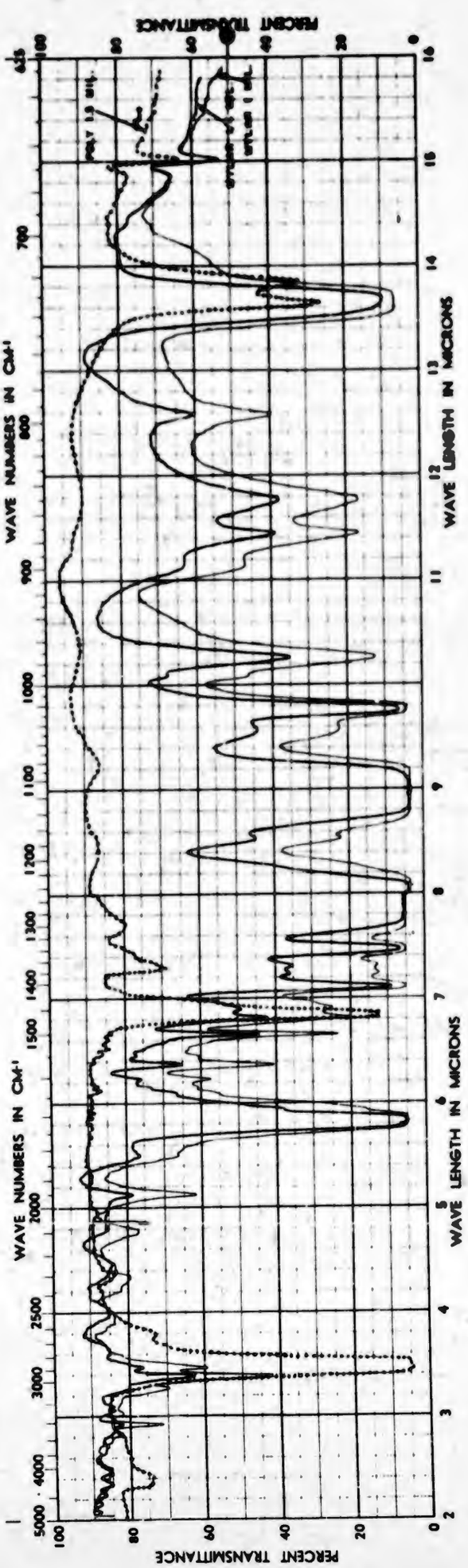
PERCENT TRANSMITTANCE
WAVE NUMBERS IN CM⁻¹
WAVE LENGTH IN MICRONS

Figure IV-1

approximately coincide with the H_2O and CO_2 bands for the atmosphere, and we would thus expect a polyethylene balloon at night to tend toward an equilibrium temperature near that of the surrounding atmosphere. The absorption between 6 and 13 microns (in the atmospheric window), however, will tend to bring the balloon to earth-ground temperature. Unfortunately, Figure IV-1 gives little information in this region, as the 100% transmittance point is arbitrary. In running the spectrum the operator adjusts the transmittance reading between 80 and 90 percent, with the sample in one beam of the I.R. spectrometer at 2μ, and the scanning in wavelength then is carried out. The upper base line thus includes variations of reflectance and scattering with wavelength as well as true absorption. To obtain the necessary data, equivalent runs (like Figure IV-1) must be made over a range of fabric thicknesses, so that the exponential absorption may be evaluated at each wavelength.

The Mylar curves are strongly absorbing in the atmosphere "window" region, and we would thus expect Mylar balloons to run warmer than the surrounding air in the stratosphere.

2. Average absorption in the infrared region. The absorption of black body radiation of temperature from -50° to 80°C by films of Mylar and polyethylene has been measured by a substitution method using a vacuum thermopile as detector. The average absorption of black body radiation by polythene in the wavelength band 2-16 microns has been calculated from a measurement of the absorption spectrum for that interval that was made available.* That calculation agrees with the measurement

* Based on I.R. spectrograph in Chem. Dept, University of Minnesota. Does not disagree with Figure IV-1.

as well as may be expected. It was found that the absorption by Mylar does not vary exponentially with thickness. The complexity of the absorption spectrum of Mylar for 2-16 microns makes that result plausible.

Discussion of Method

A straightforward measurement on black body radiation involves a black detector at some temperature T_d and a black body at a different temperature T_s. Energy will be transferred between them by radiation, and it is the spectrum of the net radiation that is of interest. The net absorption (+ or -) by the detector will be a geometric factor times the difference between the black body spectra for the two temperatures. If one body is much hotter than the other the contributions to the absorbed energy from various wavelengths will be distributed essentially as in the black body spectrum for the higher temperature since the amplitude of the spectrum varies as T^4.

So to study black body radiation corresponding to a given temperature neither the source nor detector (nor the environment, in practice) can have a temperature greater than that.

The radiation temperature of a cold body can be measured with a much warmer thermopile or other detector, but in the problem under discussion it is the spectrum of the net radiation between source and detector that is important.

Apparatus

The source of radiation was a slit in a cylindrical copper shell blackened inside. The shell was furnished with a heater in close thermal contact with it covered by electrical tape and aluminum foil except for the slit. The cylinder was mounted on light bakelite supports inside a

heavy brass tank opposite the detector, a linear thermopile (Cenco 81075, 40 exposed iron-constantan junctions). The heavy aluminum thermopile housing was mounted on a heavy copper shield with a slit to expose the row of free junctions the same size as that in the source and opposite it (Figure IV-2). A second copper shield with a slit was mounted directly in front of but not touching the source. Both shields were in good thermal contact with the tank.

The thermopile e.m.f. was measured with a L & N type R galvanometer with an L & N Ayrton Shunt set at .1 to give proper impedance match for fast response at the expense of sensitivity.

It was found necessary to evacuate the tank (good fore-pump) to get back adequate sensitivity.

Samples of film could be moved in the space between the collimating shields. A series of three film samples and a copper slug of the same dimensions except for thickness could be moved into position between the slits from outside the tank by means of a screw arrangement through a bellows vacuum seal.

The difference between galvanometer readings with nothing in position and the slug in position was taken as a measure of the net radiation through the slits. The difference between readings with a film sample and the slug measured the radiation transmitted by the sample.

For a measurement on black body radiation at some temperature the tank was completely immersed in a liquid bath inside a large dewar and the liquid brought to that temperature. An alcohol-dry ice bath was used for temperatures below room temperature. For higher temperatures a water bath and heater were used. The system took about an hour to come

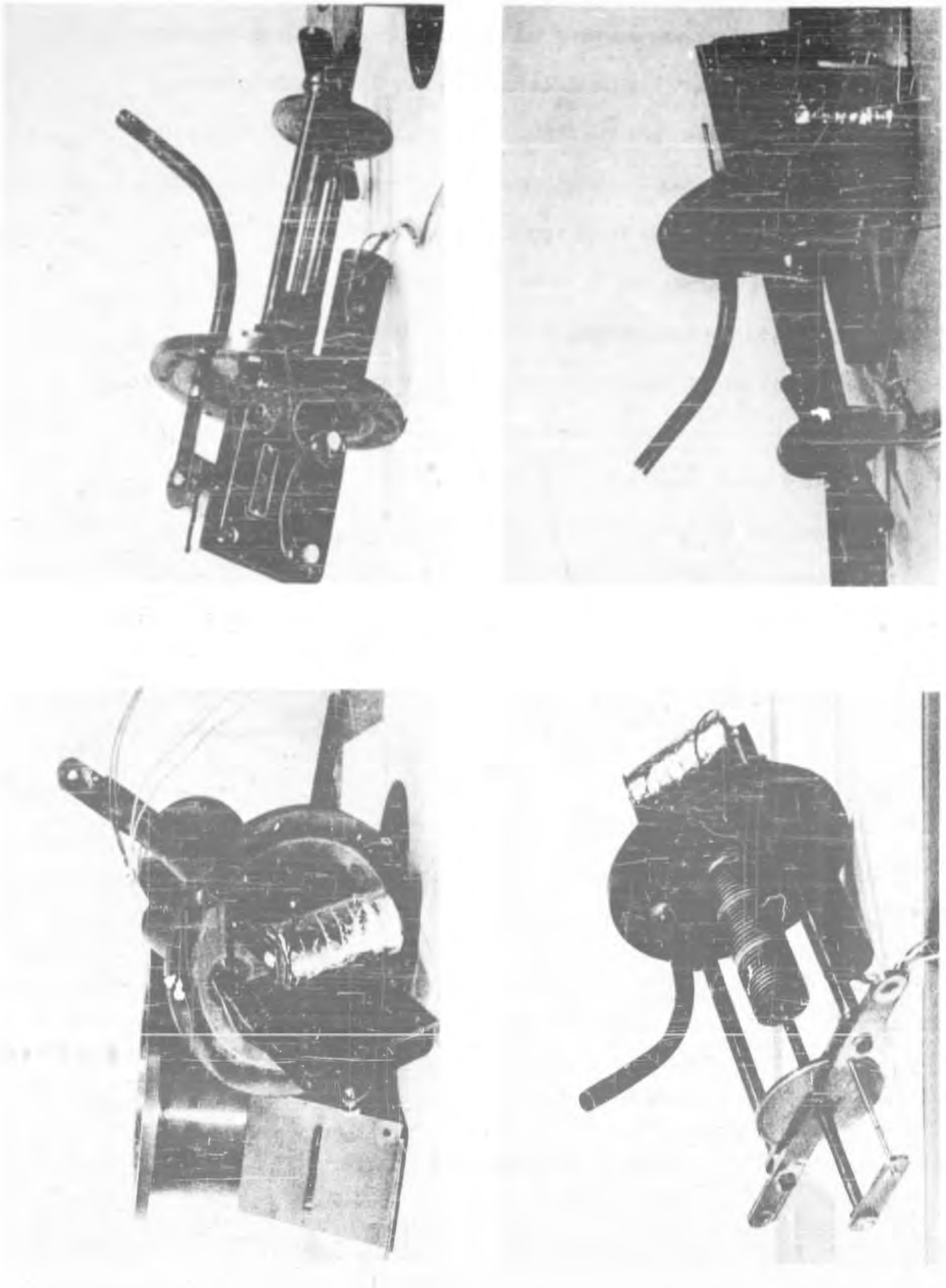

Figure IV-2. Absorption Test Cell

to thermal equilibrium after an adjustment of the bath temperature. The bath temperature was measured with a conventional bulb thermometer.

About half a watt was supplied continuously to the source heater. A constantan lead ran from the heater to a point on a copper collimator near where it contacted the tank. The e.m.f. between heater and tank could be measured to give their temperature difference. A difference less than three degrees was found to give sufficient radiation for the measurements, so the temperature of the radiation was essentially that of the bath. Six to ten runs were made for each temperature and set of samples.

Results

Table 1 gives transmission of Mylar films of different thickness for various radiation temperatures. The same results are shown in Figure IV-3. Apparently the absorption begins to be exponential at sufficiently long wavelenths, but at the shorter wavelengths characteristic of 80°C the variation with thickness suggests an absorption spectrum consisting partly of strong closely-spaced lines and partly of windows for which the material is nearly transparent.

The results on transmission of polythene are given in Table 2 and Figure IV-4. The vertical scale has been displaced between the three curves of Figure IV-4 since they nearly coincide otherwise.

For exponential absorption,

$$I = I_o \frac{(1-u)}{(1+u)} e^{-\sigma t} \qquad (7)$$

where u is the fractional reflection at each interface and σ is the absorption coefficient.

Figure IV-3. Transmission of Black Body Radiation by Mylar Films.

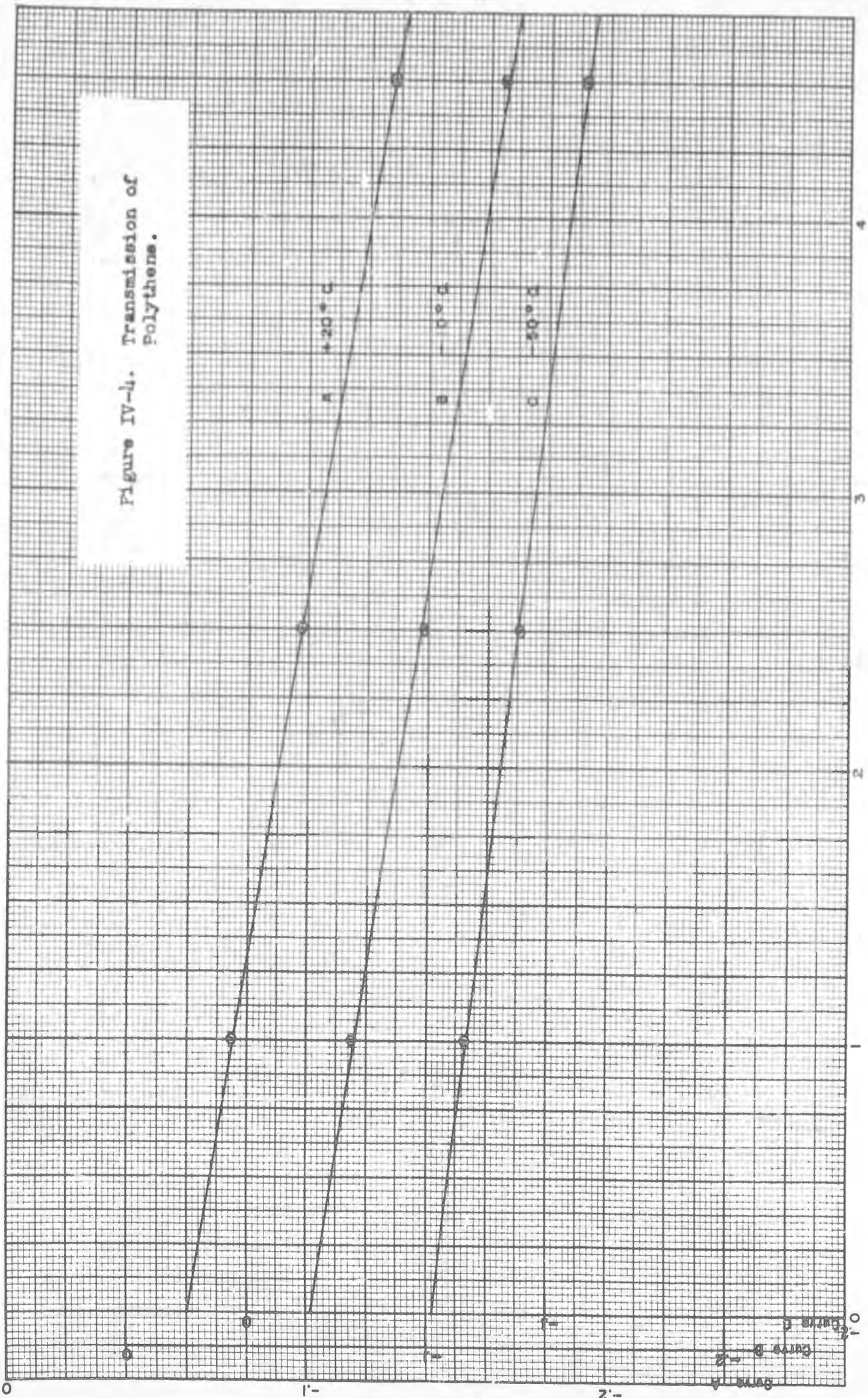

Figure IV-4. Transmission of Polythene.

$$\log_{10}(I/I_0) = \log \frac{(1-u)}{(1+u)} - .4343\,\sigma\,t \qquad (8)$$

If $\log_{10}(I/I_0)$ is plotted versus t the intercept is $\log\frac{(1-u)}{(1+u)}$ and the slope $-.4343\sigma$. Table 3 gives values of σ, $\lambda = \sigma^{-1}$ and u(%).

Table 1

Mylar Transmission

Radiation Temperature (deg.C)

Thickness (mils)	-50	-25	-5	20	40	80
.25	.71	.66	.67	.64	.63	.66
.50	.55	.56	.57	.56	.58	.61
1.00	.40	.43	.44	.46	.48	.51

Table 2

Polythene Transmission

Radiation Temperature (deg. C)

Thickness (mils)	-50	-10	20
1.0	.85	.84	.84
2.5	.81	.80	.80
4.5	.77	.75	.74

Table 3

Characteristics of Polythene

Radiation Temperature (deg. C)

	-50	-10	20
u (% reflection ea interface)	6.5	6.8	6.9
σ (mil^{-1})	.026	.033	.035
λ (mil)	40	30	28

For one set of measurements single, double, and triple one-mil foils were used instead of foils of different thickness. The variation of transmission with n, the number of films of equal thickness t, is:

$$I_n = I_o \frac{(1-u)}{(1+u)}^{n} e^{-n\sigma t} \tag{9}$$

$$\log(I_n/I_o) = -n \left[\log \frac{(1-u)}{(1+u)}^{-1} + .4343\sigma t \right] \tag{10}$$

So a semilog graph of measured values of I_n/I_o for various numbers n of foils should be a straight line through the origin. (It has been assumed that the true absorption is exponential and that reflected radiation is entirely removed from the beam.)

Figure IV-5 shows experimental results. They suggest that a component of the radiation amounting to about 3% of its energy is almost totally absorbed in the first mil. The slope of the best straight line is .059. Taking σ = .035 from Table 2, u = .05.

If the same intercept (corresponding to 3% abrupt absorption) is subtracted from the curves in Figure IV-4:

u =	.050	.053	.054	
for T =	-50	-10	20	deg. C

CALCULATIONS ON THE POLYTHENE INFRARED ABSORPTION SPECTRUM

Planck's formula for the black body radiation distribution is

$$J = c^2 h/\lambda^5 \left[\exp(ch/\lambda kT) - 1 \right] \tag{11}$$

c = the velocity of light, h = Planck's constant, k = the Boltzmann constant. Let x, y be defined by $x = T\lambda/c_2$. $y = J/T^5 c_3$.

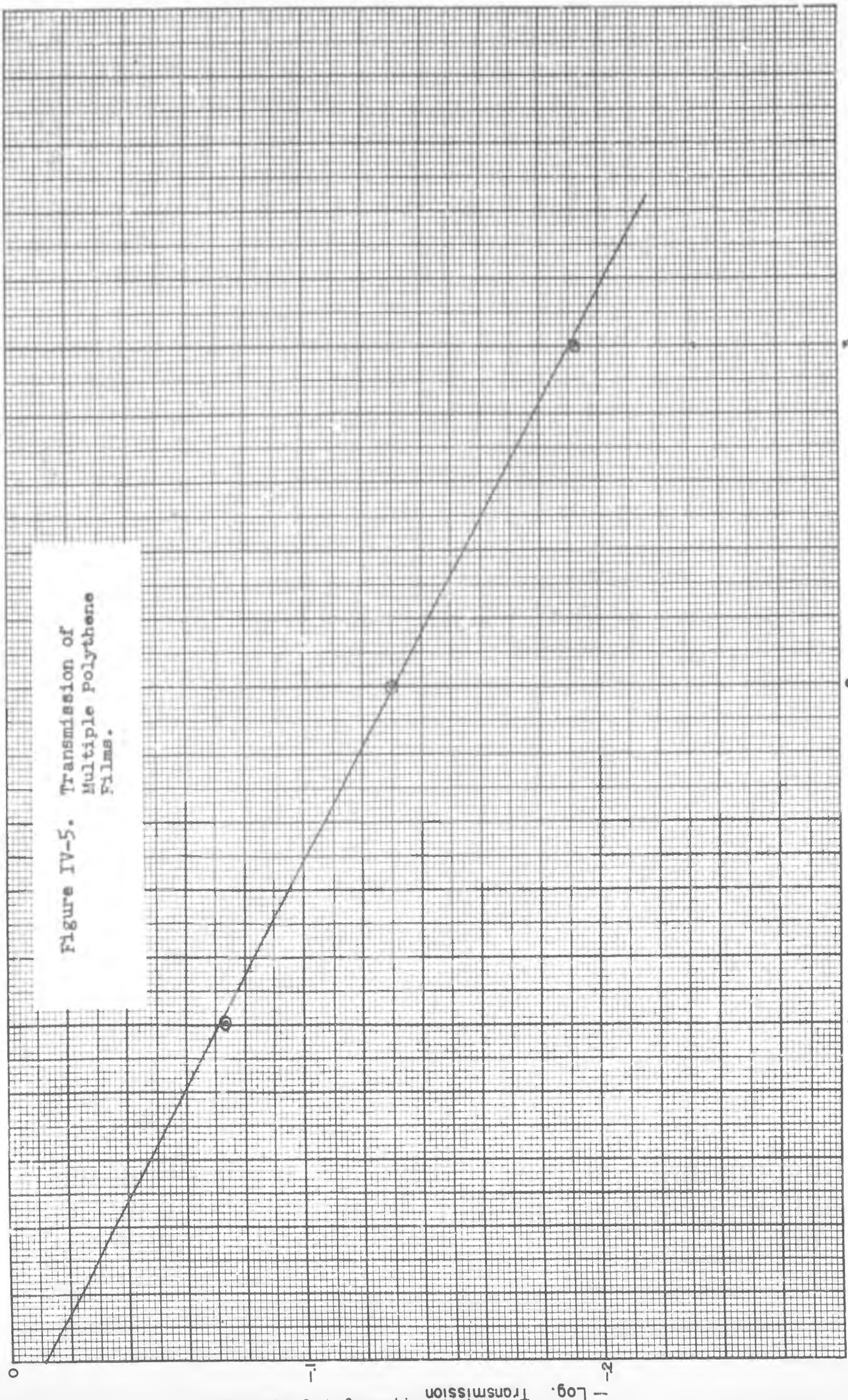

Figure IV-5. Transmission of Multiple Polythene Films.

$c_2 = ch/k = 1.43$ cm deg., $c_3 = k^5/c^3h^4 = .980 \times 10^{-13}$ watt/cm^3 deg^5.

Then Planck's equation is $y = 1/\left[x^5(e^{1/x} - 1)\right]$

$$\int_0^\infty y(x)dx = \pi^4/15 = 6.494$$

Corresponding values of y and x are to be found in Jahnke-Emde Funktionentafeln (1933) p 45. Let $q(\lambda) = 1-t(\lambda)$ where t is the fractional transmission of a sample as a function of wavelength. Then the experimental results on absorption of black body radiation correspond to:

$$\bar{\alpha}\ (T) = \frac{\int_0^\infty q(\lambda)J(\lambda,T)d\lambda}{\int_0^\infty J(\lambda,T)d\lambda} \qquad (12)$$

$q(\lambda)$ is available for the interval $\lambda = 2\text{-}16\mu$ (sample thickness 1-mil).

The following integrals have been computed:

$$\int_2^{16} J(\lambda,T)d\lambda \Big/ \int_0^\infty J(\lambda,T)d\lambda = \begin{cases} .400 & T = -50^\circ C \\ .588 & T = 20^\circ C \end{cases} \qquad (13)$$

(That is, 40% of the energy from a black body at -50°C lies in the wavelength interval mentioned. For a black body at 20°C about 60% of the energy falls in that interval.)

$$\int_2^{16} q(\lambda)\, J(\lambda,T)d\lambda \Big/ \int_2^{16} J(\lambda,T)d\lambda = \begin{cases} .174 & T = -50^\circ C \\ .173 & T = 20^\circ C \end{cases} \qquad (14)$$

If one lets $q(\lambda) = .13$ for $\lambda > 16\mu$,

$$\int_0^\infty q(\lambda)\, J(\lambda,T)d\lambda \Big/ \int_0^\infty J(\lambda,T)d\lambda = \begin{cases} .150 & T = -50^\circ C \\ .156 & T = 20^\circ C \end{cases} \qquad (15)$$

Observed values are $\bar{\alpha} = \begin{cases} .15 & T = -50^\circ C \\ .16 & T = 20^\circ C \end{cases}$

If it be assumed that the calculated values represent 10% reflection at the two surfaces of the sample and a remainder which is true absorption, the calculated absorption is:

5.0% -50°C

5.6 % 20°C

It is observed that the exponential absorption is:

2.6% -50°C

3.5% 20°C

But to make the observations fit the assumption about reflection one must assume that there is an abrupt absorption of about 3% in addition. This "abrupt" absorption is undoubtedly the effect of the absorption bands. In the bands the absorption coefficient is much larger (see, for example, the two Mylar curves in Figure IV-1). The true absorption calculated is thus in satisfactory agreement with the measured absorption, considering the approximate knowledge of the spectral absorption of polyethylene.

3. Solar Radiation. The sun as a source supplies 1.9 calories/cm/min* at the top of the atmosphere. (.134 watts/cm^2) Measurements show that polyethylene and Mylar absorb about 1%/mil in the visible region (black body at 6000°K to which the sun is equivalent.)

Figures IV-6, 7 and 8 summarize the atmospheric absorption effects, which are principally due to water vapor. These curves are computed from known absorption constants of the atmosphere for visible light.

---

* See Smithsonian Physical Tables, eg.

Figure IV-6.

ALTITUDE DEPENDENCE OF SOLAR RADIATION

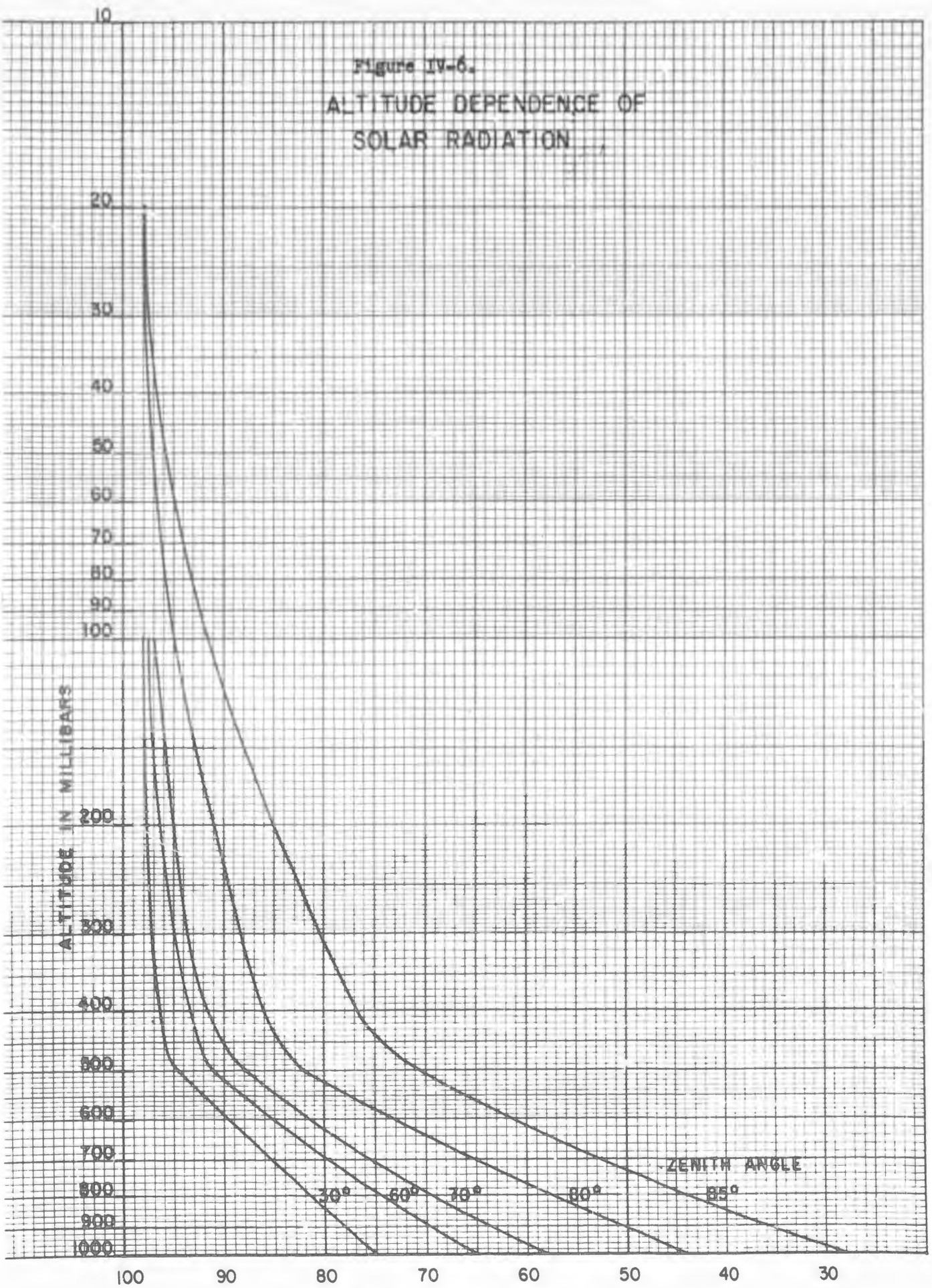

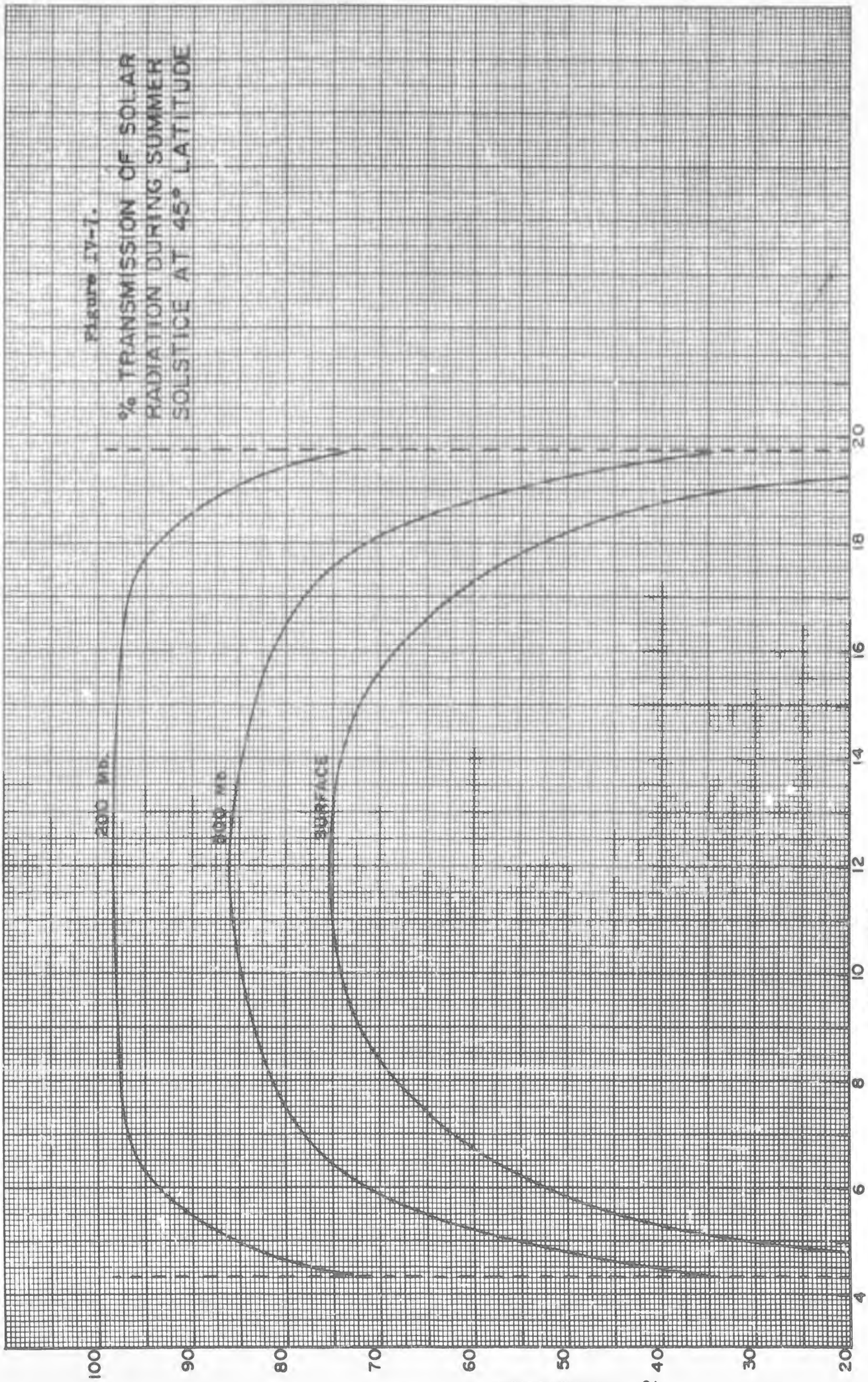
Figure IV-1.
% TRANSMISSION OF SOLAR RADIATION DURING SUMMER SOLSTICE AT 45° LATITUDE
200 MB.
800 MB.
SURFACE
LOCAL TIME
% TRANSMISSION
100
90
80
70
60
50
40
30
20
4
6
8
10
12
14
16
18
20

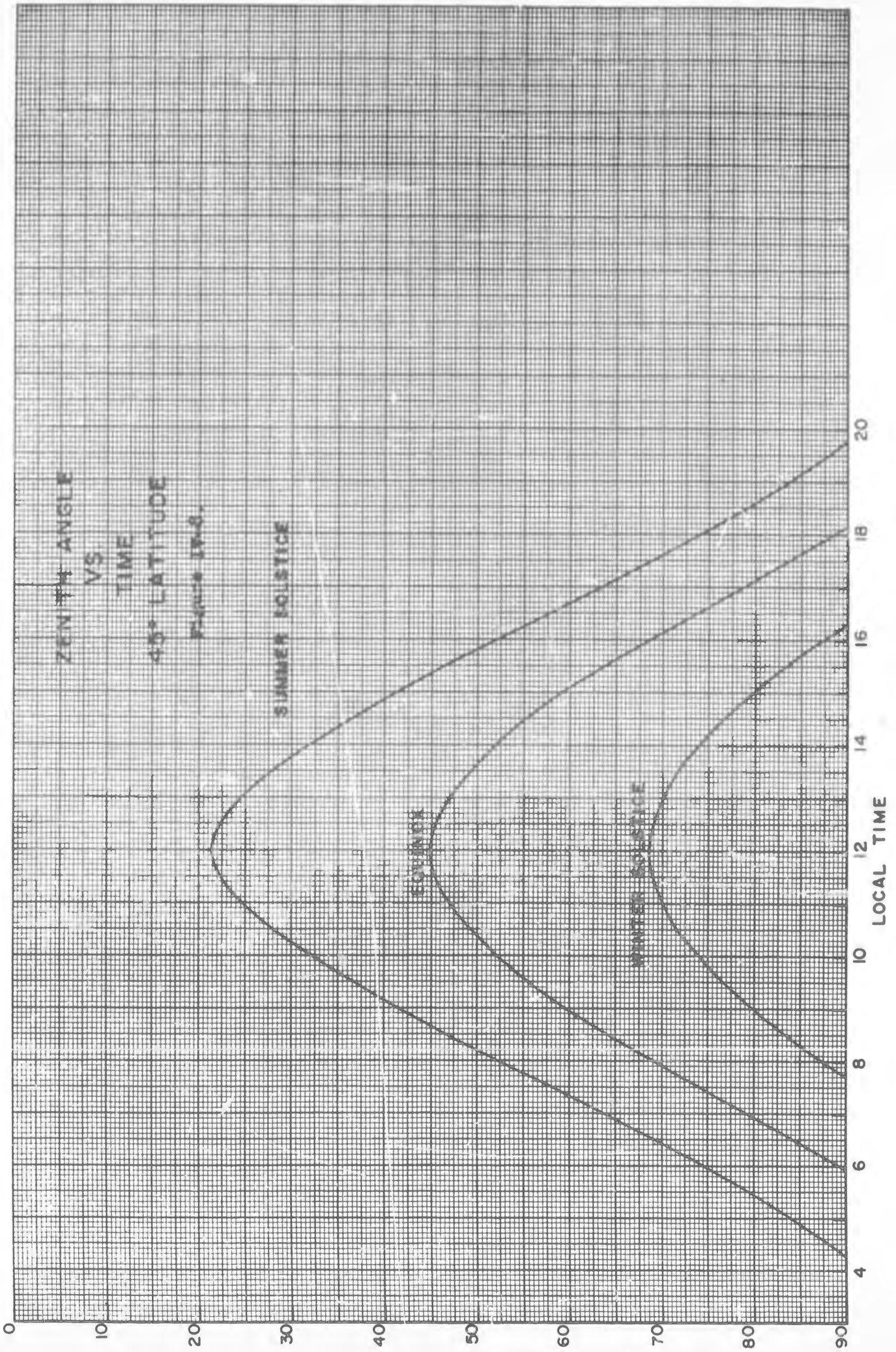
ZENITH ANGLE VS TIME
45° LATITUDE
SUMMER SOLSTICE
EQUINOX
WINTER SOLSTICE
ZENITH ANGLE IN DEGREES
LOCAL TIME
0
10
20
30
40
50
60
70
80
90
4
6
8
10
12
14
16
18
20

At the surface the energy flux increases until noon and then drops symmetrically until sunset. At 200 mb the full sunrise and sunset effects develop in about two hours. Balloons above 20 mb pressure height are exposed to the full direct radiation essentially as soon as the sun's disc clears the horizon at any time of year.

Figures IV-9, 10, and 11* are examples of the surface solar flux under various conditions of season. Figure IV-12 summarizes the fluctuation to be expected on the surface from low cloudiness.

The balloon is also subject to solar radiation scattered back from the earth. This effect may not be computed directly as above, but depends on the terrain as well as the balloon altitude. The "earth set" effect should begin at the time of ground sunset on the eastern horizon as seen from the balloon, and ends at balloon sunset. There is ample evidence that balloons in the stratosphere consistently lose lift prior to sunset on the balloon. Figure IV-13 and Table 4 are a summary of earth-set effects on Flights 1-111. The effect has a wide distribution but occurs most frequently 30-40 minutes before balloon sunset. This is about ten minutes before ground sunset occurs below the balloon, and probably indicates that the substantial portion of ground in shadow to the East has cooled the balloon fabric appreciably.

The magnitude of the sunset effect on balloons is discussed elsewhere in this report. (See Volume VI, Section VI, and Volume IX, Section VI-A.)

---

* I. F. Hand, "Heating and Ventilating", January 1950, pp 92-94. From Blue Hill Observatory Results.

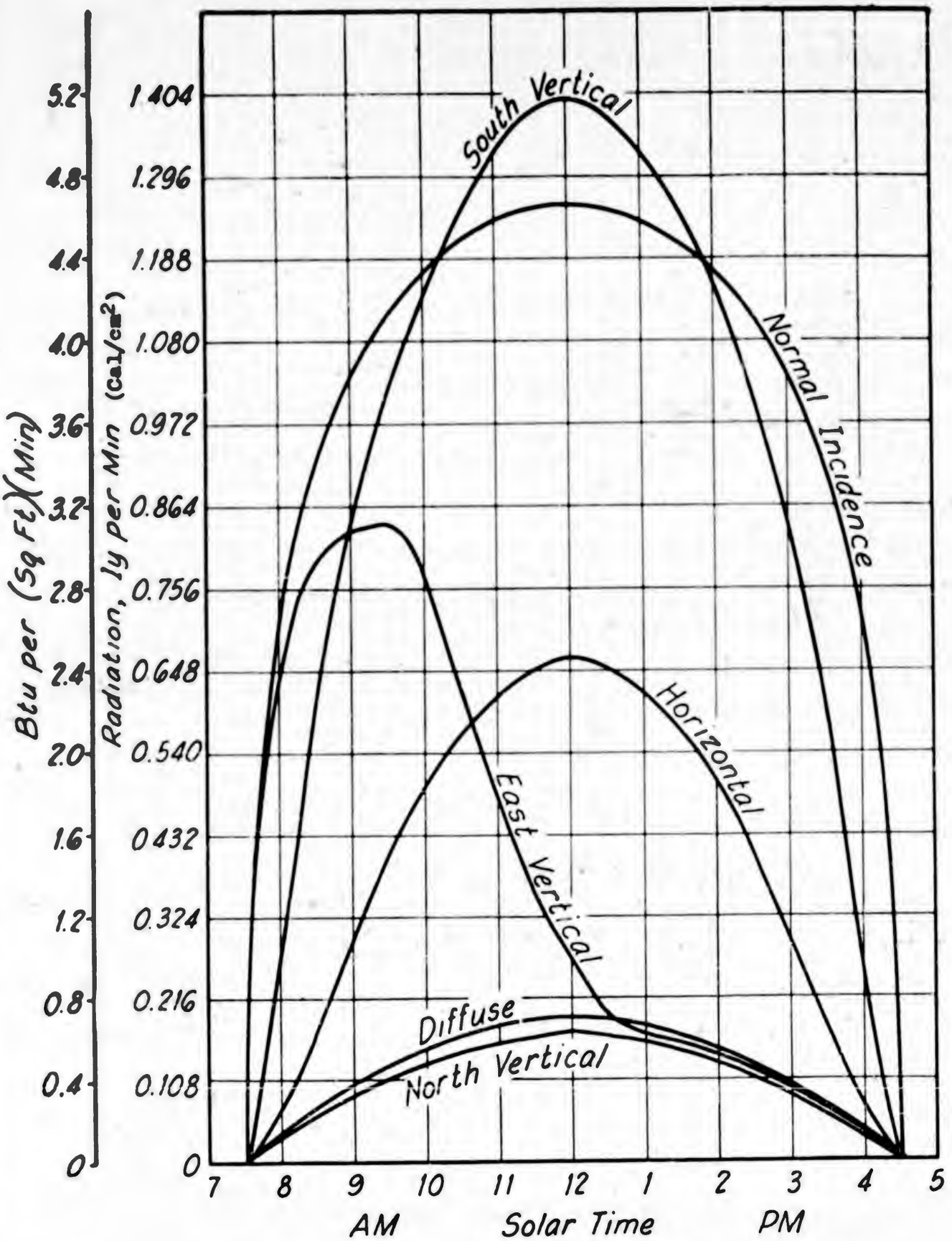

Figure IV-9. **Insolation on cloudless days, December 21, for latitude 42° N.**

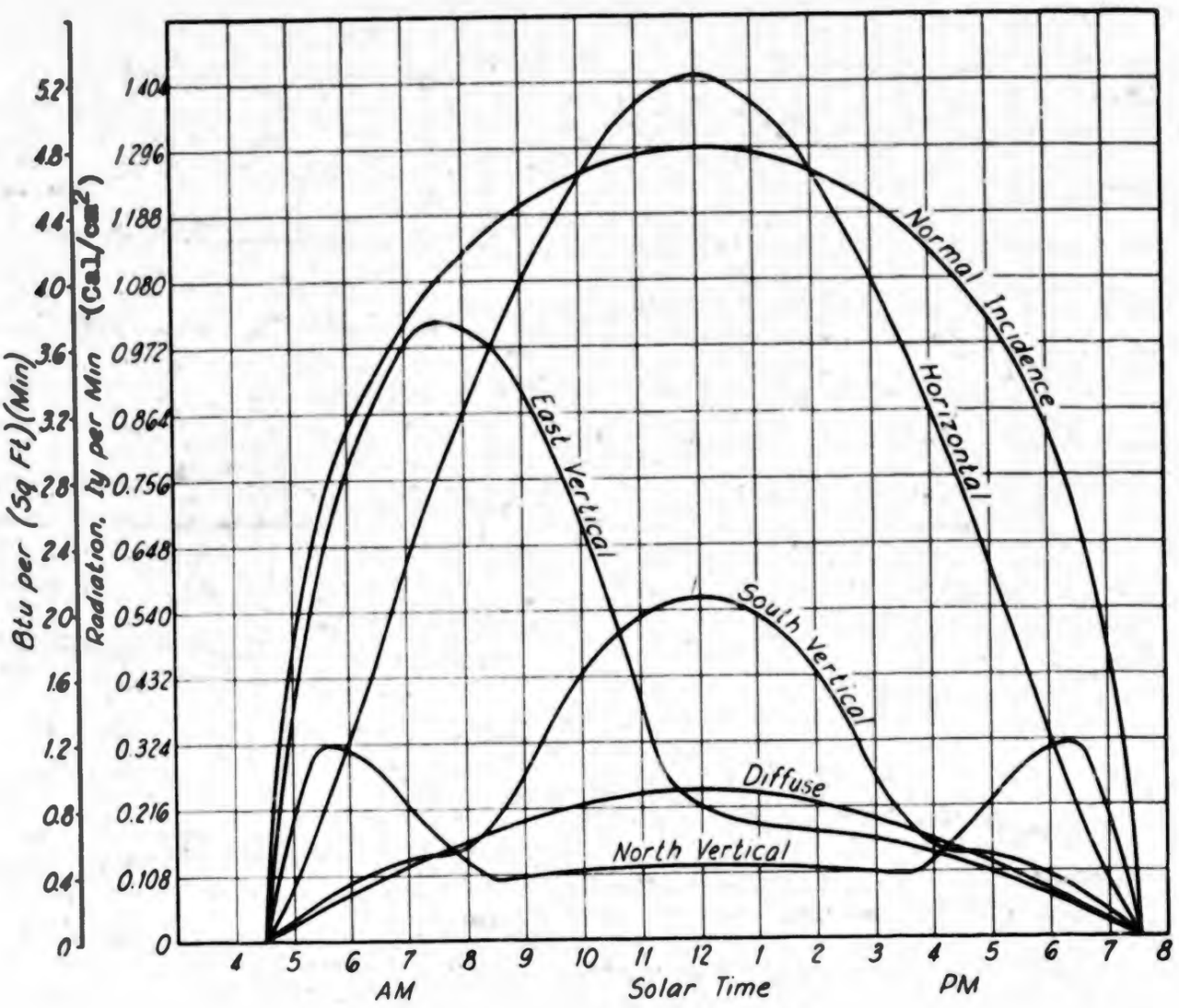

Figure IV-10.

Insolation on cloudless days, June 21, for latitude 42° N.

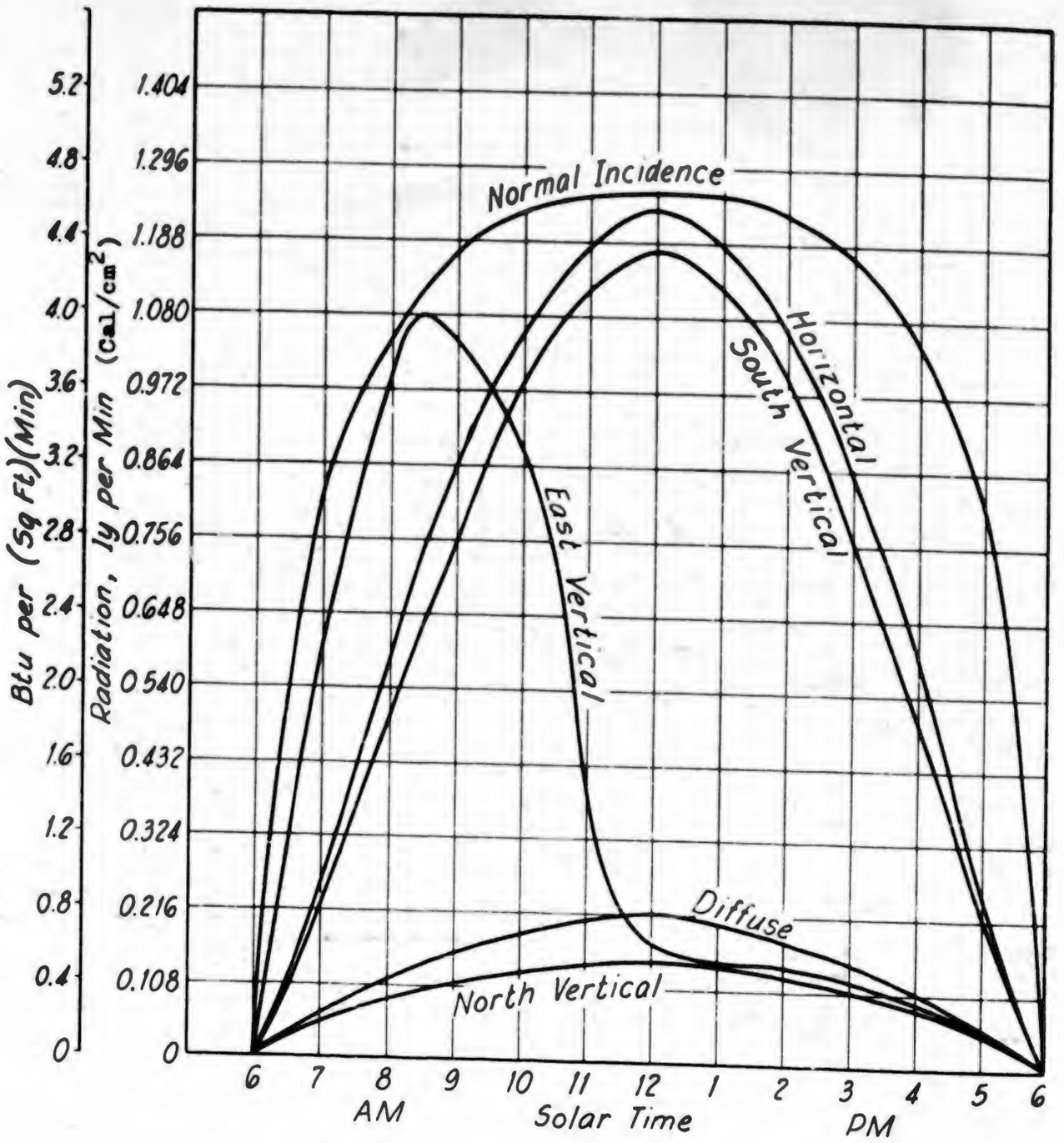

Figure IV-11. Insolation on cloudless days, March 21 and September 21, latitude 42° N.

Figure IV-12.

FREQUENCY OF OBSERVED VALUE OF SOLAR RADIATION
WITH LOW CLOUDS
SECANT z = 1.1

REFERENCE- HAURWITZ, JOURNAL OF METEOROLOGY
JUNE, 1948, VOL.5 PAGE 111

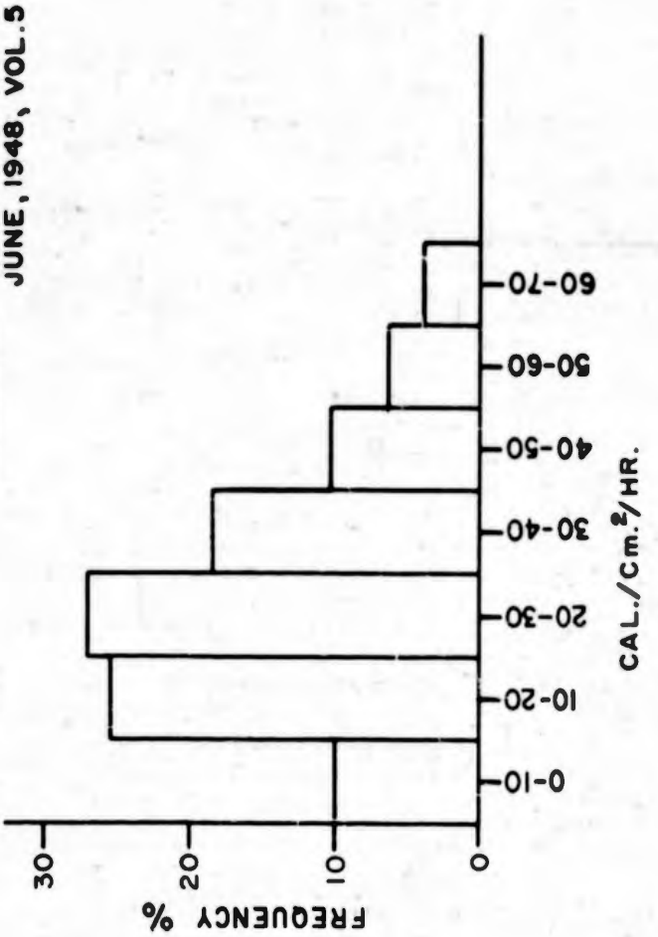

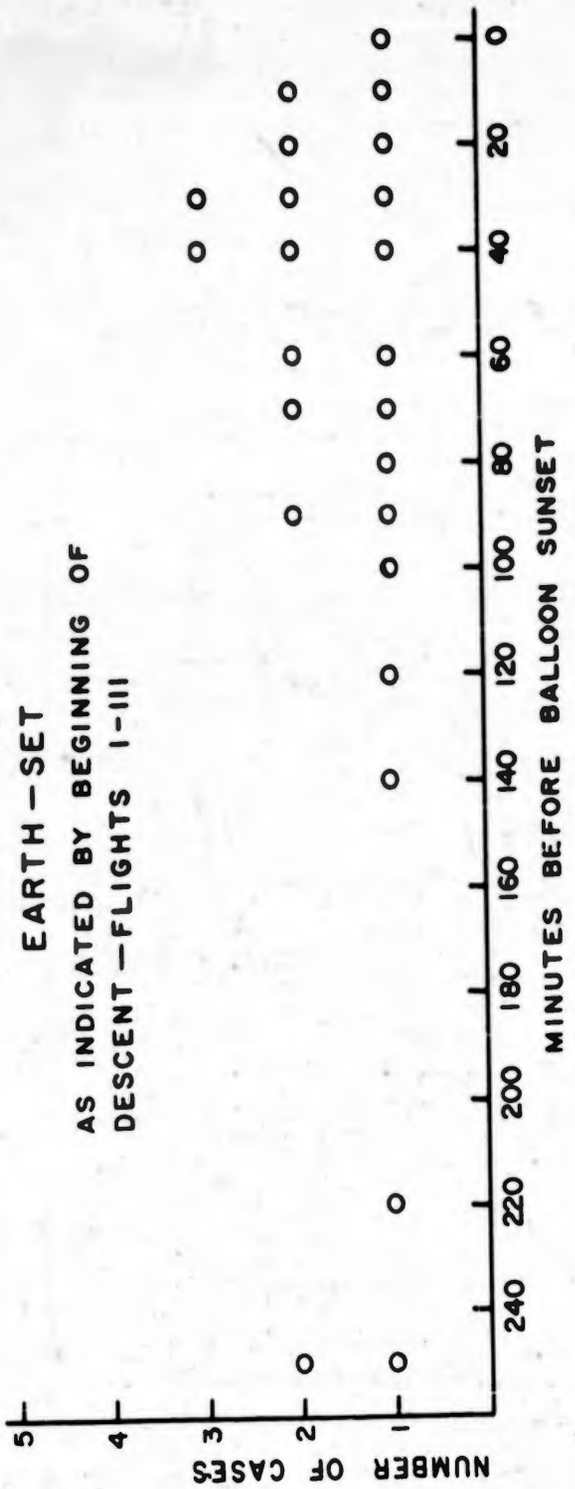

Figure IV-13.
EARTH—SET
AS INDICATED BY BEGINNING OF
DESCENT—FLIGHTS I-III

TABLE 4

Summary of Descent Data from Level Flights

Flt #	Date	Begin Descent	Sunset on Balloon	ΔT	Notes
9	4/23/52	1520 CST	1930 CST	250 min.	Bottom open.
10	4/29	1920	1940	20	Open.
12	5/12	1850	2000	70	Open.
14	5/22	1930	2010	40	Girdle on.
15	5/26	1910	2010	60	Open.
20	6/12	1920	2040	80	
24	7/8	2020	2040	20	
27	7/23	1850	2020	90	
	7/24	2010	2040	30	
28	7/29	1600	2010	250	
31	8/12	1940	1950	10	Floating below ceiling.
32	8/19	2200	1930	(-150)	" " "
40	9/26	1740	≈1750	10	
42	10/9	1710	1750	40	
	10/10	1620	?		
43	10/14	1600	≈1740	100	
47	11/4	1740	≈1730	0	
50	11/22	1650	1720	30	
53	12/7	1630	≈1700	30	
57	1/25/53	2030	2130	60	Floats little below theoretical ceiling.
63	2/23/53	2350 GMT	2430 GMT	40	
67	4/4/53	2310 GMT	2440 GMT	90	
73	5/13/53	2220 GMT	2600 GMT	220	
81	7/7/53	0040 GMT	0240 GMT	120	
		Texas Series 1953			
103	1/21/53	1610 CST	1830 CST	140	
111	2/1/53	1740 CST	1850 CST	70	

4. Computation of Atmospheric Infrared Flux. The spectral distribution of atmospheric infrared radiation has been computed for a number of cases, as a preliminary step in the estimation of the warming effect of the infrared upon the balloon. Both the radiating gases of the atmosphere (H_2O and CO_2) and the polyethylene or Mylar fabric absorb selectively in the infrared so that the spectral energy distribution is required for the warming computation.

Elsasser* has given a method of graphical integration for computing the total infrared flux across a horizontal surface in the atmosphere. While his treatment has received some criticism** it seems to be sufficiently accurate for an order-of-magnitude computation of balloon warming. Elsasser's final results give the total flux integrated over all frequencies so that, although the following computation is based on Elsasser's data, it was necessary to construct separate graphs for every spectral interval investigated.

The method may be better understood by first discussing Elsasser's method and then the modification employed.

Elsasser assumes a horizontally stratified atmosphere of infinite lateral extent, for which case expressions for the absorption or emission of a vertical beam will differ from the expression for total hemispheric flux by only a constant. Following the review by Goody and Robinson,*** the vertical flux emitted at frequency ν by a thin isothermal gas layer

---

*Elsasser W.M., 1942: Heat transfer by infrared radiation in the atmosphere, Harvard Meteorological Studies No. 6, 1942, 107 pp.

**Kaplan, L.D., 1952: J. Met., Vol. 9, p. 1

***Goody R.M. and Robinson C.D., 1953: QJRMS. p. 151

of radiating mass dm, may be written:

$$df_\nu = B_\nu \left[E_\nu (m + dm) - E_\nu (m) \right]$$

$$df_\nu = B_\nu \frac{\partial E_\nu}{\partial m} dm \qquad (16)$$

where B_ν is the black body flux per frequency interval and E_ν is the emissivity of the gas at frequency ν. The downward flux received at a horizontal surface from the gas above will be the integration of (16) performed over all frequencies and over the total mass M above this level,

$$F = \int_0^\infty \int_0^M B_\nu \frac{\partial E_\nu}{\partial m} \, dm \, d\nu \qquad (17)$$

The emissivity will vary rapidly with frequency and depend to a certain extent on temperature and pressure of the gas and it is necessary to introduce some empiricism in the evaluation of (17). Elsasser treats not E_ν but a transmission coefficient τ which has been averaged over a sufficiently large spectral interval to eliminate rapid fluctuations in emissivity (i.e. molecular bands). The transmission coefficient τ is then found to depend principally on the product of the generalized absorption coefficient and the path length, (ℓu), the function $\ell(\nu)$ being given by Elsasser's paper.*

---

* The optical path length u is in units of grams cm^{-2}. Elsasser shows by a theoretical analysis that the fractional absorption over a small frequency interval $\Delta\nu$ should, for single opaque lines and sums of lines, and for simple band spectra (but with thin layers as measured in the laboratory), be proportional to $\sqrt{\ell u}$ where ℓ depends only on the line intensity, spacing, and the half width of the lines. The function ℓ, therefore, characterizes the intensity of the square root absorption. The values of ℓ were then determined from various absorption measurements assuming the square root form for the absorption. (In some cases by estimates of the half width and line intensities.)

The evaluation of (17) then in Elsasser's notation will be:

$$F = -\int_0^{\infty}\int_{u_1}^{u_2} B_\nu \frac{\partial \tau(\ell u)}{\partial u}\, du\, d\nu \qquad (18)$$

For a given atmosphere u is a function of temperature alone and it is convenient to exchange variables making (18)

$$F = -\int_0^{\infty} d\nu \int_{T_1}^{T_2} B_\nu \frac{\partial \tau}{\partial T}\, dT \qquad (19)$$

This can be integrated by parts

$$F = -\int_0^{\infty} B_\nu\, \tau\, d\nu \Big]_{T_1}^{T_2} + \int_0^{\infty} d\nu \int_{T_1}^{T_2} \tau \frac{\partial B_\nu}{\partial T}\, dT \qquad (20)$$

Since τ is not a function of temperature by Elsasser's assumptions, (20) is equivalent to

$$F = \int_0^{T_1} \left\{Q(u_1,T)\right\} dT + \int_{T_1}^{T_2} Q(u,T)\, dT + \int_{T_2}^{0} \left\{Q(u_2,T)\right\} dT \qquad (21)$$

$u = u_1$ at $T = T_1$; $u = u_2$ at $T = T_2$

where $Q = \int_0^{\infty} \tau \frac{\partial B_\nu}{\partial T}\, dT$

The functions Q are computed in advance for different values of T and u, and a graph constructed with ordinates, essentially, of Q and T with isopleths of u. The final integration over any path representing the atmospheric (u, T) relationship is done graphically. The area of such a graph will be proportional to the flux.

The modification here was to construct separate graphs of the function which will be called Q_ν, and temperature, where Q_ν is defined

as before except that the integration over ν is performed over a relatively small interval.

$$Q_\nu = \frac{\int_{\nu_1}^{\nu_2} \tilde{\imath} \frac{\partial B_\nu}{\partial T} d\nu}{\nu_2 - \nu_1} \qquad (22)$$

The frequency interval used is of the order of 20 cm^{-1}. Values of Q_ν centered at significant points in the water vapor spectrum were computed, i.e. for the following values of ν :

200, 500, 900, 1500, 1600, 1700, 1800, 2000 cm^{-1}.

The atmospheric path-length, temperature relationship was plotted on each of these graphs and both the upward and downward components of the flux at these frequencies were computed from the area on the chart. The complete spectral distribution of the flux was then estimated by a smooth curve drawn through these eight points, interpolation being aided by referring to the appropriate black body curve.

To illustrate, the results of the flux computation (the case for 1500Z, 29 September 1953, Flight 94) computed from the St. Cloud, Minnesota, radiosonde for the levels 700 mb, 500 mb and 200 mb, are given in Figures IV-14, 15 and 16. The spectral distribution of total vertical flux across a horizontal plane (sum of upward and downward components) is plotted, as well as twice the black body flux at the temperature of the air at that level. At the two lower levels as anticipated, the total infrared flux (area under the curve) is less than the black body flux at the air temperature, while the actual flux is greater than the black body flux at air temperatures in the stratosphere.

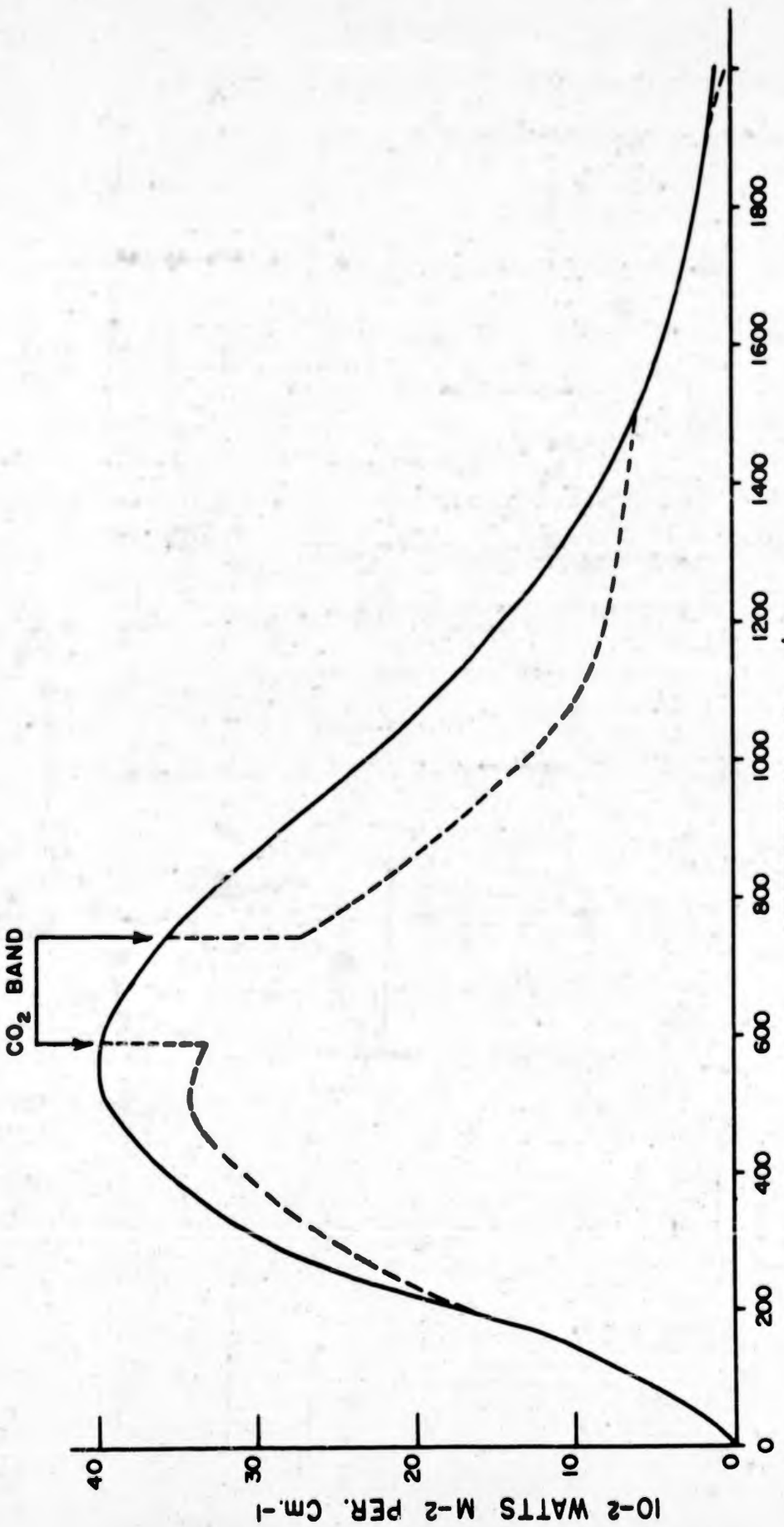

Figure IV-14. 700 mb level.

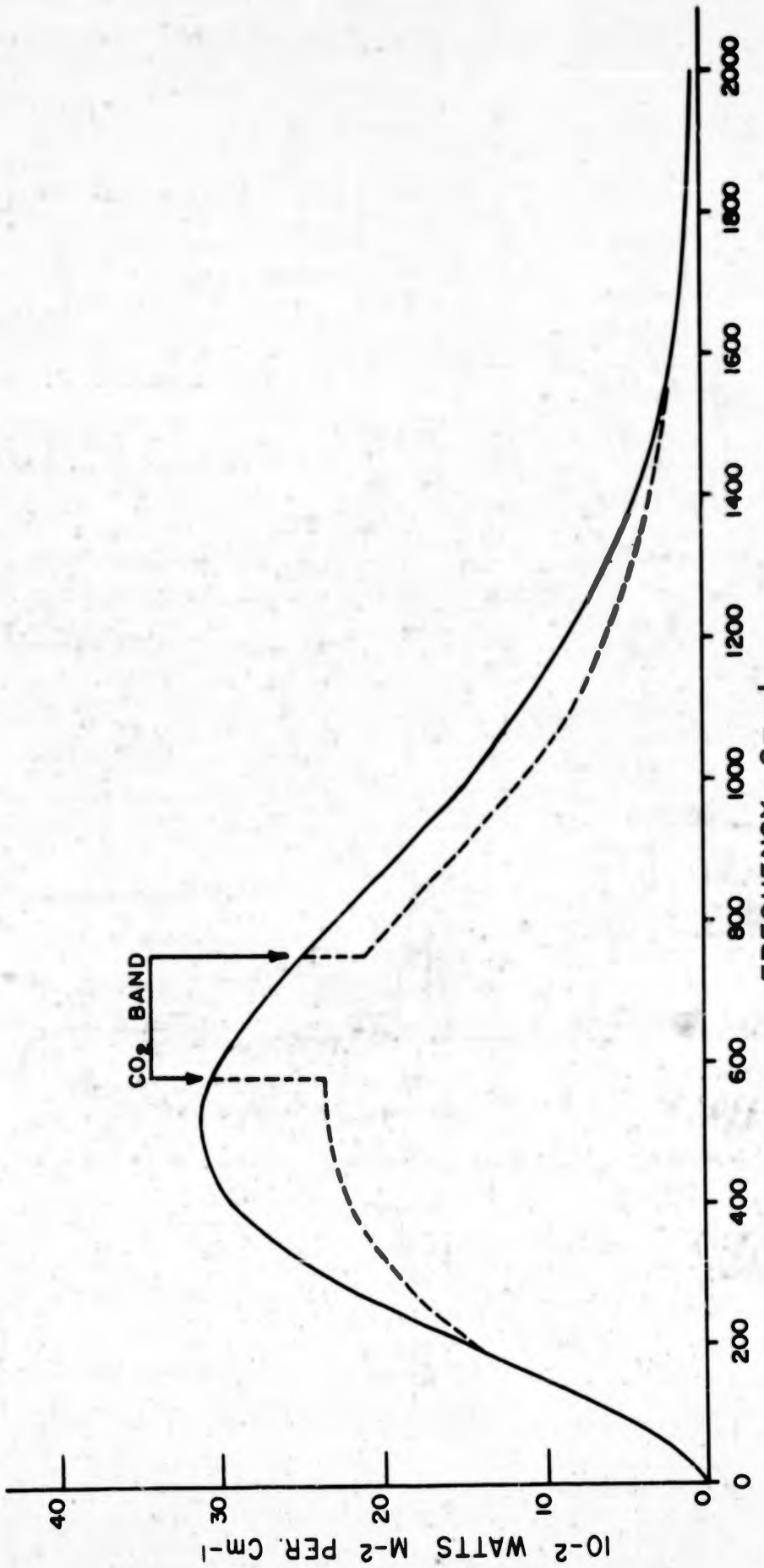

Figure IV-15. 500 mb level.

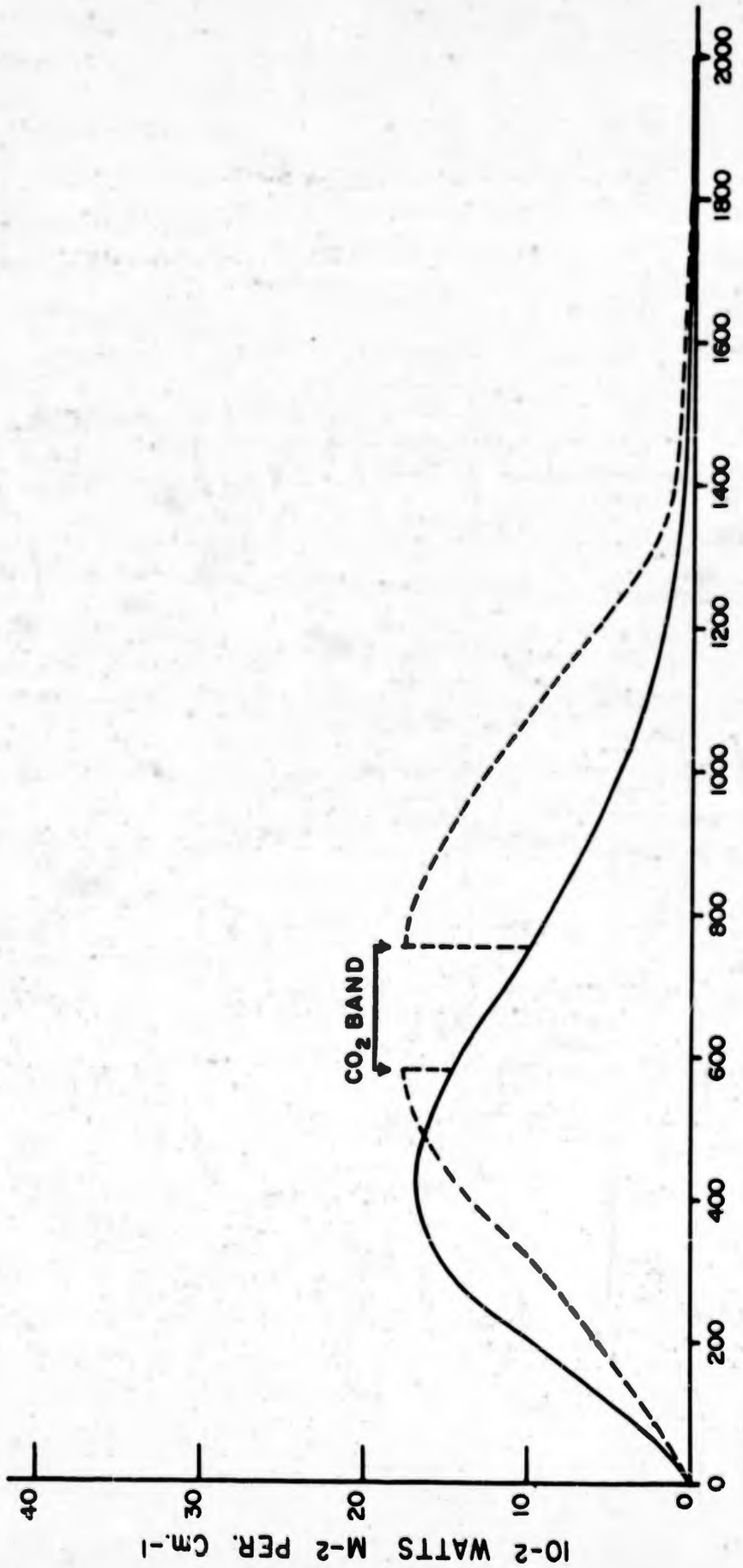

Figure IV-16. 200 mb level.

The infrared computation was made for the time of Flight 94 and for several other examples to illustrate the differences between seasons and the consistency from day to day within the season; the 27th and 29th of July, 1500Z, of 1953 were used to illustrate summer conditions, while 10 and 12 January 1954 were used as examples of midwinter.

As a check on the consistency of the computation the total flux obtained by a numerical integration of the curves for the spectral flux distribution F_ν (for example, Figures IV-14, 15 and 16) are given in Table 5 and compared with the compilation of the total flux (sum of up and down) obtained from the original Elsasser chart.

TABLE 5

Total flux intensity obtained from a numerical integration of the spectral flux distribution, $\Sigma F_\nu \Delta\nu$, compared with the total flux computed directly from Elsasser's chart (Watts, m^{-2}).

Level	$\Sigma F_\nu \Delta\nu$	Elsasser's Chart
Jan. 10		
Surface	359	375
700 mb	347	369
500	293	292
200	223*	211
Jan. 12		
Surface	343	357
700 mb	322	331
500	280	283
200	210*	208
July 27		
Surface	824	855
700 mb	655	658
500	503	501
200	332*	308
July 29		
Surface	828	846
700 mb	635	638
500 mb	498	512
200	333*	303

* F_ν curve smoothed to account for downward flux from H_2O.

TABLE 5, continued:

Level	$\sum F_\nu \Delta\nu$	Elsasser's Chart
Flight 94, 1500Z, 29 Sept 53		
700mb	591	608
500	433	446
200	292	299

The numerical summation extended only to a frequency of 2000 cm^{-1} and the neglect of the contribution from higher frequencies explains some of the differences between the first two columns of Table 5. On the whole, the interpolation of the flux distribution for a limited set of points appears satisfactory.

D. Examples of Heat Balance Calculations

1. The descent of a balloon following sunset. This is a good case to analyze, as much data is available from temperature measurements and sunset descent rates. Before sunset the superheat of the fabric, which must therefore be the superheat of the helium as the balloon is in level flight, is about 16°. Following sunset, the descent of the balloon obeys a simple empirical rule in the stratosphere

$$v = 818\ B/A^* \qquad (23)$$

where v = descent rate in ft/min.

B = balloon weight in pounds

A = weight of air displaced in pounds

This applies to large He inflated polyethylene balloons with thin film.

During descent at constant velocity v, power is developed by adiabatic compression of the balloon gas. This power can be equated to that absorbed from the sun minus the change in raciated and convected power from the fabric due to a lowering of the fabric superheat on descent. In an iso-

*See Vol. VI, p. VI-127.

thermal atmosphere, or even one with constant temperature gradient, and neglecting aerodynamic drag, the balloon gas superheat should remain unchanged as the system is in dynamical equilibrium both before and after sunset, and measurements show this to be the case.

The power developed on descent

$$P = gAv$$
$$= 818 \times g \times B \quad \text{(from Equation (23))}$$
$$= 818 \text{ ft-lbs/min/lb}$$
$$= .040 \text{ watts/gram.}$$

We now write down the heat balance equation (Eq. 1) as follows:

a) before sunset

$$0 = 0 + q_1 - q_2 + q_3 - q_4 \tag{24}$$

b) after sunset

$$0 = q_o - q_2' + q_3 - q_4'$$

The terms are as defined for Equation 1. (Sec. IV-A)

Subtracting a) from b)

$$0 = q_1 - q_o + (q_2' - q_2) + (q_4' - q_4) \tag{25}$$

The atmospheric radiation absorbed (q_3) is assumed constant before and after sunset and drops out. Using further the detailed definition of the various terms, as described in Part B,

$$q_1 - q_o = K \left[(T + \theta_1)^4 - (T + \theta_1')^4\right] + H \left[\theta_1^{4/3} - \theta_1'^{4/3}\right] \tag{26}$$

or $$q_1 - q_o = 4KT^3 (\theta_1 - \theta_1') + H (\theta_1^{4/3} - \theta_1'^{4/3}) \tag{27}$$

We now make the assumption that the convection constant H inside the balloon (He to fabric) is identical with that outside (air to fabric). There is some theoretical justification for this assumption. Then

$$q_o = H (\theta_1 - \theta_1')^{4/3} \tag{28}$$

and H may be eliminated, giving

$$\frac{q_1}{q_o} - 1 = \frac{4KT^3}{q_o} (\theta_1 - \theta_1'' + \frac{\theta_1^{4/3} - \theta_1'^{4/3}}{(\theta_1 - \theta_1')^{4/3}} \tag{29}$$

In this equation one may insert known values of q_1, q_o, K, T, and θ, and compute θ_1', the fabric superheat after sunset on descent. Although this would be a very valuable number for practical application, unfortunately it may readily be seen that values of q_1 in paticular, and K, are not well enough known to determine θ_1'. We therefore assume that θ_1' lies between θ_1 and 0. The last term in Equation 27 therefore lies between 0 and 1. We assign it the value 1 ($\theta_1' = 0$), and compute q_1, the solar absorption, as an unknown.

$$4KT^3 = 4 \times \underbrace{24.5 \times 5.67 \times 10^{-12}}_{K} \times (218)^3$$

$$= 5.76 \times 10^{-3} \text{ watts/g}$$

$$q_o = .04 \text{ watts/g}$$

$$\frac{4KT^3}{q_o} = 0.144$$

with $\theta_1 = 20^o$

$$q_1 = (.144 \times 20 + 1)\ .04$$

$$= (2.88 + 1)\ .04 = .155$$

with $E_s = .134$ watts/cm^2

$a_s = 1.16$ which is equivalent to .26%/mil thickness.

This is a maximum figure. If $\theta_1 > \theta_1' > 0$, the calculated a_s will be further reduced. Note that the laboratory value corrected for reflection but not scattering is about 1%/mil ($a_s = 4.4$).

2. Equilibrium Temperature of Film at Night.

From Equation (1) we write

$$q_2 = q_3 \qquad \text{(ignoring convection)} \tag{30}$$

$$A_e \cdot b \cdot T^4 \cdot m = E_e \cdot a_e \cdot m \tag{31}$$

$$T = \left(\frac{E_e \cdot a_e}{A_e \cdot b}\right)^{1/4} \tag{32}$$

It can be theoretically shown that for a transparent material $A_e = a_e$

$$\therefore \quad T = \left(\frac{E_e}{b}\right)^{1/4} \tag{33}$$

$$= E_e \cdot 0.643 \cdot 10^3$$

At 200 mb in winter we find (See Summary of Useful Information, Section F)

$E_e = .021$ watts/cm^2 $\qquad T = 135^\circ$ K

In summer $E_e = .031$ $\quad T = 199^\circ$ K

Both these temperatures are lower than air temperature at 200 mb except under exceptional circumstances. Convection transfer will always limit the excursions due to radiation, and therefore a calculation of this kind may be used only as an indication of the direction of the effect unless convection is quantitatively taken into account. Furthermore, we have ignored the spectral distribution of the atmospheric radiation and the selective absorption of polyethylene in this region, and have used

the absorption coefficient a_e, determined with black body radiation. At the present writing we have available the spectral distribution of atmospheric radiation from calculations (see Section IV-C-4), but the knowledge of the absolute spectral absorptivity of polyethylene fibers is not good enough at present to make a completely valid computation of q_3. At least in the case of summer conditions, it is possible that due to the earth "window" effects on the polyethylene, q_3 may be increased enough to bring T above air temperature (200-220° K are plausible air values). This emphasizes the importance of careful investigation of the spectral properties of all structurally usable films, in attempts to control film temperatures, and thereby balloon stability.

E. Preliminary Infrared Flux Measurements

In order to obtain some quantitative data on the effect of ground radiation on the balloon, a device has been developed wh ch can theoretically measure the equivalent black body temperature of the received radiation. The device is essenti .lly a simple thermistor bolometer.

Results from these measurements are very meager to date. The initial model of infrared detector was flown in conjunction with the temperature recorder on Flights 67 and 73. Flight 67 has been recovered and has given the only reliable data to date; Flight 73 has never been found.* The infrared detector was flown in subsequent flights in conjunction with the thermistor pulse generator. Unfortunately, the characteristics of this instrument are such that the shift of zero point in the detector invalidates the telemetered data. (See Vol X, Sect. IB) A satisfactory telemetering system has now been designed but has not been flown in this series of flights.

* Gondola from Flight 73 later recovered.

The infrared detector consists of three thermistors mounted in a relatively massive block such that two of them always remain at the block temperature while the third, thermistor C, attains the block temperature with the shutter closed and some other temperature dependent on ground radiation with the shutter open. See Figure IV-17. Two models of the detector have flown: the first, 2-IRD 1-540, uses three ML 419/AMT-4 thermistors, a silver chloride filter, and is suspended outside the gondola; the second, 2-IRD 2-547, uses one ML 419/AMT-4 and two Victory Engineering type 51A2 bead thermistors, a Wratten type 87 filter, and is mounted inside the gondola. Both use two thermistors as sensing elements and one as a thermometer for measuring the block temperature.

Arranging the two sensing thermistors in a bridge circuit prevents any shift in zero point due to changes in the absolute temperature of the detector block. Actually, because of slight non-uniformities in thermistors, the zero does shift to some degree with a change in temperature. With the shutter closed, both thermistors A and B attain the block temperature, T_A. After the shutter has been open for a time, radiation causes thermistor B to attain a new temperature, $T_A - \Delta T_A$, and a new resistance, $R_A + \Delta R_A$.

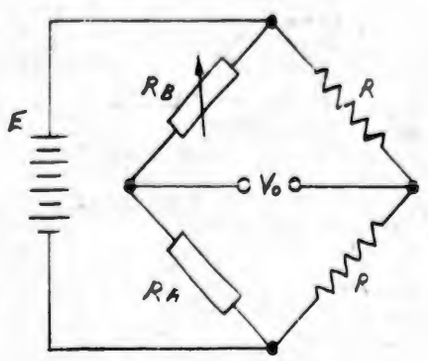

The change in bridge output is then

$$\frac{\Delta V_o}{E} = \frac{R_A}{R_A + R_B + \Delta R_A} - \frac{R_A}{R_A + R_B}$$

If $R_A = R_B$ with the shutter closed,

$$\frac{\Delta V_o}{E} = \frac{R_A}{2R_A + \Delta R_A} - \frac{1}{2}$$

$$\cong -\frac{\Delta R_A}{4R_A}$$

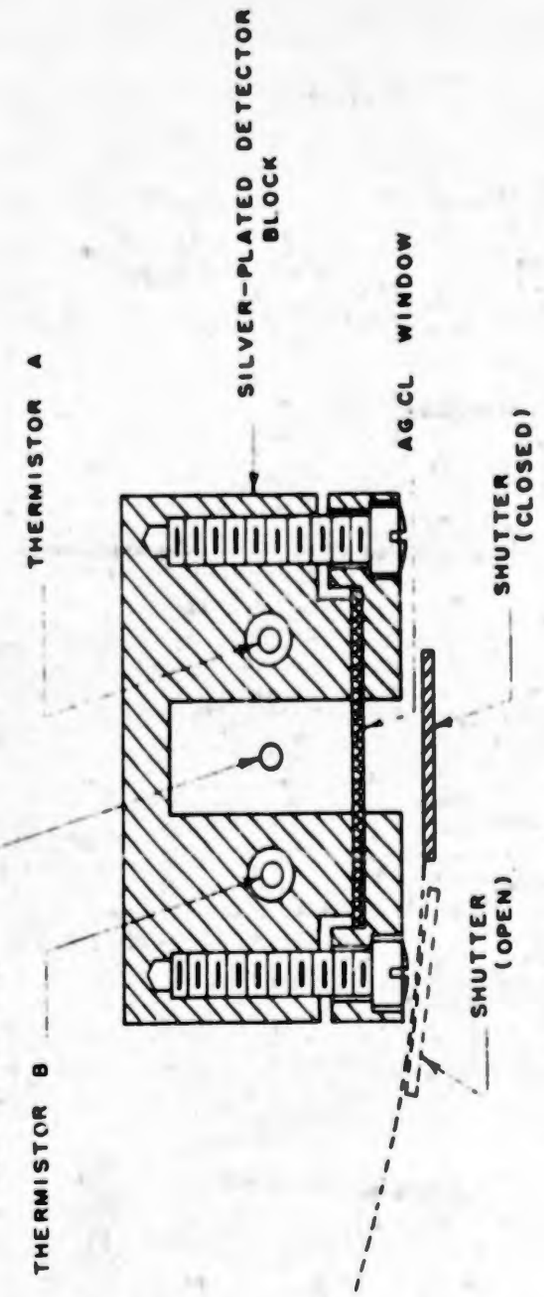

Figure IV-17. CUTAWAY VIEW OF INFRA-RED DETECTOR

The characteristic of a thermistor can be accurately expressed by the relation,

$$R = R_o e^{b\left(\frac{1}{T} - \frac{1}{T_o}\right)}$$

where R_o is the resistance at 0^oC, $T_o = 273^o$, b is a constant, and R is the resistance at absolute temperature T. This gives

$$\Delta R = -\frac{b}{T^2} R dT, \text{ or}$$

$$\frac{\Delta R}{R} = -\frac{b}{T} \cdot \frac{\Delta T}{T}$$

To relate the thermistor temperature to the incident radiation, consider the heat balance of the element per unit area of the thermistor:

a) it receives $\alpha \epsilon_g \sigma T_g^4$ watts from the ground. Here, T_g is the effective black body temperature of the radiating surface whose emissivity is ϵ_g, σ is the Stephan-Boltzmann constant, and α is a geometrical factor which takes into account the fact that the thermistor is partially concealed in the block. Since the interior of the case is highly silvered, α must be nearly unity.

b) It receives $\beta \epsilon_A \sigma T_A^4$ watts from the block, whose temperature is T_A and whose emissivity is ϵ_A. Here, β, another geometrical factor, is roughly 0.5, and ϵ_A is approximately 0.04.

c) it radiates σT_B^4 watts, where T_B is the thermistor temperature.

d) it gains (loses) heat by conduction to the block via the air in the cavity. If K is a suitable conduction constant, this loss is $K(T_A - T_B)$. The conductivity strongly governs the temperature, since if the cavity is pumped down to approximately 10^{-5} mm Hg pressure, the recorded temperature

change between conditions of shutter closed and open increases by about five times. However, for pressures between atmospheric and about 1 mm Hg, there is only a small change in sensitivity as expected from gas conduction theory. One may now write

$$\sigma T_I^4 = \alpha \epsilon_g \sigma T_g^4 + \beta \epsilon_A \sigma T_A^4 + K(T_A - T_B)$$

If $T_A - T_B = \Delta T_A$

$$T_B^4 \cong T_A^4 - 4T_A^3 \Delta T_A \qquad \text{Substituting,}$$

$$\Delta T_A \left(\frac{K}{\sigma} + 4T_A^3\right) = T_A^4 (1 - \beta\epsilon_A) - \alpha \epsilon_g T_g^4$$

$$\frac{\Delta T_A}{T_A} = \frac{1 - \beta\epsilon_A}{4\left(1 + \frac{K}{4\sigma T_A^3}\right)} - \frac{\alpha \epsilon_g}{4\left(1 + \frac{K}{4\sigma T_A^3}\right)} \left(\frac{T_g}{T_A}\right)^4$$

If the radiating surface is at the same temperature as the block, $T_g = T_A$ and $\Delta T_A = 0$, so finally

$$\frac{\Delta T_A}{T_A} = \frac{\alpha \epsilon_g}{4\left(1 + \frac{K}{4\sigma T_A^3}\right)} \left[1 - \left(\frac{T_g}{T_A}\right)^4\right]$$

Over moderate ranges of block temperature, T_A, it is sufficient to write

$$\frac{\Delta T_A}{T_A} = C_1 \left[1 - \left(\frac{T_g}{T_A}\right)^4\right] \qquad \text{where } C_1 \text{ is a constant.}$$

Making the further approximation that

$$T_A^4 - T_g^4 \cong 4T_A^3 (T_A - T_g)$$

$$\Delta T_A \cong C_2 (T_A - T_g).$$

Finally, combining expressions, the change in bridge-output voltage between conditions of shutter open and closed is

$$\frac{\Delta V_o}{E} = \frac{bC_1}{4T_A}\left[1 - \left(\frac{T_g}{T_A}\right)^4\right] \cong C_3 (T_A - T_g).$$

On Flight 67, the detector case hung in the outside air and remained colder than the apparent ground temperature. The expression above was used in the form

$$\Delta V_o = C_3 (T_g - T_A).$$

For calibration, the detector was placed in a Styrofoam box whose interior could be cooled by passing cold dry air through it. The air served the double purpose of refrigerant and dessicant to prevent fog from forming on the silver chloride window. The unit was pointed up and the top of the Styrofoam box removed to allow measurements on the radiation from a black surface which was supported a few inches above the box, covering the solid acceptance angle of the window. Data was taken with the black body at 20°C and 0°C and the detector operated between -5° and -90°, as shown in Figure IV-18. The effect of the $\frac{C_1}{T_A}$ term is apparently not serious.

During flight, the voltage output from the detector was applied to a vacuum tube voltmeter which indicated on one of the two panel meters on the temperature recorder. One of the temperature readings in the sequence of readings (Vol. X, Sect. IB) was that of the detector block temperature, the difference reading thus giving the apparent ground temperature.

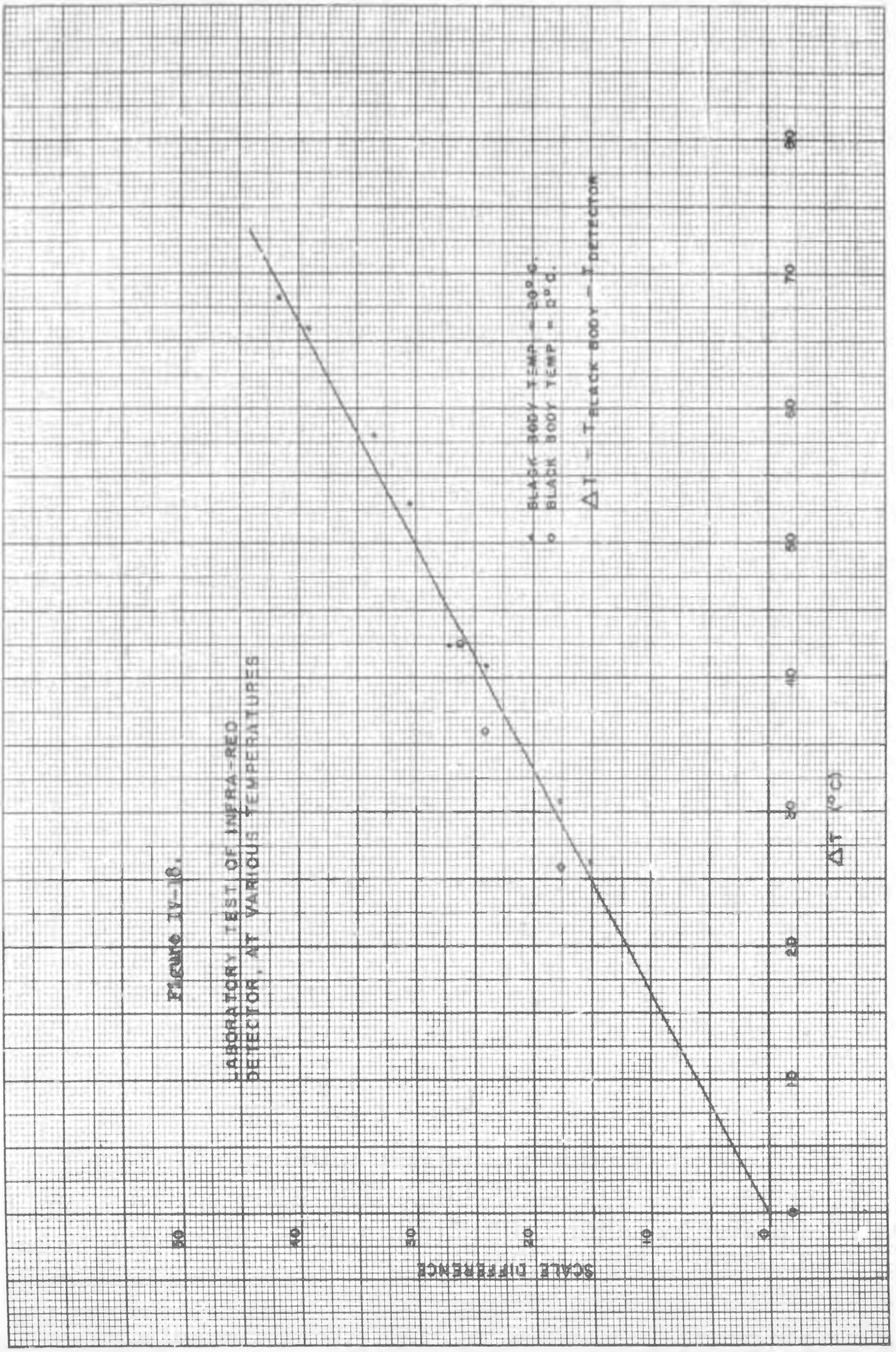
FIGURE IV-16.
LABORATORY TEST OF INFRA-RED DETECTOR, AT VARIOUS TEMPERATURES
ΔT = T BLACK BODY − T DETECTOR
BLACK BODY TEMP = 20°C.
BLACK BODY TEMP = 0°C.
SCALE DIFFERENCE
ΔT (°C)
0
10
20
30
40
50
60
70
80

Results from Flight 67 are shown in Figure IV-19. Although the block temperature varied widely, the apparent ground temperature points plot out a smooth curve, the variations most likely resulting from rapid ascent or descent causing a difference in temperature between the block and the shutter. The apparent ground temperature is shown to be roughly -7°C during the day and roughly -17° after sunset, or a total diurnal change of about 10°. This change appears to be higher than one would expect from theoretical computations but further measurements will clear up the point.

F. Summary of Useful Information

1. Solar Constant, E_s = .134 watts/cm^2

   (subject to seasonal, diurnal and altitude effects as shown in text).

2. Radiation constant b = 5.672×10^{-12} watts/cm^2/°K^4

3. $\lambda_{max} T = A$ A = .288 cm-deg Wein Displacement Law

4. Mean absorption and emissivity of films:

FRACTIONAL ABSORPTION OR EMISSIONS/cm/g/cm^3

Symbol	Wavelength Region	Mylar	Polyethylene
a_s	visible .4 - .7μ	≈ 2.9	≈ 4.4 (lab measurement) 1.16 (calculated)
a_e	infrared 1 - 15μ - 50°C radiation	217	24.5
ρ	density g/cm^3	1.38	0.9

5. Typical infrared flux in atmosphere at 200 mb. 45°Lat., up and down, clear skies.

Watts/cm^2

Winter	Summer
.021	.031

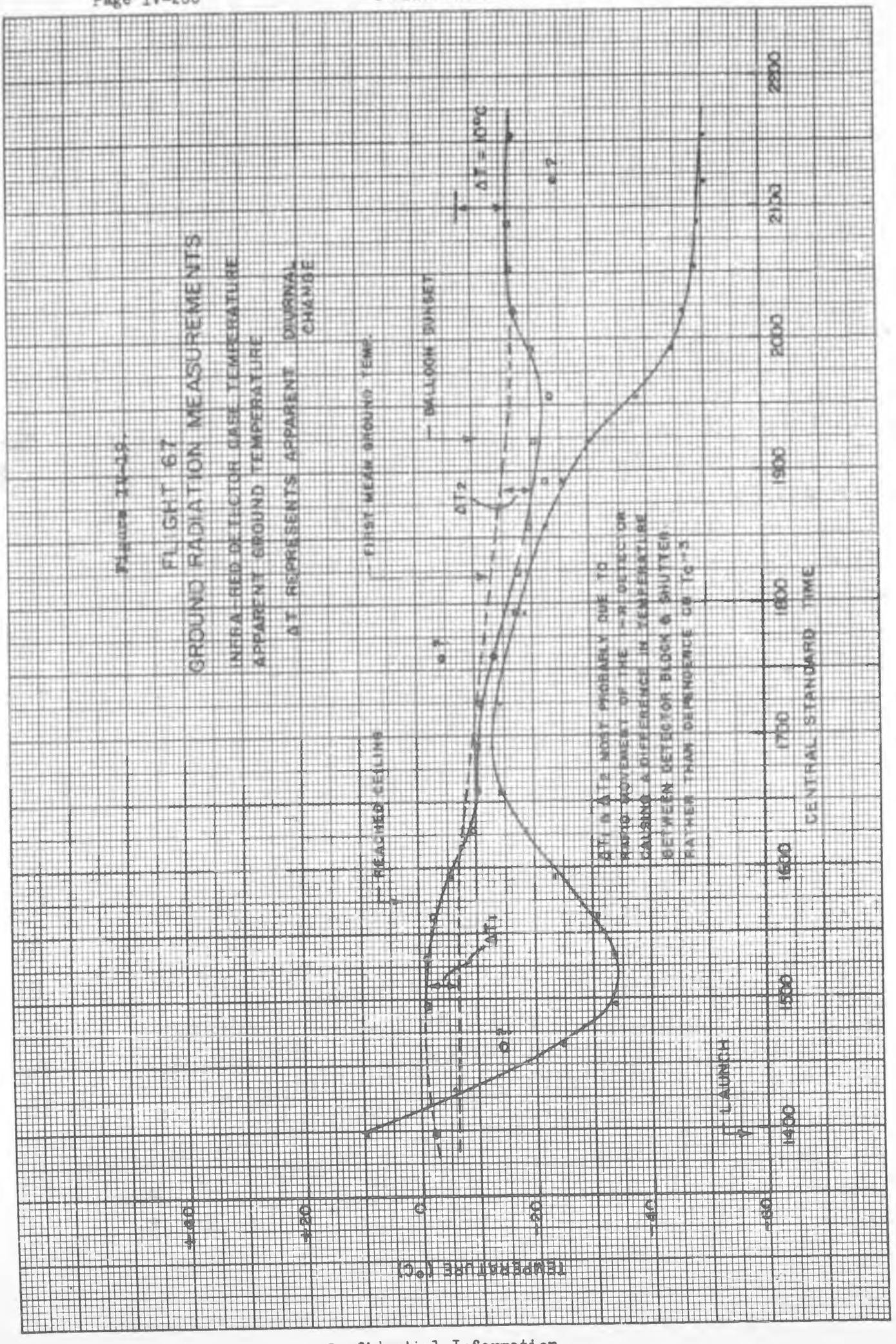
Figure IV-19
FLIGHT 67
GROUND RADIATION MEASUREMENTS
INFRA-RED DETECTOR CASE TEMPERATURE
APPARENT GROUND TEMPERATURE
ΔT REPRESENTS APPARENT DIURNAL CHANGE
FIRST MEAN GROUND TEMP.
BALLOON BURSET
REACHED CEILING
LAUNCH
ΔT = 10°C
ΔT1
ΔT2
ΔT1 & ΔT2 MOST PROBABLY DUE TO RADIO MOVEMENT OF THE IR DETECTOR CAUSING A DIFFERENCE IN TEMPERATURE BETWEEN DETECTOR BLOCK & SHUTTER RATHER THAN DIFFERENCE OF Tg-Ts
+40
+20
0
-20
-40
TEMPERATURE (°C)
1400
1500
1600
1700
1800
2000
2143
2300
CENTRAL STANDARD TIME

6. Absorption of Atmospheric Gases in the Infrared Region.

(from J. H. Shaw, Engineering Experiment Station Report, Ohio State University, June, 1951.)

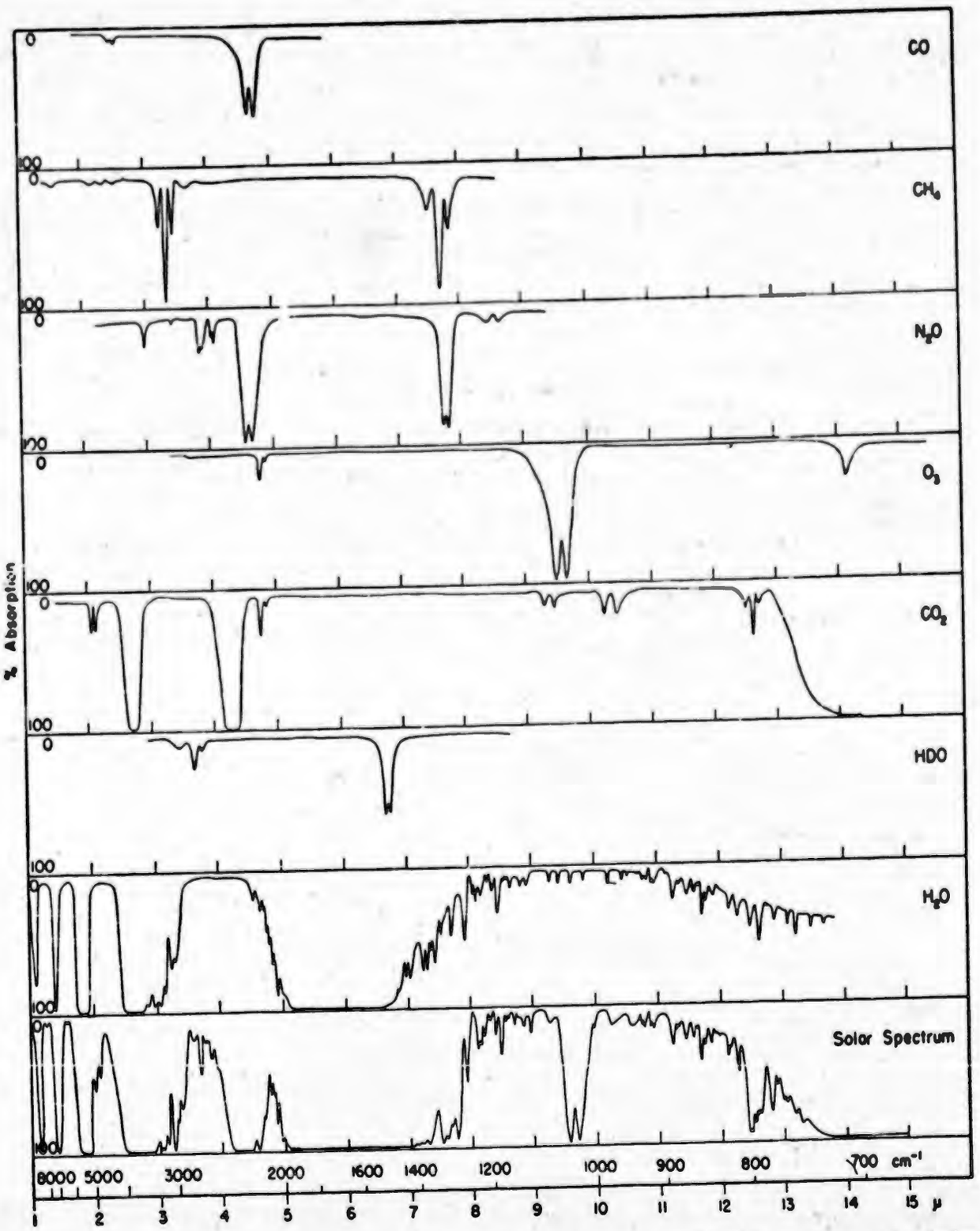

—Infrared solar spectrum, from 1μ to 15μ (*bottom curve*), with positions and relative intensities of the bands of other known atmospheric gases shown on other curves.

Figure IV-20

Section V

ANALYSIS OF BALLOON AND AIR TEMPERATURE MEASUREMENTS

A. General Description

A balloon may be regarded as a thermodynamic engine in which the work done in raising the load comes from heat transported into the gas (Volume V, Sec. VI). If one assumes the gas to be at a uniform temperature, convection theory serves as a guide to an estimate of the heat transport (Volume I, Sec. IV). A mean buoyancy temperature is obtainable from gross considerations of the flight, i.e., rates of rise and descent, changes of altitude during ballast drops, etc., or in the step flights, from knowledge of the tow balloon free lift from the tensiometer data. Details of the heat flow, however, can be obtained only from actual temperature measurements of the balloon gas and outside air. In addition, a direct measure of the temperature relations holding in a balloon provides a graphic illustration of balloon behavior and an independent check on vertical flight constants obtained from ballast, tension, and rise rate data.

To date, five flights have been flown specifically for the purpose of obtaining direct measurements of balloon temperatures. These are Flights 57, 63, 67, 73, and 81. Two step flights, Flights 91 and 94, have also included measurements of the tow balloon temperature. Other flights including measurements of air temperatures and temperatures inside the gondola are listed in Table I.

Evidence exists, based on observations of dips and rises in balloons floating below ceiling altitude at night, plus the equilibrium warming of

TABLE I

Temperature Instruments Flown, By Flight

Flight	Measuring Instrument	Air Temps.	Gondola Temps.	Balloon Temps.	Infrared Flux
57	Rec.	2		3	
63	Rec.	2		6	
67	Rec.	2		7	1
68	TPG	1	1		
69	TPG	1	1		
71	TPG	1	1		
72	TPG	1	1		
73	Rec.	2		7	1
74	TPG	1	1		
75	TPG	1	1		
76	TPG	1	1		
77	TPG	1	1		
78	TPG	1	1		1
79	TPG	1	1		1
80	TPG	1	1		1
81	TPG	1	2	7	1
83	TPG	1	1		
84	TPG	1	1		
86	TPG	1	1		1
87	TPG	1	1		1
90	TPG	1	1		
91	BTT	1	1	3	1
92	TPG	1	1		1
94	BTT	1		2	
95	TPG	1	1		

Rec. = Temp.-Pressure Recorder
TPG = Thermistor Pulse Generator
BTT = Balloon Temp. Telemeter

the balloon gas with altitude,* that the infrared radiation from the ground and the atmosphere must be considered in the heat balance of the balloon. In order to obtain some quantitative measurements of this radiation, a device was developed which in principle can measure the total incident radiation. Results from such measurements have proved unsatisfactory to date because of the difficulty of perfecting a suitable transponder to modulate the telemetering system. An improved transponder for these measurements has been developed and will be flown in subsequent flights.

B. Experimental Methods

Temperature measurements of both balloon gas and outside air have been made using white thermistors.** A description of their coating has been given by Brasefield***, who quotes tests at Johns Hopkins to show that they have low emissivity in the visible and high emissivity in the infrared. Averaging the emissivity over the solar spectrum, he arrives at a figure of 6% for the mean emissivity in the visible. Our own measurements in the 10-μ region show them to be black, indistinguishable within about 10% from an Aqua-Dag coated thermistor. This color property (white in the visible, black in the infrared) is desirable for air temperature measurements since the absorption of sunlight is small, and what heat may be so gained can be dissipated by radiation characteristic of the thermistor temperature. The thermistors are vulnerable to radiation from

---

* See Sect. G of this report for discussion of altitude warming.
** Freiz Instrument Company, type ML 419/AMT-4.
*** J. Met. 5, 147 (1948).

the earth, but this is nearly balanced by the radiation to free space at ordinary air temperatures.

For measurements within the balloon gas, the situation is slightly worse. The fabric radiates to the thermistor in the region where the thermistor is black. At worst, the thermistor will then read the fabric temperature. The effect is not serious, however, for a number of reasons:

a) the fabric is essentially transparent in the infrared.*

b) the conductivity of helium is much greater than that of air, clamping the thermistor temperature more effectively to that of the gas.

c) the fabric temperature in any case cannot be too different from that of the gas to be measured.

In order to obtain measurements of the air temperature, one need only mount or suspend one or more thermistors in such a manner that air is free to circulate about the element, and at a sufficient distance from the gondola so that radiation effects from this source are negligible. The two methods which have been employed are 1) mounting the thermistor(s) on the ends of 6-inch shiny wires connected to a Lucite plate which is suspended at a distance of about five feet from the gondola on an aluminum pole (Figure V-1); and 2) dangling a thermistor below the gondola on an eight-foot length of fine twisted-pair lead.

To obtain balloon gas temperatures at various points, thermistors are dangled on leads of appropriate length from points on the fabric. Because of the extreme fragility of the thermistor element, each is mounted on a wooden stick of low heat capacity and surrounded by a helix of wire

---

* See Volume IX, Section IV.

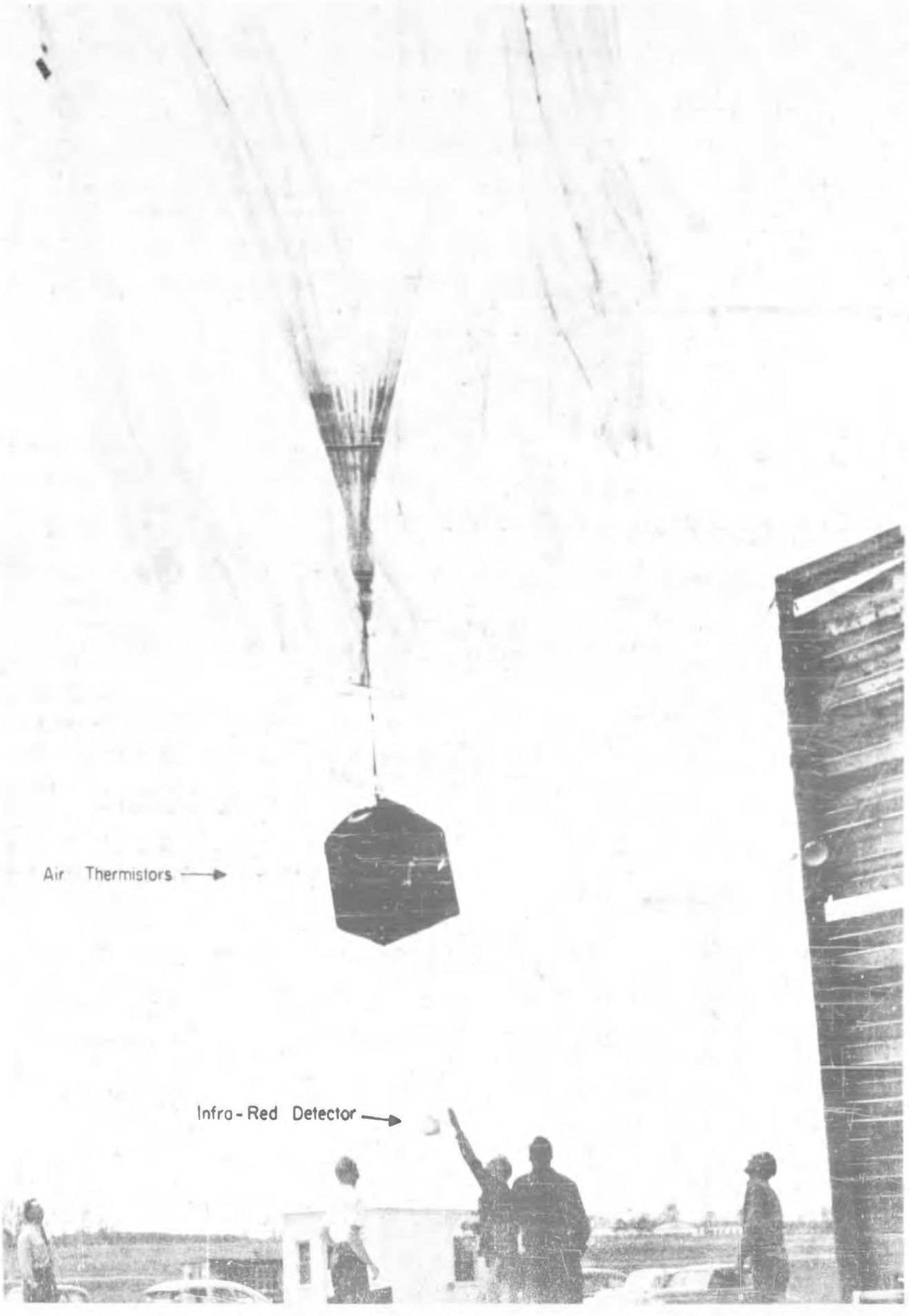

Figure V-1. Flight 73 at launch, showing method of suspension of air thermistors on pole and infrared detector below the gondola.

which serves to prevent breakage by falling against the fabric (Cf. Figure I-2, Volume X, Section I). This assembly is encased in an aluminum sphere, around which the appropriate length of lead wire is wound, and the sphere is released into the balloon gas at such a pressure that when the lead wire has unrolled and the sphere fallen off, the thermistor hangs free in the balloon gas. For a description of the thermistor dropper, see Volume X, Section I. To date, thermistors have been flown in seven positions within the balloon; these positions are illustrated in Figure V-2.

Two types of instruments have been used to measure temperatures during flight. The first of these, flown on Flights 57, 63, 67, and 73, is a device which sequentially switches the various thermistors to a vacuum tube voltmeter, whose output meter is photographed. Periodically, precision resistors are switched into the circuit for self-calibration. Success of the flight depends on recovery of the instrument. The second type of instrument is a Thermistor Pulse Generator. This is essentially a bootstrap relaxation oscillator into which the various thermistors are switched, and which produces spaced pulses, the interval between them being proportional to the thermistor resistance. This instrument also calibrated during flight by switching in precision resistors periodically. For the step flights, the pulse generator is used in conjunction with a low power 10-mc transmitter which relays the temperature information from the tow balloon down to the main gondola. A receiver in the gondola then applies the pulses to a regular telemeter channel. For a complete description of both these instruments, see Volume X, Section I.

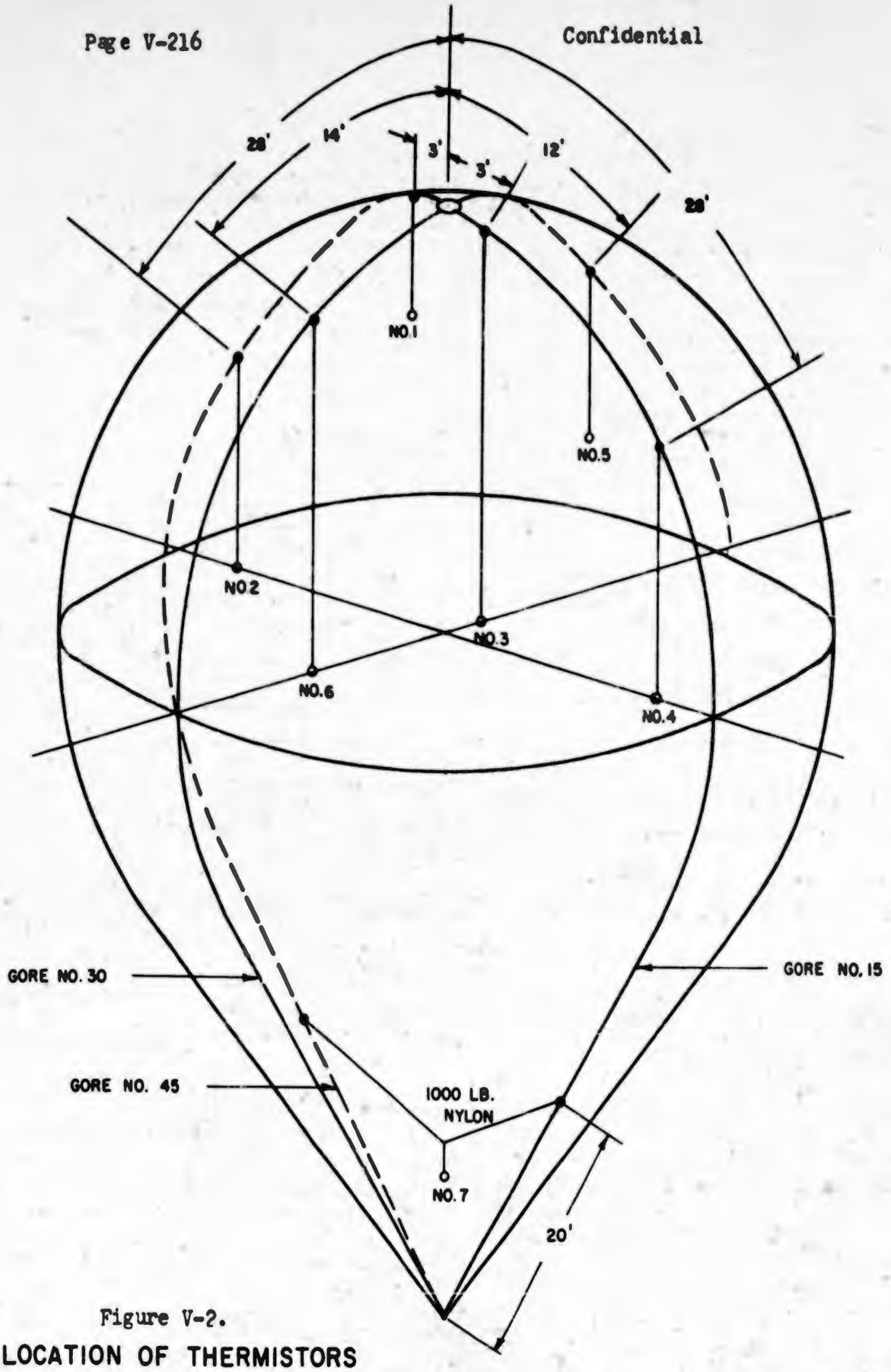

Figure V-2.
LOCATION OF THERMISTORS
IN BALLOON

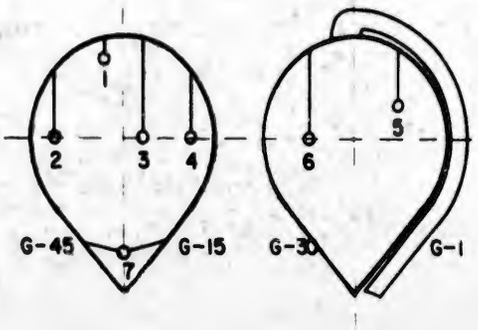

C. Properties of Thermistors

The thermistors, purchased from Friez Instrument Corporation, have been found to be quite uniform. If, for some average thermistor, the calibration is found to be $R = R_s(T)$ (Figure V-3), then all others tested are found to fit $R_k = \lambda_k R_s(T)$, where λ_k is a number characteristic of a given thermistor lying within $\pm$ 4% of unity. Calibration of a thermistor can thus be made at a single temperature. Assuming $\lambda = 1.00$ for all thermistors leads to errors of only about 1°C at temperatures below -10°C.

For the understanding of balloon phenomena, temperature errors of as high as 5°C might be tolerated if the difference between balloon gas and outside air can be determined to within $\pm$ 2°. Since forced ventilation is not feasible for any but the outside air thermistors, and then only during rapid ascent or descent, it was necessary to make some laboratory tests to see how large a temperature error would be made by failing to ventilate the thermistors. This was done in two ways. In the first way, a thermistor was mounted in a large metal bell jar which had two diametrically opposed Lucite windows. Light from a sealed beam lamp was allowed to shine through one window and to emerge from the other. The incident window was double, with cooling water circulated through the space between the panes. The thermistor lay horizontally in the light beam 18 inches from the lamp face, the latter being outside the bell jar. The radiation intensity was determined by a separate calorimetric measurement in which the beam passed through the window into a dewar flask of blackened water. In this way, the intensity at 18 inches was measured to be 0.13 watts/cm^2, or very closely one solar constant (0.132 watts/cm^2). The spectral distribution

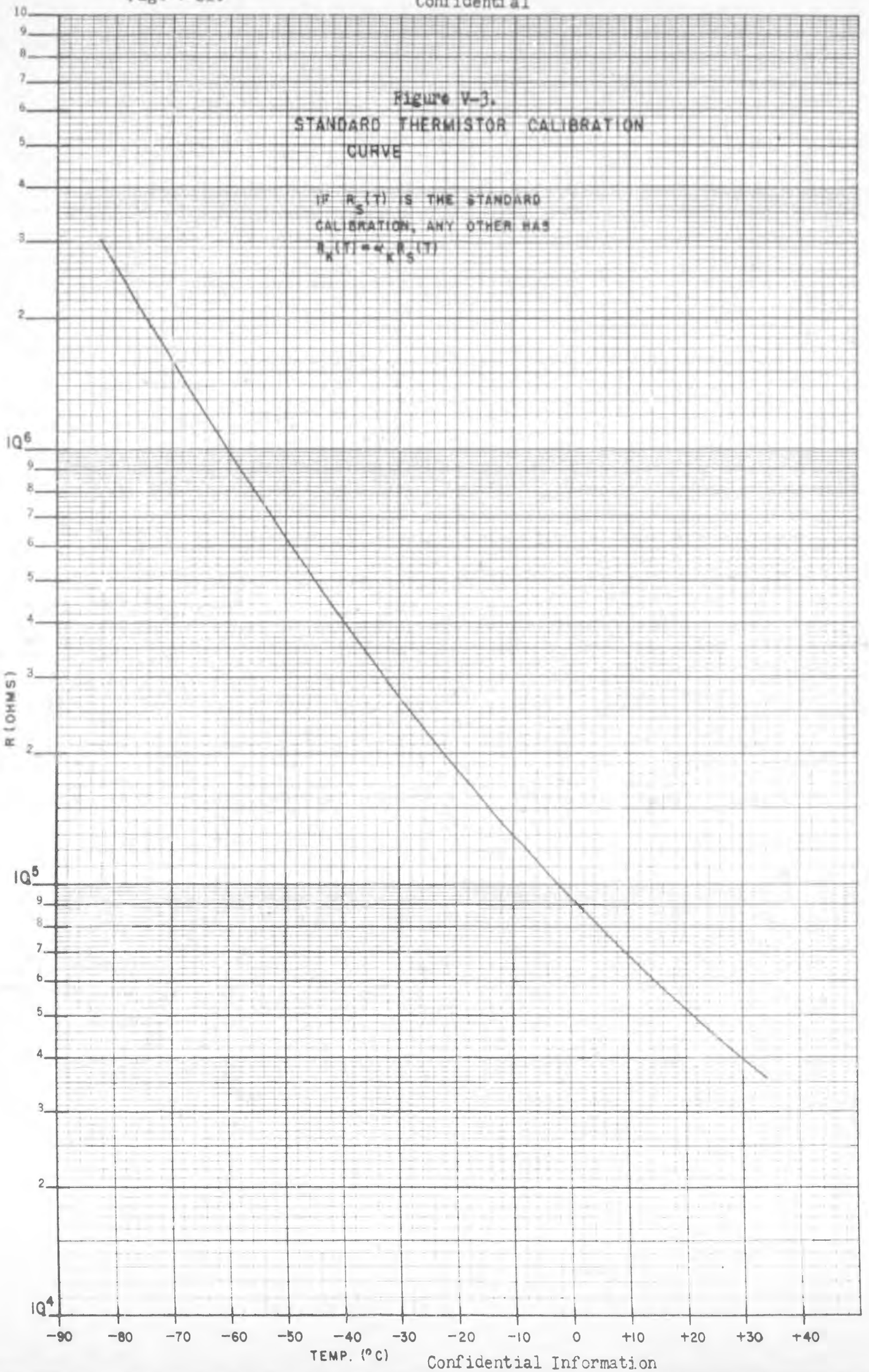

Figure V-3.
STANDARD THERMISTOR CALIBRATION CURVE

IF $R_S(T)$ IS THE STANDARD CALIBRATION, ANY OTHER HAS $R_K(T) = \alpha_K R_S(T)$

of the test radiation favors the red end of the spectrum and is cut off in the near infrared by the Lucite and the water. Table II gives values of the temperature rise above room temperature ambient.

TABLE II

Temperature Rise, ΔT, of a White Thermistor Illuminated by One Solar Constant of Tungsten Radiation

Pressure	ΔT (°C) Air	ΔT (°C) He
1 Atm	1.3	0.7
20 cm Hg	1.4	1.5
10 cm Hg	1.5	2.2
4 cm Hg	1.7	2.4
1 cm Hg	3.4	2.5

From the table, it is seen that at the highest altitude reasonable (1 cm Hg), an air temperature error of approximately 3°C may be made, and a difference between helium and air temperatures of about 1°C. This is within the limits considered satisfactory. It must be pointed out that the thermistor could also lose heat by radiation to the jar. This loss for a temperature rise ΔT is, per unit area of thermistor, $4\sigma T^3 \Delta T$. For the temperature rises given, this is less than 10^{-2} solar constant and is negligible.

The second method for determining temperature rise in the absence of ventilation was to heat the thermistor in the bell jar by passing a current through it and simultaneously measuring the resistance. The current was 60-cycle AC applied through a condenser. The AC voltage across the thermistor was measured with a vacuum tube voltmeter decoupled by a condenser. The resistance was measured by an ohmmeter connected to the thermistor through a low-pass filter.

Figure V-4 shows the equilibrium temperature rise as a function of the electric power dissipated in the thermistor.

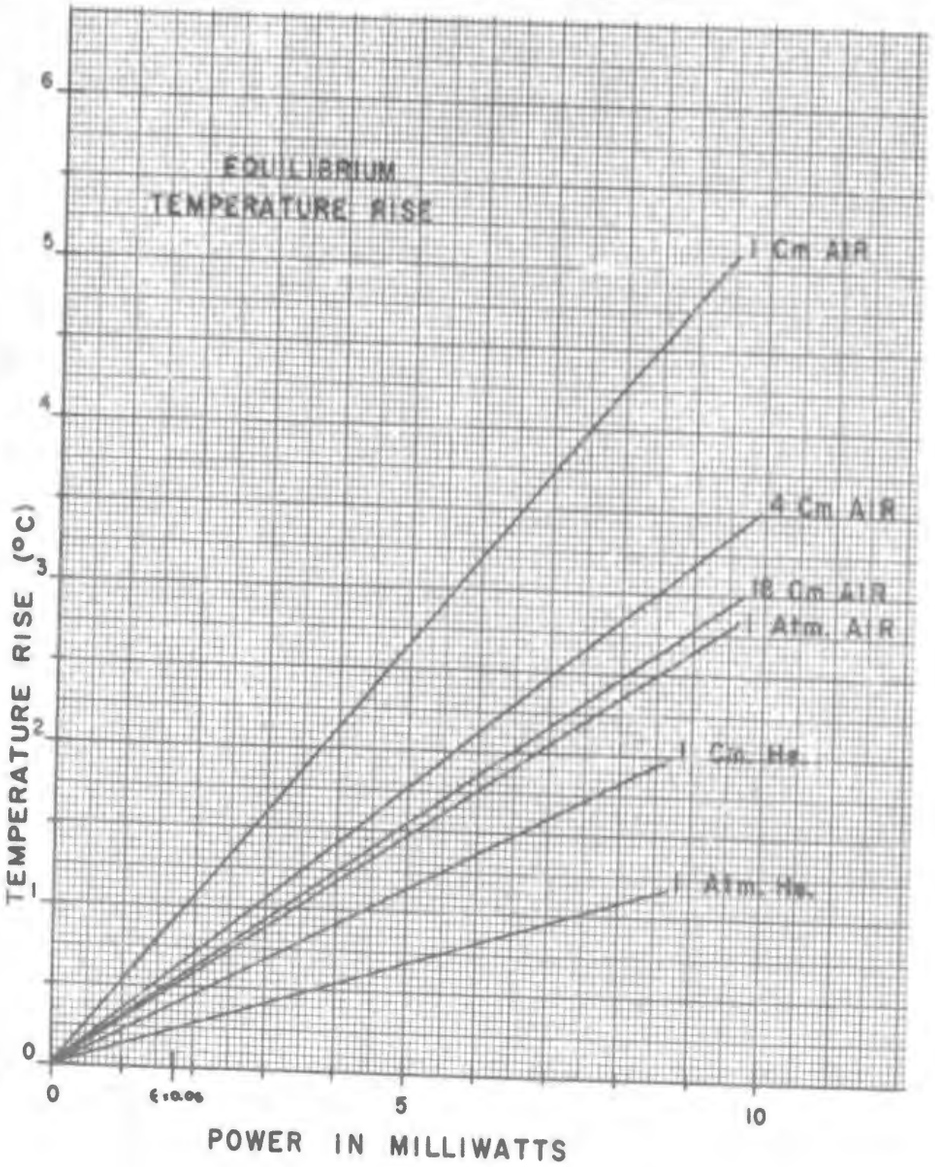

Figure V-4.

Using the thermistor dimensions (0.066 cm dia., 3.3 cm length) and the solar constant (0.132 watts/cm^2), an emissivity of 0.06 corresponds to the abcissa shown (ϵ = 0.06) and gives an expected temperature rise in sunlight of 0.9°C in air at 1 cm pressure and about half this for helium. The data is roughly consistent with that of the previous measurement if we take the emissivity as 15-20% for the incandescent light spectrum, a

not unreasonable figure. Figure V-5 shows the time taken for the thermistor to reach equilibrium is approximately one minute. This is entirely adequate for the present purpose.

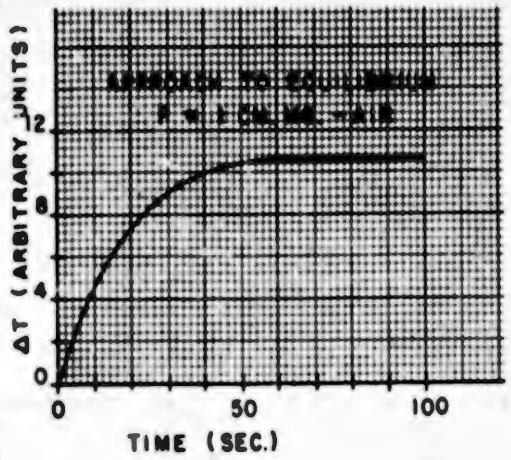

Figure V-5.

We may conclude that the temperature error without ventilation will be on the order of 1°C and that no correction need be applied to the observed values.

D. Flight Summaries of the Temperature Flights

Five flights were launched to obtain direct temperature measurements of the balloon gas. The first of these, Flight 57, was a straightforward flight without ballast drops or unusual behavior. The next four temperature flights, 63, 67, 73, and 81, were launched so as to reach ceiling in time to attain temperature equilibrium before the balloon descended at sunset due to loss of solar radiation, and dropped a known amount of ballast at a predetermined altitude to cause a bounce in height with a subsequent loss of balloon superheat.* Flights 63, 67, and 81 show similar behavior, Flight 57 indicates anomalous characteristics, and Flight 73 has never been recovered.** All of these flights used a Winzen 1-mil double-walled 73-ft-dia. taped balloon.

---

* See Volume IX, Sect. VI, C & D, for a discussion of this type of response to release of a ballast increment.

** Gondola from Flight 73 later recovered.

1. Flight 57

Flight 57 was launched from Pierre, S. D., at 1527 GMT on 25 January 1953. The ground temperature at launch was -10°C, but no readings were taken on this flight of balloon gas temperatures prior to launch. Measurements of air temperature and of temperatures at points 1, 2, and 3 in the balloon were taken during flight. The balloon ascended with a slightly increasing rate of rise to a ceiling of 27 mb, where it floated level until after the film in the temperature recording camera had passed through.

Figure V-6 shows a comparison of the air temperature readings with the temperature sounding from Rapid City at approximately the same time. At launch time, Rapid City reported 12.8°C on the ground. The comparison is seen to be extremely close, although the stations are 150 miles apart. In any case, the comparison serves only as a check on the accuracy of the thermistor readings.

The balloon gas and air temperatures vs time are plotted in Figure V-7. Thermistor 1 was released into the gas almost from the start of the flight; the other two were released at a higher altitude. These points are indicated on the plot by dotted lines; thermistor 2 appears to have fallen against the fabric and begins to read gas temperatures only from 1638 GMT on.

The air temperature decreases as expected until 1614 GMT when the balloon entered the stratosphere, after which it increases and eventually stabilizes at -58°C. Thermistor 1, which is near the top of the balloon at ceiling, but which is near the center of the gas bag during most of the ascent, is seen to follow the air temperature very closely, but to get steadily warmer than the air, maintaining a positive superheat at all times.* At the tropopause, it continues to get warmer than the outside air and there-

*This behavior has never reappeared in any subsequent temperature flight.

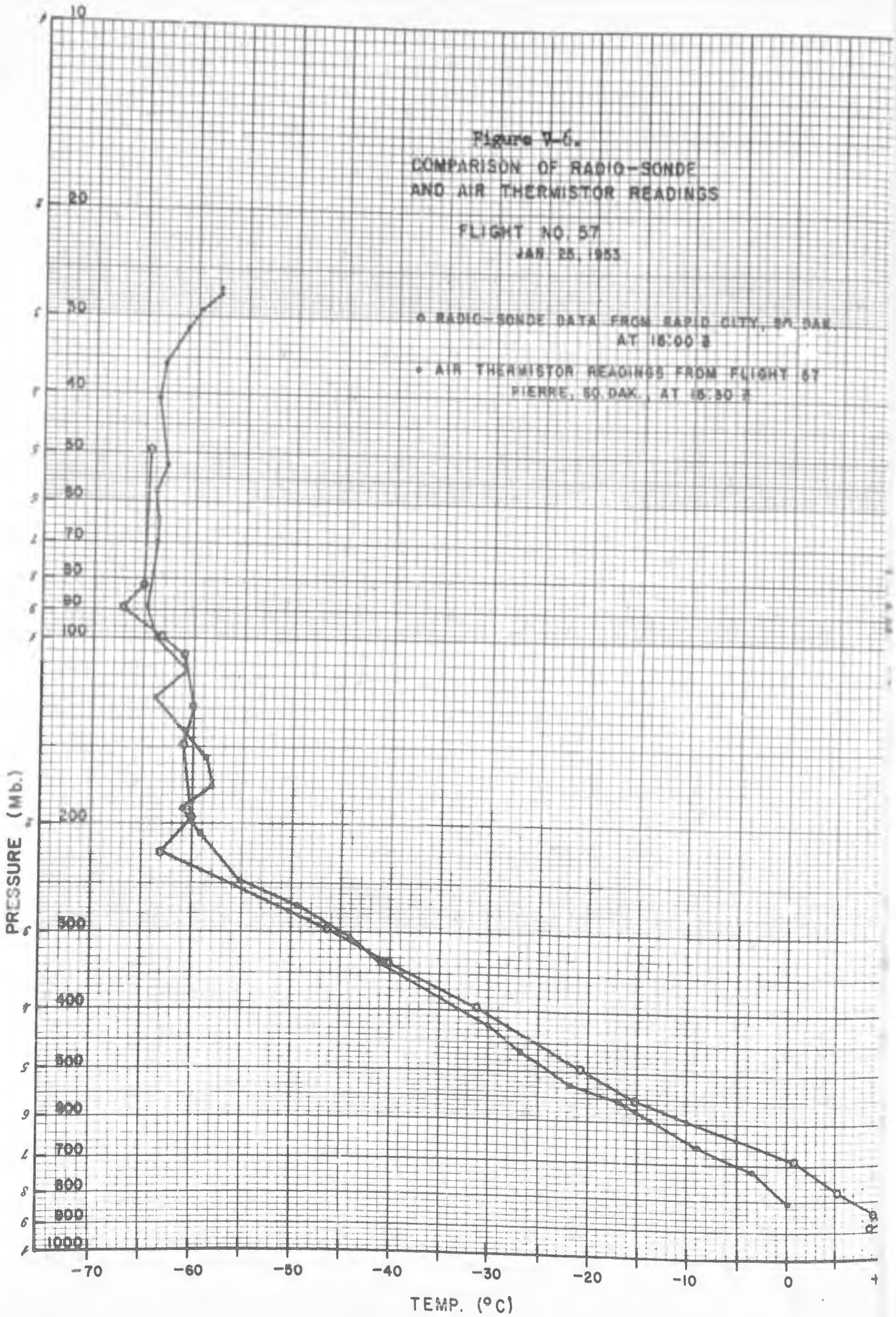
Figure V-6.
COMPARISON OF RADIO-SONDE
AND AIR THERMISTOR READINGS
FLIGHT NO. 57
JAN 25, 1953
○ RADIO-SONDE DATA FROM RAPID CITY, S. DAK.
AT 18:00 Z
• AIR THERMISTOR READINGS FROM FLIGHT 57
PIERRE, S. DAK., AT 18:30 Z
PRESSURE (Mb.)
10
20
30
40
50
60
70
80
90
100
200
500
400
500
600
700
800
900
1000
-70
-60
-50
-40
-30
-20
-10
0
+
TEMP. (°C)

Fig. V-7
N GAS and AIR
MPERATURES
ght No.57
January, 1953

1630 1640 1650 1700 1710 1720 1730 1740 1750 1800 1810 1820 1830 1840 1850 1900 1910 1920 1930 1940 1950 2000

fore its rate of change of temperature changes sign. When the balloon stops rising, the temperature rises rapidly to about -17°, which represents a superheat of almost 40°. Thermistor 2, which becomes free in the gas at 1638 GMT, follows a curve very similar to that of 1 and finally reaches an equilibrium temperature about two degrees warmer than 1. Thermistor 3, free in the gas after 1649 GMT, warms at roughly the same rate but reaches an equilibrium temperature of about -35°, or a superheat of about 23°.

Since no subsequent flight has shown such tremendous temperature gradients within the balloon, it is most reasonable to suppose that thermistors 1 and 2 became electrically shorted, either in the balloon or in the recording instrument. The resistance corresponding to -15° is about 160 kilohms, and to -35° is 330 kilohms, these values agreeing with the paralleling of the two thermistor resistances.

This flight was successful in that it pointed out sources of error to be avoided in subsequent flights, and that it indicated the feasibility of using thermistors for these measurements.

2. Flight 63

This flight was launched from Pierre, S. D. at 2043 GMT on 23 February 1953. The ground temperature at launch was -0.5°C compared with a mean of about +4.0°C for the balloon gas. The balloon gas reading was obtained by releasing thermistor 7 into the gas just previous to erection of the inflated bubble and launch; the readings were recorded on one section of the recorder intended for recording readings from the infrared detector which was not ready for flight at this time.

Flight 63 rose at an almost constant rate and reached a ceiling of 27.5 mb at 2247 GMT, where it remained level until ground sunset at about

2400 GMT. The balloon then descended at about 160 ft/min until balloon sunset, when its rate increased to about 350 ft/min. At a pressure of 77 mb, a pressure release mechanism dropped 25 pounds of ballast, causing an altitude bounce of 1181 ft. This was not quite sufficient to level the balloon and it continued to descend at a rate of about 43 ft/min. The film in the temperature recording camera had run through by the time the load cut down at 0740 GMT.

The flight moved steadily eastward from Pierre, passing over Minneapolis at about 0600 GMT, and cut down in the vicinity of Rhinelander, Wisconsin. The balloon was reported in the following day but the gondola was not discovered until November 2, 1953. Vandals had destroyed almost all of the equipment in the gondola including the up and down cameras, but had stopped just before demolishing the temperature recorder. Although the instrument was damaged, the film was uninjured and developed perfectly.

Figure V-8 shows a comparison of the air temperature readings during ascent with a Rapid City temperature sounding at 1500 GMT. The dashed line between 280 mb and 175 mb indicates that no air temperature readings were being taken as the balloon passed through the tropopause; the variations at high altitudes are also lost because of the relatively long interval between air temperature readings.

The plot of balloon gas and air temperatures vs time is given in Figure V-9. This plot is typical of the behavior shown by other temperature flights. Although the accuracy of the recorder for high temperatures is low, due primarily to reading errors, the initial superheat is seen to be approximately $+4.0^{\circ}$. Thermistor 1 is free in the gas from 1503 GMT on, and shows the balloon gas temperature remaining close to that of the air

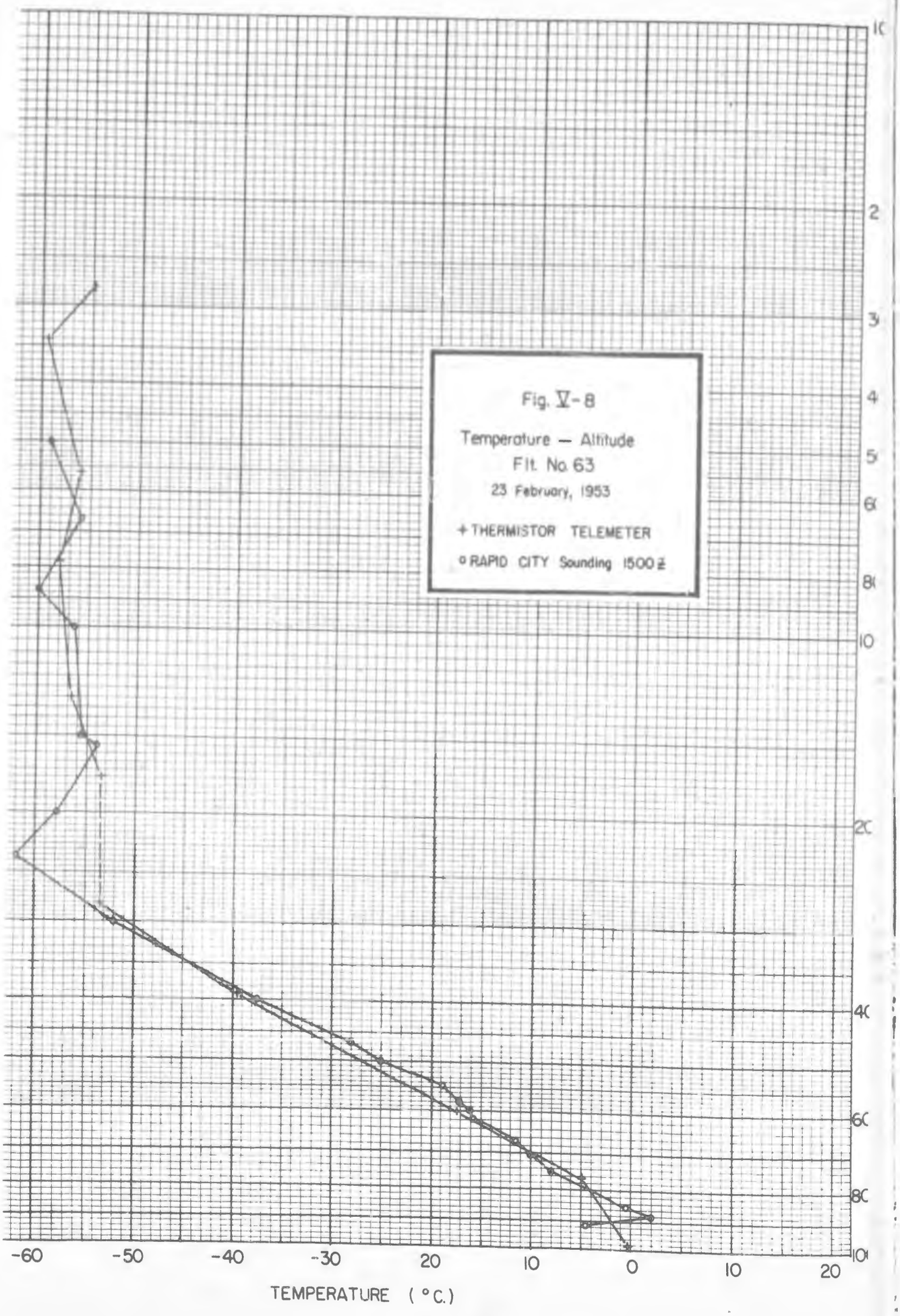
Fig. V-8
Temperature — Altitude
Flt. No. 63
23 February, 1953
+ THERMISTOR TELEMETER
o RAPID CITY Sounding 1500 Z
-60
-50
-40
-30
20
10
0
10
20
TEMPERATURE (°C.)

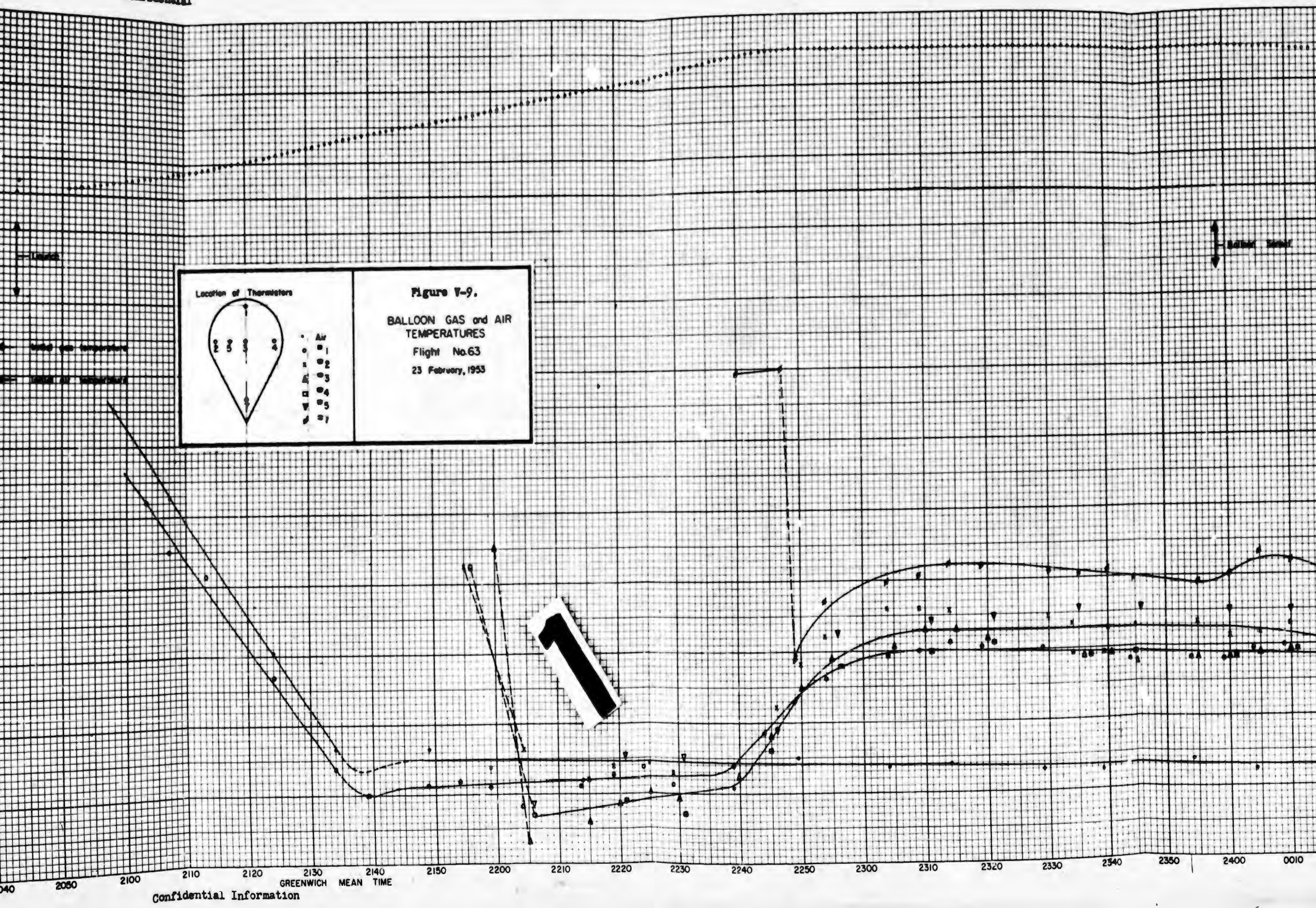
Location of Thermisters
Air
1
2
3
4
5
7
Figure V-9.
BALLOON GAS and AIR TEMPERATURES
Flight No.63
23 February, 1953
2040
2050
2100
2110
2120
2130
2140
2150
2200
2210
2220
2230
2240
2250
2300
2310
2320
2330
2340
2350
2400
0010
GREENWICH MEAN TIME

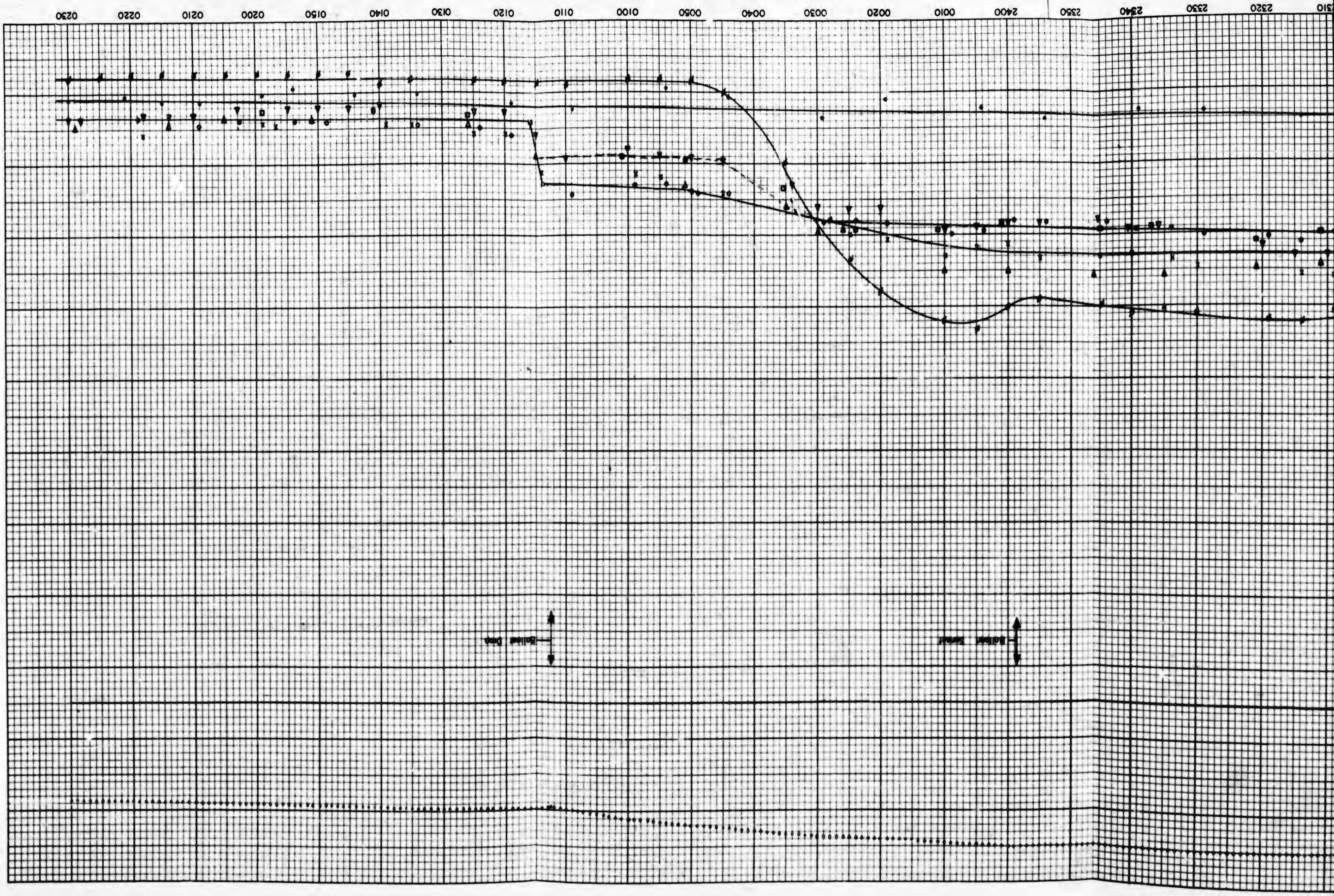
0230
0220
0210
0200
0150
0140
0130
0120
0110
0100
0050
0040
0030
0020
0010
2400
2350
2340
2330
2320
Boiler Drum
Radial Sensor

but decreasing at a slower rate with altitude and remaining below air temperature until past the tropopause. As the balloon ascends through the stratosphere, the gas temperature appears to warm somewhat, while the air temperature remains approximately constant. The points at which thermistors 2 through 5 become exposed to the gas are again shown with dashed lines. During this latter portion of the ascent, from about 2205 to 2240 GMT, the gas temperatures show wide variation which suggests considerable agitation of the gas, since reading errors cannot account for the large differences shown.

Within twenty minutes after reaching ceiling altitude, the balloon has come to temperature equilibrium, with a mean superheat of about + 21°. This superheat is maintained as the balloon floats level until ground sunset at 2400 GMT. Temperatures 1, 3, and 4 during the level portion of the flight seem to have essentially the same value, which is different from that shown by temperatures at positions 2 and 5. If these latter two positions are maintained warm because of, for example, the sun shining on that particular side of the balloon, one would expect position 1 to be at almost the same temperature as that shown at positions 2 and 5 (cf. Figure V-2, this section). It is not sufficient to assume that 2 and 5 are reading high or that 1, 3, and 4 are reading low because of calibration errors, since at balloon sunset, 3 and 4 are still lowest, but 1 has become approximately equal to 2 and 5. In addition, after the ballast drop, all thermistors read within 2° of each other, as would be expected, since earth radiation alone could not maintain any appreciable gradient. A tentative conclusion from these considerations is that a temperature difference of at least 2° exists between points 2 and 3, when point 2 is nearest the side of the balloon facing the sun.

The behavior of thermistor 7 on this flight is quite significant. It was included in the flight to obtain a value of the initial superheat of the balloon gas at launch. The thermistor was released into the bottom third of the balloon just previous to launch and it was expected that the thermistor would be broken by the agitation of the fabric during ascent. It apparently suffered no damage, however, and gave readings throughout the flight. Figure V-9 shows this thermistor reading to be approximately 0° until just previous to the balloon's levelling at ceiling. As the cone at the bottom of the balloon opened during the last part of the ascent, the thermistor again became exposed to the gas. This point is shown by the dashed line at 2247 GMT. The thermistor immediately assumes a temperature of -41° and then warms with the other thermistors, but attains an equilibrium temperature about 7° warmer. At ground sunset, the balloon begins to descend and thermistor 7 again becomes enclosed by the fabric. This is reflected in the sudden increase of 4°, followed by a gradual decrease to just below air temperature as the fabric at this portion of the balloon cools.

Assuming that thermistor 7 retained its carbonate coating and was held distant from the fabric by the ½-inch radius of the protective helix (cf. Figure I-2, Vol. I,), gas convection would maintain the thermistor temperature at very nearly the fabric temperature, since the gas in this region of the balloon is thermally isolated. One can thus estimate the fabric temperature during the level flight as approximately -26°, or about 10° warmer than the mean gas temperature during level flight. This very rough estimate is not to be taken too seriously for a number of reasons:

1) thermistor 7 is situated in a region of the balloon where the tapes are most concentrated and one would expect this region to be warmed

by solar radiation to a temperature greater than the mean fabric temperature.

2) it is quite possible that some or all of the carbonate coating on the thermistor was rubbed off during the ascent, causing the thermistor to absorb solar radiation more effectively.

3) the readings from position 7 during level flight are from a position surrounded by gas, and though the thermistor is again enclosed by the fabric just after ground sunset, the fabric temperature in this region might have changed considerably during the late afternoon as the zenith angle of the sun increased.

It will be worthwhile to attempt to measure fabric superheat by suspending a thermistor in such a manner that it is distant from the fabric by about one inch. This will allow the gas near the fabric to clamp the thermistor temperature by means of convection, and since the gas temperature at this distance cannot be appreciably different from the fabric temperature, some indication of the fabric superheat and mean temperature can be obtained.

The behavior of thermistor 7 after sunset is apparently indicative of the fabric temperature in a region where the fabric no longer surrounds any lift gas. As shown, it drops fairly rapidly to about 2° below air temperature and remains there for the duration of the film record.

The temperature behavior at positions 1 through 5 after ground sunset at 2400 GMT is typical. Beginning at 2400 GMT, the balloon temperatures gradually decrease, representing a gradual loss of superheat. At balloon sunset, this decrease increases its rate somewhat but the total balloon superheat remains almost at its daytime equilibrium value. During this period, the time-altitude curve shows the balloon to be descending,

the rate of descent increasing after balloon sunset.* At 0113 GMT, the balloon has reached an altitude of 77 mb, and the release of a ballast increment of 25 pounds causes the balloon to bounce rapidly upward, in turn causing the gas to cool by expansion. As shown in Figure V-9, the gas temperature drops to within about 3° of air temperature, retaining a positive superheat. Numerical relations holding between temperature, ballast, and altitude during this bounce are summarized in the following table. For a discussion of the calculations, see Part G, this section.

TABLE III. Temperature and Altitude Changes during Ballast Bounce, Flight 63

ΔW	Δh	Adiabatic ΔT_{gas}	Measured ΔT_{gas}	T_{air}	Measured $\Delta T/T$	Change in Aero Drag	$\frac{\Delta W}{G}$
25#	1181 ft.	4.73°	9.0°	216.0°	4.17%	0.6%	4.85%

The balloon continues to descend after dropping ballast, and the superheat is again maintained at + 3° during this slow descent. For a description of the relations holding between temperature and altitude changes, see Part G, this section.

At 0230 GMT, the film in the temperature recording camera had run through, well before the flight termination at 0740 GMT.

3. Flight 67

This flight was launched from Pierre, S. D., at 1956 GMT on 5 April 1953. The air temperature on the ground at launch was 7.8°, but the thermistor at the bottom of the balloon broke upon release into the gas and there is, consequently, no measured value for the initial superheat

*For a discussion of this effect, see Part G, this section.

on this flight. Measurements were taken at five points in the balloon and at two points in the outside air, as well as measurements of infrared flux from the ground. During transfer of the gas to the upper portion of the balloon just after launch, some of the balloon fabric draped down onto the pole supporting the air thermistors. Although neither of the two was broken, their readings indicate that most probably they were forced back against the aluminum pole and consequently gave readings which are both high and erratic during sunlight but which smooth out after balloon sunset. The erroneous temperatures do not appear to be serious during ascent because of ventilation but are undoubtedly high by about 4° at ceiling.

As shown in Figure V-10, the air thermistor readings during ascent give values which lie uniformly between air temperatures recorded at Rapid City and St. Cloud. The balloon evidently floated in a region of rapid temperature change.

The behavior of the balloon temperatures on this flight is very similar to that shown in Flight 63. In Figure V-11, Thermistor 1, which is released into the gas shortly after launch, shows the balloon gas to be colder than the outside air until somewhat past the tropopause, when the gas steadily warms. The points at which thermistors 2, 3, 4, and 5 dropped free into the gas are again shown with dashed lines. Thermistor 3 apparently fell into the fabric and broke. The mean gas temperature when the balloon reached valving ceiling at 2142 GMT appears to be -49.5°, the same as air temperature. The gas warms and by 2200 GMT has apparently stabilized at about -32°, representing an equilibrium superheat of + 21.5° at a ceiling of 28 mb. The maximum temperature difference indicated is about 4° between thermistors 1 and 2. This measured difference does not completely disappear after balloon sunset, when the two still read about

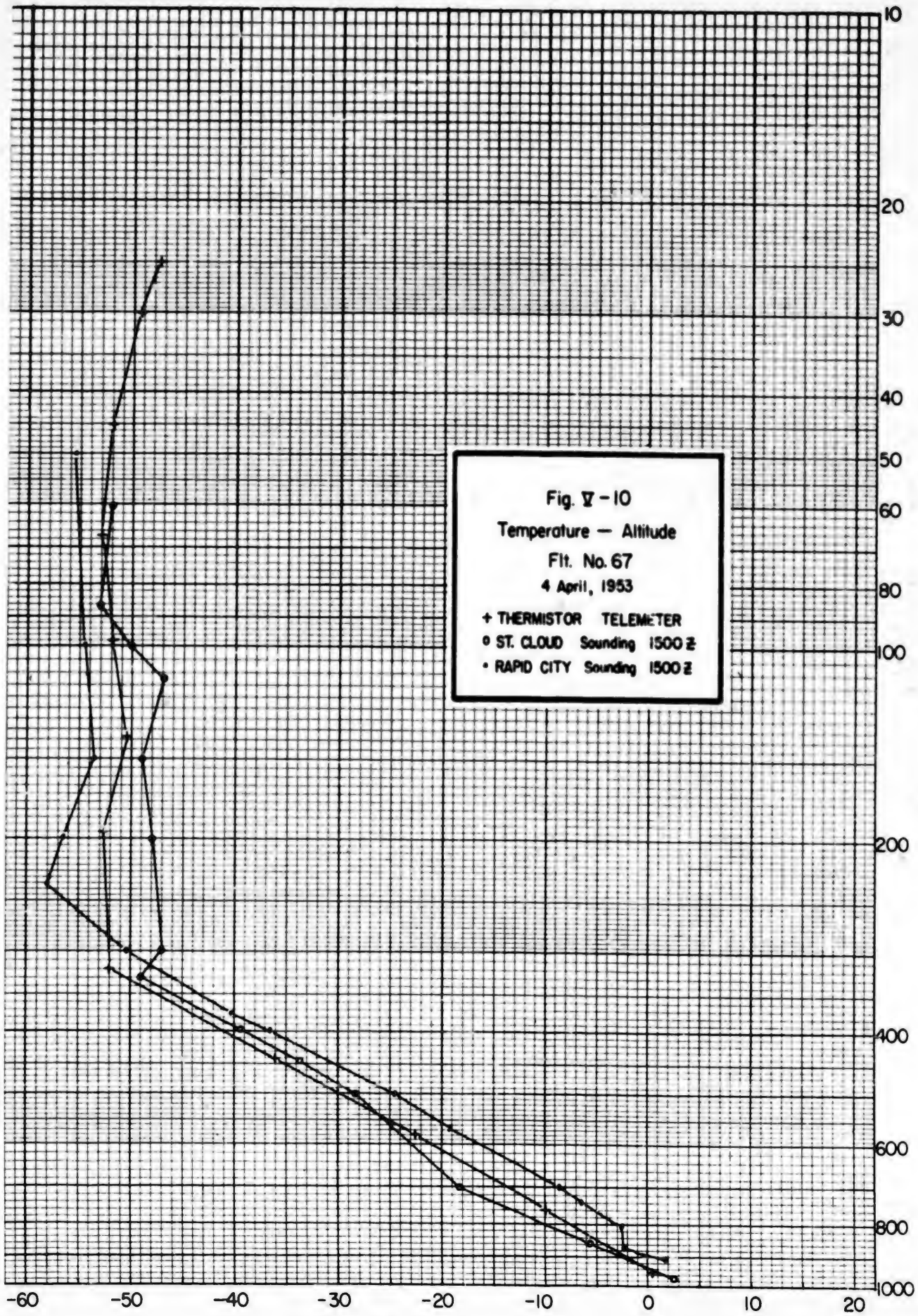
Fig. V - 10
Temperature — Altitude
Flt. No. 67
4 April, 1953
+ THERMISTOR TELEMETER
o ST. CLOUD Sounding 1500 Z
• RAPID CITY Sounding 1500 Z
10
20
30
40
50
60
80
100
200
400
600
800
1000
-60
-50
-40
-30
-20
-10
0
10
20
TEMPERATURE (°C.)

1.5° to 2° different. This would appear to be a systematic error in the readings, but would still indicate a gradient of about 2° at ceiling, assuming that solar effects would not enhance the difference readings because of, for example, loss of carbonate coating on thermistor 2.

Similar to Flight 63, the gas temperatures during the late afternoon begin to decrease slightly, and decrease somewhat more rapidly after balloon sunset, while still maintaining an appreciable superheat. During this period, the balloon loses altitude as shown in the time-altitude curve. At a pressure of 70 mb, the balloon drops 32.7 pounds of ballast and bounces rapidly upward, cooling the lift gas by expansion. The gas temperature drops rapidly to approximately -53°, within about 2° of air temperature, as shown. This superheat of 2° is then maintained as the balloon continues to descend.

The temperature relations holding during this bounce are given in Table IV.

TABLE IV.
Temperature and Altitude Changes
During Ballast Bounce, Flight 67

ΔW	Δh	Adiabatic ΔT_{gas}	Measured ΔT_{gas}	T_{air}	Measured $\Delta T/T$	Change in Aero Drag	$\frac{\Delta W}{G}$
32.7#	1580 ft.	6.31°	14.5°	219.0°	6.62%	0.2%	6.03%

4. Flight 73

This flight was launched from Minneapolis at 1847 GMT on May 13, 1953. The air temperature at launch was 8.6°, and the gas temperature just previous to launch, measured with thermistor 7, was 19.4°. Thus, the initial superheat measured +11°. This value appears to be high, representing a superheat before the balloon gas and fabric have come into

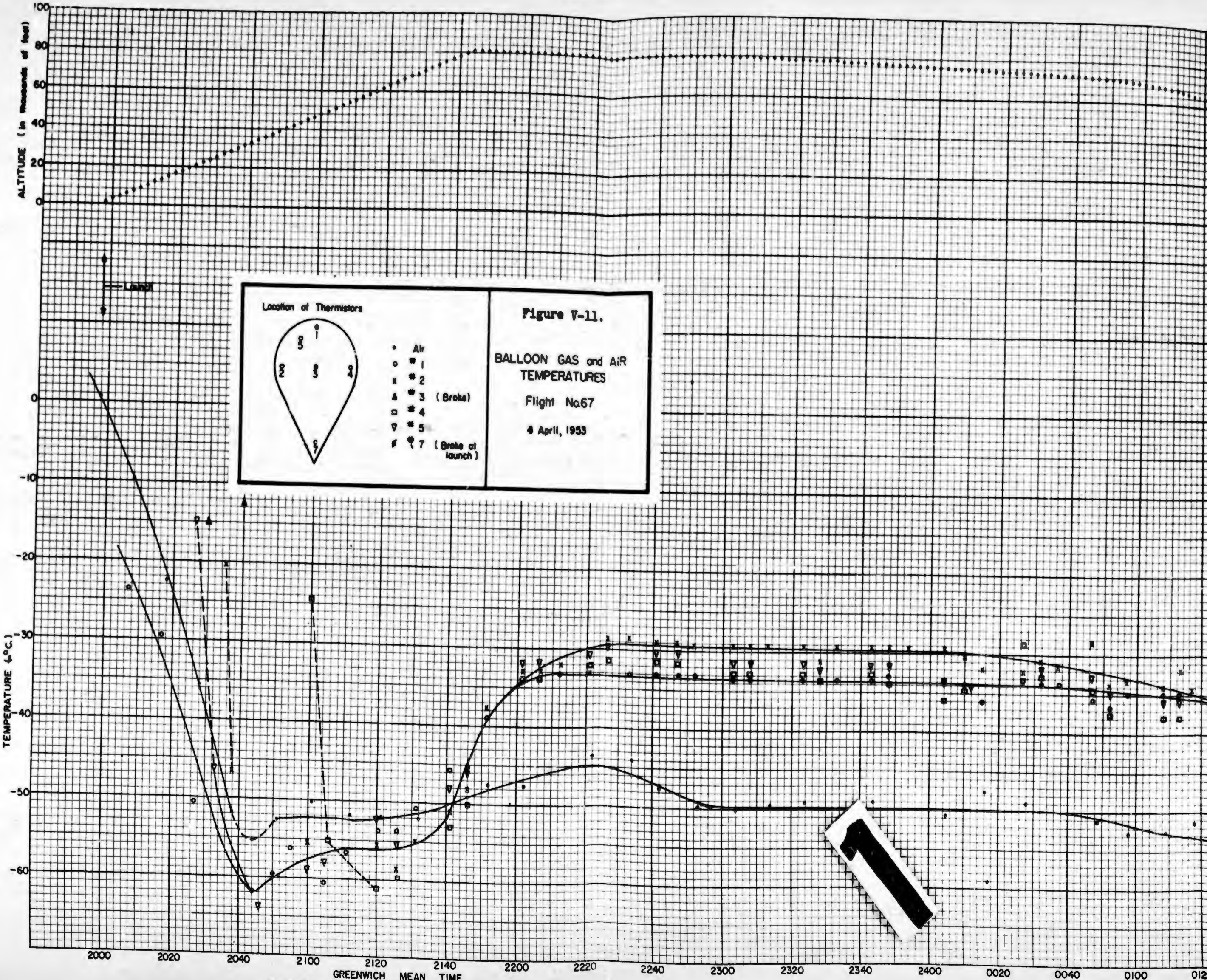

Figure V-11.

BALLOON GAS and AIR TEMPERATURES

Flight No.67

4 April, 1953

11.

and AIR
RES
7

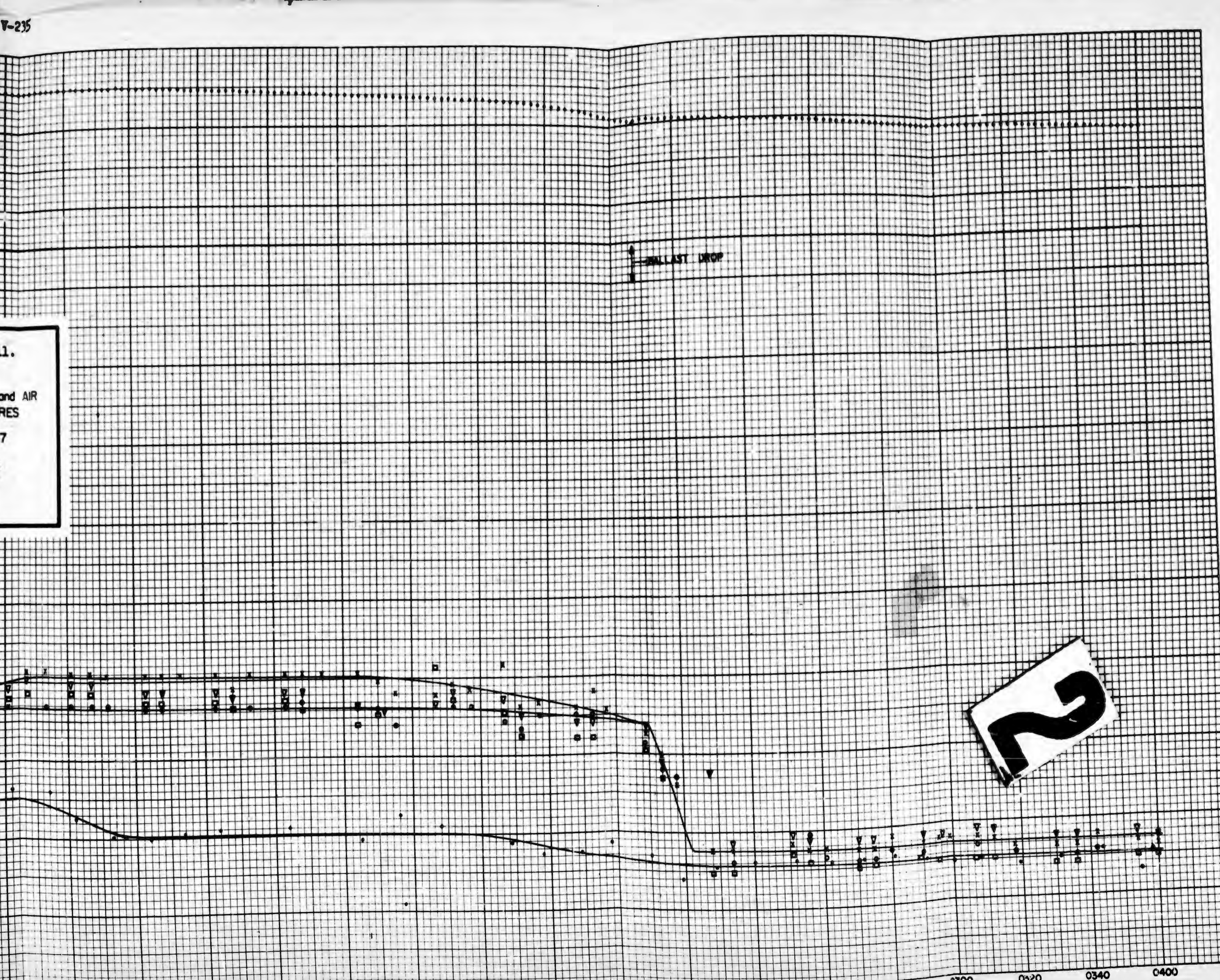

radiation equilibrium with the ground and atmosphere.* Measurements of temperatures at six points in the balloon gas and of air temperature at two points were taken, in addition to measurements of ground infrared flux. The gondola from this flight free-fell somewhere in the vicinity of Jump River, Wisconsin, and has never been recovered. Consequently, no temperature data is available.**

5. Flight 81

Flight 81 was launched from Minneapolis at 1912 GMT on July 7, 1953. It included measurements of gas temperature at six points, air temperature, gondola interior temperature, and measurements of infrared ground flux. In place of the temperature recorder, two temperature pulse generators telemetered the temperature information on two channels of the commutated transmitter (Vol. X, Sect. II). The temperature data, as well as the Olland cycle pressure data were, however, recorded on a multichannel 16-mm recording camera (Vol. X, Sect. I). The flight remained in the vicinity of Minneapolis and although the gondola has never been recovered, a good telemetered record was obtained.

At launch, the air temperature on the ground was 25.5°, while the gas temperature measured 20.1°, corresponding to a superheat of -5.4°. These temperatures were measured by reading thermistor 7 in the balloon and an air thermistor suspended at five feet from the ground with an ohmmeter. The pulse generator, however, just after launch, gave erroneous readings which are high by as much as 30° initially. Since the pulse generator is

---

* For a discussion of this effect, see Part G, this section.
** The gondola from Flight 73 was later recovered.

sensitive to leakage resistance, some effect dependent on a rapid ascent from the ground must be responsible. This behavior of the pulse generators has appeared in several subsequent flights, and has been attributed to sensitivity to moisture on the plugs and leads. Redesigning of the pulse generator has eliminated this sensitivity.

Comparing the temperature-altitude sounding from St. Cloud with the air temperature telemetered (Figure V-12), it becomes obvious that in addition to the initial error caused by the ascent, the air temperature readings are suspect by at least 5° in the stratosphere. This appears from the plot of balloon and air temperatures as well (Figure V-13), where the air temperature points are not only badly scattered but show a larger decrease in temperature at sunset than one would expect from the loss of altitude. In addition, the measured value of superheat during level flight is on the order of 6.5°, which appears to be unreasonable in view of the results obtained from Flights 63 and 67.

Assuming that the air thermistors are abnormally heated during the day for some reason, but decrease to near the correct value after sunset, one can estimate the mean air temperature during level flight at ceiling as -53°. This value agrees reasonably well with the extrapolated temperature from the St. Cloud sounding. Comparing the balloon gas temperatures with this assumed value gives a superheat of about +15°, which, although still low, is much closer to the values recorded on other flights. Since the balloon temperatures were measured with a different pulse generator from that which measured air temperatures, and appear to be of the expected order of magnitude, one is justified in taking some quantitative results from these assumptions.

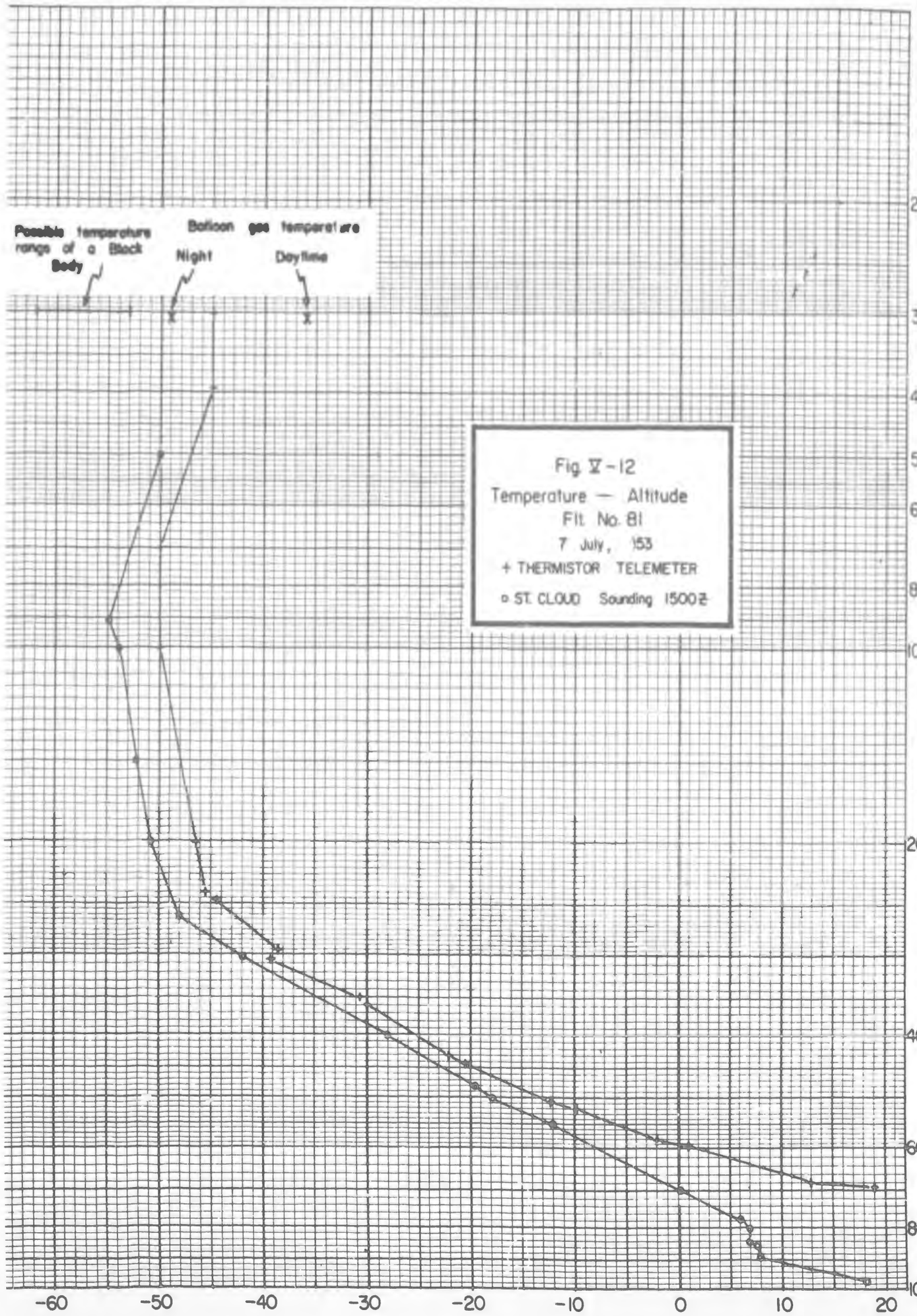
Possible temperature range of a Black Body
Balloon gas temperature
Night
Daytime
Fig. V-12
Temperature — Altitude
Flt. No. 81
7 July, 153
+ THERMISTOR TELEMETER
○ ST. CLOUD Sounding 1500Z
-60
-50
-40
-30
-20
-10
0
10
20
TEMPERATURE (°C.)

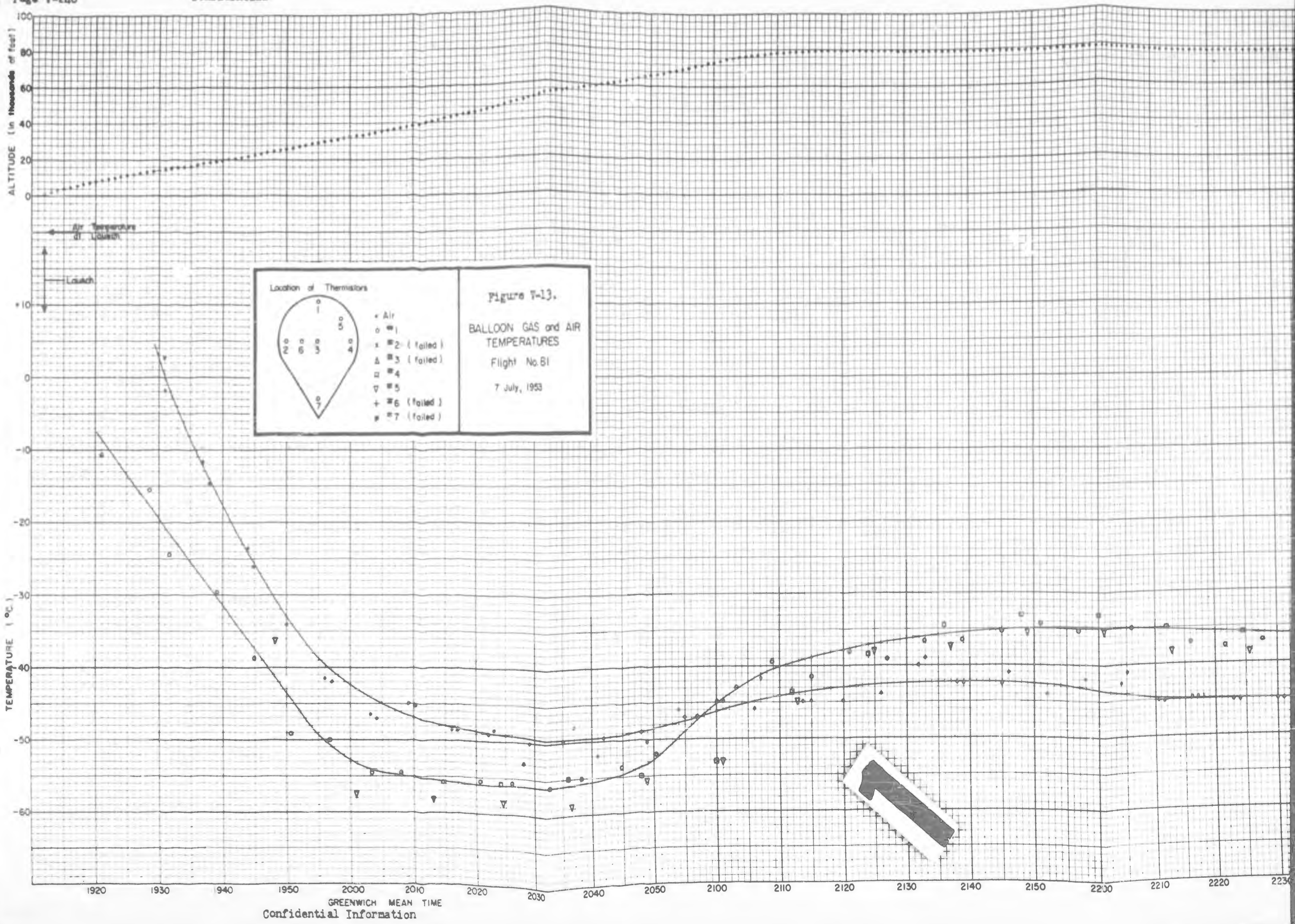

Figure V-13.

BALLOON GAS and AIR TEMPERATURES

Flight No. 81

7 July, 1953

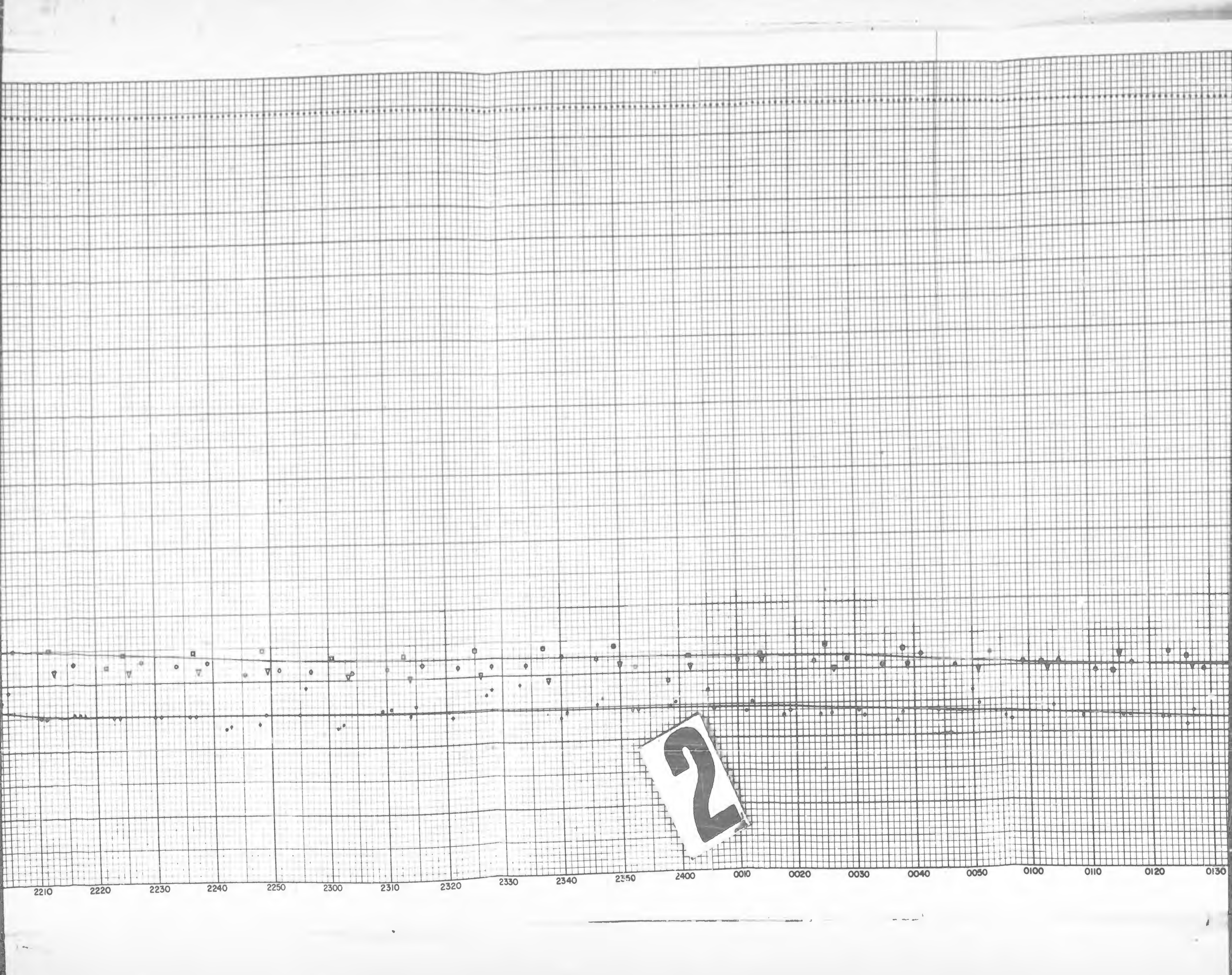
2210
2220
2230
2240
2250
2300
2310
2320
2330
2340
2350
2400
0010
0020
0030
0040
0050
0100
0110
0120
0130

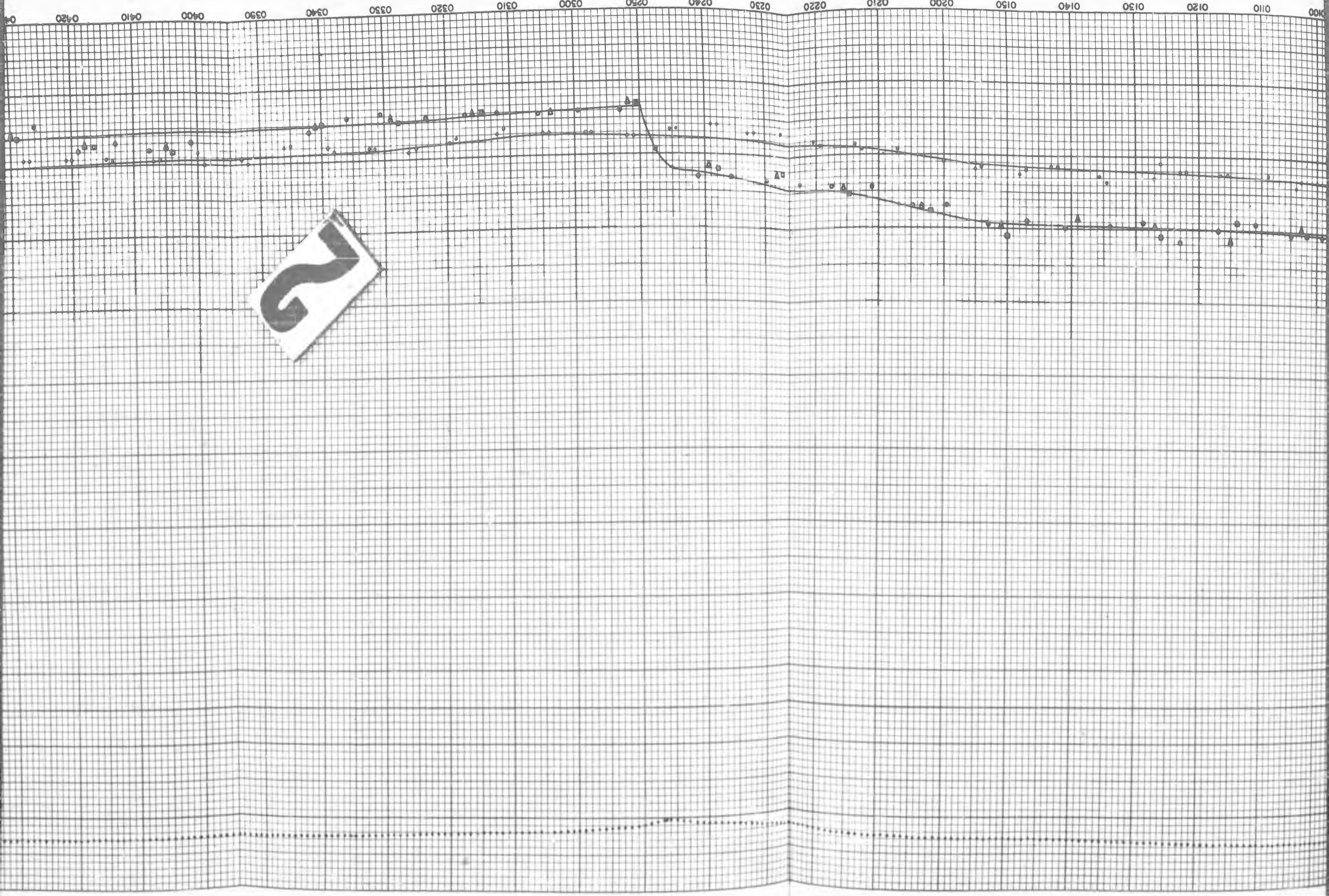
0100
0110
0120
0130
0140
0150
0200
0210
0220
0230
0240
0250
0300
0310
0320
0330
0340
0350
0400
0410
0420


0210
0220
0230
0240
0250
0300
0310
0320
0330
0340
0350
0400
0410
0420
0430
0440
0450
0500
0510
33

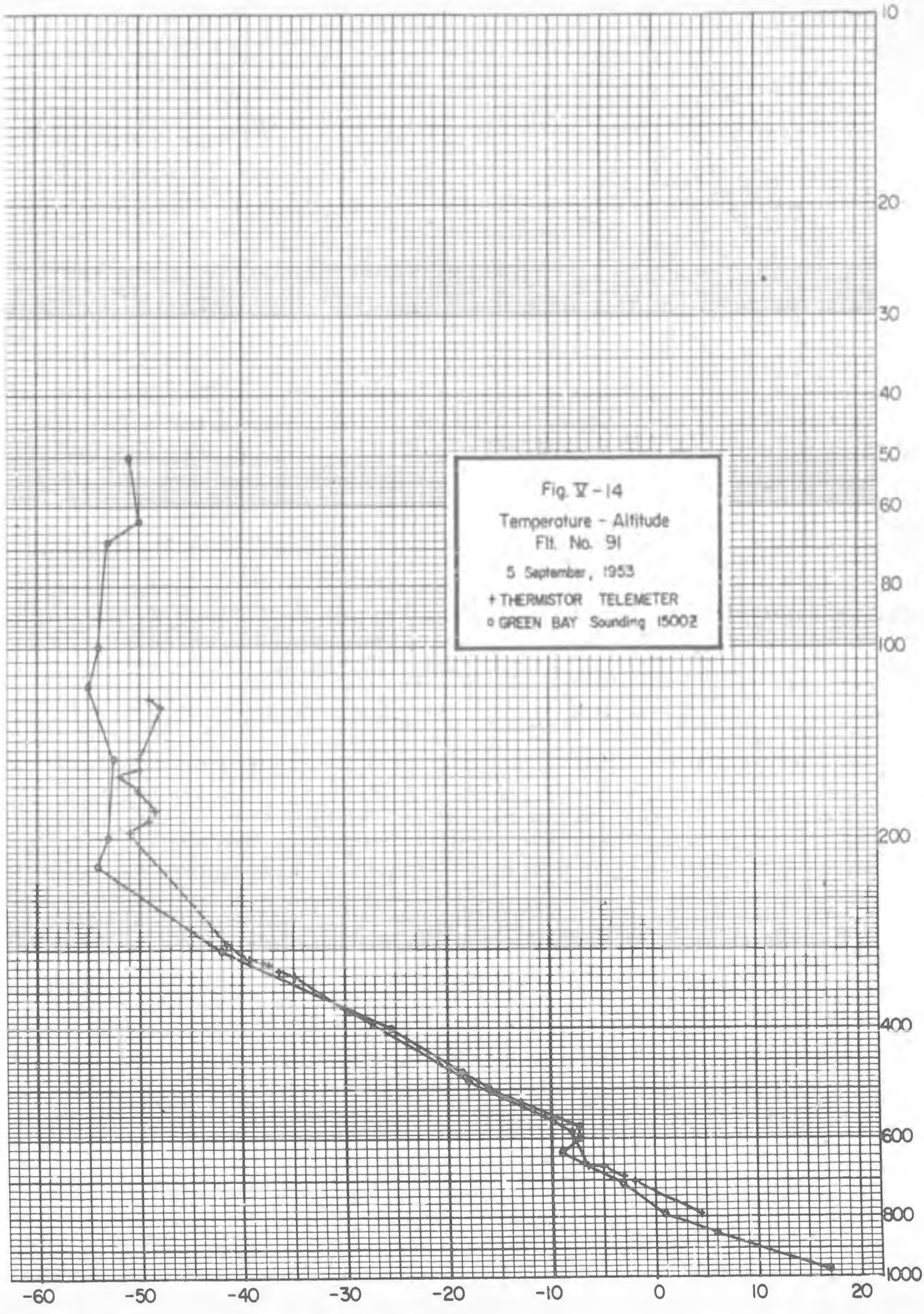
Fig. V - 14
Temperature - Altitude
Flt. No. 91
5 September, 1953
+ THERMISTOR TELEMETER
○ GREEN BAY Sounding 15002
10
20
30
40
50
60
80
100
200
400
600
800
1000
-60
-50
-40
-30
-20
-10
0
10
20
TEMPERATURE (°C.)

Because of the telemetering difficulty, air temperatures are readable for only an hour after reaching the second step at 30,000 ft, and disappear until 1715 GMT, when the flight had floated level at 49,000 ft for about 40 minutes. Gas temperatures are readable only during the first step at 12,500 ft and for the first 28 minutes of the ascent to the second step. As shown in Figure V-14, the temperature sounding from Green Bay, Wisconsin, agrees surprisingly well with the air temperatures measured, except in the region of 130 mb, where rapid winds appear to have existed.

Figure V-15 is the plot of air and balloon gas temperatures vs. time. As shown, the equilibrium superheat on the first step is $+1^{\circ}$. The behavior of the gas during the ascent to the second step is characteristic of the temperature flights previously described. The gas remains colder than the outside air during ascent and presumably warms after attaining equilibrium, as indicated by the tensiometer. Only one gas thermistor is plotted in this figure, since the balloon had not attained sufficient altitude to drop the other two by the time the temperature telemeter failed.

2. Flight 94.

Flight 94 was launched from Minneapolis at 0131 GMT on September 28, 1953. Measurements of two balloon temperatures and of the outside air temperature were taken. At launch, the air temperature was 11.3° and the balloon gas temperature at this time was apparently about 5°, giving an initial superheat of about -8°. Figure V-16 shows the behavior of these temperatures during the time the balloon was held down prior to launching. Apparently, the balloon loses heat quite rapidly after sunset due to radiation to free space. One would expect this effect to be enhanced in the Minnesota launching method because of the overlapping of several layers of

E. Flight Summaries of Temperature-Instrumented Step Flights

Beginning with Flight 91, thermistors were flown in the step flight tow balloon,* using a pulse generator connected to a low-power 10-mc transmitter which relayed the temperature information from the tow balloon down to a receiver in the gondola, which then keyed the commutated transmitter on one channel. Impractically long leads from the balloon thermistors to the gondola, and possible fouling of the weigh-off cable by these leads, are thus avoided. The tensiometer measurements, which are considerably more accurate for measurements of the mean balloon gas superheat, are relative only, since absolute values of the superheat depend on an exact knowledge of the initial superheat. Measurement of temperatures serves also to point out possible discrepancies in tensiometer readings. Where both temperature and tension readings are good, the ability of the thermistors to read the mean balloon temperature can be evaluated.

1. Flight 91

This flight was launched from Minneapolis at 1217 GMT on September 5, 1953. The air temperature at launch was 7.8° and the gas temperature measured 7.4°, giving an initial superheat of -0.4°. These values were measured using a Wheatstone bridge on the air thermistor later flown in flight and on a thermistor suspended in position 7. During flight, temperatures were measured at points 1, 2, and 3 in the tow balloon and in the outside air.

The pulse generator used for telemetering temperatures on this flight apparently performed satisfactorily during the entire flight, but an incorrect time constant in the gondola receiver caused erratic telemetering.

---

* See Section VI of this volume for a discussion of step flights.

The balloon gas temperatures during ascent show behavior similar to the previous temperature flights: the gas remains colder than the outside air for some time past the tropopause, then steadily warms and reaches equilibrium about 20 minutes after attaining ceiling. Using the assumption that the mean stratospheric air temperature is -53°, the gas superheat at altitude is +15°, with a maximum difference of 3° between thermistors 4 and 5. After balloon sunset, the superheat decreases slightly, and at the ballast drop at 0247 GMT, decreases suddenly to about 3° below air temperature, which at this time can be assumed to be accurate as plotted. The amount of ballast dropped was more than sufficient to account for sunset effect, which is reflected in both the time-altitude and time-temperature curves.

The numerical results comparing temperatures with ballast dropped are given in Table V.

TABLE V.
Temperature and Altitude Changes
During Ballast Bounce, Flight 81

ΔW	Δh	Adiabatic ΔT_{gas}	Measured ΔT_{gas}	T_{air}	Measured $\Delta T/T$	Change in Aero Drag	$\frac{\Delta W}{G}$
35#	1900 ft.	7.6°	9.5°	220.0°	4.31%	0.2%	7.1%

This flight, which was the first to use the pulse generator for measuring balloon temperatures, indicated that the method was feasible but subject to further errors. The desirability of having temperatures directly telemetered more than compensated for this, since otherwise no data at all would have been obtained from this flight.

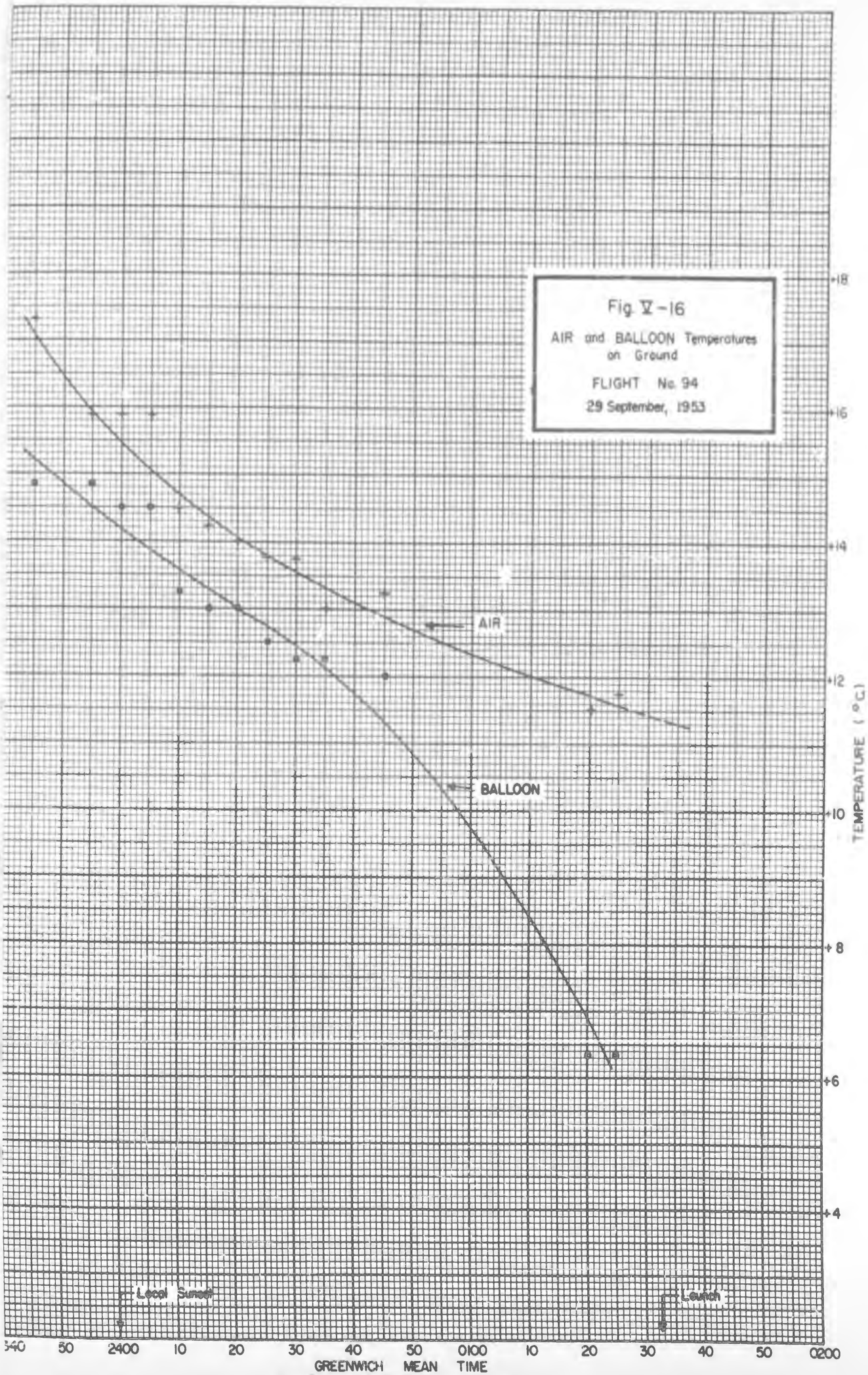
Fig. V-16
AIR and BALLOON Temperatures on Ground
FLIGHT No. 94
29 September, 1953
AIR
BALLOON
Local Sunset
Launch
+18
+16
+14
+12
+10
+8
+6
+4
TEMPERATURE (°C)
2340
50
2400
10
20
30
40
50
0100
10
20
30
40
50
0200
GREENWICH MEAN TIME

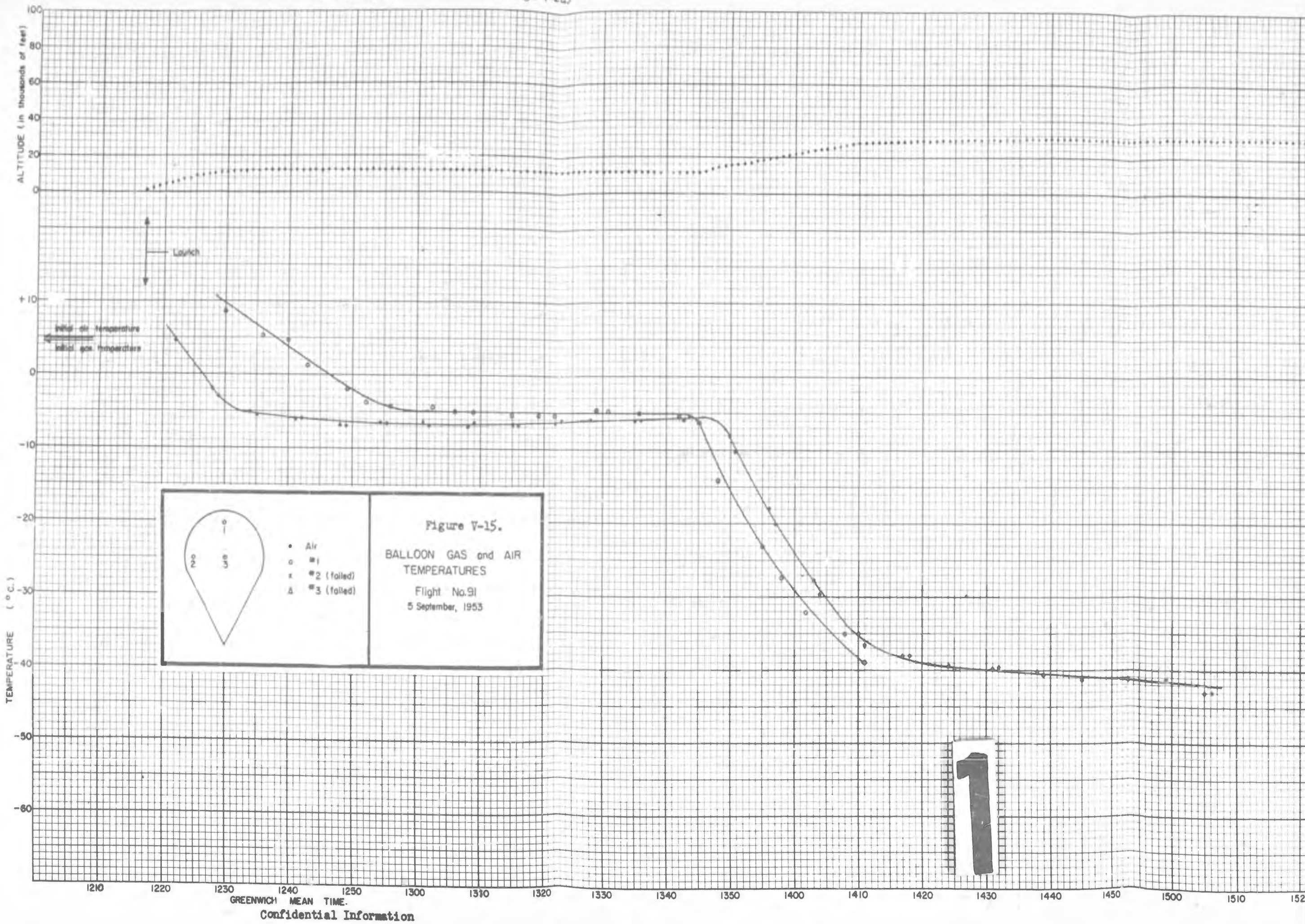

Figure V-15.

BALLOON GAS and AIR TEMPERATURES

Flight No. 91

5 September, 1953

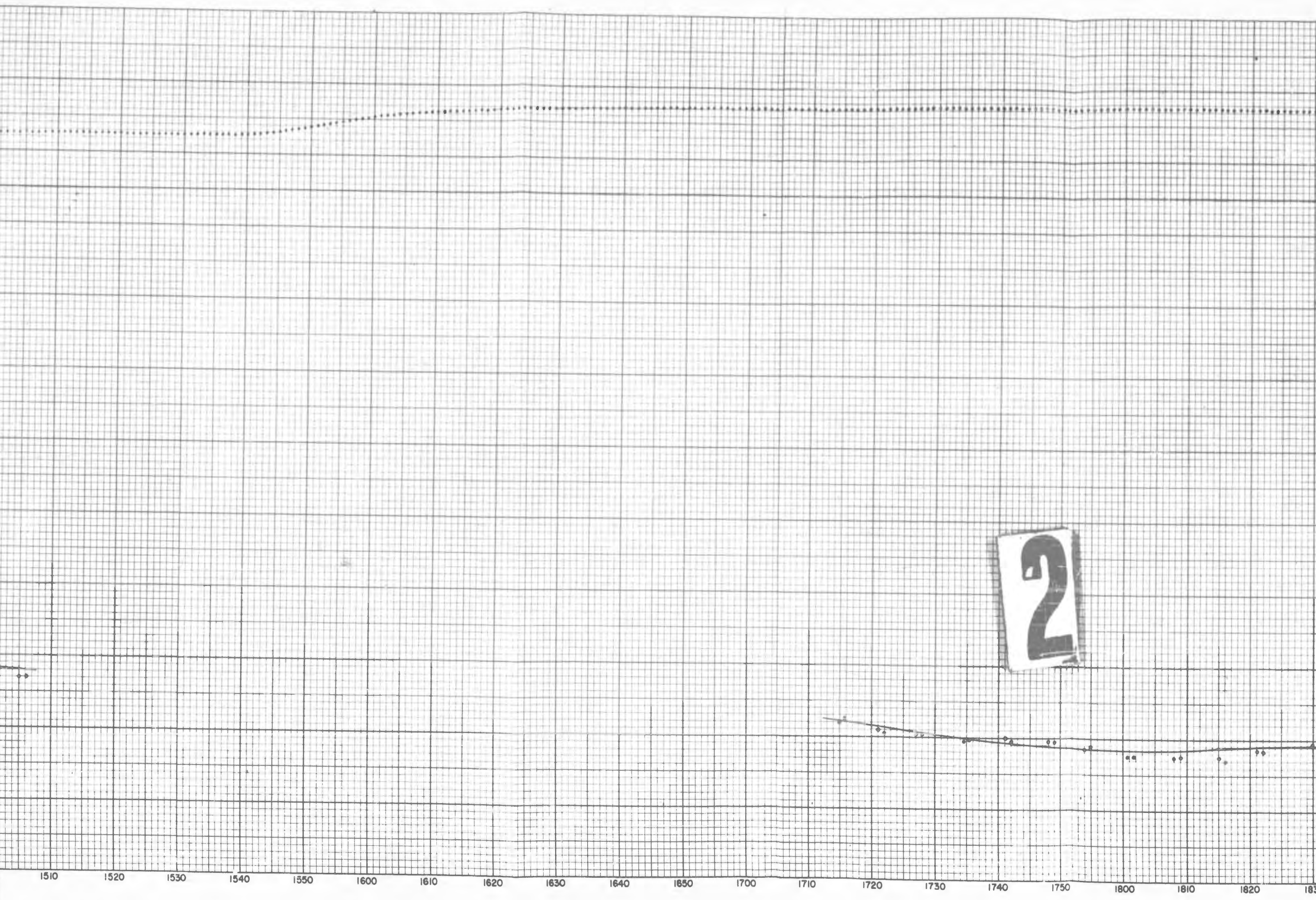
2
1510
1520
1530
1540
1550
1600
1610
1620
1630
1640
1650
1700
1710
1720
1730
1740
1750
1800
1810
1820

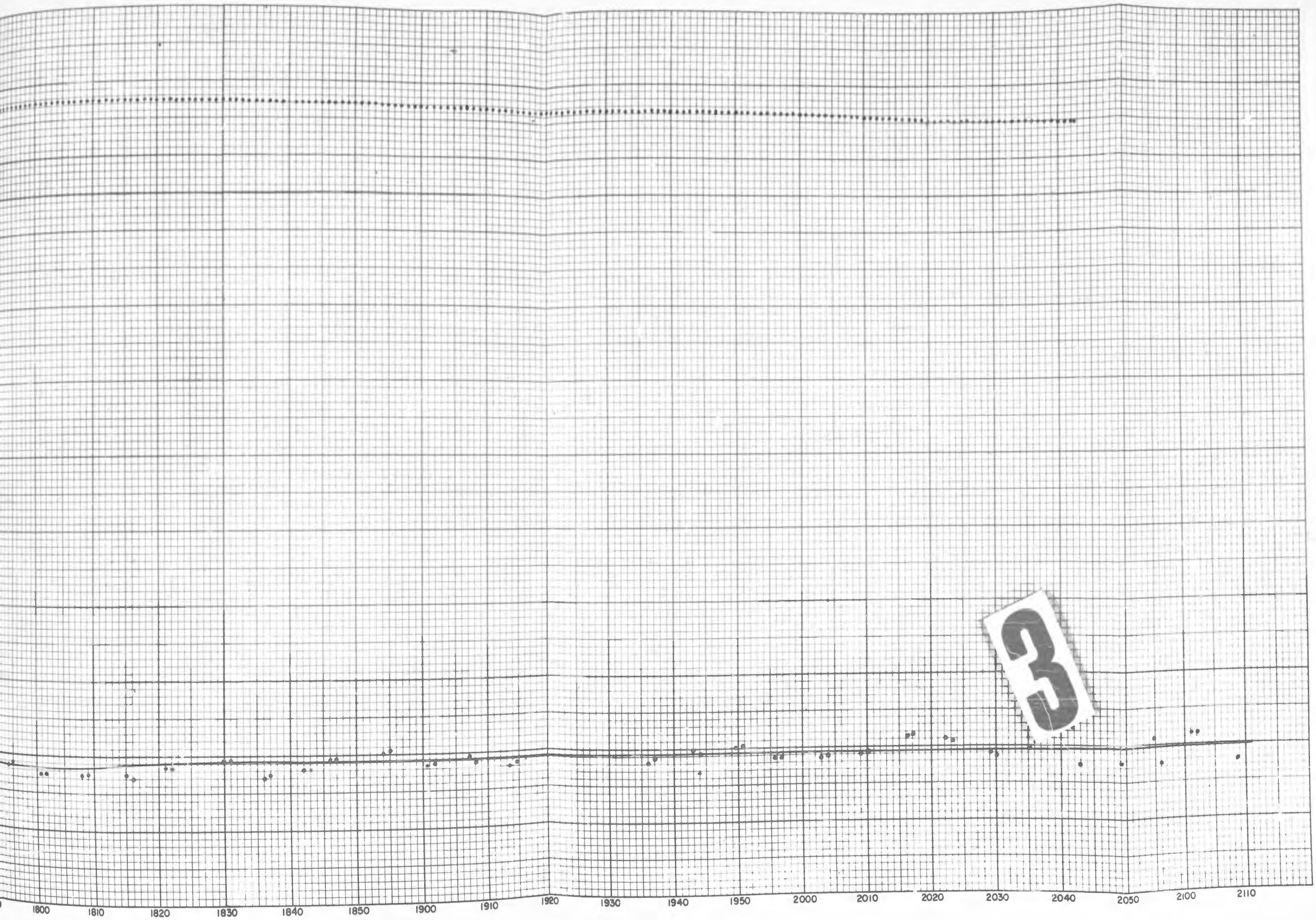
3
1800
1810
1820
1830
1840
1850
1900
1910
1920
1930
1940
1950
2000
2010
2020
2030
2040
2050
2100
2110

balloon fabric, but measurement of temperatures on a tied-down balloon over a 24-hour period will give more qualitative data. This will be reported on in a later volume.

The temperature pulse generator, during the entire first step and somewhat past having reached equilibrium on the second step at 19,500 ft, indicates abnormally high temperatures for both gas and air. From Figure V-18, it appears that the cause of the discrepancy slowly disappears during the second step and that the temperatures indicated at 0300 GMT are probably correct. The sounding points are plotted from this time on and show close agreement with the Green Bay sounding at 1500 GMT. See Figure V-17.

Both balloon thermistors indicate very close agreement, and one would expect to find no great difference throughout the balloon unless a powerful heat source such as the sun were present. The equilibrium value for the superheat at 20,000 ft from the time-temperature curve is $+1^{\circ}$. As shown, the ascent to the third step was very erratic, and this is reflected in the air and gas temperatures. From 0347 to 0405 GMT, the balloon floated level at 29,000 ft with a measured equilibrium superheat of -3°. During the ascent to the fourth step, the balloon temperatures show the characteristic decrease with a subsequent increase after the balloon reaches equilibrium. The gas temperatures, however, continue to increase, and never attain a true equilibrium value. Comparison of the temperature curves with the time-altitude and time-tension plots shows that most probably the lead balloon began to leak some time after 0500 GMT, causing the balloon system to descend, thereby compressing the balloon gas with consequent warming.

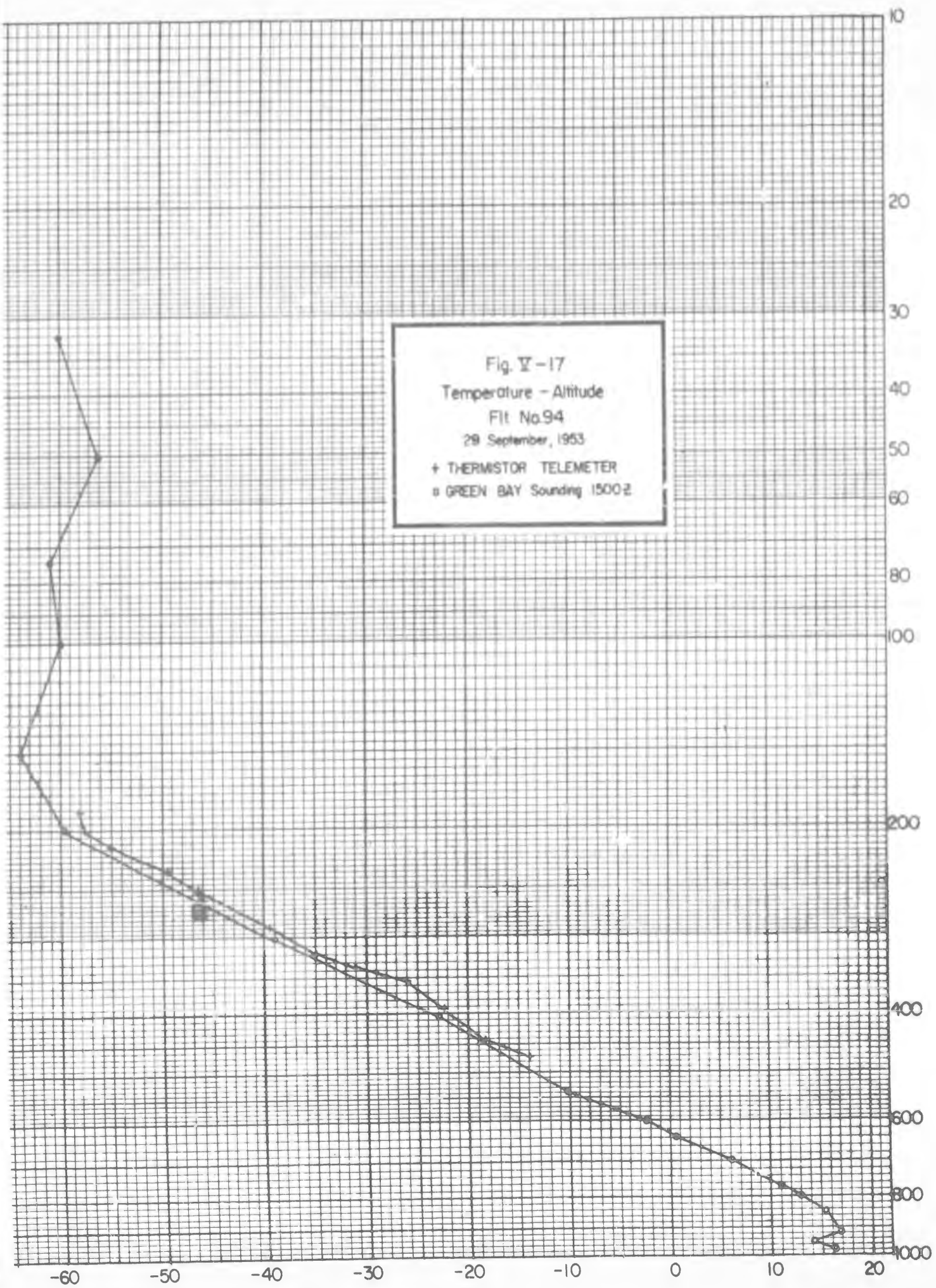
Fig. V-17
Temperature - Altitude
Flt No.94
29 September, 1953
+ THERMISTOR TELEMETER
o GREEN BAY Sounding 1500Z
10
20
30
40
50
60
80
100
200
400
600
800
1000
-60
-50
-40
-30
-20
-10
0
10
20
TEMPERATURE (°C.)

The direct temperature measurements in this particular flight proved useful in correcting an erroneous initial reading of the tensiometer. The measured value of the initial free lift was 89 pounds, but the equilibrium tensiometer readings at the first three steps show values of 59#, 61#, and 65#, which would indicate a large loss of superheat. Calculation of an initial free lift from the measured equilibrium superheat values and the tensiometer values gives a corrected value of 76.6# for the initial free lift.

TABLE VI.
Calculation of Initial Free Lift from Temperature and Tension Data, Flight 94

Time	p(mb)	F(#)	Meas. θ	$\Delta\theta$	T_{air}	$F_o = F + G\frac{\Delta\theta}{T}$
0130	1000	F_o = ?	-8.0°	--	--	--
0250	470	59	0.0°	+8.0	259°	76.5
0304	475	61	-1.0°	+7.0	259°	76.3
0350	321	65	-3.0°	+5.0	238°	76.9

Another interesting result from Flight 94 is shown in Figure V-19, where the superheat is plotted vs. time. The rate of loss of superheat during ascent is shown to be very nearly constant at -1.2°/1000 ft, even though the rates of ascent during the periods plotted vary from 194 ft/min to 497 ft/min. This flight is the only one whose temperature points are both sufficiently accurate and plotted close enough together in time to indicate this behavior clearly. For comparison, the adiabatic expansion for helium is -4°/1000 ft, which sets a maximum.

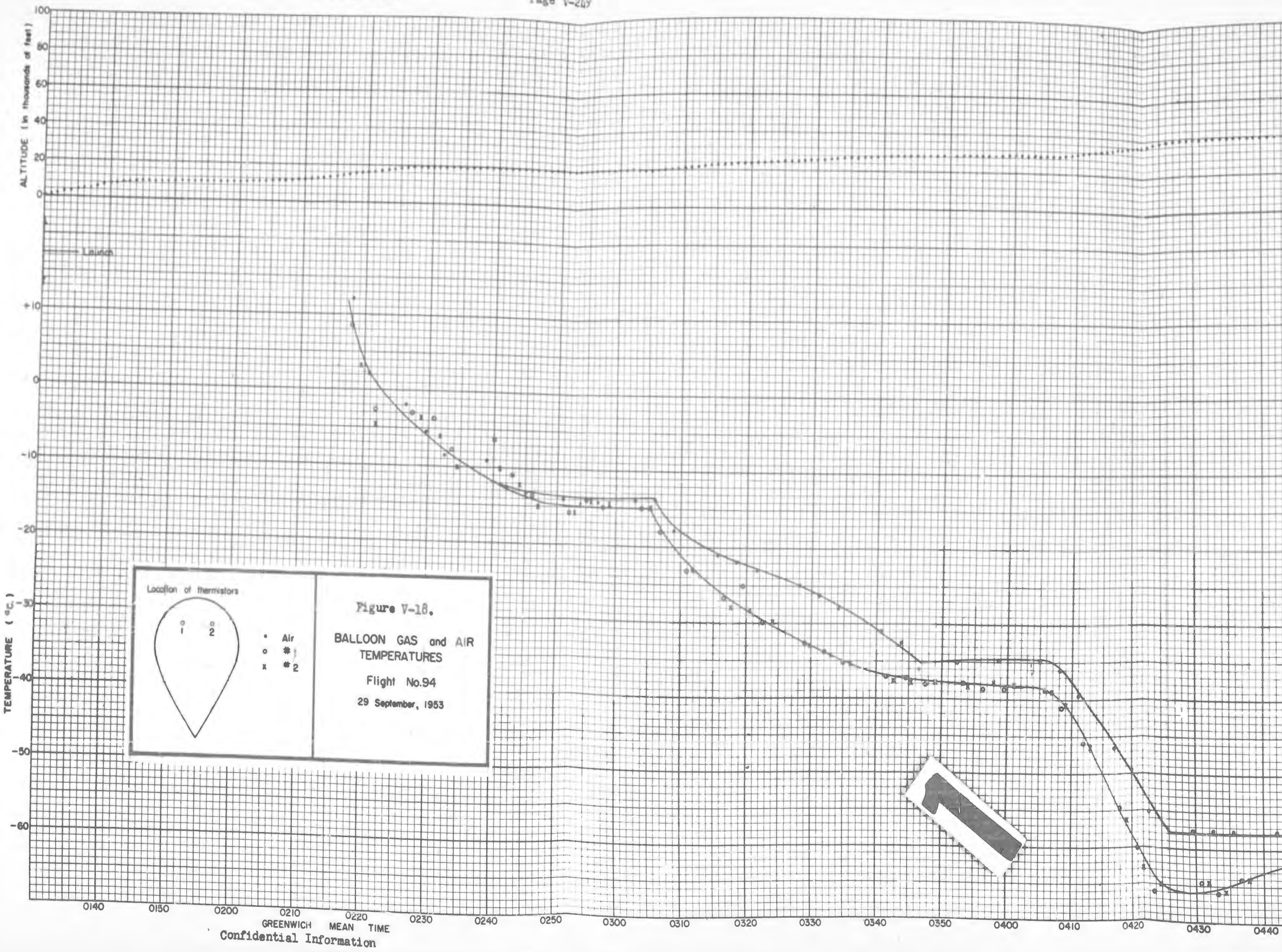

Figure V-18.

BALLOON GAS and AIR TEMPERATURES

Flight No.94

29 September, 1953

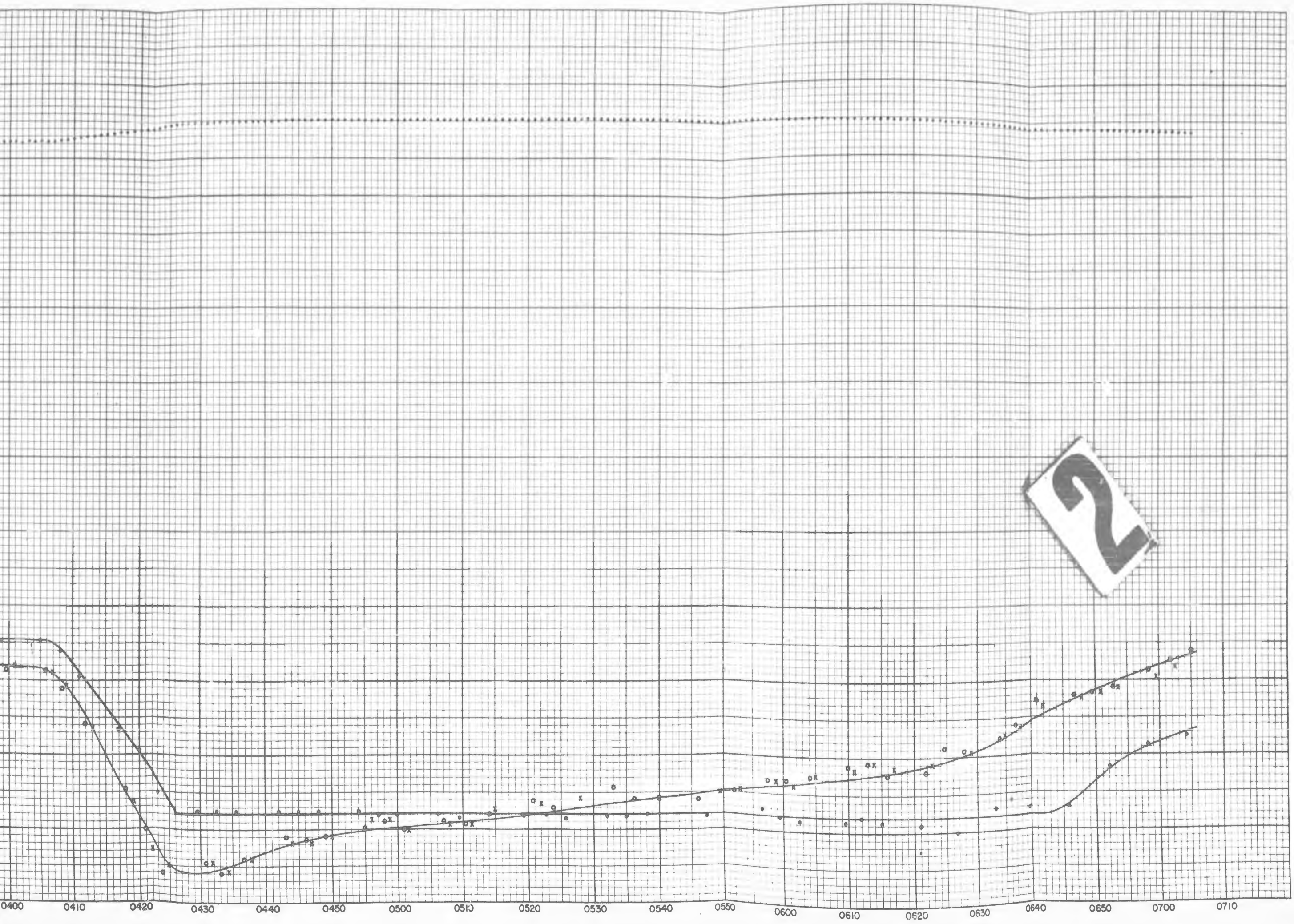
2
0400
0410
0420
0430
0440
0450
0500
0510
0520
0530
0540
0550
0600
0610
0620
0630
0640
0650
0700
0710

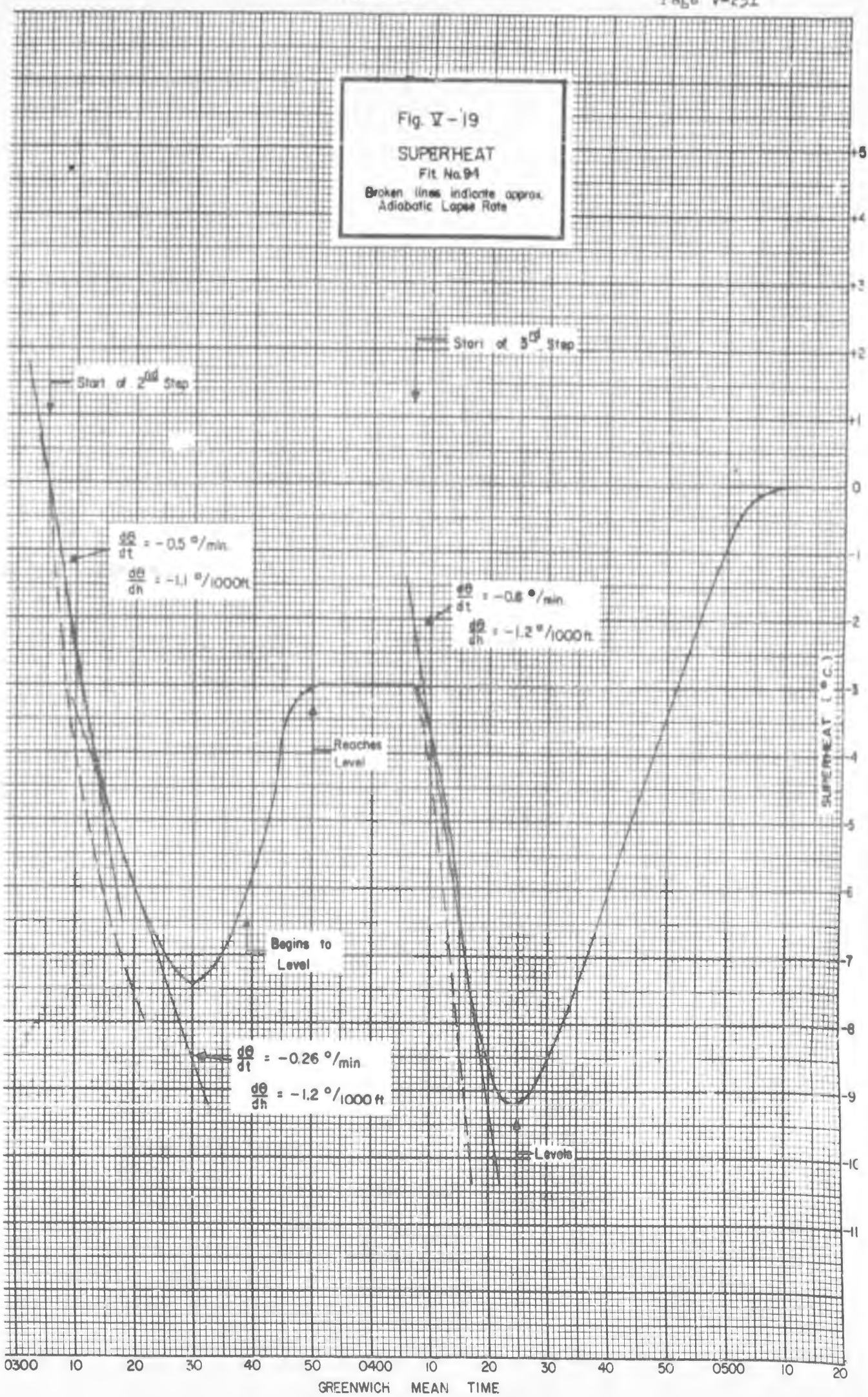
Fig. V-19
SUPERHEAT
Flt No. 94
Broken lines indicate approx. Adiabatic Lapse Rate
Start of 2nd Step
Start of 3rd Step
dθ/dt = -0.5 °/min.
dθ/dh = -1.1 °/1000ft.
dθ/dt = -0.8 °/min.
dθ/dh = -1.2 °/1000 ft.
Reaches Level
Begins to Level
dθ/dt = -0.26 °/min.
dθ/dh = -1.2 °/1000 ft.
Levels
SUPERHEAT (°C.)
+5
+4
+3
+2
+1
0
-1
-2
-3
-4
-5
-6
-7
-8
-9
-10
-11
0300
10
20
30
40
50
0400
10
20
30
40
50
0500
10
20
GREENWICH MEAN TIME

F. Description of Results from Other Temperature Measurements

Beginning with Flight 68, all flights using the standard size gondola were flown with one or more temperature pulse generators. Measurements on these flights included those of outside air temperature, temperatures at some point of interest inside the gondola, in addition to measurements of infrared flux from the ground. It is of importance to have a good air temperature measurement in the region in which the balloon is floating so as to obtain accurate values for the rates of rise and descent as well as the lapse rate at a particular level. Temperatures inside the gondola were of interest to explain erratic behavior of some flight components. Unfortunately, the last of the three, measurement of infrared flux, proved to be completely unfeasible with this type of telemetering circuit. A different unit has been developed which will perform adequately for these measurements and will be reported on in a later volume.

The temperature soundings for all flights are shown with the time-altitude curves (Volume XII, Section I.) Wherever possible, comparison soundings from nearby Weather Bureau stations are included.

It would be superfluous to plot out temperatures inside the gondola vs. time. During the day, the interior temperatures remain between $+10^{\circ}$ and $+30^{\circ}$ and decrease to a minimum of -15° about an hour after midnight. The points of measurement have included the free air inside the gondola, the structural members of the gondola or certain pieces of equipment. Even in Flight 81, where the bottom of the gondola was exposed to the outside air, the temperature of the infrared detector case, which is thermally well connected to the gondola frame, has apparently stabilized at -20° at midnight. The gondola at this time floated at about 37 mb.

G. Analysis of Temperature Measurements

Figures V-20 and V-22 are plots of the expected air and balloon gas temperatures vs. time during the two types of flights which have been instrumented for temperature to date.

In Figure V-20, typifying Flights 63, 67, and 81, the ground temperature at launch is arbitrarily taken as 5°. As the balloon ascends after launch at 0H10, the air temperature decreases uniformly to -59° at the tropopause, increases to -55° and then remains constant throughout the flight. The balloon gas, which is taken initially as -1° (an initial superheat of -6°), decreases with the air but at a slightly lower rate. At the tropopause, the gas, although still colder than the outside air, begins to warm, maintaining $\Delta\theta_a$ constant, and thus the thermodynamic drag constant. This rate of increase continues until the balloon begins to valve off its aerodynamic drag,* when the gas warms rapidly to an equilibrium value of -36°.

During level flight throughout the day, the balloon maintains its equilibrium superheat, but at ground sunset at 3H10, the balloon begins to descend, and increases its rate of descent at balloon sunset which usually occurs about 20 minutes later for a flight at 80,000 ft. One may regard the balloon system during sunset descent as a thermodynamical feedback loop, in which, when solar radiation is removed and the balloon gas attempts to cool, a minute loss of lift causes a descent with consequent compression and warming of the lift gas to such a degree that the process is continuous. The balloon thus descends at such a rate as to maintain the superheat it attained during level flight, except for a small decrease required to compensate for aerodynamic drag. This aerodynamic "friction" results in the net loss of superheat $\Delta\theta_b$. At a predetermined altitude, the gondola releases

* See Vol. IX, Section VI-C and D, for a discussion of balloon behavior during valving.

Figure V-20.
TYPICAL AIR and BALLOON
TEMPERATURES for
DAYTIME TEMPERATURE FLIGHT

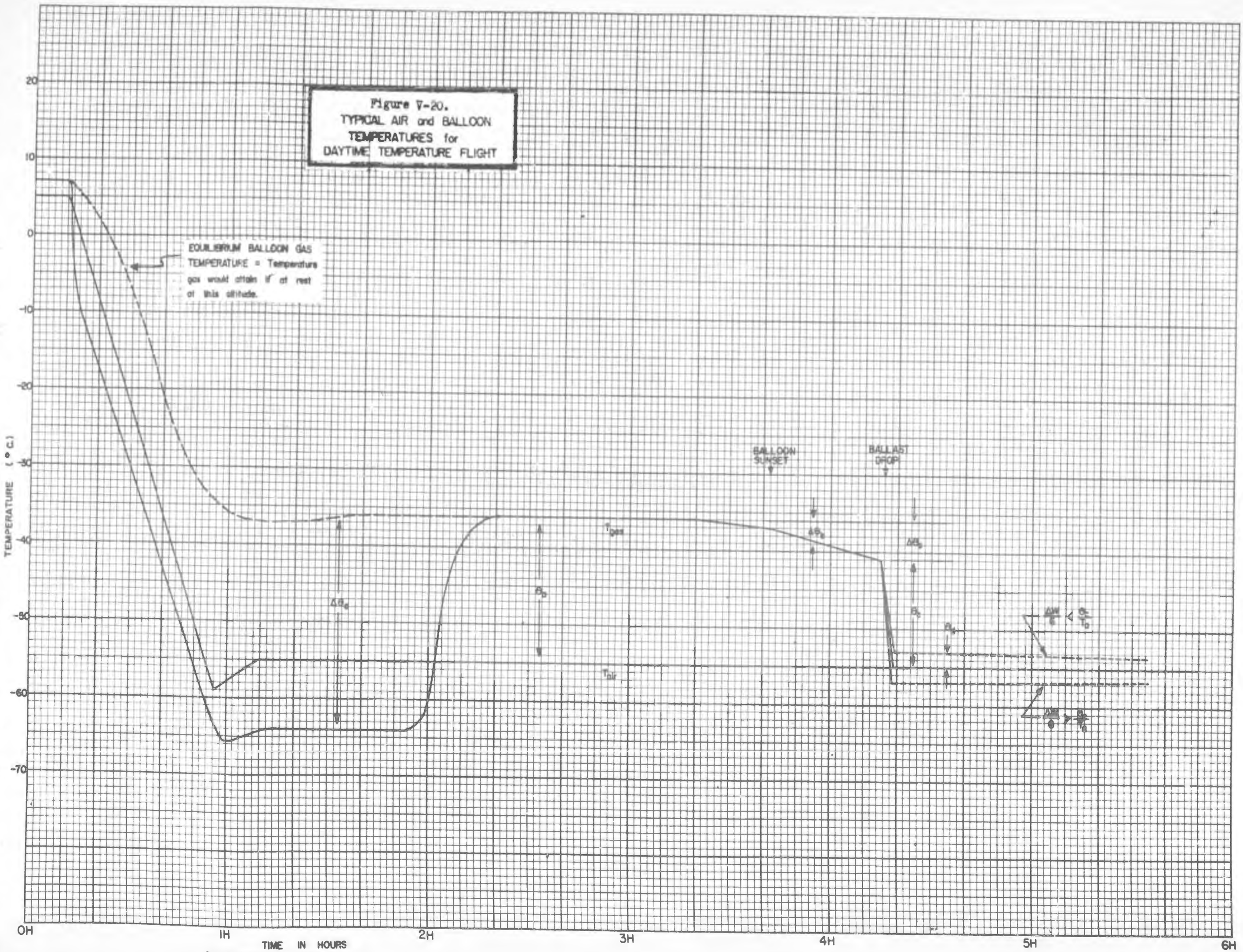

a known amount of ballast, ΔW, whereupon the balloon, having now an excess lift, bounces rapidly to a new altitude. Three cases apply here, depending on the amount of ballast dropped:

a) if the ballast dropped is less than enough to cause the balloon to rise sufficiently such that expansion of the gas drives its temperature to air temperature*, the balloon will retain some superheat and will continue to descend so as to maintain this superheat.

b) if the ballast dropped is just sufficient to drive the gas temperature to air temperature*, the system is in equilibrium at this altitude and will continue to float level until radiation again drives the balloon up, for example, at the next sunrise.

c) if the ballast dropped is more than enough to drive the gas temperature to that of air*, the superheat will become negative and the balloon will rise at such a rate to maintain this negative value, until the balloon begins to discharge gas.

These three cases are illustrated by dotted lines in Figure V-20. The superheats in the non-equilibrium cases are not quite maintained, again because of aerodynamic drag.

The dashed curve from launch to 2H20 represents the equilibrium value of superheat for a balloon floating level at an altitude corresponding to that reached by the balloon at this time. A clear idea of this quantity can be obtained from Figure V-21. This curve was plotted from the tensiometer data on Flight 80 converted to superheat by assuming an initial super-

*In principle, the equilibrium temperature at night need not be air temperature, since infrared flux from the ground could clamp the gas temperature to some higher value. Our experiments, however, with helium-filled polyethylene balloons in the stratosphere seem to indicate that the night-time equilibrium temperature is that of the air.

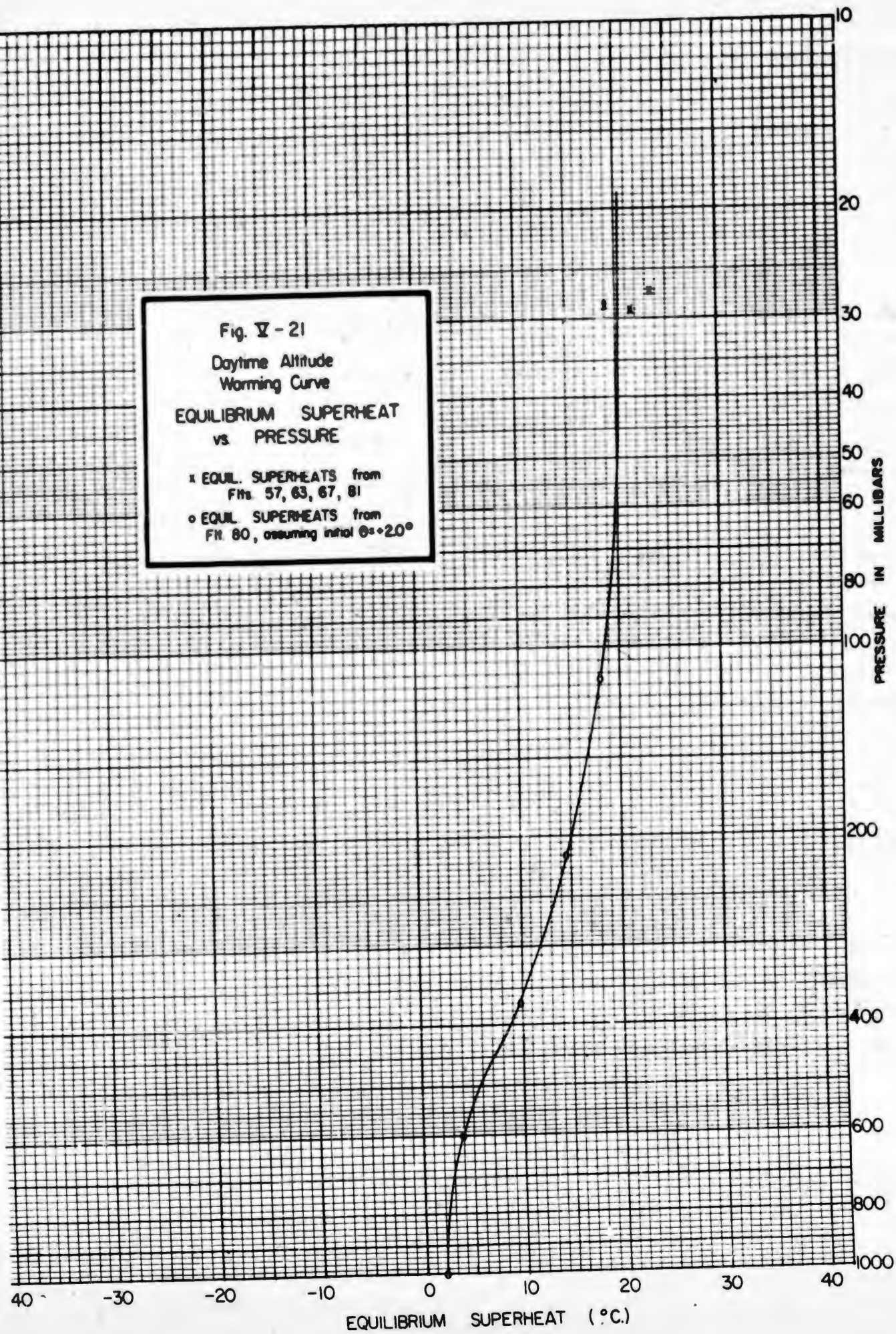
Fig. V - 21
Daytime Altitude
Warming Curve
EQUILIBRIUM SUPERHEAT
vs PRESSURE
x EQUIL. SUPERHEATS from
FMs 57, 63, 67, 81
o EQUIL. SUPERHEATS from
FM 80, assuming initial θ=+2.0°
10
20
30
40
50
60
80
100
200
400
600
800
1000
PRESSURE IN MILLIBARS
40
-30
-20
-10
0
10
20
30
40
EQUILIBRIUM SUPERHEAT (°C.)

heat of $+2.0^{\circ}$. See Table VII.

TABLE VII
Equilibrium Superheats from
Tension Data - Flight 80.

p(mb)	F(#)	ΔF	T_{air}	$\frac{\Delta F}{G}$	$\Delta \theta$	Equil. θ
1000	76	--	289	--	--	Assumed 2.0°
600	80	4	270	0.74%	2.0°	4.0
370	93	17	246	3.15%	7.8°	9.8
215	107	31	220	5.74	12.6°	14.6
112	116	40	217	7.41	16.1°	18.1

For descent after sunset, the equilibrium value of superheat is that attained by the balloon during level flight during the day; and after each ballast drop, the equilibrium superheat is that which the balloon attained after having bounced to its new altitude. For calculations of thermodynamic drag, altitude warming, and temperature changes during ballast bounces, the following relations hold true:

(a) during ascent, the difference between the measured superheat and the equilibrium superheat, $\Delta\theta_a$, divided by the mean air temperature in the region considered multiplied by the air displaced, G, is equal to the thermodynamic drag:

$$G\frac{\Delta\theta_a}{T_a} = \text{thermo drag.}$$

(b) during the descent after sunset, the difference between the measured superheat and the superheat measured at level flight, $\Delta\theta_b$, divided by the mean air temperature in the region considered and multiplied by G, is again the thermodynamic drag:

$$G\frac{\Delta\theta_b}{T_a} = \text{thermo drag.}$$

(c) at the ballast bounce, the difference between the superheat measured before and after the bounce, $\Delta\theta = \theta_c - \theta_d$, is equal to the percentage of the mass of air displaced dropped as ballast, minus the difference between the percent aerodynamic drag before and after the ballast drop. θ_d in this expression can be positive or negative, as shown:

$$\frac{\theta_c - \theta_d}{T_a} = \frac{\Delta W}{0} - \% \text{ aero drag difference.}$$

Table VIII gives calculations which show the relations between measured temperatures, thermodynamic and aerodynamic drags calculated from the nomographs, and ballast drops for all flights which have contained temperature measurements. The values of the equilibrium superheat at various altitudes used in computing $\Delta\theta$ during ascent were taken from Figure V-21. After level flight, the equilibrium superheats were taken from the temperature data for each flight individually, so as to eliminate, as far as possible, systematic errors.

Figure V-22 represents the expected behavior of night-time step flights, as typified by measurements on Flights 91 and 94. The air temperature decreases in steps corresponding to the balloon altitude, except for the last step, where the system passes through the tropopause on the ascent to the last step. The balloon gas, on the ascent to each step, decreases with the air, remaining colder than the air, and after a short warming time, attains an equilibrium temperature.

The data on these two flights is not sufficient to provide quantitative temperature comparisons with tension readings for reasons previously noted, but assuming that the equilibrium superheat changes only slowly at night with altitude, one can compute the thermodynamic drag during ascents by assuming the equilibrium superheat to be that attained by the balloon at equilibrium on the step. Values of thermodynamic drag so computed are given in Table VIII.

TABLE VIII.
Calculations of Temperature changes, Drags, and Ballast Drops

Flt. θ	t Time	θ (θ air displaced)	p (mb)	v (ft/min)	T_{air} (°F)	L (°/1000')	T_{gas} (°F)	θ (°F)	Equil. θ from Fig. V-21	Δθ from Fig. V-21	Meas. Equil. θ	Δθ from Meas. θ	$\frac{\Delta\theta}{T_0}$	Ballast $\frac{\Delta B}{B}$	Nomograph Zero Drag	Nomograph Thrust Drag
57	1544	519	600	767	240.0	-1.75	—	—	—	—	—	—	—	—	4.2%	6.6%
	1600		140	850	214.0	-1.26	—	—	17.0	—					3.3	9.2
	55		30	850	213.0	+1.05	218.5	+5.5	20.0	-14.5			6.81%		2.0	14.0
	1700		27	0	214.0	0	237.5	+23.5	20.0	+3.5			1.4%		—	—
63	2055	516	820	563	270.0	-2.36	263.0	-7.0	+2.5	-9.5			3.52		2.5	4.1
	2100		700		262.0	-1.20	256.0	-6.0	3.0	-9.0			3.44		2.4	6.3
	08		600		255.0	-0.60	249.5	-5.5	4.0	-9.5			3.72		2.3	7.5
	16		500		246.0	-2.12	241.5	-4.5	5.5	-10.0			4.06		2.4	4.6
	32		300	675	222.0	-1.90	219.0	-3.0	12.0	-15.0			6.76		2.8	6.0
	44		200	675	219.0	+1.14	213.5	-5.5	15.0	-20.5			9.36		2.5	11.8
	55		150	650	218.0	-0.57	214.5	-3.5	17.0	-20.5			9.40		2.0	8.8
	2206		100		217.5	-0.14	213.5	-4.0	18.5	-22.5			11.35		1.8	9.5
	13		80		217.0	-0.14	213.5	-3.5	19.0	-22.5			11.35		1.7	9.5
	22		60		216.5	+0.29	214.5	-2.0	19.5	-21.5			9.94		1.5	10.2
	34		40		215.5	-0.33	215.5	0.0	20.0	-20.0			9.28		1.3	9.0
	43		30		215.0	+1.10	220.5	+5.5	20.0	-14.5			6.75		1.2	12.0
	2320		28.5	0	216.5	0	235.5	+19.0	20.0	-1.0			—		—	—
	2015		32	146	216.0	+1.10	233.5	+17.5			19.0	-1.5	0.70		0.1	4.0
	45		45	337	214.0	-0.33	227.0	+13.0			19.0	-6.0	2.81		0.4	5.8
	0100		60	415	213.5	+0.29	226.0	+12.5			19.0	-6.5	3.04		0.6	5.6
	13		75	—	213.5	—	217.0	+3.5			12.5	-9.0	4.21	4.85	—	—
	55	467	75	43	213.5	-0.14	216.5	+3.0			3.5	-0.5	0.23		~0.0	1.2
67	2014	542	600	661	256.0	-1.81	—	—	4.0				—		3.1	6.1
	20		500		248.0	-1.98	237.0	-11.0	5.5	-16.5			6.66		2.9	5.8
	27		400		238.0	-2.23	227.0	-11.0	8.5	-19.5			8.19		2.8	5.4
	36		300		228.0	-2.23	216.5	-7.5	12.0	-19.5			8.70		2.6	5.4
	48		195	538	221.0	0.00	212.5	-8.5	15.5	-24.0			10.85		1.5	8.4
	56		150	725	221.0	+0.20	216.5	-4.5	17.0	-21.5			9.73		2.6	10.2
	2108		100		221.0	-0.15	214.0	-7.0	18.5	-25.5			11.55		2.2	10.0
	14		80		221.0	-0.10	217.5	-3.5	19.0	-22.5			10.20		2.0	10.1
	21		60		221.0	+0.10	219.5	-1.5	19.5	-21.0			9.50		1.8	10.8
	30		45		221.0	+0.10	221.0	0.0	20.0	-20.0			9.05		1.6	10.8
	40		30		223.0	+0.45	225.5	+2.5	20.0	-17.5			7.85		1.5	13.5
	2240		29	0	220.5	0	242.0	+21.5	20.0	+1.5			—		—	—
	0030		37	123	221.0	+0.10	240.0	+19.0			21.5	-2.5	1.13		<0.1	2.8
	0110		53	272	221.0	+0.10	237.5	+16.5			21.5	-5.0	2.26		0.2	5.5
	46		70	—	219.0	—	221.0	+2.0			16.5	-14.5	6.62	6.03	—	—
	0200	504	74	68	218.0	0.00	220.0	+2.0			2.0	~0	~0		<0.1	1.7
81	1912	493	1000	0	298.5	—	293.5	-5.0	2.0	-7.0			2.35		—	—
	27		650	533	270.0	-1.98	255.5	-14.5	3.5	-17.5			6.48		2.2	4.5
	30		600		265.5	-1.98	252.0	-13.5	4.0	-17.5			6.60		2.1	4.5
	39		500		256.0	-2.26	244.0	-12.0	5.5	-17.5			6.84		2.0	4.1
	47		400	690	245.0	-2.09	234.0	-11.0	8.5	-19.5			7.96		3.2	5.6
	56		300		230.5	-1.90	221.5	-9.0	12.0	-21.0			9.11		2.9	6.1
	2010		200		222.0	-0.55	218.5	-3.5	15.0	-18.5			8.33		2.6	9.2
	20		150		221.0	-0.20	217.5	-3.5	17.0	-20.5			9.28		2.4	9.3
	32		100	698	219.0	-0.20	218.0	-1.0	18.5	-19.5			8.90		2.1	9.3
	38		80		219.0	+0.40	218.5	-0.5	19.0	-19.5			8.90		1.9	10.8
	47		60		221.5	+0.40	221.5	0.0	19.5	-19.5			8.80		1.8	10.8
	56		45		222.0	0?	226.5	+4.5	20.0	-15.5			6.98		1.6	9.8
	2108		30		222.0	0?	227.0	+5.0	20.0	-15.0			6.76		1.4	9.8
	30		30	0	220.0	0	235.0	+15.0	20.0	-5.0			—		—	—
	0110		35	70	222.0	0?	234.0	+12.0			+15.0	-3.0	1.35		~0.0	1.8
	0211		55	300	220.0	+0.40	226.0	+6.0			+15.0	-9.0	4.09		~0.3	5.6
	47		68	—	220.5	—	217.0	-3.5			+6.0	-9.5	4.31	7.10	—	—
	0305	452	54	139	220.0	+0.40	217.0	-3.0			3.5	+0.5	0.23		~0.1	3.2
91	1200	567	1000	0	281.0	—	280.5	-0.5			—	—	—		—	—
	1300		660	0	266.5	—	268.5	+2.0			—	—	—		—	—
	40		660	0	267.0	—	268.0	+1.0			—	—	—		—	—
	50		570	690	263.0	-2.28	257.0	-6.0			?	—	—		3.3	5.0
	1400		430		249.0	-1.94	243.5	-5.5			?	—	—		3.1	5.9
	10		330		238.0	-2.13	235.0	-3.0			?	—	—		2.9	5.5
	1500		288	0	229.5	—	—	—			—	—	—		—	—
	1800		118	0	218.5	—	—	—			—	—	—		—	—
94	0120	567	1000	0	284.8	—	279.5	-5.3			—	—	—		—	—
	0250		700	0	259.0	—	259.0	0.0			—	—	—		—	—
	0304		690	0	259.0	—	258.0	-1.0			—	—	—		—	—
	10		435	420	255.0	-1.45	252.0	-3.0			-3.0	0.0	0.00		1.1	4.8
	20		393	194	250.5	-1.31	245.0	-5.5			-3.0	-2.5	1.00		0.2	2.8
	30		363		246.5	-1.31	240.0	-6.5			-3.0	-3.5	1.42		0.2	2.9
	40		335		242.0	-4.68	236.0	-6.0			-3.0	-3.0	1.24		0.2	~0.2
	50		320	0	238.0	-2.03	235.0	-3.0			-3.0	0.0	0.00		—	—
	0400		317	0	238.0	-2.03	235.0	-3.0			—	—	—		—	—
	10		295	497	235.0	-2.03	233.0	-2.0			-5.5?	—	—		1.4	4.7
	20		252	497	223.0	-2.64	214.5	-8.5			-5.5?	-3.0	1.35		0.9	3.5
	30		198	~0	215.5	-0.31	208.0	-7.5			-5.5?	-2.0	0.93		0	~0.0
	40		192	0	215.5	—	210.0	-5.5			-5.5?	0.0	—		—	—
	50		187	0	215.5	—	212.0	-3.5			—				—	—
	0500		185	0	215.0	—	213.0	-2.0			—				—	—
	20		182	0	215.0	—	215.0	0.0			—				—	—

Figure V-22.
TYPICAL AIR and BALLOON TEMPERATURES for NIGHTTIME STEP FLIGHT

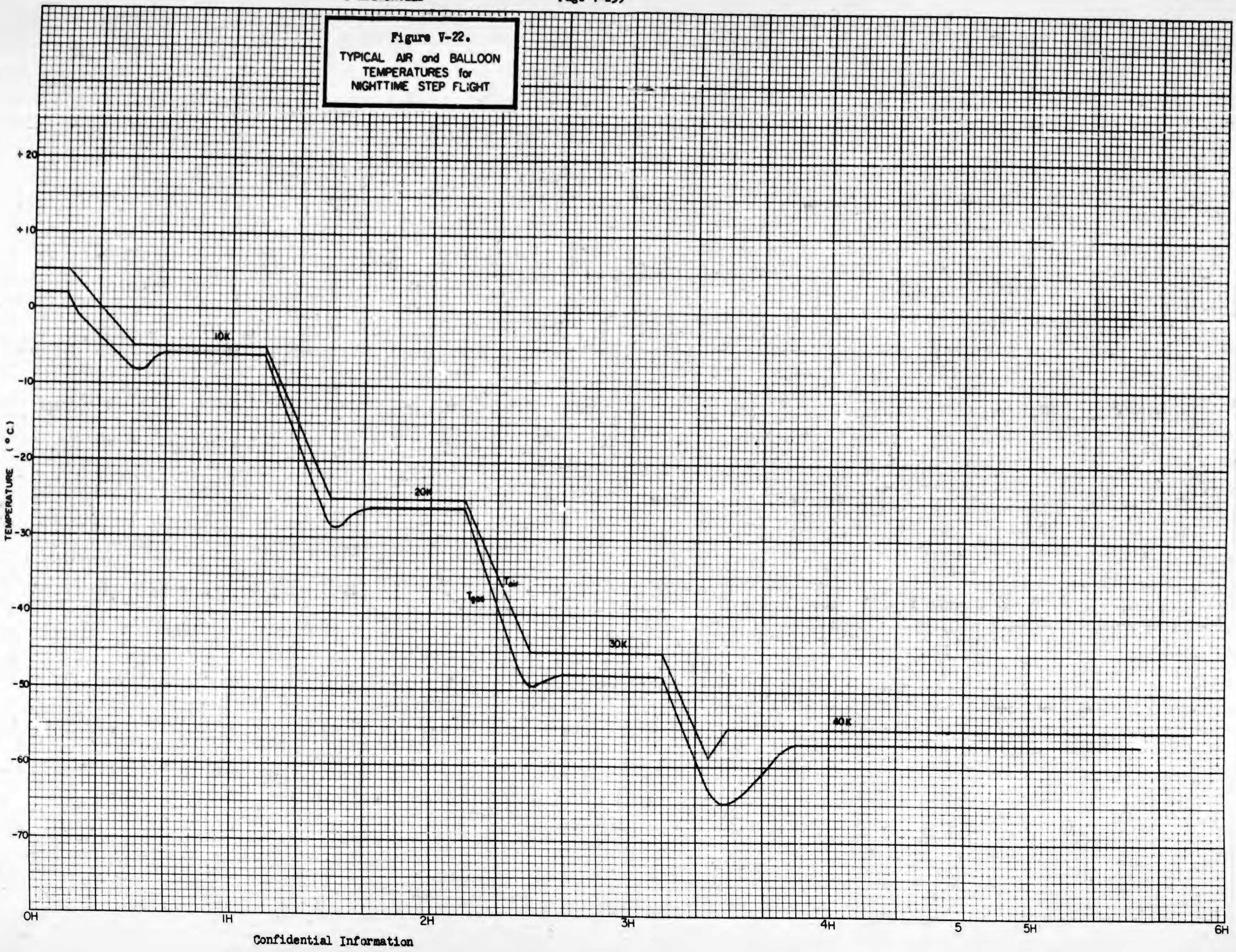

Section VI

VERTICAL FLIGHT

A. Step Flight Techniques

Introduction. Early in the project it was recognized that the constants which go into the equation of vertical motion of plastic balloons would have to be evaluated by experiments. It was obvious that it would be necessary to measure the velocity at various altitudes corresponding to a known free lift. It was also surmised that due to the radiation fields present and the variations in air temperature with altitude the balloon might gain or lose free lift as the altitude changed, and the ground weigh-off alone would lead to completely wrong results if used in the drag equation. Measurements on a continually rising balloon would not separate the altitude warming from the various drag terms in the equation of vertical motion and accordingly methods of stopping the balloon and weighing it at various altitudes were considered.

The first approach to the problem of measuring the velocity corresponding to known free lifts at various altitudes was by means of radio controlled flights in which it was attempted to valve gas to level a rising balloon or to force a balloon at equilibrium to descend. The ballast dropped by radio control would give the balloon a known free lift and then measurement of the corresponding upward velocity would evaluate the flight constants at each level. A great deal of effort was put into the radio controlled flights on this project -- approximately 19 flights in all were attempted, in which a system was set up to operate the valve motors, ballast sequence droppers which dropped fixed amounts in a predetermined order by command,

and also cut down the flight by command.* Many difficulties were encountered with this system and only very meager information was obtained due to failures of all kinds, of which the failure of the radio circuit to be consistently reliable was only partially the cause. There was also a fundamental difficulty in flying a balloon by remote control because the altitude data came in slowly and it was necessary to make decisions about dropping ballast or valving gas on the basis of insufficient data. Sometimes the pressure readings were uncertain for some reason and this complicated the latter problem. Flight 56 is an example of this situation. On later flights in this radio controlled series, altitude warming was to be measured by use of the tow balloon technique. In view of the known difficulties, it was finally decided to discard the radio controlled flight as a means of getting the flight constant data. Following this the idea of the step flight was developed and it was obvious from the start to be such a superior method that effort was henceforth concentrated on this technique.

The principle involved was to provide a platform composed of a balloon of suitable size, for example a 30-ft diameter polyethylene balloon, whose altitude could be exactly controlled to fit a predetermined schedule. The altitude control was obtained by dropping ballast and having the balloon full at all times so that the pressure altitude was proportional to the gross load remaining on the always full balloon. The balloon to be studied would be moored (above) to this platform balloon by a cable and the lift of this "tow" balloon would be measured by a tensiometer and the results would be telemetered. The pressure altitude, temperatures and other relevant data would also be telemetered. No radio control would be used; rather, mechanical timers and programmers would be included with the system to schedule the

---

* See Volume V, PP. VII-207 to 338, of this series of reports.

release of the ballast to control the altitude. The desired form of time-altitude curve best suited to evaluate the flight constants seemed to consist of a number of steps in which the platform balloon first valved and levelled at a low altitude. Then the successive steps where the system was level would be separated by portions in which the system rose at a constant velocity. The equilibrium weigh-off would be obtained on the level portion of the step if sufficient time were allowed for the tow balloon to reach thermal equilibrium at that level. The total drag would be determined on the rising portion of the step by measuring the decrease in tension of the tow balloon as the platform balloon controlled the altitude. It was also anticipated that the aerodynamic and thermodynamic parts of the drag could be separated, as the aerodynamic part would come in rapidly as soon as the upward motion of the step was begun and the thermodynamic part of the drag would come in slowly as equilibrium was established on the rising part of each step and could then be separated from the aerodynamic part. The success with which the thermodynamic and aerodynamic drag and altitude warming can be evaluated from the step flight curves will be discussed in the results of the step flights.

In executing the step flights, the project was faced with a whole new series of problems. One of these was the design of a suitable ballasting device which would release gross load in the proper way to give the desired time-altitude curve. It was decided to approach the problem in sections and to develop the platform by itself first. Accordingly a ballasting scheme was worked out, as described in the Ballasting section, and a balloon selected for the platform (General Mills 30-ft diameter type 301C, 2-mil 24 gore, cone-on-sphere design, with 90° cone angle equipped with a duct appendix.) A

flight was made, number 68, to prove out the platform, and was completely successful. The details of the time-altitude curve and the information obtained from it will be discussed in a later section. The old style telemetering system which keyed a transmitter directly with the Olland Cycle was used to transmit pressure and air temperature data on this flight. Following this successful beginning a considerable amount of time was spent working out further problems. One of these was a completely new telemetering system which could transmit a number of different pieces of information simultaneously. One needed to know the tension in the tow balloon cable, the air temperature, pressure and other temperatures in the tow balloon itself.

The telemetering of temperatures from the tow balloon presented another problem as no wires or connections could be used between the two balloons because of the possibility of fouling the weigh-off cable. Accordingly, a complete transmitting system was built to hang on the bottom of the tow balloon, including a temperature pulse transmitter and a cycling device to look at all the different thermistors in the tow balloon. This data was transmitted on 10 mc to the gondola hanging below the platform balloon where it was fed into the main telemetering system through a small receiver and transmitted back on the high powered carrier to the receiving point.

The selection of the platform balloon depended on the range of altitudes desired. It was selected so that the troposphere and the lower portion of the stratosphere would be covered by the step flights reported in this series. It was decided to use for the tow balloon the 73-ft double-wall one-mil cone-on-sphere balloon manufactured by Winzen Research, Inc., which had been used in a great deal of the work of the project, and for which a

great deal of data on sunset effects, rise rate, etc. was available. Further data on this same balloon would then be obtained on the step flights for comparison. This balloon had proven to be very durable, very successful in flying and to have low leakage.

A further problem was that of launching the assembly consisting of a platform balloon with nearly a thousand pounds of displaced air on the ground and the tow balloon which was of large size. Because of the necessity of the interconnecting cable, shock or snap in launching had to be avoided because of the possibility of damaging the tensiometer device carried in the platform balloon. The launching techniques are described in the paragraphs below, as well as the systems used for ballasting. The analysis of the flights is also contained in this section of the report. Details of the instrumentation used on the step flights including the telemetering system, temperature system, etc., will be found in the instrumentation section of this report, Volume I, Section I.

It was surmised that the observed warming with altitude might be partly the slow onset of sunrise, and computations showed (see Section IV of this volume) that the solar radiation was increasing during the early steps of a daytime flight. However, it was necessary to launch step flights as soon after sunrise as possible because of the need for low wind conditions. To separate this diurnal effect from the altitude warming, several one-step 50 kilo feet flights were made in which the tow balloon was weighed off through sunrise and sunset. It was realized that to be complete the radiation effects should be investigated throughout a 24-hour day, at a series of altitudes, and at various seasons of the year. The flights reported herein represent only a beginning of the study. Table I presents a summary of step flights through Flight 100, giving the purpose and results of ten such flights.

TABLE I. SUMMARY OF STEP FLIGHTS THROUGH FLIGHT 100

Flight No.	Purpose	Comments
68	Test of Platform Balloon. 500 ft/min 10-20-30-40-50 k. ft.	Completely successful. Gave absolute value of air temperature using balloon as a gas thermometer.
78	1st Step Flight using 70-ft tow balloon. 500 ft/min 14-24-34-44-54 k.ft. Daytime	Launching failure. Safety blowdown fired prematurely with gondola 8 feet off ground. Both balloons destroyed.
79	Repeat of 78.	Successful time altitude curve but tensiometer failed for unknown reasons.
80	Repeat of 78.	Successful flight. Gave daytime warming and drags at 500 ft/min.
86	Night step flight 500 ft/min. 14-24-34-44-54 k. ft.	Leaky 20' tow balloon caused flight to descend at Rice Lake 5 miles from launch site.
87	Repeat of 86	Successful flight. Gave night altitude warming and drag constants.
90	Single step. Level at 54,000 to measure diurnal changes.	Tensiometer failed early in flight. No significant data.
91	Two step 14-34-54 k.ft. 750 ft/min rise. Daytime.	Gave good data most of the time.
92	Single step. Level at 54,000 ft to measure diurnal changes	Very successful round-the-clock weigh off in stratosphere. Gave sunrise and sunset effects.
94	Repeat of 86	Good data on three of four steps on nighttime warming and drag terms.

Ballasting. The achievement of the time-altitude curve for the platform balloon resolved itself into dropping the ballast in such a way that the balloon would rise with constant velocity. If we assume the approximate exponential relation between atmospheric height and density, then the total gross of the system should be changed exponentially with time to achieve constant velocity. The first approach was to consider the behavior of a tank of liquid in which the velocity of efflux of the liquid was proportional to the height of the liquid. Then /the time-altitude curve could be established by turning on and off a valve to get the rising portion at the correct time. A number of experiments were conducted in order to establish a viscous flow of efflux from a tank which would give a mass flow proportional to pressure head. These experiments were not successful as in order to establish the viscous flow such long thin tubes would be necessary as to make the physical situation impracticable.

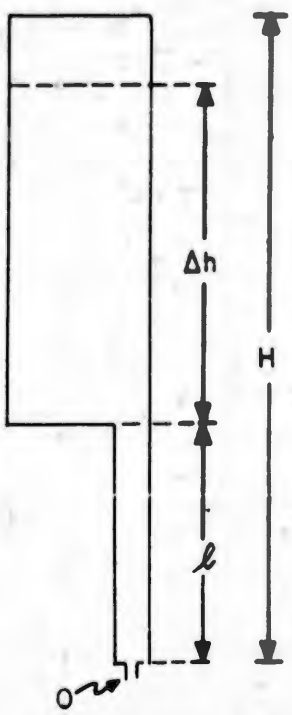

Figure VI-1.

One considers a tank (Figure VI-1) of fluid height H composed of a cylindrical reservoir of height Δh and a hose of length ℓ. The mass discharge rate of the orifice O is

$$\frac{dm}{dt} = C.\rho v a = C.\rho . a\sqrt{2gH} \qquad (1)$$

where C is the discharge coefficient for the orifice to be determined by experiment, a is the orifice area, ρ the fluid density, and g the acceleration of gravity. The total gross dropped is

$\Delta h.A.\rho$ where A is the tank cross-sectional area. Since the time-altitude schedule is divided into steps, a separate tank may be used for each, with the tank parameters to be adjusted so that during each step the mean rate is the same as the true exponential mean and the total gross released corresponds to the change in pressure height.

For true exponential ballasting (w = gross load)

$$\frac{dw}{dt} \sim w$$

While from equation (1)

$$\frac{dw}{dt} \sim H^{\frac{1}{2}}$$

and accordingly

$$w = \text{const.}\ H^{\frac{1}{2}}$$

$$2\,d\,w = \text{const.}\ H^{-\frac{1}{2}} d\,H$$

This gives

$$2\,\frac{d\,w}{w} = \frac{d\,H}{H}$$ as the differential relation to be satisfied.

Approximately then

$$2\,\frac{\Delta w}{\bar{w}} = \frac{\Delta H}{\bar{H}}$$ where $\bar{w}$ and $\bar{H}$ are the mean values of gross and fluid height during the step. We have, also, from the tank geometry, that

$$\Delta W = \rho A \Delta h$$

$$\Delta H = \Delta h$$

$$\bar{H} = \ell + \frac{\Delta h}{2}$$

The computation of tank heights and hose lengths begins by selecting the altitude of the level sections of the flight. These were nominally 10, 20, 30, 40 and 50 kilofeet on flight 68, and were changed to 14, 24,

34, 44 and 54 kilofeet for most other flights using this ballasting system. Once the tank size calculations had been made it was easy to change the rise rate by adjusting the orifice size, or combine steps where 10 kilofeet is insufficient to establish equilibrium on ascent (e.g. Flight 91). As shown in Table II (Flight 68), the air pressure, temperature, density and the corresponding weight of system at each altitude were computed from standard atmosphere tables. The volume of the platform balloon was taken from manufacturer's data and later evaluated exactly from the experiments. No account was taken of changes of tension caused by altitude warming. Table III gives similar computations for flights after 68. The ballast to be dropped during ascent, the mean weight during ballasting, $\Delta w/w$ and $\Delta H/\overline{H}$ could then be determined. A correction has been made to the gross weight (-50 lbs) for the free lift of the tow balloon. The altitude warming was unknown at the beginning. Knowing the tank cross section, A (.87 ft) and the density of the ballast liquid (Skelly "S", ρ = 53.3 lbs/ft^3), $\underline{\Delta h}$ could then be determined and $\underline{\ell}$ knowing $\underline{H}$. The relative orifice sizes were also determined using relation (1). One of these orifices had to be set by trial and error to give the correct rate. On Flight 68 for example, on the first step at 500 ft/min the mean rate had to be 195/20 = 9.75 lbs/min. The calculations were also carried out for water to be used in laboratory checking of equipment.

The can dimensions and orifice sizes computed for step flights after 68 are given in Table IV. Laboratory flow tests on a typical tank (#4, Flight 68) are shown in Figure VI-2. The points (experiment) are seen to approximate quite well the desired exponential curve (straight line). The ratio of initial to final flow ratio (6.6/4.1) is equal to the ratio of the gross load of the platform balloon at the beginning and end of the step (234/145). The

TABLE II.

(1) Alt.	(2) Press.	(3) Temp.	(4) Density	(5) Wt. of System	(6) Ballast Drop	(7) Mean Alt. During Ballast	(8) $\frac{\Delta w}{w}$	(9) $\frac{\Delta h}{h}\left(2\frac{\Delta w}{w}\right)$	(10) Δh ft.*	(11) $\bar{h}$	(12) $\bar{h}-\frac{\Delta h}{2}$ l	(13) $(\sqrt{h})^2$
10K	696	268	2.6	700								
					195	602	.324	.648	4.23	6.53	4.42	6.4
20	465	248	1.87	505								
					151	429	.353	.706	3.28	4.64	3.00	4.46
30	300	228	1.31	354								
					120	294	.409	.818	2.60	3.18	1.88	3.05
40	188	218	.865	234								
					89	190	.468	.936	1.93	2.06	1.10	1.93
50	117	218	.537	145								

	(14) $\bar{M}$ Kerosene lbs/min	(15) $\sqrt{\bar{h}}$	(16) $\frac{\bar{M}}{\sqrt{\bar{h}}}$	(17) Area of Orifice	(18) Dia. of Orifice	(19) Wt. of Water	(20) Wt. of Water for 10-min. test with one tank
10K							
	9.7	2.53	3.83	1	1	238	119
20							
	7.05	2.12	3.32	.865	.93	184	92
30							
	6	1.75	3.42	.891	.94	146	73
40							
	4.95	1.39	3.56	.93	.96	108	54
50							

*Area of 2 bases is .88 ft^2
46.1 #/ft kerosene
$P_{kerosene}$ = .82

TABLE III

(1) Alt.	(2) Press. mb	(3) Temp. °K	(4) Density	(5) Gross Wt.	(6) Gross Wt. -50	(7) Ballast Drop	(8) Mean Wt. During Ballast $\bar{w}$	(9) $\frac{\Delta w}{w}$	(10) $\frac{\Delta h}{h}$ $(2x\frac{\Delta w}{w})$	(11) Δh ft.	(12) $\bar{h}$ ft.	(13) $\bar{h} - \frac{\Delta h}{2}$ ℓ
14K	595	260	2.29	659	609							
						177	520	.340	.680	3.86	5.68	3.75
24	392	241	1.63	482	432							
						130	367	.354	.708	2.84	4.01	2.59
34	251	221	1.14	352	302							
						114	245	.465	.930	2.49	2.68	1.44
44	156	216	.715	238	188							
						72	152	.473	.946	1.57	1.66	.87
54	96.5	218	.443	166	116							

	(14) $\bar{M}$ Kerosene lbs/min	(15) $\sqrt{\bar{h}}$	(16) $\frac{\bar{M}}{\sqrt{\bar{h}}}$	(17) Area of Orifice	(18) Dia. of Orifice
14K					
	8.9	2.35	3.79	1	1
24					
	6.5	1.97	3.30	.87	.94
34					
	5.7	1.60	3.56	.94	.97
44					
	3.6	1.25	2.88	.76	.87
54					

TABLE IV

Can Dimensions for Step Flights After 68

Step in 1000 ft	Dropped Wt-Kerosene in lbs	Liquid Ht in Can in ft	Hose length to orifice	Orifice Diameter in in.	Time to Empty
14-24	172	3.74	3.71	.216	20' 32"
24-34	128	2.78	2.57	.195	20' 39"
34-44	112	2.44	1.44	.206	20' 40"
44-54	72	1.57	.88	.186	20' 43"

Area of cans = .88 ft^2

Rate for 14-24 = 8.6 lbs/min

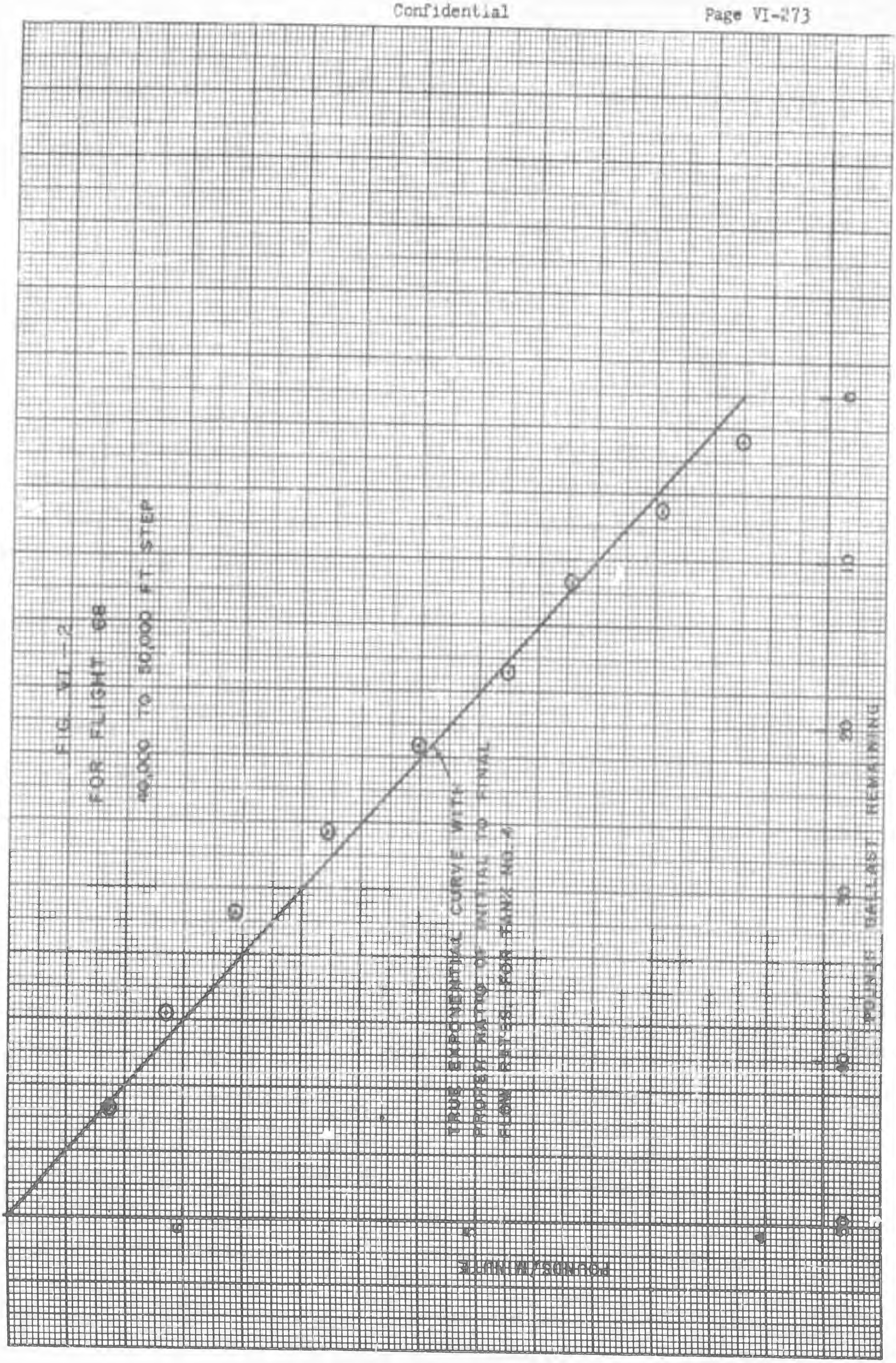
FIG. VI - 2
FOR FLIGHT 68
40,000 TO 50,000 FT STEP
TRUE EXPONENTIAL CURVE WITH PROPER RATIO OF INITIAL TO FINAL FLOW RATES FOR TANK NO. 4
POUNDS BALLAST REMAINING
POUNDS/MINUTE
6
10
20
30
40
50
6
5
4

orifice has not been adjusted. The release of the ballast was started at each step by dropping the proper hose from a tied-up position. The hose-dropping method was used to eliminate magnetic or mechanical valves. However, this method was not without problems. The single hoses became stiff at stratosphere temperatures and did not straighten when released. (This fact was learned from down camera photos.) This was corrected by introducing a section of thinner walled hose near the tank. Brass sylphons were also tried,but tended to crack and leak after some use; further, the Skelly "S" fluid becomes viscous at -75°C and solid at -80°C and it was suspected that either the freezing of the Skelly "S" or the freezing of water contaminate caused failure of ballast flow in certain cases. Of the step flights controlled by the release of liquid ballast, only the first attempt (Flight 68),in which the platform balloon alone was flown, was 100 percent successful. Because of these difficulties, a method using steel shot ballast and an altitude servo mechanism was developed and has been used on recent flights. This device was flown after Flight 100 and accordingly will be reported later in the program.

Another possible alternative to the straight cans and hoses described above would be a series of shaped cans in which the cross-section was varied as a function of height in such a way as to take into account the density lapse of the atmosphere. This shape could also include the aerodynamic drag force on the balloon if desired.

Launching Procedure. Figure VI-3 is a schematic of the complete step flight assembly as it appears when airborne. The platform balloon below carried the ballast tanks. The instrumentation gondola is hung inside these tanks on the end of the tow cable, and its weight constitutes the

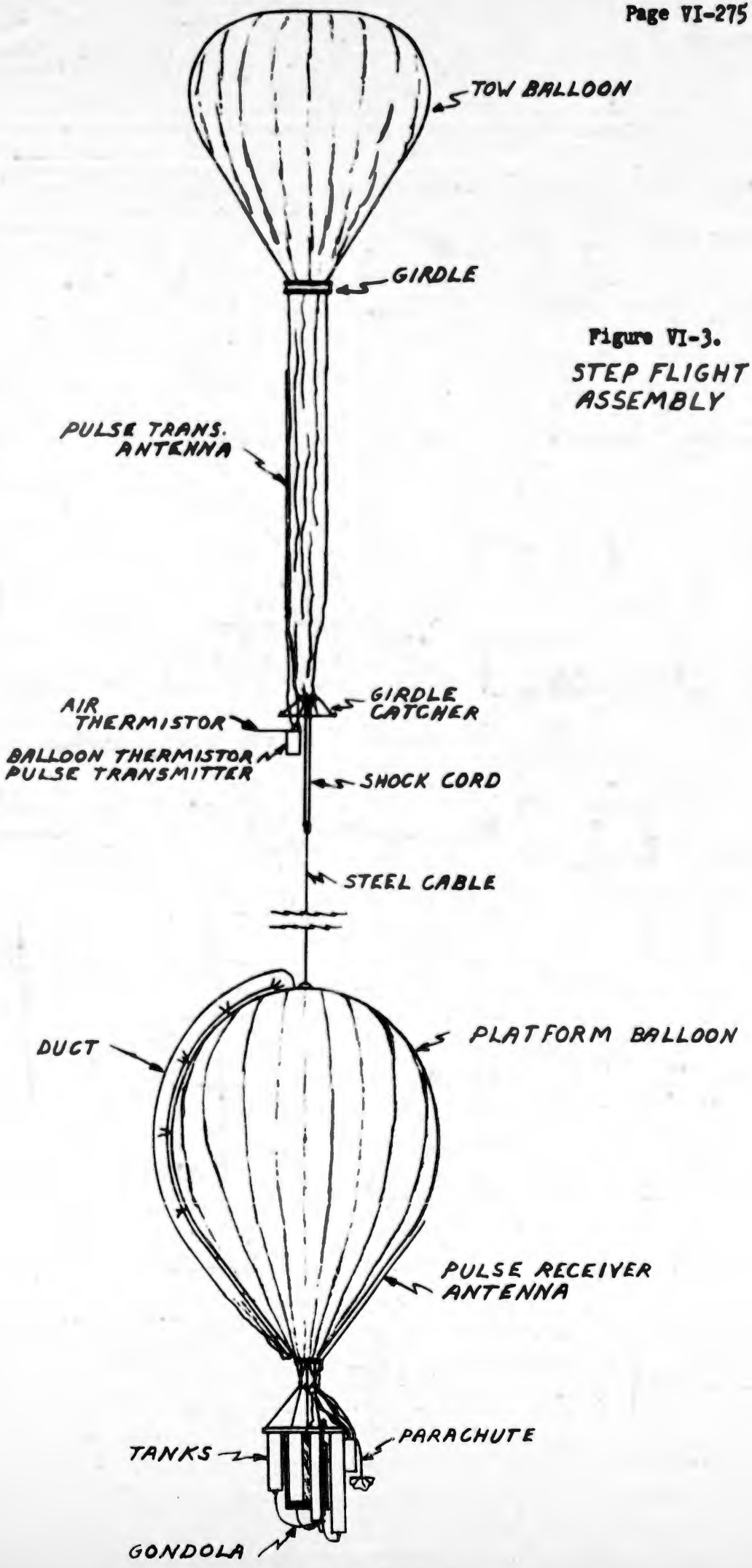

Figure VI-3.
STEP FLIGHT ASSEMBLY

payload of the tow balloon. (See Figure VI-4 for detail.) The tow cable passes through a gas tight grommet in the bottom of the platform balloon and out through a similar grommet in the top and then to the tow. The tensiometer connects the ballast frames to the tow cable just above the instrumentation gondola, and measures the unbalance of the tow. The cable tension exceeds this unbalance by the instrument gondola weight. In Flights 78 and 79 the payload of the tow was hung directly on the tow balloon in the form of sand, and the cable tension was then the total unbalance. It was observed on Flight 79 that the tension behaved in an anomalous manner and oscillated continually. Accordingly the cable tension was increased on successive flights by transferring the payload to the bottom of the cable. The instrumentation gondola formerly hung on the ballast can assembly was transferred to the tow cable for this purpose. Where higher rise rates were investigated the tow unbalance was made higher to allow larger changes due to drag. Practice finally centered about a tensiometer range of 300 lbs and an unbalance of about 160 lbs.

This required that the platform balloon on launching have enough lift to support the instrumentation gondola in addition to its regular load of ballast. The tow balloon on the other hand, had to be launched with its net lift appearing as free lift, until it reached its position above the platform and took up the instrument load. The total free lift of the assembly thus always consisted of the net lift of the tow (approximately 250 lbs) plus the small free lift given the platform to get it off the ground (approximately 20 lbs). It was found by experience that this free lift of up to 20% was not too high.

The launching technique evolved into the simple procedure of inflating the two balloons simultaneously, connecting the tow balloon to the tow cable with a length of shock cord, and releasing both together. The tow balloon was always folded by the Minnesota launching method so that an accurate weigh-off could be obtained. It was found on Flight 80 that if this balloon was launched in the usual way the very large free lift and corresponding high velocity surge upward would brush off the canopy before it could be inflated. Flight 80 went all the way to the 10,000-ft first level with the inflated lower 1/3 of the balloon held horizontal. The tow cable on one end and the spilled upper 2/3 of the balloon on the other end retained it in that position. The gas passed into the top, however, and finally erected the balloon properly without damage. Following this experience, the practice was made of letting the gas transfer in the tow balloon while it was on the ground and then releasing it quickly before any wind damage resulted to the fully extended cell. Very smooth launchings resulted from following this procedure. Several recent flights, to be reported later, used a General Mills platform launch for the tow (50% air inflation) balloon with similar good results.

Prior to the first step flight (78) great difficulties with the launch were anticipated. An elaborate scheme was devised and executed on this flight for maneuvering the tow balloon into position over the platform balloon using control lines from the ground. The steps usually taken on the ground to launch a large balloon by the Minnesota method were then carried out by these lines remotely with the balloon 100 ft above the ground, namely corset release, diaphragm rip cord, top inflation, etc. Although this launching was a failure for other reasons than the use of

this technique, it was found to be an unnecessary complication. Release of both balloons simultaneously from the ground with the introduction of a shock cord in the tow line was found to be simpler and superior in every way.

Because of the large lift of the platform balloon, special rigging and handling techniques were developed. These are illustrated in the schematic diagram, Figure VI-4, and the photograph, Figure VI-5. The 30-ft diameter 2-mil balloon (GMI #301-C) was equipped with an aluminum fitting at the balloon to replace the usual load harness. (Figure VI-6.) This fitting securely clamped all the tapes and provided rings for the suspension ropes. The gas was admitted to the balloon through an aluminum tube on the center of this fitting. The tow cable also came down through this tube as shown and through the rubber grommet. In the photograph the bottom of the duct appears in the upper right corner.

The platform balloon was moored by three blocks (A-A-A , Figures VI-4 and VI-5) to the ground on the corners of a 30-ft triangle. The lift was measured by a torque wrench with the balloon secured by a single block. (Figure VI-7.) When the inflation had reached about 80% the balloon was maneuvered over the load using the three blocks. The ballast tanks and instrument gondola were carried by a derrick on the back of the project stake truck, and were secured to the balloon by the harness and the two snaps (B-B, Figures VI-4 and VI-5). The blocks were than slackened and the three attachment snaps A-A-A were removed. The inflation was continued until weigh-off was obtained. Then the entire assembly could be lifted gently off the derrick hook and walked out into launching position.

The inflation and weigh-off of the tow proceeded as in the Minnesota

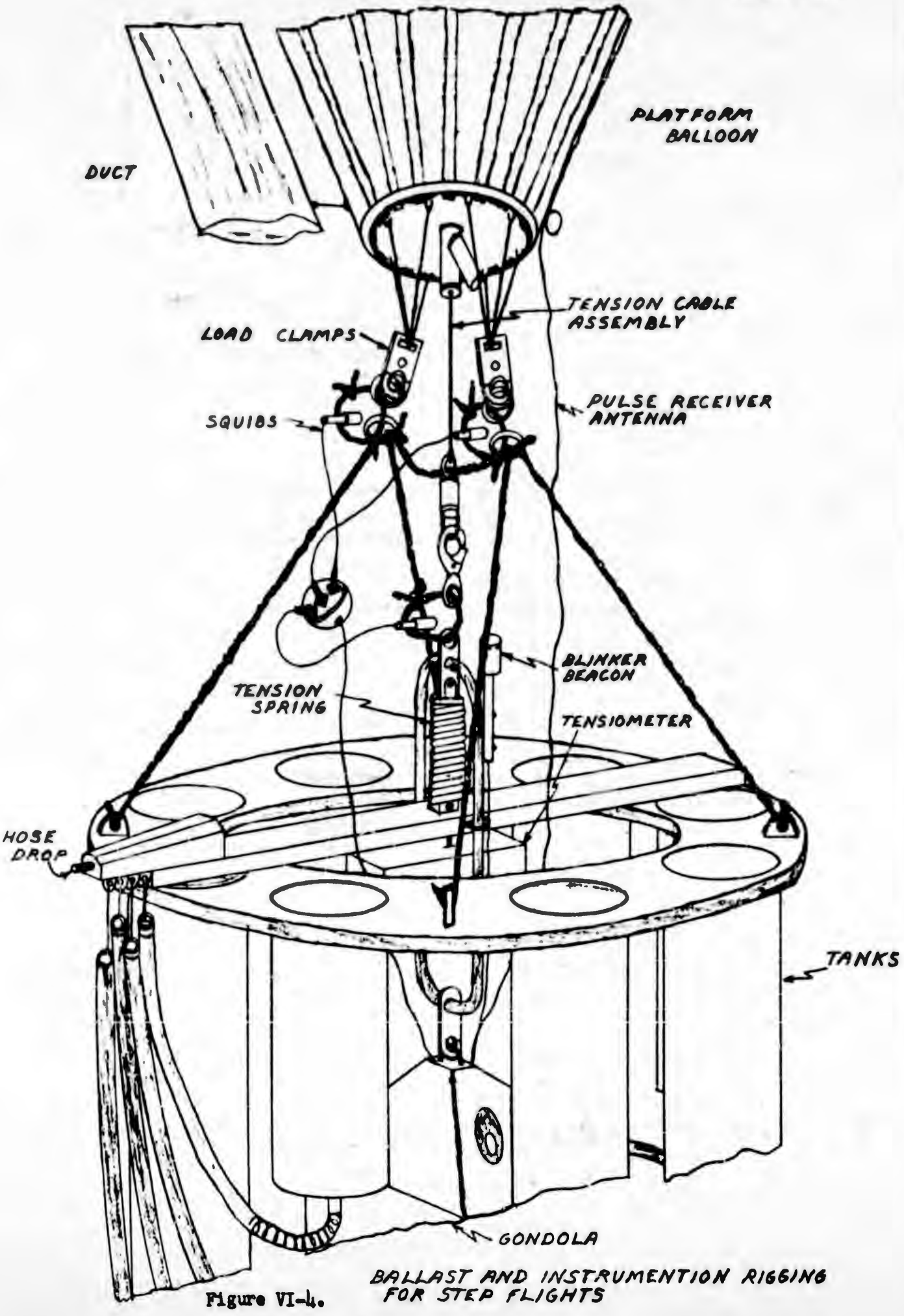

BALLAST AND INSTRUMENTION RIGGING FOR STEP FLIGHTS

Figure VI-4.

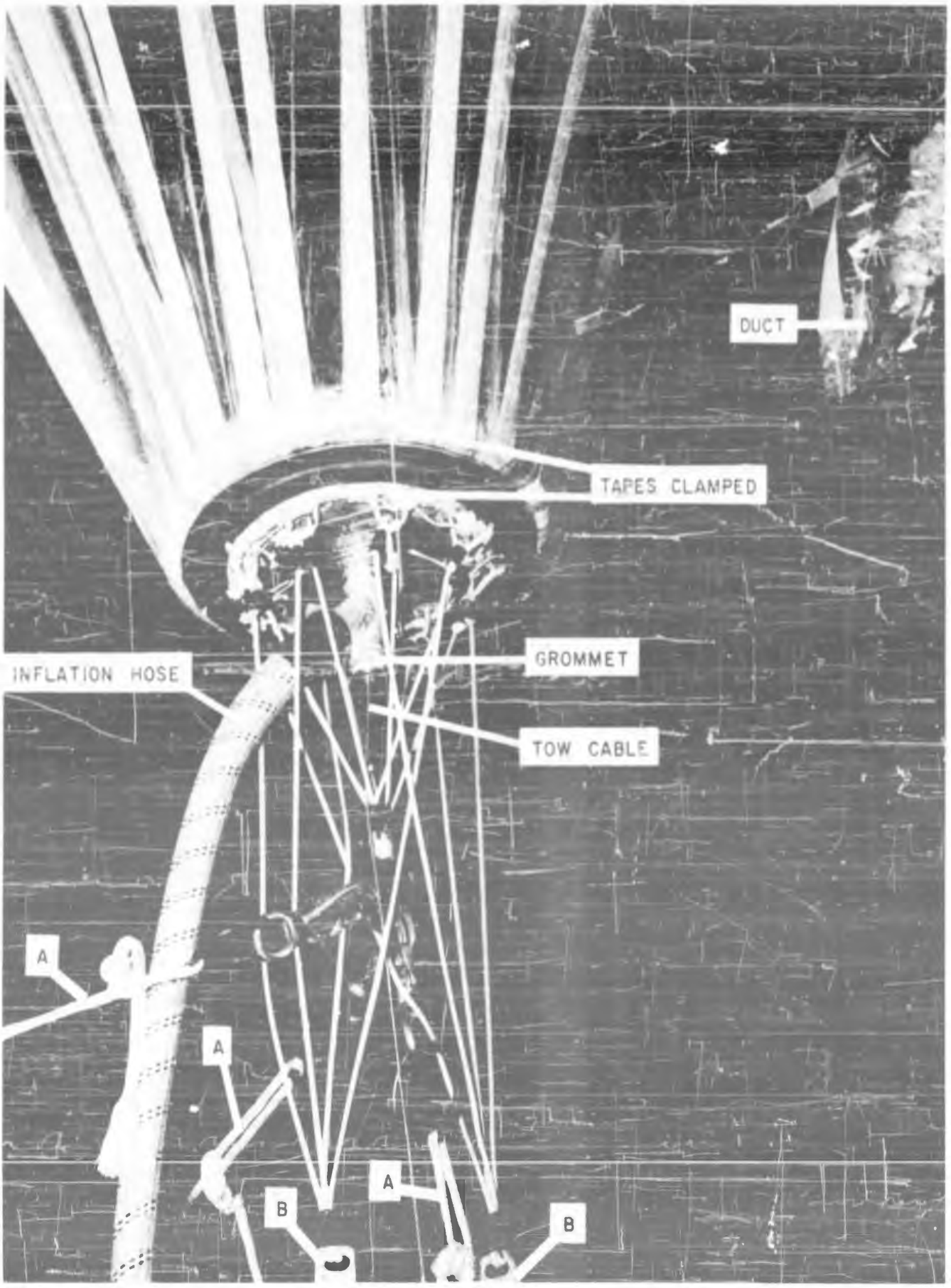

Figure VI-5. Close-up of platform balloon showing special bottom fitting and handling harness with three blocks secured by snaps to central rings (A-A-A) and snaps for attaching ballast tanks (B-B). Note inflation tube connected to side arm of aluminum pipe. A 500-lb aircraft type tow cable comes out of the pipe through grommet. In the upper right corner may be seen the bottom of the duct with the tie string securing it to the balloon. This balloon was approximately one-half inflated at the time the picture was taken.

Figure VI-6. View of bottom plate of platform balloon prior to inflation on the ground.

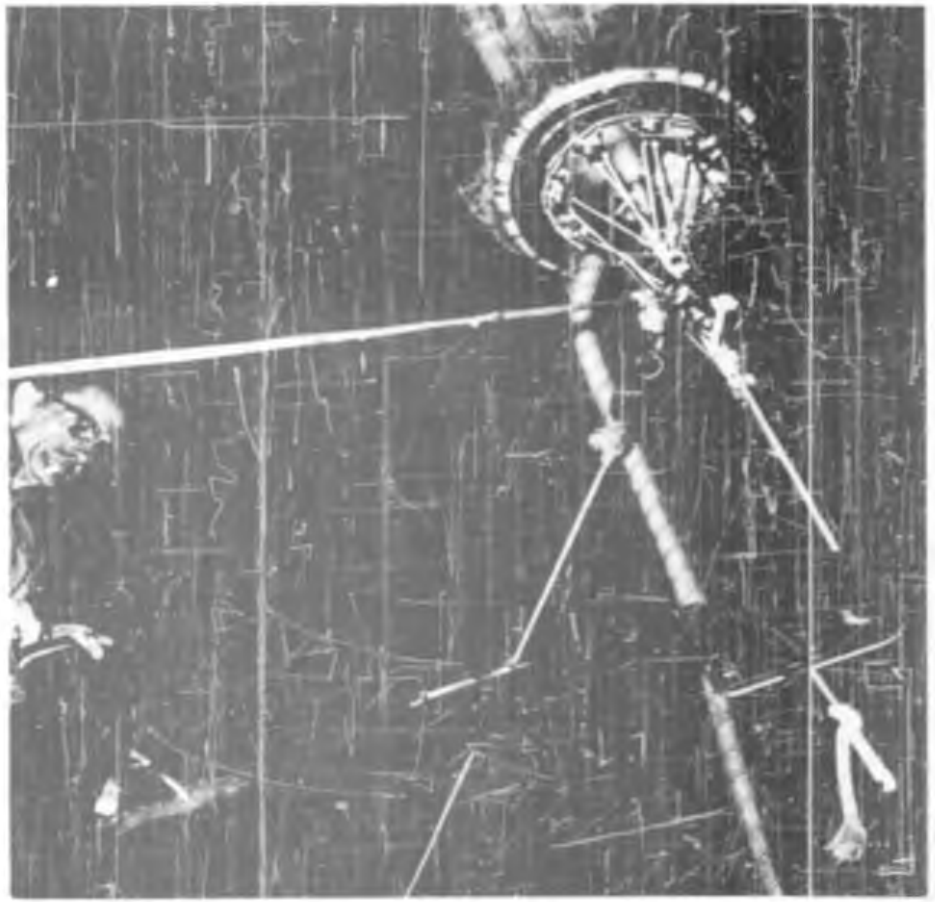

Figure VI-7. Weigh-off of platform balloon using torque wrench during initial steps of inflation. Note that balloon is moored by one of the lines from the block. The other two are slack at this stage before balloon is maneuvered over to pick up the load.

launch method. The final weigh-off was always made with sandbags as permitted by the low wind conditions chosen for step flight launchings. Figure VI-8 shows a step flight ready for launching. The corset has been removed from the tow balloon preparatory to transferring the gas to the top. The platform balloon is almost completely full and is supporting the ballast tanks and instrument gondola. The tow cable and shock cord connect the two balloons. Figure VI-9 shows the assembly in the air with the tow balloon transferring gas to its top. The improved technique of transferring gas prior to release is not shown in Figure VI-9.

B. Analysis of Step Flights

Of the step flights that have been made up to the series ending at Flight 100, four flights with level regions at a number of altitudes have been selected, and one flight has been selected which measured the tension on the tow balloon throughout a 24-hour period,in order to show the diurnal effect of the balloon lift at a fixed altitude. These step flights are: Flight 80, Flight 87, Flight 91, and Flight 94, and the 24-hour constant level step flight is Flight 92. The flights have been replotted in this section in a way which displays all of the pertinent data about the step flight in one series of graphs. All of the properties measured on the flight are plotted as a function of altitude. Beginning at the left of the graph is velocity in feet per minute, followed by tension in pounds, followed by hours after sunrise or sunset, followed by temperature in degrees Kelvin. It is possible, then, by looking across these graphs at a fixed altitude, to determine all the parameters of the system and to see how the tension behaved as a function of altitude and rate, etc., in

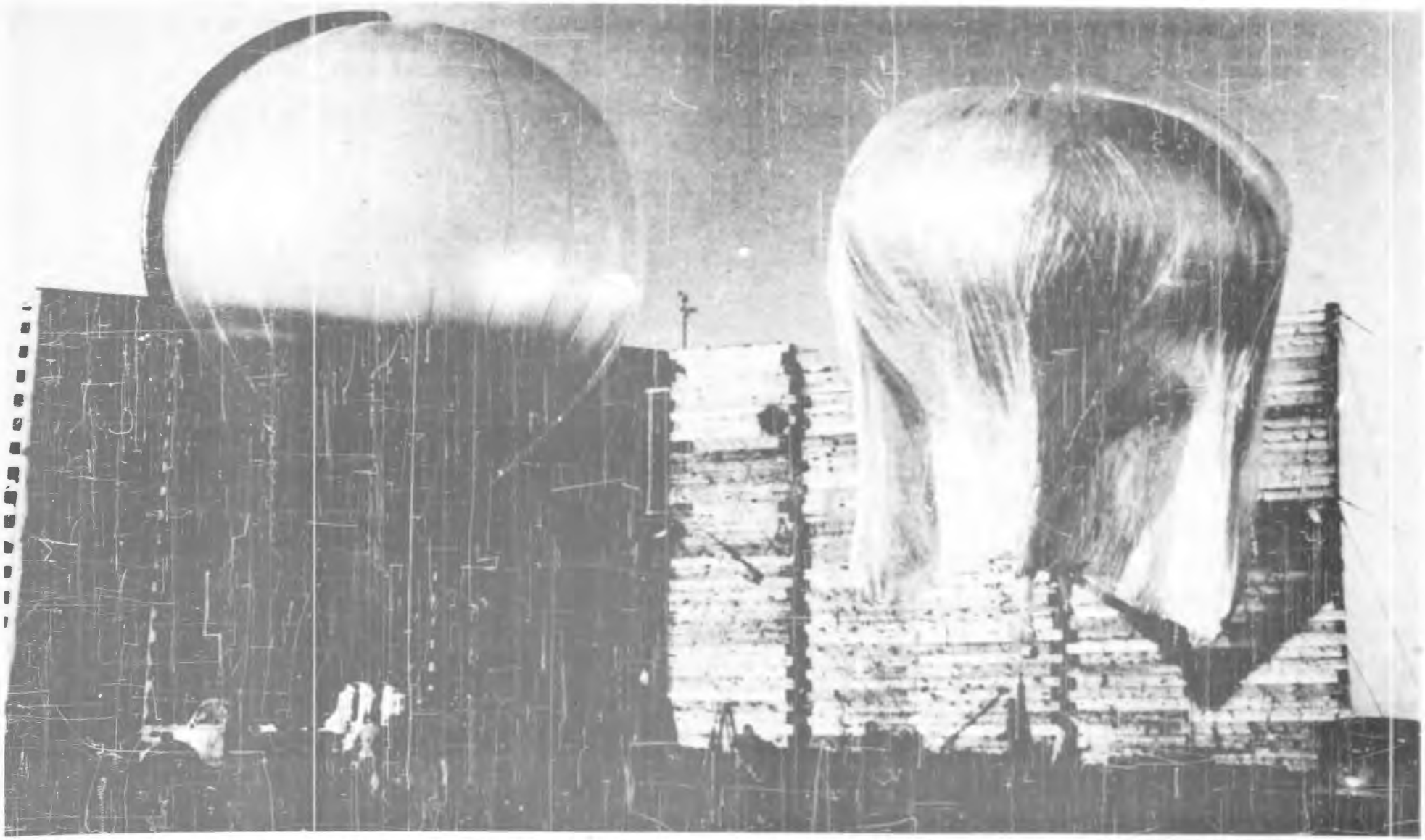

Figure VI-8. Step flight ready for launching. Tow balloon at right has free lift of about 150 lbs (weight of one man, note figure). Corset has been removed but diaphragm rip cord has not been pulled yet. Platform balloon at left is weighed off ready for release and is almost completely full. Note that duct is collapsed for only a few feet up from bottom showing that zero pressure level is very close to bottom of balloon. Upon release, platform balloon will begin to valve almost immediately and by the time flight reaches 10,000 ft will have valved off the free lift of the system.

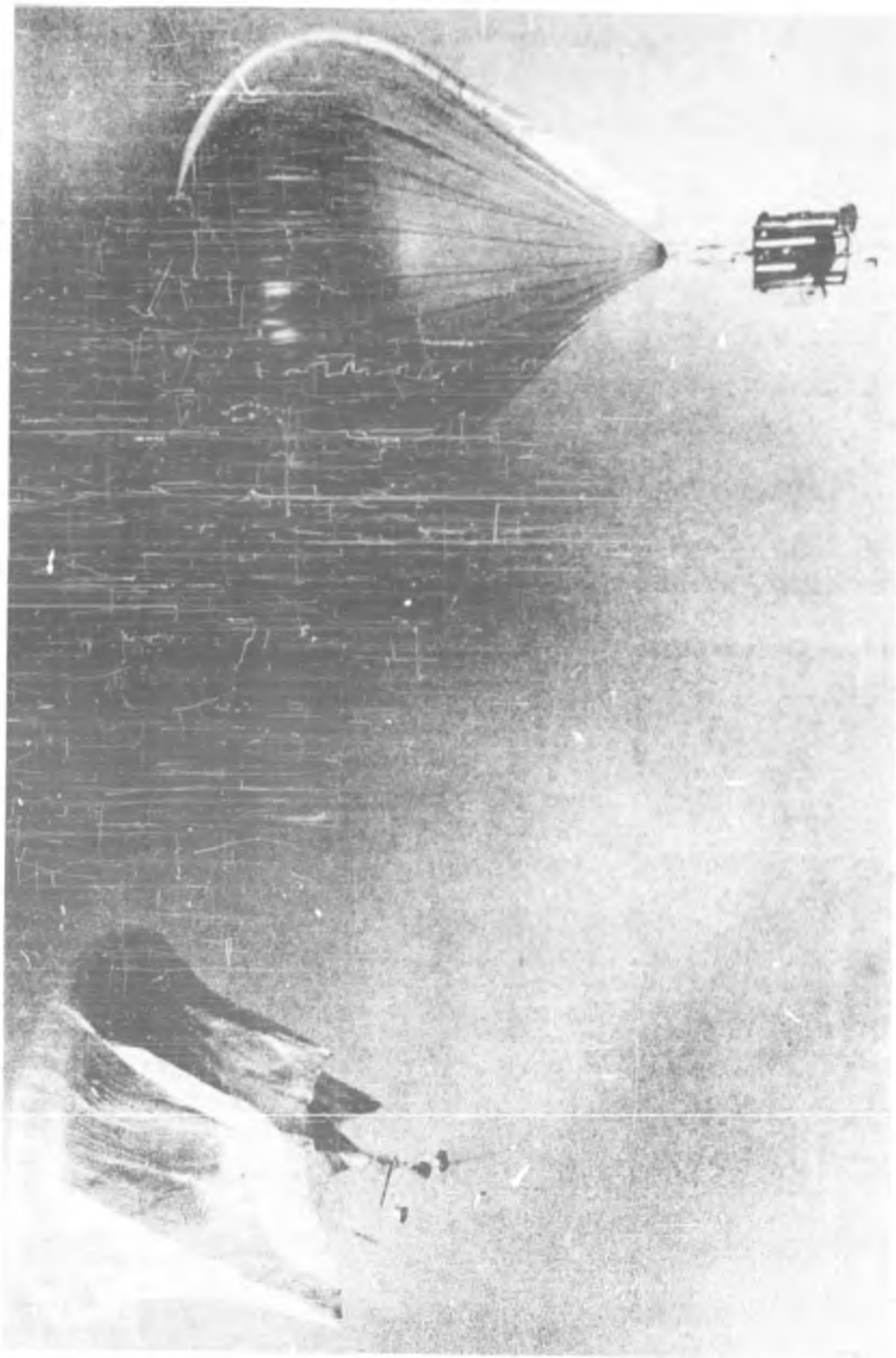

Figure VI-9. Step flight after launching. Tow balloon at left is transferring gas from bottom to top section. Note much flattened shape due to aerodynamic pressure with high rise rate. This tow balloon carries a down camera on small arm, a temperature transmitting unit in dark package, and ballast in bottom package. Shock cord extends down below this for a short distance.

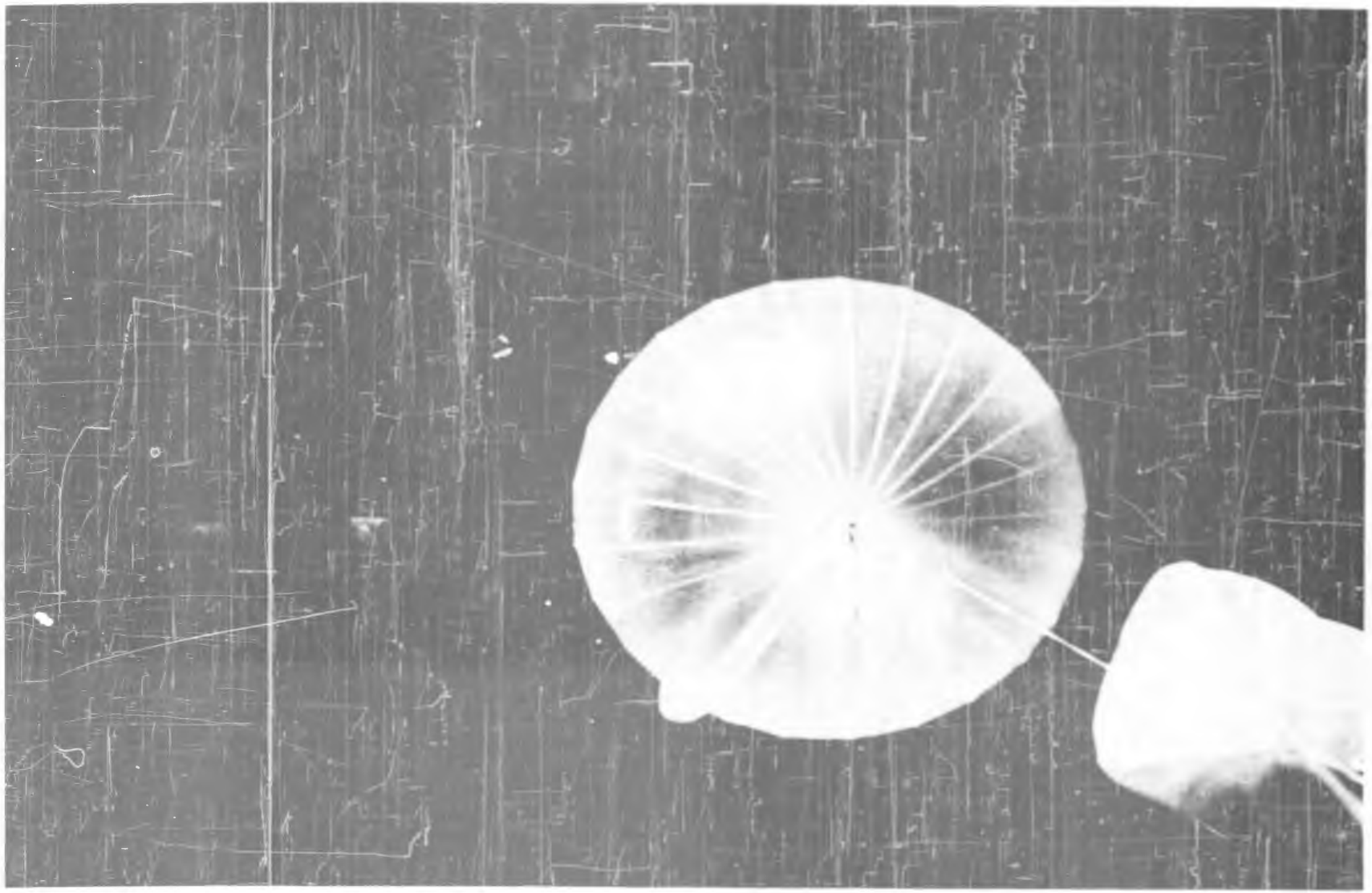

Figure VI-10. Top view of platform balloon in flight over St. Croix River near Hudson, Wisconsin, taken by down camera on tow balloon. White object in corner is drag parachute to deploy main parachute if assembly fails. Duct appendix coming out from a point near top of platform balloon can be seen. In this photograph one can see also that platform balloon shape has a scalloped appearance showing that center of each gore is apparently carrying more tension than tapes themselves. This is presumably due to inaccuracies imposed by making a spherical balloon of flat gore segments of finite width.

these flights in which a balloon was essentially tied to a platform and its tension measured as a function of the rate of rise and altitude. Consider first Flight 80, which is Figure VI-11. Examination of the rate of rise vs. altitude curve shows that approximately a constant rate of 510 ft/min was maintained on the first step, 470 ft/min on the second step, and 360 ft/min on the third. The acceleration characteristics of the double balloon system are shown by the way in which the rate of rise changes with altitude, as shown by the velocity vs. altitude curve at the left. The solid tension curve shows the way in which the tension between the balloons behaved as the rate of rise changed in the way indicated by the curve on the left. For example, the lowest value of tension obtained on the first step, after the initial leveling of the balloon at 600 millibars, was 58 lbs. It can be seen by the way the tension has been changing that equilibrium tension has still not been obtained. The fact that the tension sweeps down in an arc from 80 lbs to 58 lbs shows the very pronounced effect of thermodynamic drag. If the drag were all aerodynamic, as soon as the rate was established, at approximately 580 millibars, the tension would have reached its minimum and constant value. In contrast to this, it can be seen that, although the rate of rise is constant, the tension is still changing by the time the ballast flow ceases and the rate begins to decrease at an altitude of approximately 470 millibars. The tension climbs as the balloon slows down and finally reaches an equilibrium value of 93 lbs after the balloon has essentially come to rest and all of the warming has taken place. A similar description of the tension curve applies to the next step, in which the balloon was also in the troposphere with a somewhat lower rate and a somewhat lower

total drag. The top and third step is quite interesting in view of the fact that the rate of rise was less, only about 370 ft/min, but the total drag of the balloon at this rate, indicated by the difference in tension between approximately 113 lbs and 80 lbs, is very much larger than it was on the step below, in which the rate was even higher. The reason for this great increase in drag is very obviously due to the fact that the balloon has now entered the stratosphere and the thermodynamic drag has increased because of the constant lapse rate indicated by the temperature vs. altitude curve on the extreme right. One of the most outstanding and somewhat unexpected results of this step flight is indicated in the tension vs. altitude curve by the dotted line. It shows quite clearly that a balloon which is weighed off on the ground at 76 lbs, if it were to be weighed off at 600 millibars would pull with a force of 80 lbs, if it were to be weighed off at an altitude of 370 millibars it would pull with a force of 93 lbs, and if it were to be weighed off at an altitude of 115 millibars it would pull with a force of 116 lbs. This very pronounced "warming with altitude" is an evidence that during the daytime, as in Flight 80, the balloon acquires lift as it rises to the stratosphere. This increase in lift with altitude comes about because the gas acquires a higher relative temperature with respect to the outside air, and has been responsible for obscuring the change in drag which occurs at the base of the stratosphere in conventional time-altitude curves. It can be seen in Flight 80 that although the drag goes up in entering the stratosphere, as is clearly evident in the tension curve, so does the lift that the balloon would possess if brought to rest because of the warming with altitude. Warming with altitude should be an extremely important

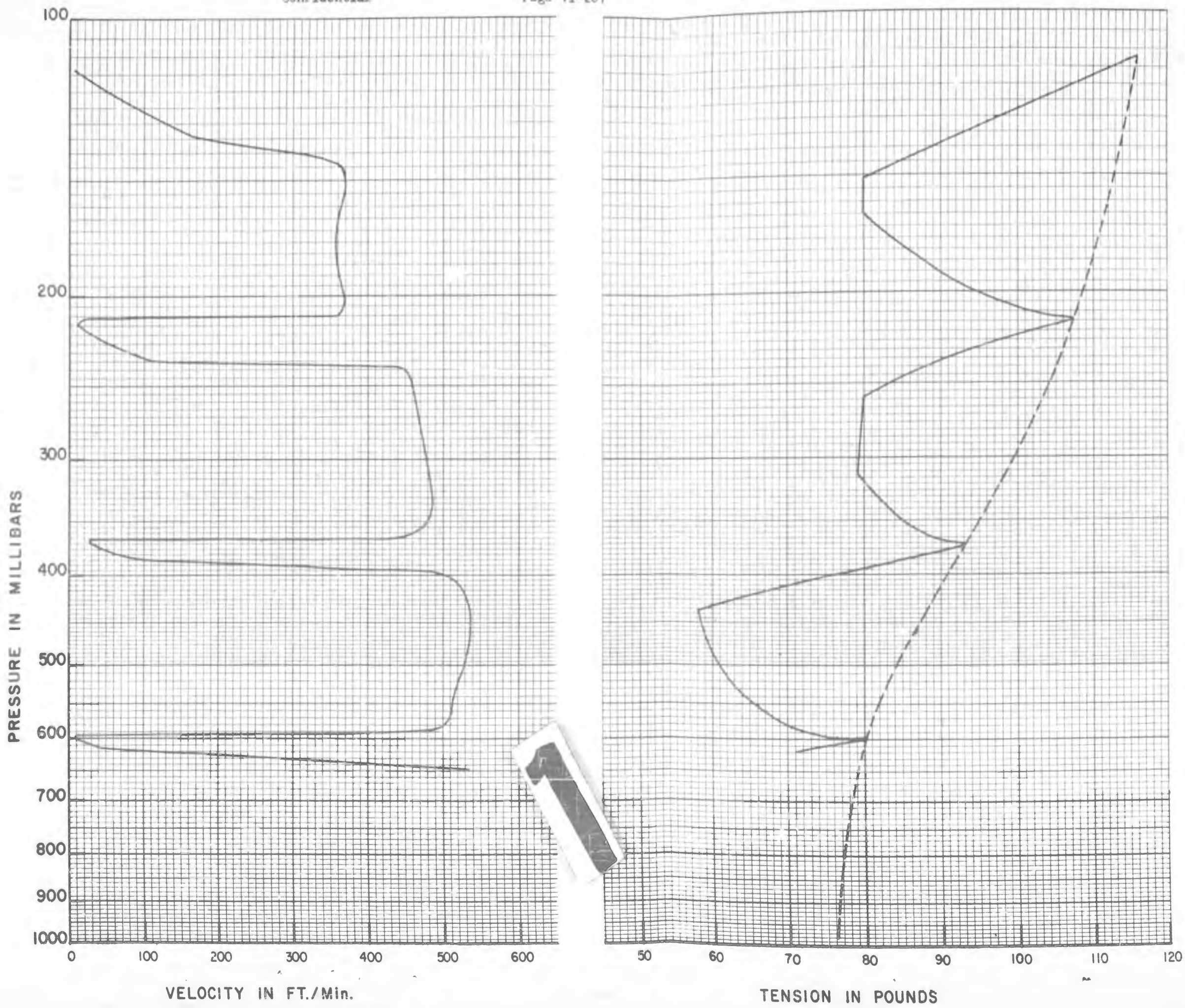

Figure VI-11. Confidential Information

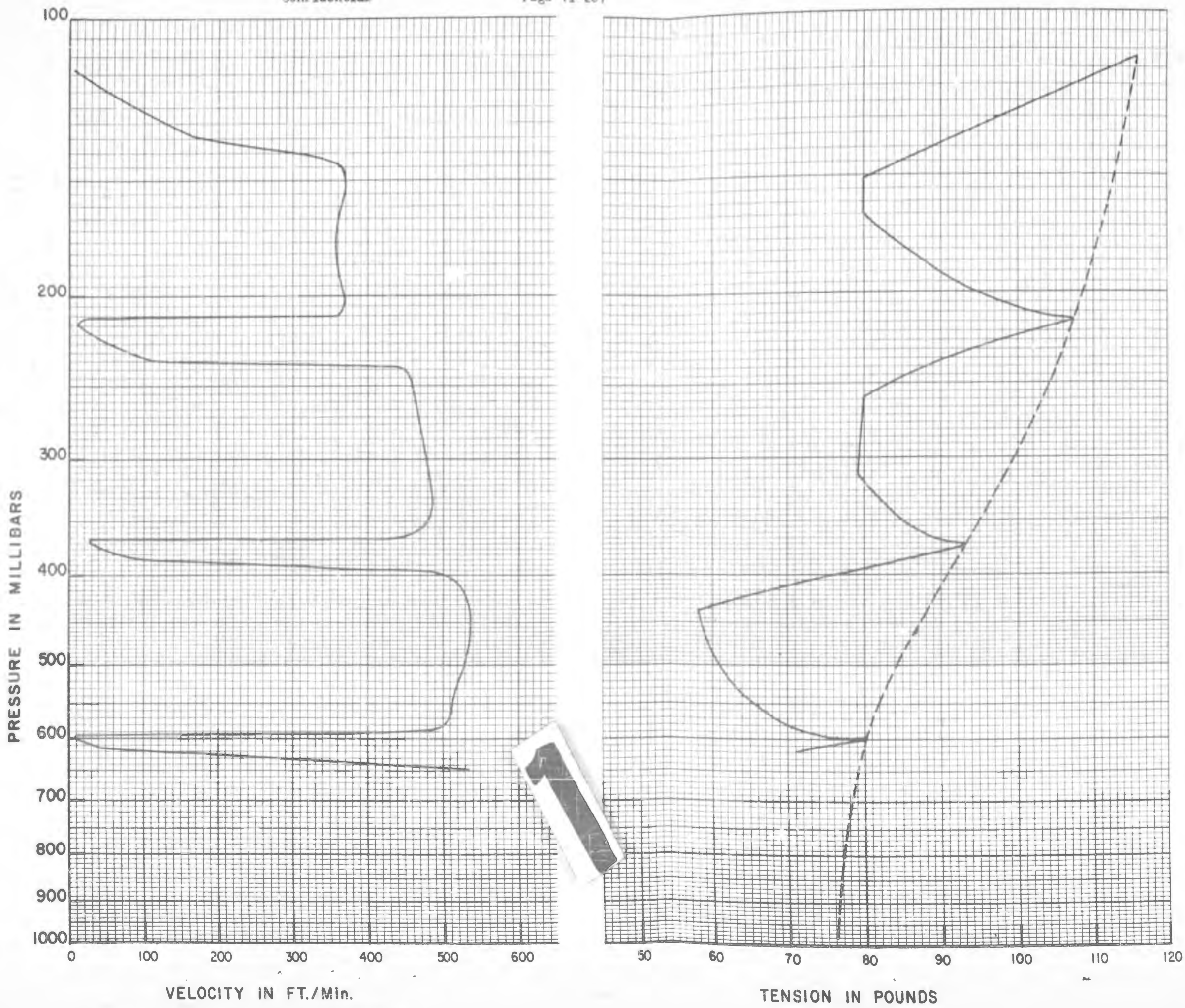

Figure VI-11. Confidential Information

FLIGHT 80

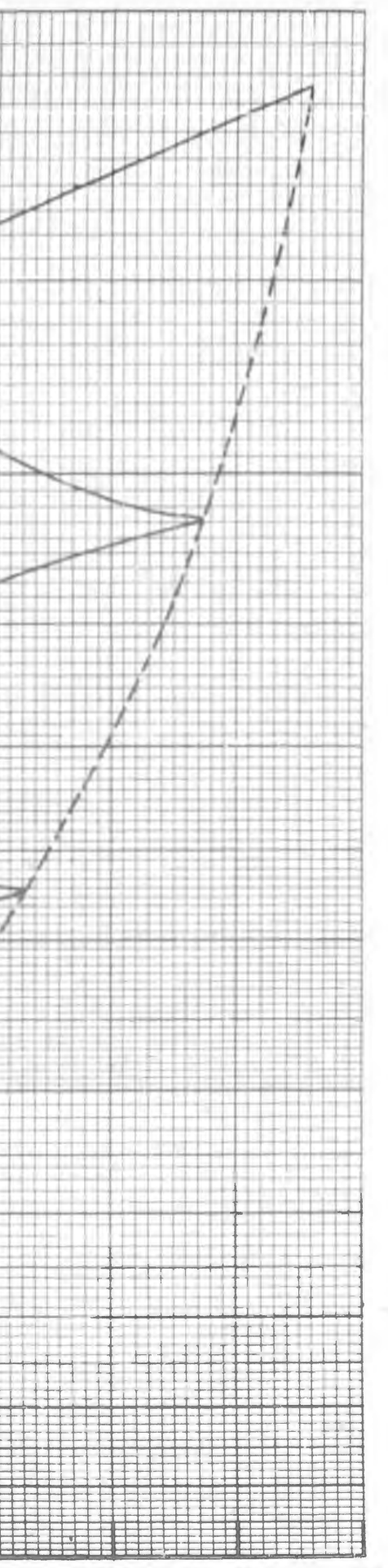

HOURS AFTER SUNRISE

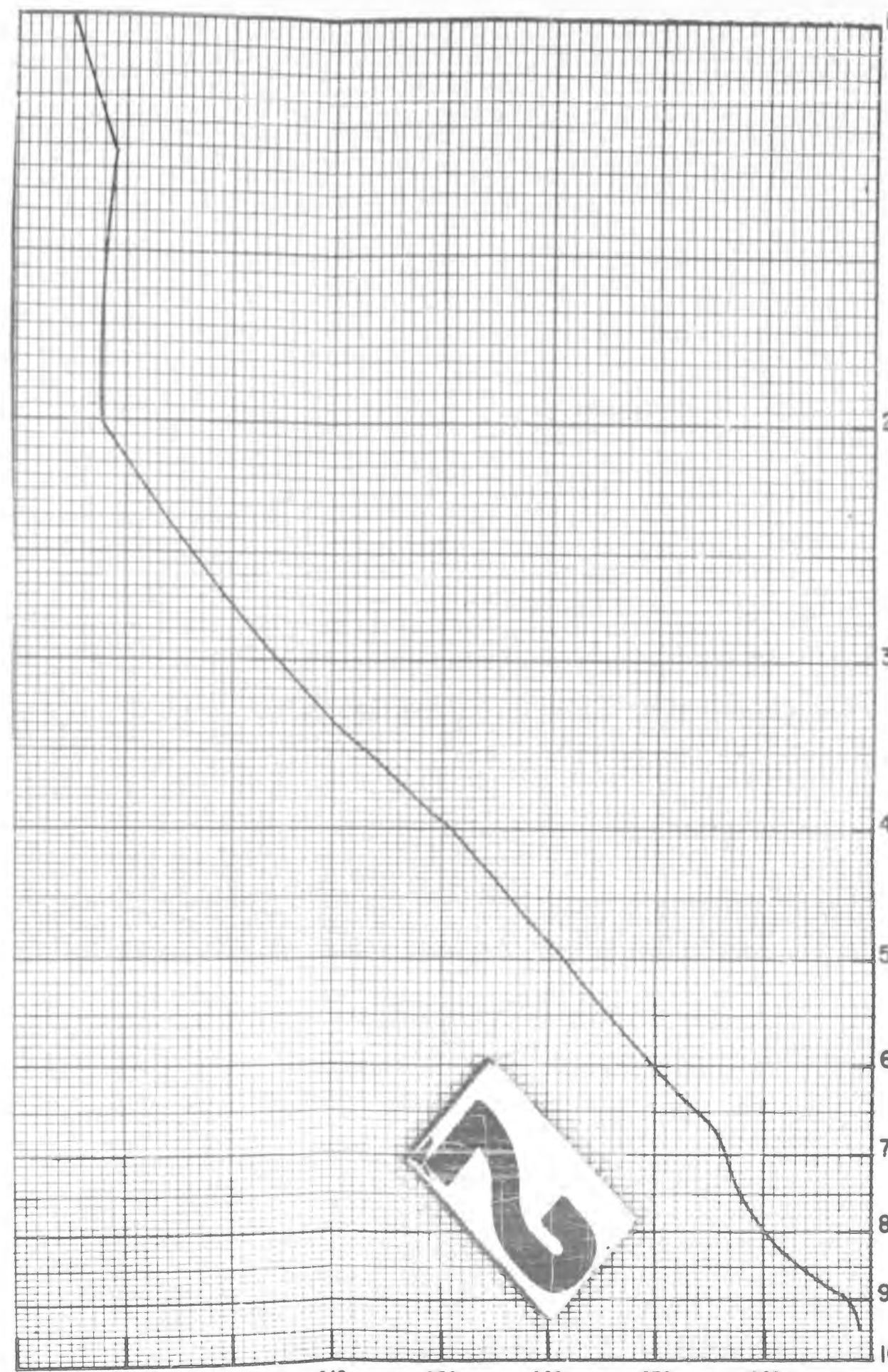

TEMPERATURE IN DEGREES KELVIN

factor in "balloon behavior" and the type of warming evidenced in the daytime, as shown in Flight 80, will produce a deleterious effect on balloon performance. The fact that the tension increases as the balloon rises to higher altitudes means that a balloon which loses some lift when floating level at a given altitude, as it descends will lose still more lift, since equilibrium tension at lower altitudes has a lower value. The kind of warming-with-altitude curve that would be desirable for stable balloon performance would be one that does just the reverse of that indicated by Flight 80, namely, one in which the tension decreases at higher altitudes along the dotted line corresponding to the one drawn in the Flight 80 data. Such a balloon system would be statically stable, since loss of lift at increasing altitudes would be gained back on returning to a lower altitude.

Flight 87 (Figures VI-12 and VI-13) was the next successful step flight and was performed at night. Here the rate of rise on the first step was about 470 ft/min, on the second about 420, and on the third about 600 ft/min. The tension vs. altitude curve on the night flight looks quite different from that in the daytime. At the beginning of the first step, it can be seen that the tension snaps down abruptly from 59 lbs to 46 lbs, and then is almost at equilibrium throughout the step. This is a definite indication that the drag here was almost all aerodynamic and there was essentially no thermodynamic drag on this step. The same thing is true on the second step, where the drag is somewhat less because of the lower rate, and is to a somewhat lesser extent true on the third step. On the third step the drag is somewhat larger but this is accounted for by the fact that the third step has a higher rate than the other two.

Confidential

FLIGHT 87

TENSION THROUGH SUNRISE

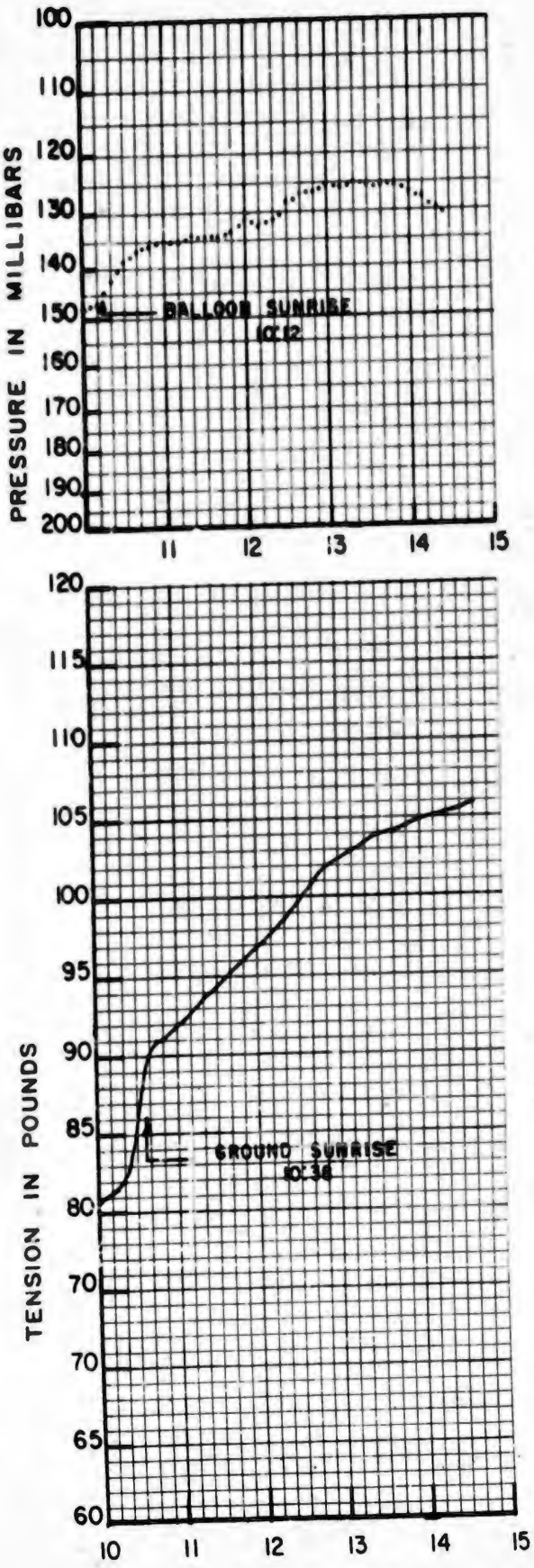

Figure VI-12.

Unfortunately,this flight never got into the stratosphere because of the fact that the tropopause was so high, approximately 150 millibars. The principal features of interest in this flight are the small thermodynamic drag for a rising balloon at night, and the fact that the warming-with-altitude curve looks quite different from that of Flight 80. Instead of increasing steadily with altitude, the curve first drops from 65 lbs to 59 lbs, going from the ground to the first step, and then increases from this step to 150 millibars, in which the tension has risen to 80 lbs. Because of this type of warming-with-altitude curve, it is evident that a balloon launched with a marginal free lift at night could very well rise to an altitude between 1000 mb and that indicated by the minimum of the tension curve,approximately 640 millibars, and float there in a stable situation. Although the step flights only reach altitudes somewhat below 100 millibars, independent data at night seems to indicate that the tension curve at equilibrium, corresponding to the dotted curve, would drop again from 80 lbs to something in the vicinity of 60 lbs by the time an altitude of approximately 20 millibars is reached. Such a tension curve represents a stable situation above an altitude of 100 millibars, in which a descending balloon can acquire lift by going to lower altitudes. The extrapolation of the time-tension curve at equilibrium to higher altitudes is based on flights in which balloons have been leveled at lower altitudes and ballast was dropped at night. Such a balloon system will start off with an appreciable rate of rise, but will have an ever-decreasing rate and may in fact level off well below its theoretical ceiling. It is believed that this cooling with altitude above 100 millibars represents a percentage change in lift of about 3-4%, and is demonstrated on our Flight 42.

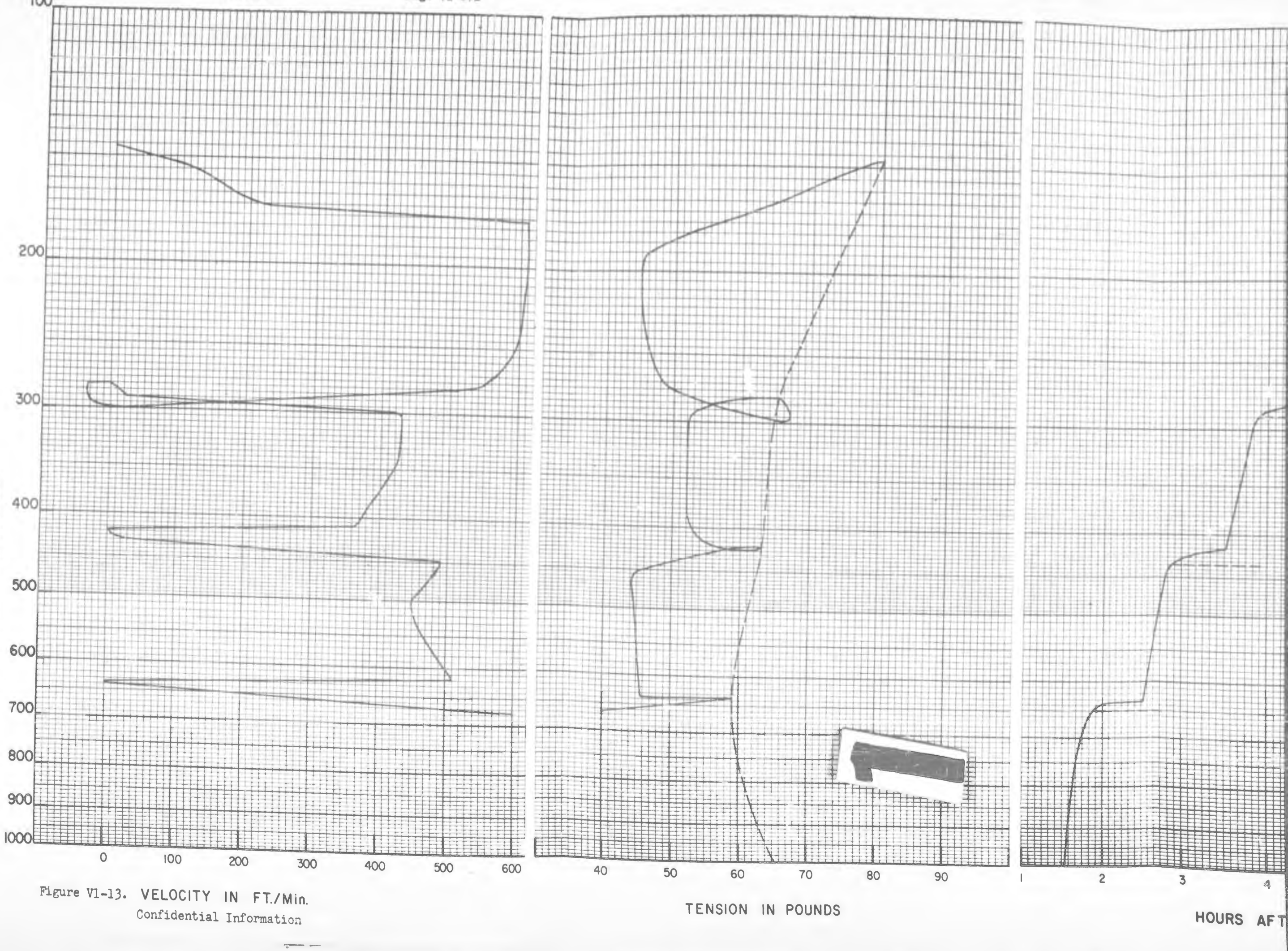

Figure VI-13. VELOCITY IN FT./Min.

Confidential Information

FLIGHT 87

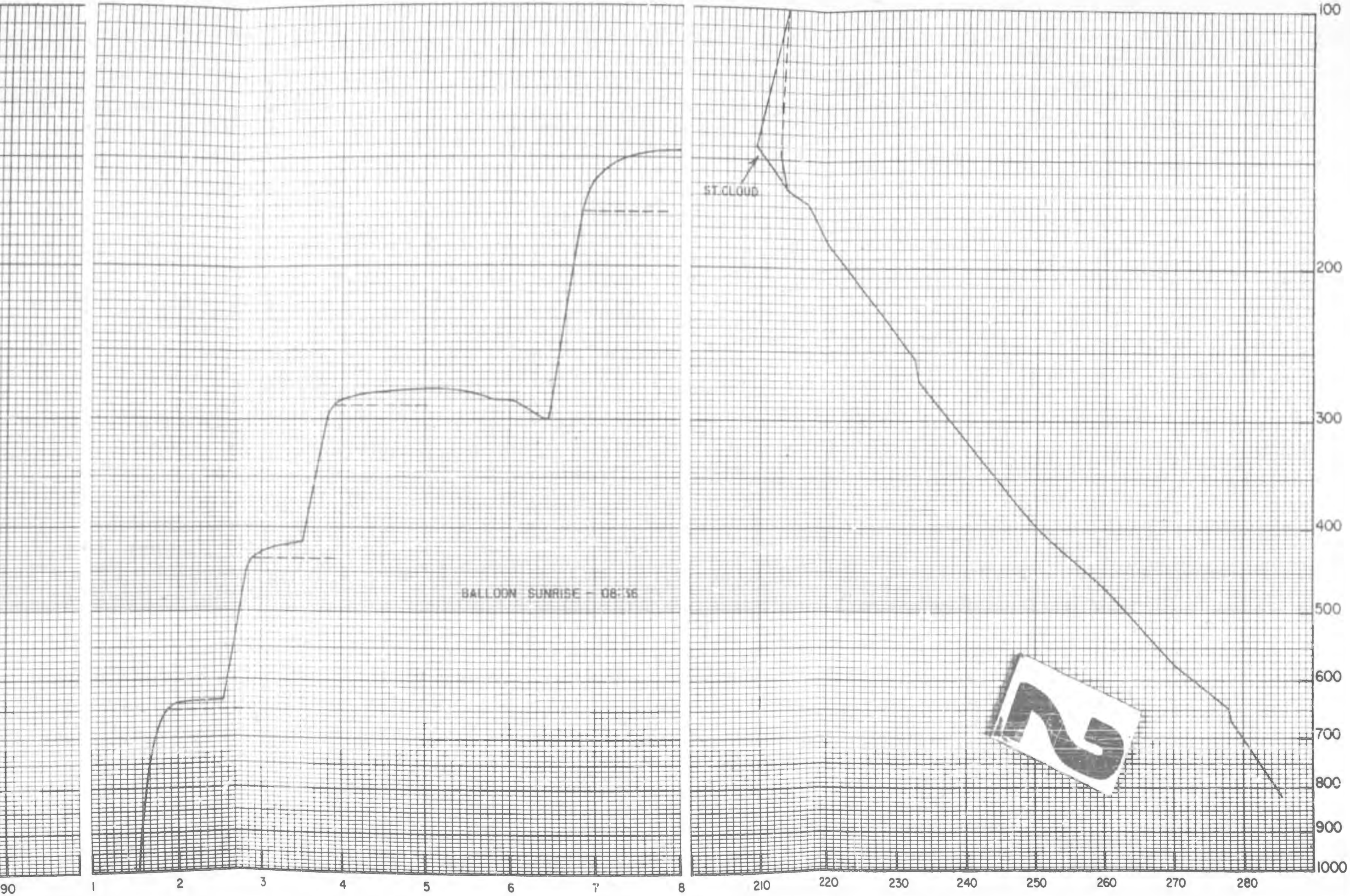
ST. CLOUD
BALLOON SUNRISE – 08:56
100
200
300
400
500
600
700
800
900
1000
90
1
2
3
4
5
6
7
8
210
220
230
240
250
260
270
280
HOURS AFTER SUNSET
TEMPERATURE IN DEGREES KELVIN

The next successful step flight was Flight 91 (Figure VI-14), which instead of being a three-step flight was a two-step flight at a higher rate of rise. The rate of rise on the first step was 700 ft/min and on the second was 670 ft/min, and the magnitudes of the tension change from balloon at rest to balloon in motion agree reasonably well with those obtained on Flight 80, another daytime flight. Unfortunately, the data were lost at the top of the last step and it is therefore impossible to obtain the complete warming-with-altitude curve. It appears, in this flight, that instead of a steady warming with altitude as indicated in Flight 80, there is a very slight cooling with altitude going from the ground to an altitude of 650 millibars. This would again represent a situation in which a balloon with very marginal free lift could be trapped at low altitude. It should be pointed out here that in this flight the change in tension with altitude and time indicates very clearly that a large part of the drag is thermodynamic and that it comes about from the change in temperature of the gas as the balloon rises. It is interesting to note that in the top step of this flight the aerodynamic drag can be quite nicely separated from the thermodynamic drag at the rate of 670 ft/min. Considering the last point where dotted line ends, the tension drops very abruptly from 172 lbs to 154 lbs as the rate of rise is acquired. This change in tension of 18 lbs represents the aerodynamic drag at this altitude and at this rate. It can be seen that the thermodynamic drag is appreciably larger, since it is represented by the difference between 154 lbs and 120 lbs, or 34 lbs thermodynamic drag. The presence of this large amount of thermodynamic drag in the stratosphere (as indicated by the temperature-altitude curve on the right) is also indicated in the curve by the extremely

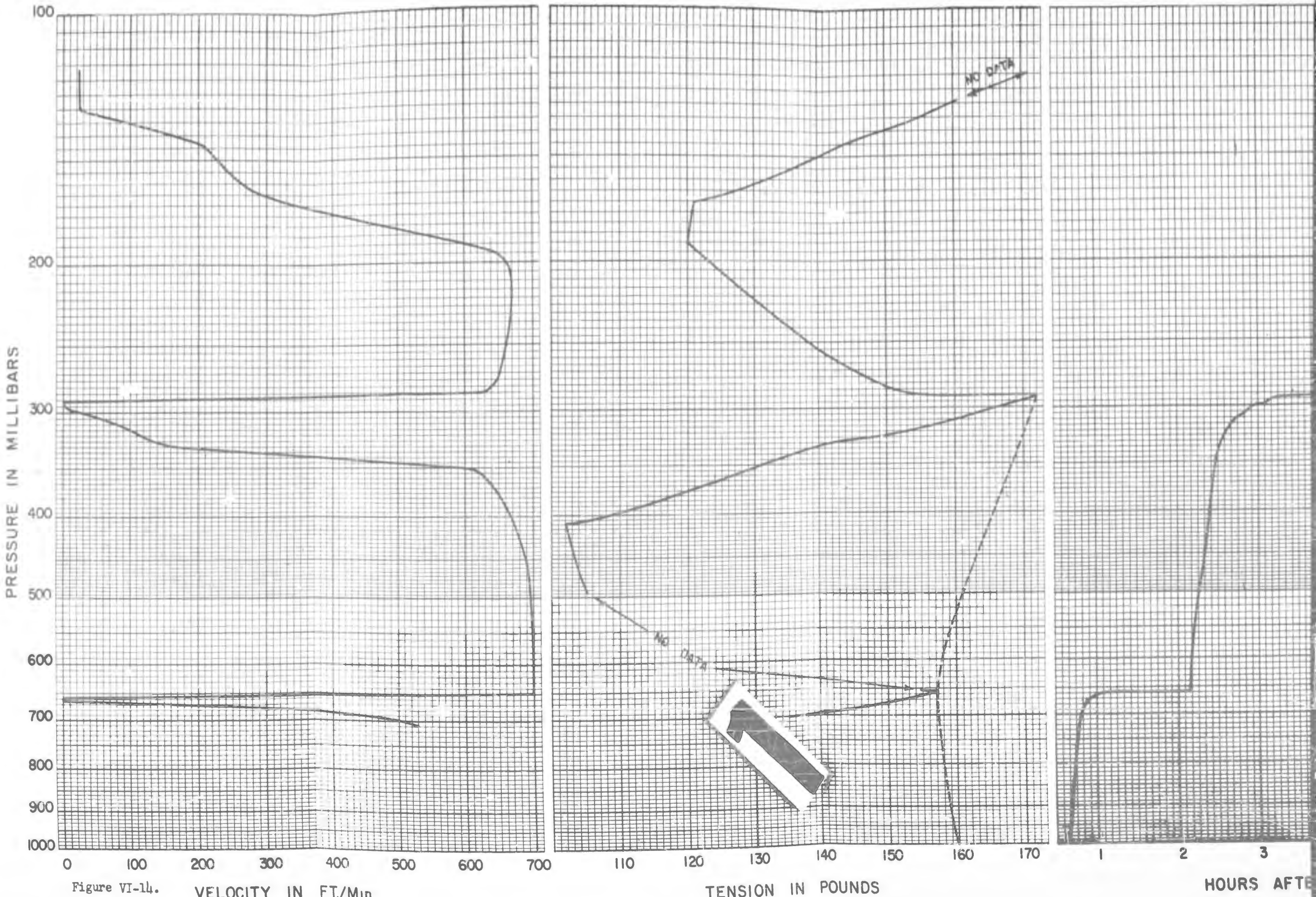

Figure VI-14.

Confidential Information

FLIGHT 91

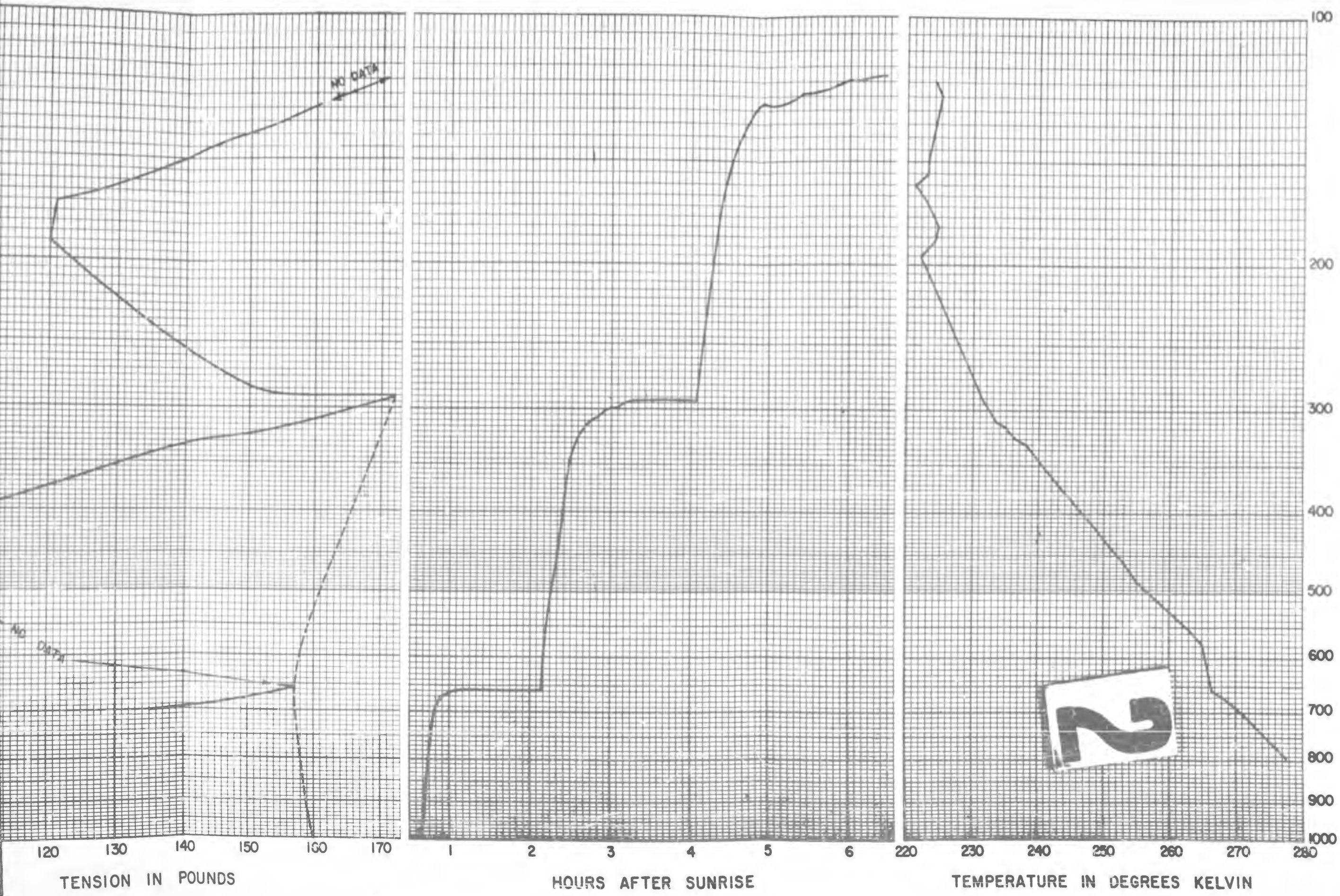
NO DATA
NO DATA
120
130
140
150
160
170
TENSION IN POUNDS
1
2
3
4
5
6
HOURS AFTER SUNRISE
220
230
240
250
260
270
280
TEMPERATURE IN DEGREES KELVIN
100
200
300
400
500
600
700
800
900
1000

slow change of tension between altitudes of 170 and 135 millibars, as the balloon warms up. The thermodynamic drag for a rising balloon can be acquired relatively rapidly, since the rising balloon can cool its gas by expansion until it reaches the proper equilibrium temperature, and this is represented by the top step between altitudes of 290 and 190 millibars. A balloon which is coming to rest, however, must get rid of the thermodynamic drag by warming its gas at a rate which depends only on the time constant for convection, which time is approximately 15 minutes.

The last step flight of the several step type of this series is Flight 94 (Figure VI-15). This is again a nighttime step flight, and in this flight the ballasting system did not behave as well as might be expected, which is responsible for the erratic behavior of the velocity vs. altitude. It does,however, show the same principal characteristics that were shown on Flight 87, namely, that the thermodynamic drag at night in this altitude range is much less pronounced than it is in the daytime. As soon as the balloon starts moving the tension drops very rapidly, showing equilibrium values which one would expect if the thermal effects on the balloon were not as important as the aerodynamic effects. It also shows the type of warming-with-altitude curve found in Flight 87 at night, in which the tension first drops as the altitude increases and then rises again. This again indicates a situation in which a balloon could be trapped by losing as much as 10 lbs free lift in rising from the ground to an altitude of about 600 millibars.

The data so far seem to indicate that if the balloon loses lift in the first portion of its ascent its lift will reach a minimum value in the region near 600 millibars pressure. In Flight 94 again we were unable to reach the stratosphere because of the very high altitude of the tropopause.

FLIGHT 94

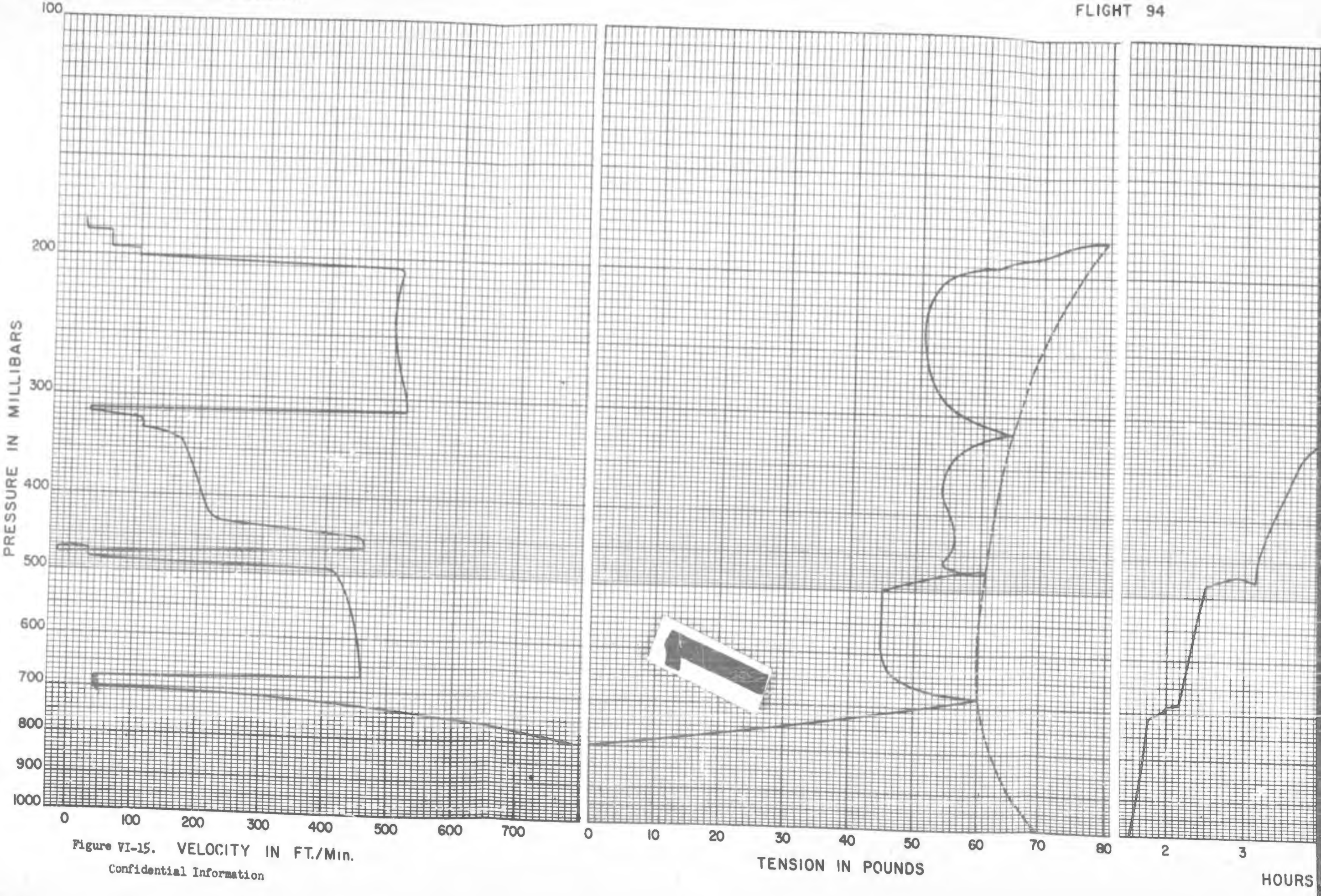

Figure VI-15.

FLIGHT 94

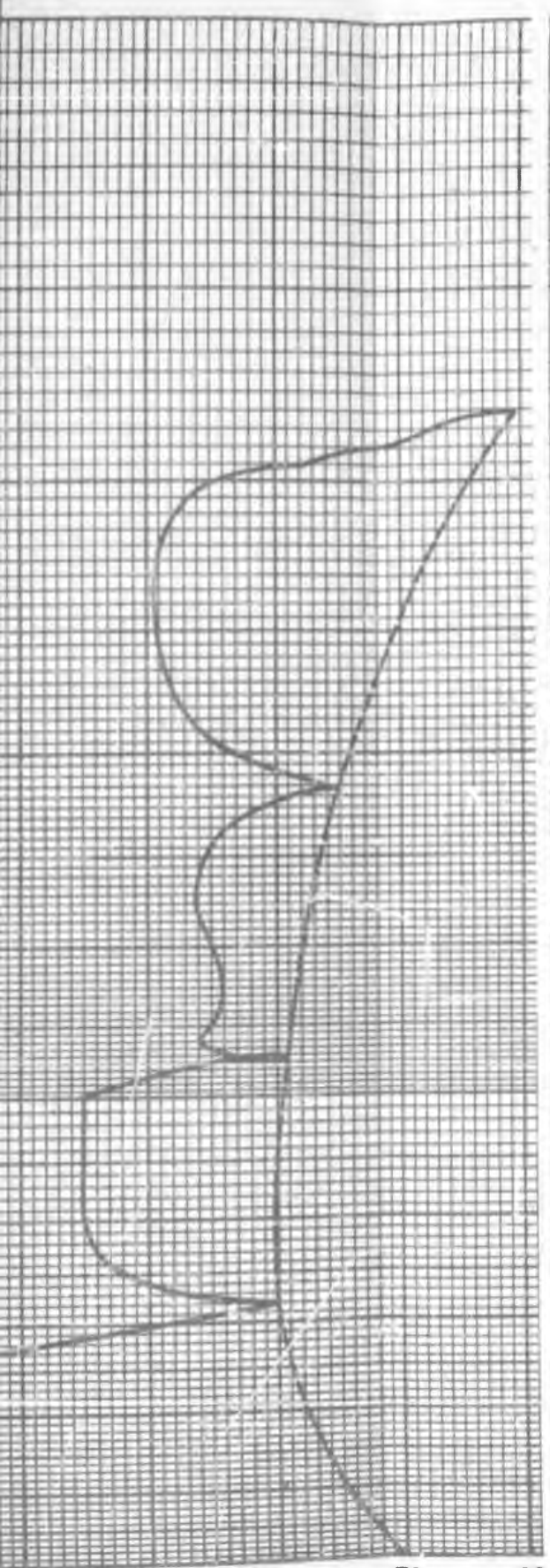
40
50
60
70
80
IN POUNDS

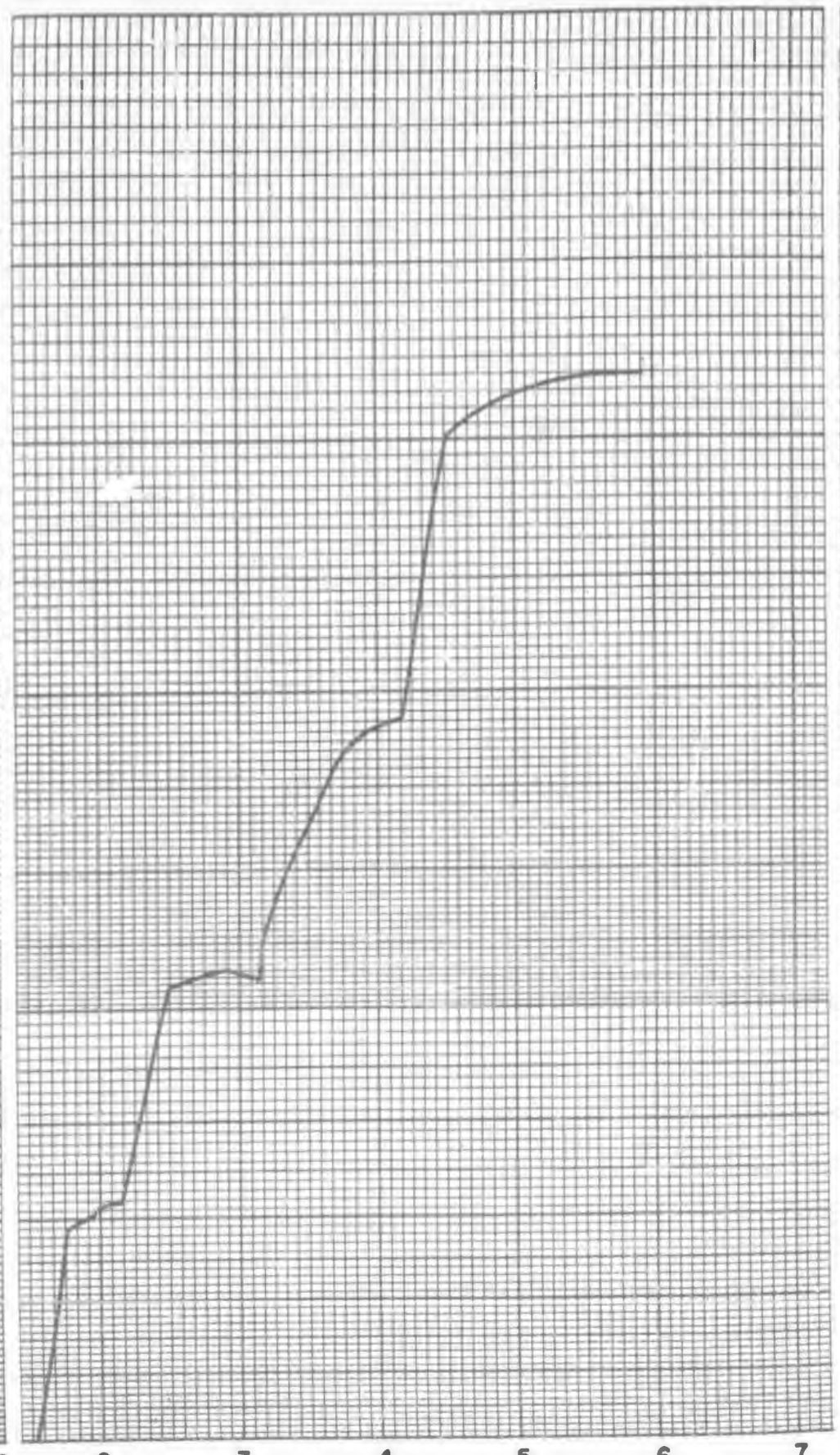
2
3
4
5
6
7
HOURS AFTER SUNSET

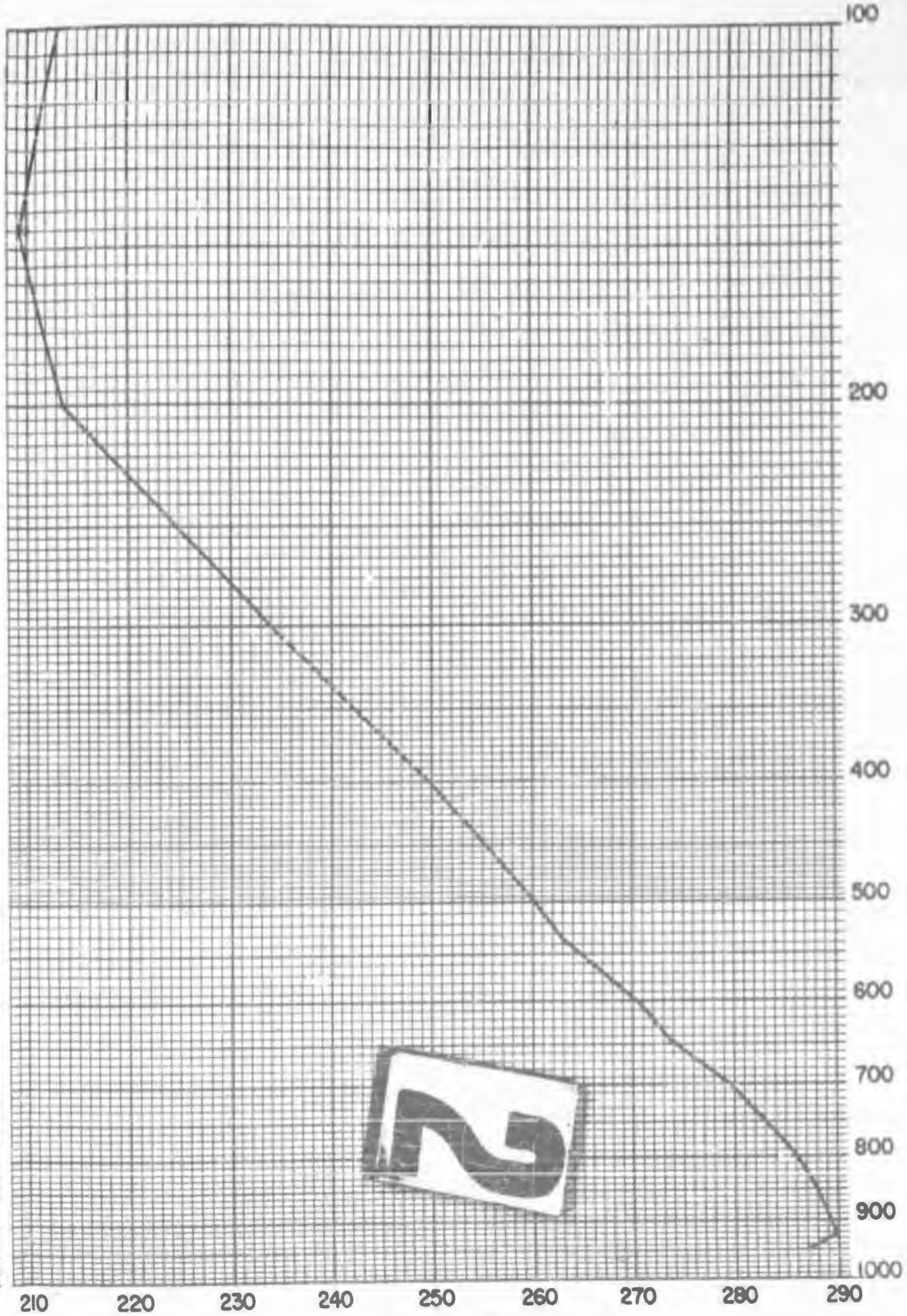
100
200
300
400
500
600
700
800
900
1000
210
220
230
240
250
260
270
280
290
TEMPERATURE IN DEGREES KELVIN

The curve of Flight 92 (Figure VI-16) shows the tension measured in a two-balloon step flight type of setup, when the balloons were allowed to float through a 24-hour period. The altitude was maintained by using a follow-up ballasting system of the type invented by Howell at Tufts for MOBY DICK work. Because of the temperature sensitivity of this particular follow-up system, the altitude curve is not perfectly smooth and does not steadily rise as one would expect if the system were working properly. The principal conclusions, however, are not altered by this fact, since all that is required in a step flight is that one precisely know the time-altitude curve as well as the time-tension curve. At time 1130 GMT the balloon system had reached its ceiling, as indicated by the time-altitude curve, and sunrise occurred at 11:26. It can be seen that the tension rose at sunrise and had risen from 192 to 228 lbs after five hours had elapsed. With some oscillations up and down, the tension remained constant until 2330, at which time sunset caused the tension to decrease to a final nighttime value of 186 lbs. Comparison of the time-altitude curve and the time-tension curve on this flight shows the fact that the thermodynamic drag can develop at very low rates. For example, consider the section 1650-1700 GMT. At 1650 the balloon begins to rise with a very slow rate of rise, but the tension drops down immediately by 8 lbs as soon as this rate of rise is established. Following through the time-tension and time-altitude curves, one can see immediate reflection of small rates of rise in the changes of tension in the time-tension curve. The aerodynamic drag at these very low rates is essentially negligible, and the changes of tension reflected here are produced by changes of temperature of the inside gas. The balloon system in this flight was quite tight; the total solar effect, average of sunrise

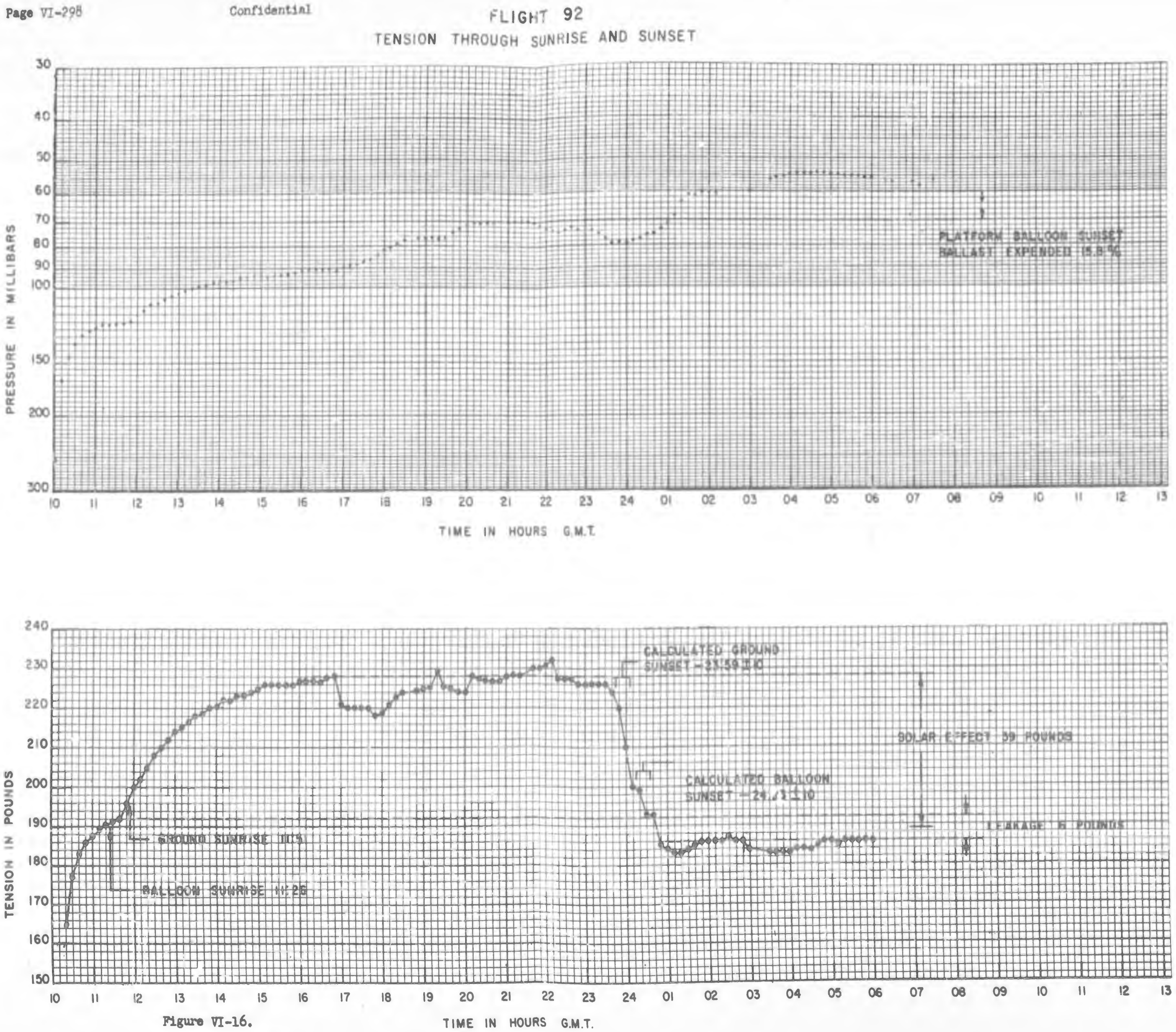

Figure VI-16.

Confidential Information

and sunset effects, directly measured by the change in tension, was 39 lbs, and the leakage was estimated to be six pounds through the period of almost 24 hours. The sunset effect amounts to 5.3% of the daytime air displaced on this flight, which used as a tow balloon a double-wall taped Winzen balloon. A ballasting system which drops ballast to keep the system level may very well over-ballast, as shown by the platform balloon's sunset ballast indicated on the top half of the curves on Flight 92. Although the sunset effect was only approximately 6%, the platform balloon expended 15.8% at sunset. This over-ballasting is probably characteristic of any ballasting system which can drive the balloon to ceiling and allow it to valve gas. For comparison with the sunset effect measured on Flight 92, Table V summarizes the sunset effects measured in situations where the balloon did not valve gas, and for which the sunset effect could therefore be calculated.

C. Equations of Motion and Nomographs

Flight 80 was the first successful step flight which gave values for the drags at various altitudes at the rate of about 400 ft/min. As soon as this flight was made, the data were analyzed in terms of the equations of motion of the balloon proposed earlier in the project (see Volume V, Section VI). The aerodynamic drag coefficients and the thermodynamic drag coefficients were determined from Flight 80 on various steps; and, assuming the functional form of the equations previously quoted, thermodynamic and aerodynamic drag nomographs were constructed. (Figures VI-17 and VI-18). It should be pointed out that the aerodynamic drag coefficient based on the cross-sectional area of the equivalent sphere--that is, the drag coefficient calculated assuming that the balloon has a cross-sectional area equal

TABLE V. SUNSET EFFECT MEASUREMENTS ON 2-MIL 73-FT DIAMETER CELLS

Flight No.	Date	Pre-(Sunrise (Sunset Altitude	Post-(Sunrise (Sunset Altitude	Sunset Effect (% of Daytime Air Displaced)	Daytime Air Displaced	Sunrise or Sunset	How Measured
63	2/23/53	28 mb	75 mb	6.0	516	Sunset	Ballast. Bounce with residual downward rate.
67	4/4/53	29 mb	70 mb	6.2	546	Sunset	Ballast. Bounce with residual downward rate.
81	7/7/53	30 mb	54 mb	4.2	492	Sunset	Ballast. Bounce with residual upward rate.
42	10/10/52	22 mb	150 mb	6.8	489	Sunset	Ballast. Bounce with residual upward rate.
87	8/4/53	150 mb	150 mb	4.7	513	Sunrise	Tension through sunrise.
90	8/12/53	100 mb	100 mb	5.1	495	Sunrise	Tension through sunrise.
92	9/16/53	100 mb	100 mb	5.4	671	Sunrise	Tension through sunrise.
92	9/16/53	70 mb	70 mb	5.1	671	Sunset	Tension through sunset.

AERODYNAMIC DRAG NOMOGRAPH

D = PRESSURE IN MILLIBARS (ASSUMES STANDARD ATMOSPHERE)
P = PERCENT AERODYNAMIC DRAG OF AIR DISPLACED
v = RATE OF RISE IN FEET/MINUTE
G = AIR DISPLACED IN POUNDS

DRAG COEFFICIENT FROM FLIGHT 80

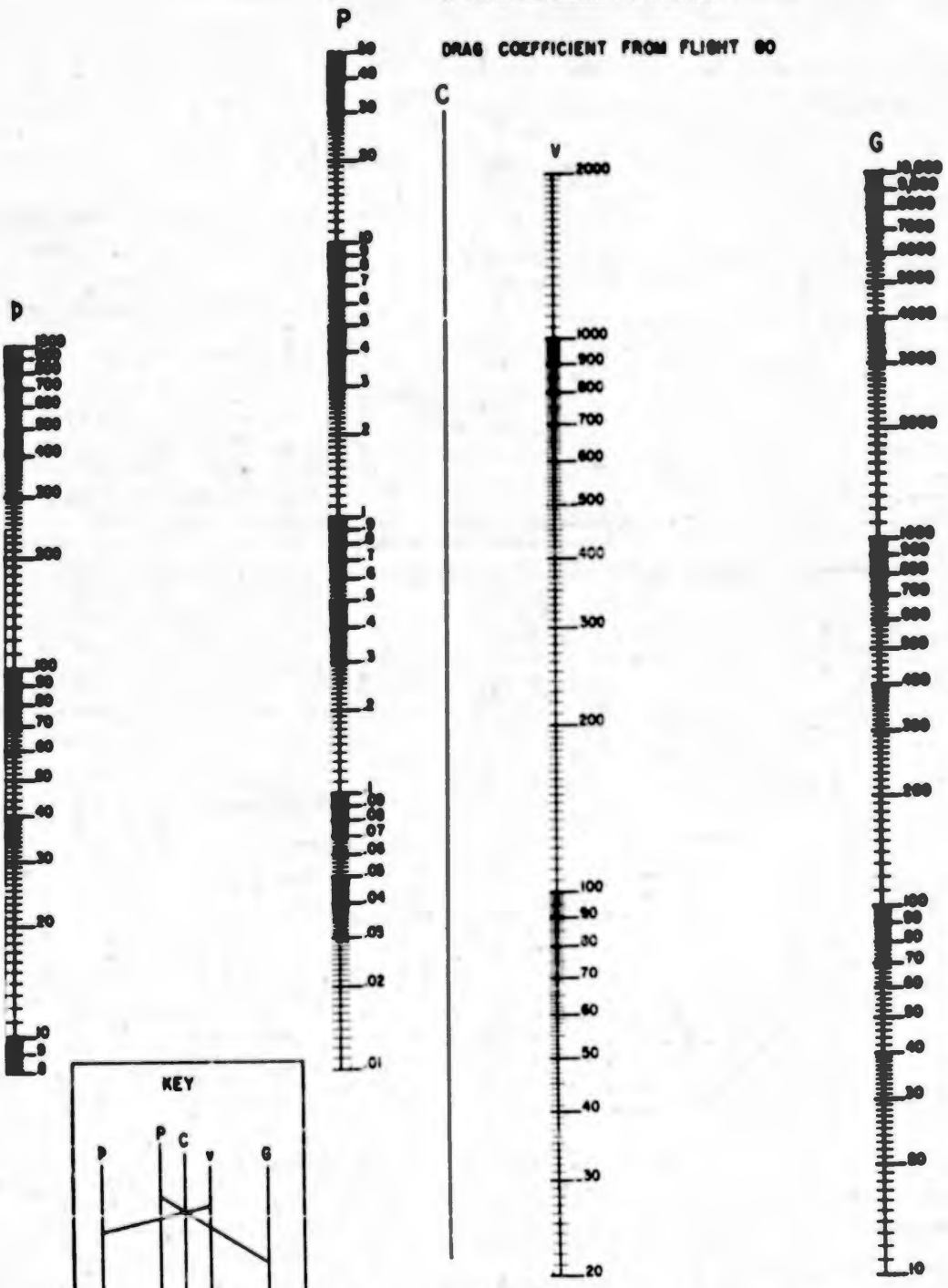

Figure VI-17.

DEPT. OF PHYSICS U. OF MINN. BALLOON PROJECT			SECT. S & T	
DWG. NO.	SHOP DWG. NO.	DRAWN BY	CHECKED BY	DATE
25-RP-252		[illegible]		8-25-53
AERODYNAMIC DRAG NOMOGRAPH			MOD. 1	
			MOD. 2	
			MOD. 3	

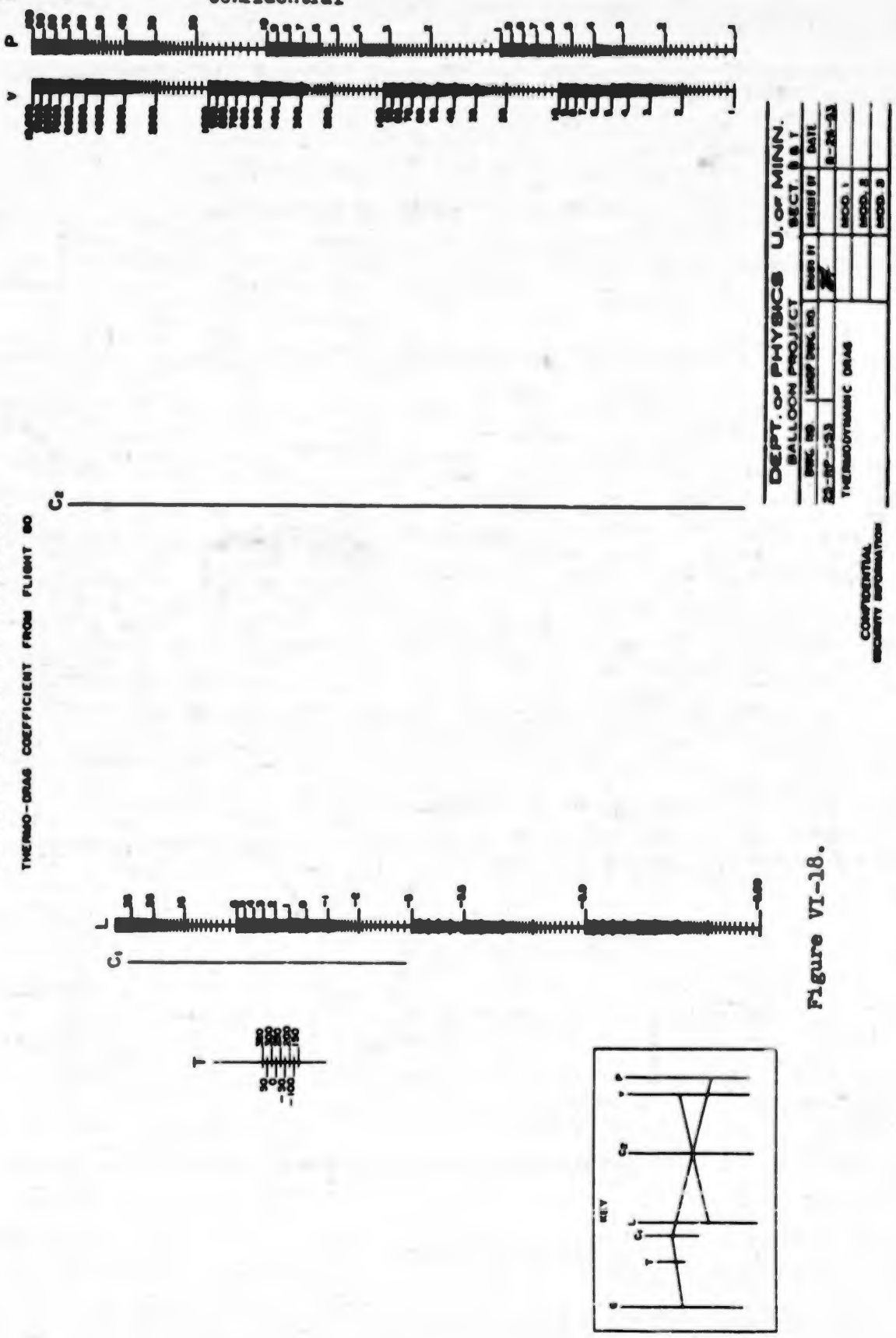
THERMODYNAMIC DRAG NOMOGRAPH
G = AIR DISPLACED IN POUNDS
T = AIR TEMPERATURE
L = dT/dh = ATMOSPHERIC TEMPERATURE GRADIENT
v = RATE OF RISE IN FEET/MINUTE
P = PERCENT THERMO-DRAG OF AIR DISPLACED
THERMO-DRAG COEFFICIENT FROM FLIGHT 80
P
v
Cd
L
CL
T
G
KEY
DEPT. OF PHYSICS U. OF MINN.
BALLOON PROJECT
THERMODYNAMIC DRAG
CONFIDENTIAL
SECURITY INFORMATION

Figure VI-18.

to that of a sphere the volume of which is equal to the volume of the balloon at the altitude in question--gives a value for C_d, the drag coefficient, of approximately .27. This value is not unreasonable and is the average of the values obtained on three steps.

Since the original construction of these two nomographs, they have been used and applied to various results of other step flights. It has been found that the nomographs agree reasonably well with any situation in which the balloon is rising during the daytime or descending at night, but that they give too high a thermodynamic drag for balloons which are ascending at night, and no data is available for balloons descending during the day. It appears that the conduction problem is quite different for a balloon which is ascending in the night versus one which is ascending during the daytime, and future work of the project, we hope, will clarify this situation.

These nomographs, however, are extremely useful in estimating what percent free lift will be required to produce a given rate of rise for a balloon system at a given altitude and in an atmosphere with a particular lapse rate. The use of the nomographs consists in the following procedure: If one is given a velocity, a gross load, and a pressure, it is possible with the aerodynamic drag nomograph to solve for the percent aerodynamic drag of air displaced. Using the thermodynamic drag nomograph, with the gross load, the lapse rate, and the velocity, it is possible to solve for the percent thermodynamic drag of air displaced. The sum of these two percentages, thermodynamic and aerodynamic, gives the total percent required to produce the specified rate. If one is given the rate of rise of the balloon, it is, of course, possible to work backwards and infer from this rate of rise what the percent aerodynamic and thermodynamic drags must have been. The thermodynamic drag nomograph is useful in other ways, for example,

if one wished to know how much warming a balloon would undergo after reaching ceiling at a given rate, one knows that this warming is related to the so-called thermodynamic drag which the balloon has before reaching ceiling. From the nomograph at a given rate one can calculate what the percent thermodynamic drag is; one knows then that this percent thermodynamic drag will also be the percentage change in temperature of the gas in the balloon after reaching ceiling. This is also the percentage loss in lift which the balloon can suffer in case it over-valves upon reaching ceiling.

In using the nomographs, it should be emphasized that they appear to hold within an accuracy of perhaps 10% if applied to cases in which balloons rise during the day or descend at night. A general mathematical treatment which covers all situations of rising and descending balloons will have to take into account the difference which occurs for a balloon rising at night as opposed to a balloon rising during the daytime etc. A preliminary indication of the general features which this mathematical description will need to have is included in the section of Radiation Heating of Balloons. (Section IV, this Volume)

D. Correlations with Other Flights

Calculations concerning Flight 56:

Flight 56 was the only radio-controlled flight constants experiment that gave significant data and this experiment was not completely successful. Figure VI-19 shows the details of the interesting portion of the time-altitude curve plotted on a very large scale by plotting the phase angle of the Olland Cycle directly and attaching a scale of feet to this plot. The descent during daylight at the start of the graph is due to the cutting of the tow

at 48,000 feet. The balloon descended at a rate of 530 ft/min until 34 pounds of ballast are dropped by the first command operation. The balloon then bounces upwards 730 ft, slowly rounds off and descends at 88 ft/min for about six minutes until a second ballast of 32 pounds was dropped. The balloon then bounces upward 2980 ft and establishes a new upward rate of 160 ft/min. If we consider the temperature sounding for the day and the bounce following the second ballast drop, we find that the adiabatic temperature change was 10.6° so that this represents 4.8% of the ambient temperature of 220° at that point in the atmosphere. The fractional ballast drop of the gross load is 5.6%. The disagreement between these two of .8% is to be associated with non-adiabatic processes occurring in the bounce such as aerodynamic drag and heat conduction into the balloon, and the agreement is about as good as one obtains in examples of this kind.

We now proceed to analyze the rates and ballast drops in terms of the flight constants nomographs (see Figures VI-17 and VI-18). On the initial descent we have 695 lbs of displaced air and the nomograph gives for the rate of 530 ft/min 8% thermodynamic drag and 1.3% aerodynamic drag which totals 64.6 or 65 lbs total drag. This is in fair agreement with the weigh-off values of -60 lbs for the main balloon provided there is no warming with altitude. However, if the warming with altitude is similar to that measured in summer step flights this warming would be 6.5% at this altitude, so that the main balloon instead of being 60 lbs heavy would be only 15 lbs heavy, so that the rate of 530 ft/min is in complete disagreement with this negative free lift. The downward velocity following the dropping of 34 pounds of ballast and the initial bounce is 88 ft/min.

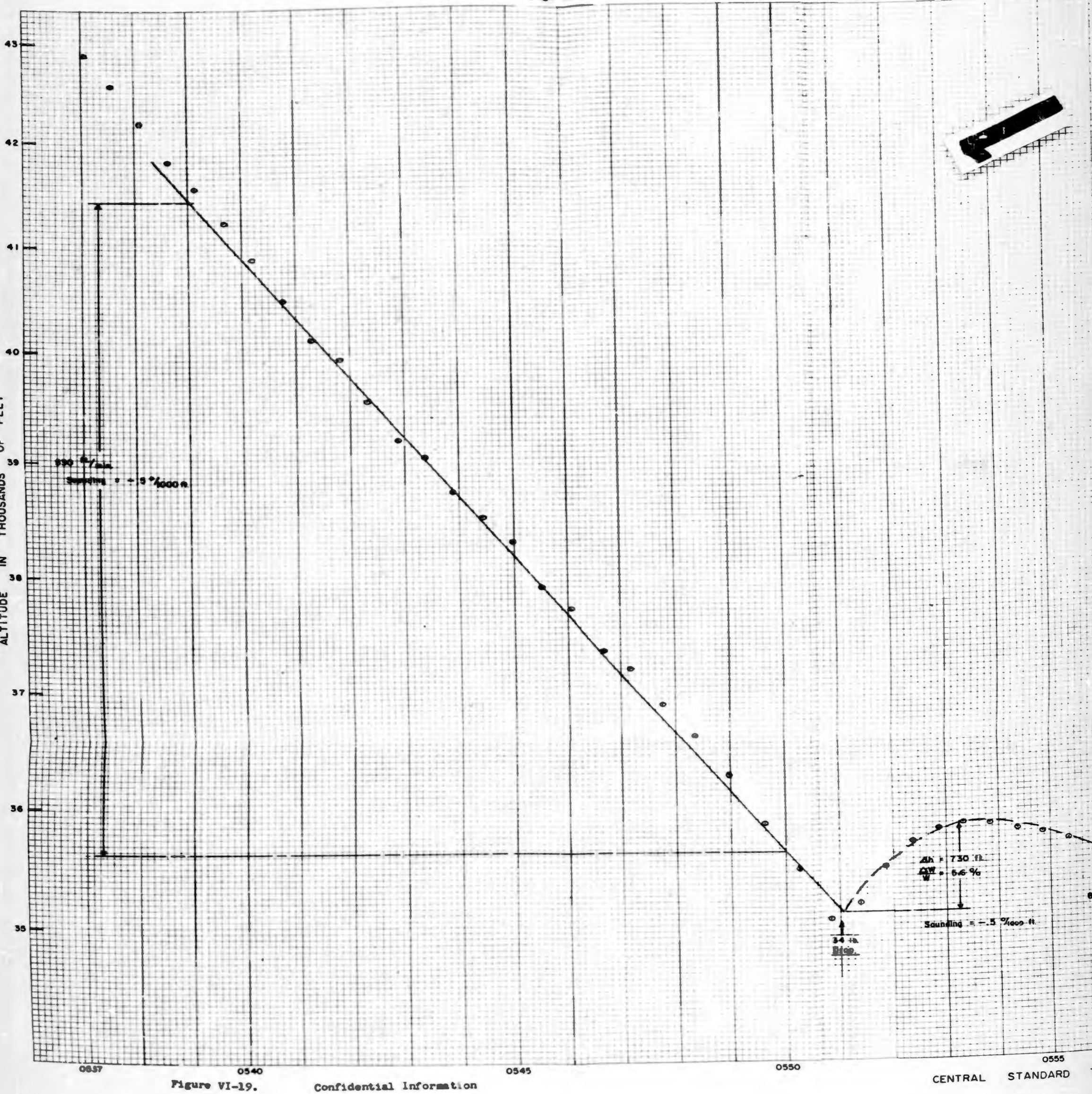

Figure VI-19. Confidential Information

nfidential

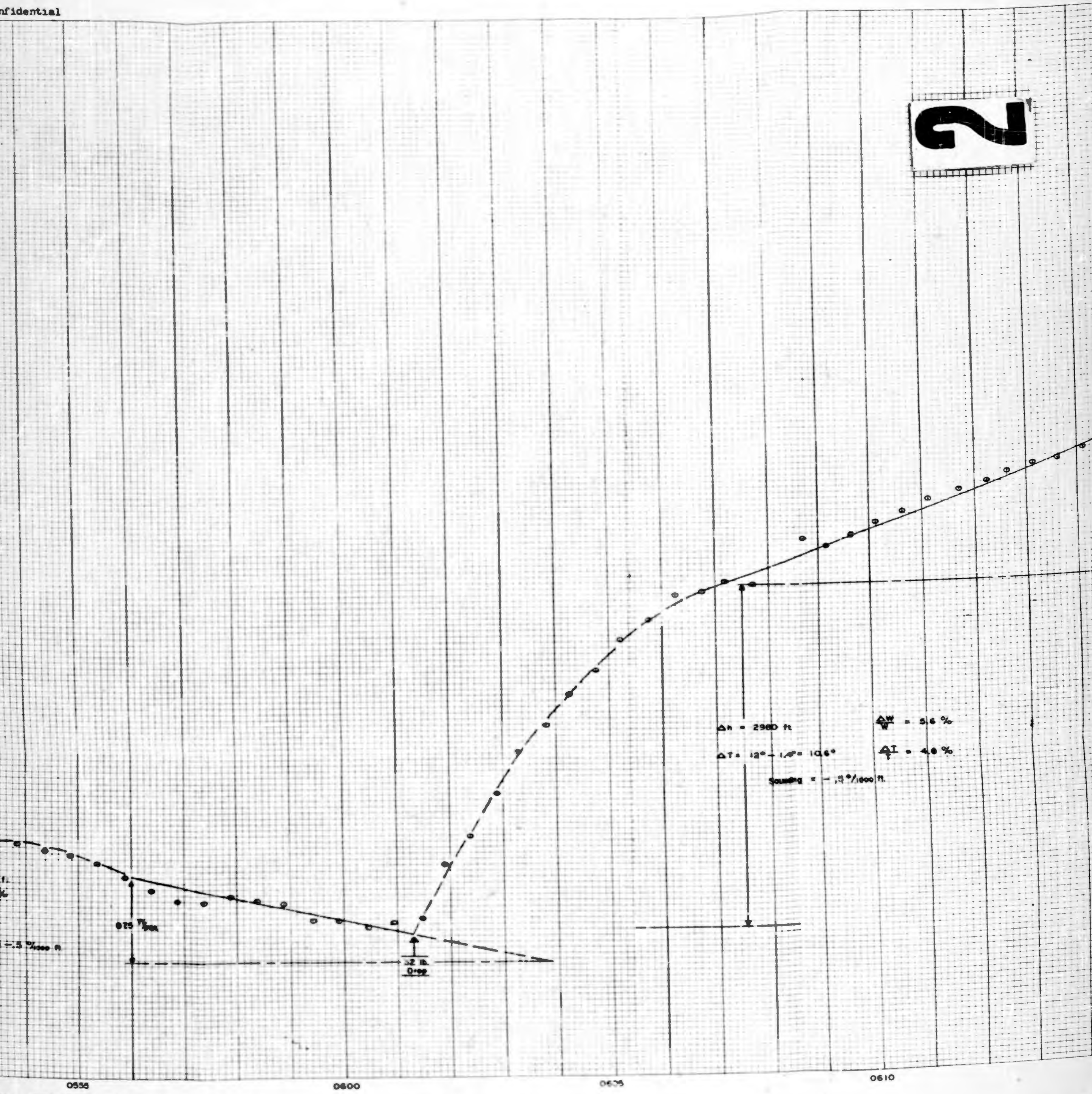

AL STANDARD TIME

160 ft/min

Δh = 2980 ft

ΔT = 12° − 1.4° = 10.6°

Sounding = − .9°/1000 ft.

$\frac{\Delta w}{w}$ = 5.6 %

$\frac{\Delta I}{I}$ = 4.8 %

22 lb. Drop

3

0600 0605 0610 0615 06

There is 13 lbs which is practically entirely thermodynamic, the aerodynamic drag being negligibly small at this rate. Therefore the difference in drag, according to the nomographs, between the descent of 530 ft/min and the descent following ballast of 88 ft/min, is 52 lbs of drag, whereas 34 lbs of ballast was actually dropped. This is, like the first case, in serious disagreement. A change in drag before and after the second ballast drop is such that the initial drag,which was just calculated, was 13 lbs. Then after 32 lbs of ballast drop, the rise rate is 160 ft/min, which gives 23 lbs thermodynamic drag and .8 lbs aerodynamic drag, or a total of 24 lbs of drag. The total change in drag is 24 plus 13 or 37 lbs, which is to be compared with 32 lbs of ballast drop. This is not in such serious disagreement as the previous case. We next compare the overall change in drag from the initial descent to the final ascent and we find that the total change in drag is 65 plus 24 or 89 lbs and the total ballast drop is 66 lbs. This is in rather serious disagreement. This flight is to be compared with flights in which the balloon was descending at night, for instance following sunset in which just the sunset effect in ballast was dropped which leveled the balloon. These cases are found to be in excellent agreement with the flight constant nomographs for thermodynamic and aerodynamic drag. It is therefore concluded that the descent and ascent in daytime with the sun on the balloon are different than the descent and ascent at nighttime without the sun, which is possibly due to the superheat of the balloon which is higher in the daytime and there may be differences in ascent and descent because of the extra superheat.

E. Fundamental Superpressure Calculations

This section is intended to present the ultimate limiting situation which exists for the case of a superpressure balloon which is floating, either just carrying itself, or carrying itself and some load. It is rather interesting that it is possible to write two equations--one expressing the structural relationship between the bursting superpressure, the tensile strength, the thickness and radius of the balloon, the other expressing the fact that the balloon system must be buoyant—and by solving these equations to get a third equation which expresses the fractional superpressure which a balloon system can maintain without bursting and still be able to flo t carrying its load. The resulting equation depends only on the atmospheric temperature and on the breaking length of the material involved, for a balloon which carries no load. For a balloon which carries a load, it also depends on the air displaced in units of the balloon weight. The solution of these equations leads to fractional superpressure values for various materials and various configurations which will be the ultimate obtainable for the balloon system. The first equations, $(1)_s$ and $(1)_c$, are the structural equations expressing the bursting superpressure of the balloon in terms of the tensile strength, the thickness of the material, and the radius at the equator of the balloon, for a perfect sphere and for a balloon made as a cylinder balloon and given enough material so that it does not develop circumferential stress.

Structural equations:

$$\Delta P_B = \frac{2\,\bar{f}\cdot t}{R} \qquad (1)_s \text{ sphere}$$

$$\Delta P_B = \frac{\bar{f}\cdot t}{r} = \frac{2\,\bar{f}\cdot t}{R} \qquad (1)_c \text{ cylinder}$$

r = meridian radius of curvature of infinite superpressure cylinder at equator

R = radius of balloon at equator

$\bar{F}$ = tensile strength of material

t = thickness of material

ΔP_B = bursting superpressure

The buoyancy equations $(2)_s$ and $(2)_c$ are derived as follows:

Mass of air displaced = Mass of helium + mass of balloon and load.

$$\rho_A V = \rho_{He} V + \rho_B \cdot \frac{G}{W} V$$

$$(\rho_A - \rho_{He}) V = \rho_B \cdot \frac{G}{W} V$$

$$\frac{P}{\bar{R} T} (M_A - M_{He}) V = \rho_B \cdot \frac{G}{W} V$$

$$P = \rho_B \cdot \frac{G}{W} \cdot \frac{\bar{R}T}{M_A - M_{He}} \qquad (2)$$

Where ρ_A = density of air

ρ_{He} = density of helium

ρ_B = density of balloon

V = balloon volume

M_A = molecular weight of air

M_{He} = molecular weight of helium

P = pressure at which the system floats

G = mass of air displaced

W = mass of balloon

$\bar{R}$ = universal gas constant

T = temperature, $^{\circ}$ absolute.

For a sphere:

$$\rho_B = \frac{\rho_p \quad t \cdot 4\pi R^2}{\frac{4}{3} \pi R^3} = \frac{3 \rho_p \cdot t}{R} \qquad (2)_s$$

For a cylinder it can be shown that

$$\rho_B = 6 . \frac{\rho_p \ t}{R} \qquad (2)_c$$

where, in addition to the quantities previously defined, ρ_p is the density of the plastic.

Solving equations (1) and (2) simultaneously, for the case of the sphere and cylinder, gives the resulting equations $(3)_s$ and $(3)_c$, where F is the fractional superpressure which the balloon has when it is just being stressed to ultimate and is floating at a pressure P. It is interesting that this fractional superpressure does not depend directly on the thickness of the balloon. It is, for example, the fractional change in temperature of the balloon system which can be allowed without having the balloon become slack.

Equations $(1)_s$ and $(2)_s$ can be solved simultaneously, as can $(1)_c$ and $(2)_c$, to give the fractional superpressure allowable for a system that is just buoyant. The result is

For a sphere

$$F = \frac{\Delta P_B}{P} = \frac{2}{3} \frac{(M_A - M_{He})}{\bar{R} T} \frac{\mathcal{F}}{\rho} \cdot \frac{W}{G} \qquad (3)_s$$

And for a cylinder

$$F = \frac{\Delta P_B}{P} = \frac{1}{3} \frac{(M_A - M_{He})}{\bar{R} T} \frac{\mathcal{F}}{\rho} \cdot \frac{W}{G} \qquad (3)_c$$

The following table gives design values for the tensile strength, density, and the ratio of tensile strength to density, for Mylar and polyethylene.

Equation $(3)_s$ and $(3)_c$ can be solved for Mylar and polyethylene:

Material	F	ρ	$\frac{F}{\rho}$
Mylar	$5000\#/in^2$	$.0500\#/in^3$	$10^5 \frac{\text{pounds force - in.}}{\text{pounds mass}}$
Polyethylene	$1000\#/in^2$	.036	2.8×10^4

These figures are not the yield strength figures given in the manufacturers' data, but are rather figures which have been obtained by experience with superpressure balloons on the ground. For example, a number of cases of Mylar cylinders have been tested and have been found to fail at equivalent tensile strengths of from 6,000 to 9,000 lbs/in^2. The figure in the table of $5,000\#/in^2$ is deemed to be an upper limit design value, as is $1000\#/in^2$ for polyethylene. The value of the constant in Equation (3) is evaluated below, finally resulting in Equations $(4)_s$ and $(4)_c$ which express the fractional superpressure allowed for spheres and cylinders, with $\frac{F}{\rho}$ for the tensile strength-to-density ratio, i.e. the breaking length, and for balloons which have a weight W and displace the amount of air G.

$$\frac{M_A - M_g}{\bar{R}\ T} = \frac{(28.8 - 4)}{33400(220)}$$

at stratosphere temperature of 220° K.

$$\frac{M_A - M_g}{RT} = \frac{24.8}{3.34 \times 2.2 \times 10^6} = 3.37 \times 10^{-6}$$

so

$$F_{sphere} = 2.26 \times 10^{-6} \frac{\mathcal{F}}{\rho} \cdot \frac{W}{G} \qquad (4)_s$$

$$F_{cylinder} = 1.13 \times 10^{-6} \frac{\mathcal{F}}{\rho} \cdot \frac{W}{G} \qquad (4)_c$$

Finally, substituting the values for $\frac{\mathcal{F}}{\rho}$ for Mylar and polyethylene gives the table of values of F below.

Material	Sphere	Cylinder
Mylar	.226 $(\frac{W}{G})$	.113 $(\frac{W}{G})$
Polyethylene	.063 $(\frac{W}{G})$	.031 $(\frac{W}{G})$

This table is quite significant since it gives upper limit values for various situations. Consider the entry for Mylar sphere, .226 $(\frac{W}{G})$. This entry means that the maximum superpressure which can be obtained with a Mylar spherical balloon which has no weight hanging on it except the weight of the material, that is $\frac{W}{G} = 1$, would be 22.6%. It would be impossible, without exceeding the 5,000#/in^2 value, to obtain a higher percentage supe pressure for this balloon. Similarly, a polyethylene cylinder not carrying any load will be able to superpressure only 3% when stressed to 1000#/in^2. If the Mylar spherical balloon first referred to were actually carrying a load equal to the balloon weight, $\frac{W}{G}$ would be $\frac{1}{2}$, and the maximum possible superpressure obtainable would be 11.3% for this balloon system. It should be emphasized that these figures are the maximum values which one could hope to obtain in practice with these balloon systems. The fact that the balloon volume did not enter is not surprising; given a value for the weight of the load to be carried, and choosing a value for $\frac{W}{G}$ consistent with the superpressure demanded, will determine a floating

altitude for the balloon system once the value of the weight of the balloon or the load to be hung upon it is selected. The design of the system, say, to superpressure out sunset, would go then somewhat as follows. If one were to make a Mylar cylinder carrying a load equal to the balloon weight, such a cylinder would be able to superpressure out half of 11.3%, or 5.6%, at sunset. If the sunset effect on the balloon were 5.6% or less, such a balloon system would be able to superpressure sunset out. If the sunset effect were larger than this, obviously it would be impossible to go through sunset with the balloon system.

A number of experiments have been carried out with Mylar cylinders, a few with poly cylinders, and one with a Mylar sphere. It is believed, because of the fact that Mylar does not stretch and from the results of this test, that it is not feasible to make spherical Mylar balloons because they would need to be tailored so perfectly that it would be impractical to manufacture them. If they are not tailored to the exact spherical shape, then they are too small in one direction or the other, the tension will become twice as great as anticipated, and the balloon will fail. The figures in the table, however, do show that it is possible, in principle, to make a balloon carry sufficient superpressure to allow it to pass through sunset with a load on it equal approximately to the balloon weight. Perhaps the most favorable practical situation is represented by the Mylar cylinder, which, carrying a load equal to its own weight, will superpressure out 5.6% sunset effect. Direct measurements of the sunset effect on ¼-mil 20-ft Mylar slack balloons indicate that the sunset effect on these is about 3%, or appreciably below the value which might be achieved with a Mylar cylinder. As has been indicated in Section III, Volume IX, some success

has been achieved with small balloons in getting the leaka
down to diffusion leakage. The value of this leakage for t
is high enough so that the addition of superpressure to ge
effect increases the leakage to the point where the ballast
pay for leakage may be as much as the sunset ballast dema
These flights with small Mylar superpressure cylinders, howe
that it is possible to add a great deal of stability to a fr
flight by providing enough superpressure. A moderate valu
pressure, say 1 or 2% of the floating pressure, is adequate
very level time-altitude curve. Such a low value of the sup
be maintained for a period of 6-8 hours, a time adequate for
purposes in studying trajectories at very constant altitude.
some interest also to investigate the possibility of ballasti
the superpressure in flight, and if the ballast demand is sm
will be stable but will climb as ballast is expended and the
weight of the balloon system decreases. In the work of the
Balloon Project it is very profitable to use superpressure t
stability, but it appears that superpressuring balloons to e
sunset effect will be too costly in terms of ballast to just
tional complicati on. It is possible, however, that several
be made in which the sunset effect is superpressured out, si
the magnitude of the sunset effect on the balloon system by
the value of the superpressure.

UNCLASSIFIED